UNIVERSIDADE FEDERAL DO RIO GRANDE DO SUL
FACULDADE DE FARMÁCIA
PROGRAMA DE PÓS-GRADUAÇÃO EM CIÊNCIAS FARMACÊUTICAS

Desenvolvimento e caracterização de sistemas de liberação contendo kaempferol para administração intranasal e oral

MARIANA COLOMBO

PORTO ALEGRE, 2019

UNIVERSIDADE FEDERAL DO RIO GRANDE DO SUL
FACULDADE DE FARMÁCIA
PROGRAMA DE PÓS-GRADUAÇÃO EM CIÊNCIAS FARMACÊUTICAS

Desenvolvimento e caracterização de sistemas de liberação contendo kaempferol para administração intranasal e oral

Tese apresentada por **Mariana Colombo** para obtenção do TÍTULO DE DOUTORA em Ciências Farmacêuticas.

Orientador: Profa. Dr. Letícia Scherer Koester

PORTO ALEGRE, 2019

Tese apresentada ao Programa de Pós-Graduação em Ciências Farmacêuticas, em nível de Doutorado da Faculdade de Farmácia da Universidade Federal do Rio Grande do Sul e aprovada em 29.03.2019, pela Banca Examinadora constituída por:

Profa. Dr. Elizandra Braganhol
Universidade Federal de Ciências da Saúde de Porto Alegre (UFCSPA)

Profa. Dr. Karina Paese
Universidade Federal do Rio Grande do Sul (UFRGS)

Prof. Dr. Tiago Caon
Universidade Federal de Santa Catarina (UFSC)

CIP - Catalogação na Publicação

Colombo, Mariana
Desenvolvimento e caracterização de sistemas de liberação contendo kaempferol para administração intranasal e oral / Mariana Colombo. -- 2019.
249 f.
Orientadora: Letícia Scherer Koester.

Tese (Doutorado) -- Universidade Federal do Rio Grande do Sul, Faculdade de Farmácia, Programa de Pós-Graduação em Ciências Farmacêuticas, Porto Alegre, BR-RS, 2019.

1. kaempferol. 2. nanoemulsão. 3. administração intranasal. 4. dispersão sólida. 5. administração oral. I. Scherer Koester, Letícia, orient. II. Título.

Elaborada pelo Sistema de Geração Automática de Ficha Catalográfica da UFRGS com os dados fornecidos pelo(a) autor(a).

Este trabalho foi desenvolvido no Laboratório de Desenvolvimento Galênico da Faculdade de Farmácia da UFRGS e no Laboratório de Sinalização Purinérgica e Câncer, Departamento de Bioquímica da UFRGS. Agradecimentos a Capes e a FAPERGS, órgãos que financiaram a bolsa de estudos e o desenvolvimento deste trabalho, respectivamente.

AGRADECIMENTOS

À Universidade Federal do Rio Grande do Sul, à Faculdade de Farmácia e ao Programa de Pós Graduação em Ciências Farmacêuticas, responsáveis por toda minha formação acadêmica.

À minha orientadora Prof. Dra. Letícia Koester pela oportunidade, incentivo e amizade desde a iniciação científica.

Ao laboratório 22 da Bioquímica, em especial ao Prof. Fabrício Figueiró, Prof., Ana Battastini e a bolsista Amanda por todo suporte nos experimentos.

Aos professores Helder, Valquíria e Ortega, pela amizade e conhecimento transmitido em todos esses quase 10 anos de LDG.

Aos queridos amigos e colegas de laboratório que alegraram todos os meus dias. À Gabi, no início como bolsista e logo depois como amiga e colega de pós-graduação. Em especial à Luana, Lucélia, Kleyton, Nessa e Tainá, pela amizade dentro e fora do laboratório. Ao pessoal do LDG do tempo da minha iniciação científica, meus primeiros incentivadores da vida acadêmica.

À minha família, em especial aos meus pais, irmão, avós, tios e dinda pelo amor e apoio durante toda minha trajetória.

Ao Fabrício pelo companheirismo, incentivo e amor durante todos esses anos. E principalmente por agora ser pai da nossa maior conquista que está a caminho, Caetano.

APRESENTAÇÃO

De acordo com as normas vigentes no Regimento do Programa de Pós-Graduação em Ciências Farmacêuticas da Universidade Federal do Rio Grande do Sul, a presente tese foi redigida na forma de capítulos, com encarte de publicações. Assim, este exemplar encontra-se estruturado da seguinte forma:

- **Introdução;**
- **Objetivo geral e objetivos específicos;**
- **Revisão da literatura;**
- **Capítulo I: Desenvolvimento de nanoemulsões contendo kaempferol para administração intranasal e avaliação da atividade citotóxica em glioma:**

  - Publicação I: "Validation of an HPLC-UV method for analysis of kaempferol-loaded nanoemulsion and its application to *in vitro* and *in vivo* tests".

  - Publicação II: "Kaempferol-loaded mucoadhesive nanoemulsion for intranasal administration reduces glioma growth *in vitro*".
- **Capítulo II: Desenvolvimento de dispersões sólidas contendo kaempferol para administração oral:**

  - Artigo científico a ser submetido: "Flavonoids delivery by solid dispersion: a systematic review".

  - Publicação II : "Solid dispersion of kaempferol: formulation development, characterization and oral bioavailability assessment".
- **Discussão geral;**
- **Conclusões;**
- **Referências.**

RESUMO

Kaempferol (KPF) é um flavonoide com diversas propriedades farmacológicas, dentre elas, podemos destacar a atividade anti-inflamatória, antioxidante e antitumoral. Entretanto, a baixa hidrossolubilidade e biodisponibilidade comprometem sua utilização terapêutica. Nesse contexto, o objetivo do trabalho foi desenvolver estratégias farmacotécnicas para melhorar as características biofarmacêuticas do KPF, no caso, nanoemulsões para administração intranasal e dispersões sólidas para a via oral. Primeiramente, um método por cromatografia líquida de alta eficiência foi validado para a quantificação do KPF em diferentes matrizes (nanoemulsão, mucosa nasal, fluido receptor e cérebro de ratos). Duas formulações foram desenvolvidas: nanoemulsão (KPF-NE) e nanoemulsão mucoadesiva contendo quitosana (KPF-MNE). Ambas nanoemulsões apresentaram tamanho nanométrico inferior a 190 nm, baixo índice de polidispersão, potencial zeta negativo pra KPF-NE e positivo para KPF-MNE e teor superior a 96%. Uma maior força mucoadesiva foi observada para KPF-MNE, bem como maior permeação através da mucosa nasal. Ainda, foi verificado que a administração intranasal da KPF-MNE aumentou o teor de KPF no cérebro de ratos em relação a KPF-NE e KPF livre. Além disso, KPF-MNE apresentou atividade citotóxica em células de glioma superior a KPF-NE, com indução de apoptose. Dispersões sólidas contendo KPF e como carreador, Poloxamer 407 (1:5, p:p), foram desenvolvidas por dois métodos de preparo (fusão e evaporação do solvente) e ambas aumentaram significativamente a solubilidade aparente e apresentaram similar perfil de dissolução em meio ácido (aproximadamente 100% em 2h). Em contrapartida, KPF livre apresentou dissolução incompleta. Após a administração oral da dispersão sólida em ratos, houve aumento significativo (aproximadamente 2 vezes) na extensão de absorção (ASC) em comparação ao KPF livre. Portanto, KPF-MNE apresenta-se como um promissor sistema de liberação para KPF através da via intranasal para o tratamento de GBM, bem como dispersões sólidas são uma estratégia eficaz para aumentar a dissolução e biodisponibilidade oral do KPF.

Palavras-chave: Kaempferol, nanoemulsões, administração intranasal, glioma, dispersões sólidas, dissolução

ABSTRACT

Kaempferol (KPF) is a flavonoid with several pharmacological properties, among them we can highlight the anti-inflammatory, antioxidant and anti-tumor activity. However, low water solubility and bioavailability compromise its therapeutic use. In this context, the objective of the study was to develop pharmacotechnical strategies to improve the biopharmaceutical characteristics of KPF. Nanoemulsions containing KPF were developed for intranasal administration and solid dispersions for the oral route. First, a high performance liquid chromatography method was validated for the quantification of KPF in different matrices (nanoemulsion, nasal mucosa, receptor fluid and murine brain). Two formulations were developed: nanoemulsion (KPF-NE) and mucoadhesive nanoemulsion containing chitosan (KPF-MNE). Both nanoemulsions had a nanometric size (less than 190 nm), low polydispersity index, negative zeta potential for KPF-NE and positive for chitosan-containing KPF-MNE, KPF content greater than 96% and compatible pH for intranasal administration. Higher mucoadhesive strength was observed for the formulation as well as increased permeation through the nasal mucosa. Intranasal administration of KPF-MNE has been shown to increase KPF content in the rat brain relative to KPF-NE and free KPF. In addition, KPF-MNE showed cytotoxic activity in glioma cells superior to KPF-NE, with induction of apoptosis. Solid dispersions containing the Poloxamer 407 as carrier (1: 5) were developed by two methods of preparation (solvent evaporation and melting method) and both significantly increased apparent solubility and showed similar dissolution profile (approximately 100% in 2h). In contrast, free KPF showed incomplete dissolution. After oral administration of the solid dispersion in rats, there was a significant (approximately 2-fold) increase in extent of absorption (ASC) compared to free KPF. Therefore, KPF-MNE presents as a promising delivery system for KPF through the intranasal route for the treatment of GBM, as well as solid dispersions are an effective strategy to increase the dissolution and oral bioavailability of KPF.

Key-words: Kaempferol, nanoemulsions, intranasal administration, glioma, solid dispersion, dissolution.

LISTA DE FIGURAS

REVISÃO BIBLIOGRÁFICA

CAPÍTULO I

Publicação I

content in the mobile phase (%); A_1: blank nanoemulsion; A_2: receptor media; A_3: porcine nasal mucosa; A_4: murine brain.

Publicação II

Figure 1. TEM analysis from developed formulations A) KPF-NE, B) KPF-MNE.

Figure 2. Histopathological sections of porcine nasal mucosa treated with A) IPA, B) PBS pH 6.4, C) NE, D) MNE, D) KPF-NE, E) KPF-MNE.

Figure 3. Force (A) and work of mucoadhesion (B) of samples measured by the mucoadhesive strength test. Data were analyzed with one-way ANOVA followed by Tukey's test. Significantly different from the control groups (**$p < 0.001$, ***$p < 0.0001$).

Figure 4. KPF concentration (ng/g of tissue) in rat's brain after 1 h of nasal administration of formulations. Data were analyzed with one-way ANOVA followed by Tukey's test. Significantly different from the control groups (**$p < 0.001$).

Figure 5. A) Antiproliferative effect of free KPF, KPF-NE and KPF-MNE at 1 μM by Trypan blue exclusion assays. B) Effect of kaempferol on C6 glioma cell line. Cell viability is presented in relation to control. Vehicle control (DMSO) did not interfere significantly with cell viability. The data represent the mean of three independent experiments performed in triplicate ± SD. Data were analyzed with one-way ANOVA followed by Tukey's test. Significantly different from the control groups (*$p < 0.05$).

Figure 6. Representative histograms of the percentage of cells in the G1, S, G2/M and sub-G1 phase of the cell cycle after treatment with free KPF, MNE, MNE+ KPF and KPF-MNE at 1 μM for 72 h. Data were analyzed with one-way ANOVA followed by Tukey's test. Significantly different from the control groups (*$p < 0.05$).

Figure 7. A–D) Representative images containing the average relative number of cells after treatment with DMSO, free KPF, MNE, MNE+ KPF and KPF-MNE at 1 μM for 72 h. E) Representative images containing the average relative number of cells after treatment with free KPF-MNE at 1 μM for 72 h. The gate settings distinguish between viable cells (bottom left), necrotic cells (top left), early apoptotic cells (bottom right) and late apoptotic cells (top right). F) Quantitative analysis of total apoptosis in cells treated with free KPF, KPF+MNE and KPF-MNE at 1 μM for 72 h. The values are presented as the means ± S.D. of three independent experiments. Data were analyzed with one-way ANOVA followed by Tukey's test. Significantly different from the control groups (*$p < 0.05$, ***$p < 0.0001$).

CAPÍTULO II

Artigo a ser submetido

Figure 1. Basic flavonoid structure.

Figure 2. Flowchart of systematic literature search.

Figure 3. Summary of records employing solid dispersion of flavonoids in terms of (A) drugs being formulated; (B) the methods of preparation (C) the carriers employed.

Publicação II

Figure 1. Diagram of phase solubility for KPF in the presence of various carriers in distilled water (mean ± S.D.; n = 3).

Figure 2. Solubility of KPF from solid dispersions composed of Poloxamer 407 at various drug: carrier weight ratio pre pared by solvent method (mean ± S.D.; n = 3). ***$p < 0.0001$, compared to the other groups.

Figure 3. Fourier transform infrared spectroscopy spectra of KPF (A), Poloxamer 407 (B), physical mixture (C), SD_{MM} (D), and SD_{SM} (E).

Figure 4. Differential scanning calorimetry thermograms of KPF (A), Poloxamer 407 (B), physical mixture (C), SD_{MM} (D), and SD_{SM} (E).

Figure 5. X-ray diffraction patterns of KPF (A), Poloxamer 407 (B), physical mixture (C), SD_{MM} (D), and SD_{SM} (E).

Figure 6. Scanning electron microscopic images of KPF (A), Poloxamer 407 (B), physical mixture (C), SD_{MM} (D), and SD_{SM} (E).

Figure 7. Dissolution profiles from different preparations of kaempferol (mean ± S.D.; n = 3).

Figure 8. KPF plasma concentration upon oral administration in rats (100 mg/kg) of pure KPF and SD_{MM} (KPF: Poloxamer 407, 1:5) (mean ± S.D., n= 4).

LISTA DE TABELAS

REVISÃO BIBLIOGRÁFICA

CAPÍTULO I

Publicação I

Publicação II

CAPÍTULO II

Artigo a ser submetido

Table 1. Summary of records that discussed solid dispersion formulations for the enhancement of the *in vitro* dissolution and/or oral bioavailability of flavonoids.

Table 2. Solid dispersion formulations of flavonoids from herbal extracts

Publicação II

Table 1. Phase solubility of kaempferol (μg/mL) at various concentrations of carriers (n=3).

Table 2. Pharmacokinetic parameters of KPF and SDMM after oral administration to rats at 100 mg/Kg (n=4; mean ± S.D.).

LISTA DE ABREVIATURAS

↑	aumento
↓	diminuição
API	do inglês, *active pharmaceutical ingredient*
AUC	do inglês, area under the curve
BCS	do inglês, *Biopharmaceutics Classification System*
BHE	barreira hemato-encefálica
CA	carreador amorfo
CC	carreador cristalino
C_{max}	do inglês, *peak plasma concentration*
CSF	fluido cérebro espinal
DS	dispersão sólida
DSC	do inglês, *differential scanning calorimetry*
EMA	do inglês, *European Medicines Agency*
EUA	Estados Unidos
FDA	do inglês, *Food and Drug Administration*
FTIR	do inglês, *Fourier transform infrared spectroscopy*
GBM	glioblastoma multiforme
HPLC	do inglês, *high-performance liquid chromatography*
HPMC	hidroxipropilmetilcelulose
HPMCAS	succinato do acetato de hidroxipropilmetilcelulose
KPF	kaempferol
KPF+MNE	tratamento com a nanoemulsão branca MNE e KPF em solução
KPF+NE	tratamento com a nanoemulsão branca NE e KPF em solução
KPF-MNE	nanoemulsão mucoadesiva contendo KPF
KPF-NE	nanoemulsão contendo KPF
MEV	do inglês, *scanning electron microscopy*
MHRA	do inglês, *Medicines and Health Products Regulatory Agency*
MM	do inglês, *melting method*

MNE	nanoemulsão mucoadesiva
NE	nanoemulsão
OMS	Organização Mundial da Saúde
PEG	polietilenoglicol
PI	polímero intumescente
PIA	polímero insolúvel em água
PS	polímero surfactante
PVP	polivinilpirrolidona
PVP-VA	polivinilpirrolidona vinil acetato
SD_{MM}	dispersão sólida preparada por método de fusão
SD_{SM}	dispersão sólida preparada por método de evaporação do solvente
SF	surfactante
SLS	lauril sulfato de sódio
SM	do inglês, *solvent method*
SNC	sistema nervoso central
TPGS	succinato de d- alfa tocoferol polietilenoglicol 1000
UE	União Europeia
XRD	do inglês, *X-ray diffractometry*

SUMÁRIO

INTRODUÇÃO

O flavonoide kaempferol (KPF) possui ação anti-inflamatória, antibacteriana, antiviral, antifúngica, antiprotozoária e neuroprotetora. KPF induz morte celular em diferentes tecidos neoplásicos (pulmão, mama, cólon, próstata, fígado, pâncreas, pele, esôfago, cérebro e ovário) principalmente por apoptose, e os mecanismos envolvidos neste processo ainda estão sendo elucidados (CALDERON-MONTANO *et al.*, 2011; CHEN e CHEN, 2013; DEVI *et al.*, 2015). Em gliomas, além de inibir a invasividade e migração das células, KPF induz apoptose celular através da geração de ROS e é capaz de sensibilizar células cancerígenas aos efeitos citotóxicos de fármacos como doxorrubicina (SHARMA *et al.*, 2007; SIEGELIN *et al.*, 2008; JEONG *et al.*, 2009; NAKATSUMA *et al.*, 2010; SEIBERT *et al.*, 2011).

Gliomas são os tumores primários mais comuns e malignos do Sistema Nervoso Central (SNC) em adultos (SATHORNSUMETEE *et al.*, 2007). Dentro dos tumores astrocíticos, os tumores de alto grau são os mais comuns, destacando-se glioblastoma multiforme (GBM), astrocitoma de grau IV (VAN WOENSEL *et al.*, 2013). O prognóstico para GBM é péssimo, pois mesmo com o tratamento preconizado (recessão cirúrgica, radioterapia e tratamento farmacológico) a sobrevida do paciente é de em média 14,6 meses desde o diagnóstico (ROBINS *et al.*, 2009; VAN WOENSEL *et al.*, 2013). A falha na terapia se deve principalmente à natureza infiltrante, ausência de especificidade terapêutica, quimiorresistência intrínseca e a barreira hematoencefálica (BHE) que limita a entrada dos quimioterápicos no SNC (VAN MEIR *et al.*, 2010; LIU *et al.*, 2014).

Diversas estratégias são utilizadas para aumentar a entrada dos fármacos no SNC (ALAM *et al.*, 2010). Dentre elas, a via de administração intranasal tem se mostrado promissora por diversas razões: ser uma via não invasiva; promover entrega direta do fármaco ao cérebro, evitando a limitação imposta pela BHE; evitar o metabolismo de primeira passagem, o que poderia diminuir a fração de fármaco ativo; possibilitar a utilização de baixas doses, evitando possíveis efeitos adversos; possibilitar a autoadministração. O fármaco consegue alcançar o cérebro diretamente através da região olfatória e/ou ramificações do nervo trigêmeo, ou indiretamente através da porção de fármaco que atinja a circulação sistêmica e consiga transpor a BHE (ALAM *et al.*, 2010; ILLUM, 2012; KOZLOVSKAYA *et al.*, 2014). Entretanto,

a via nasal pode apresentar algumas desvantagens como o *clearance* mucociliar, degradação enzimática e baixa permeabilidade do epitélio nasal a determinados fármacos.

Neste contexto, nanoemulsões são alternativas para contornar tais obstáculos, pois apresentam o potencial de aumentar a absorção de fármacos e o tempo de retenção na cavidade nasal (VINOGRADOV *et al.*, 2002; SOOD *et al.*, 2014). Além disso, o uso de quitosana nas formulações, devido a sua capacidade de abrir as junções oclusivas, favorece a permeação dos ativos, bem como o aumento do tempo de permanência na cavidade nasal, devido às propriedades mucoadesivas (CASETTARI e ILLUM, 2014).

A partir do exposto, considerando a atividade do KPF contra gliomas, a seletividade imposta pela BHE aos fármacos, a potencialidade da nanotecnologia e a via de administração intranasal em aumentar a distribuição no tecido cerebral, o presente trabalho propõe, o inédito desenvolvimento de nanoemulsões contendo kaempferol para aplicação intranasal visando ao aumento da penetração cerebral e, assim, ao tratamento de glioblastoma multiforme.

Apesar das diversas atividades farmacológicas já citadas, KPF possui baixa biodisponibilidade oral, atribuída principalmente a sua baixa hidrossolubilidade (log P 3,11), o que limita sua aplicação terapêutica por esta via de administração tão consagrada (ROTHWELL *et al.*, 2005; CALDERON-MONTANO *et al.*, 2011; CHEN e CHEN, 2013; DEVI *et al.*, 2015). KPF é classificado como classe II no Sistema de Classificação Biofarmacêutica, tendo sua absorção oral controlada pela etapa de dissolução (XIE *et al.*, 2014). Portanto, aumentar a solubilidade do KPF no trato gastrointestinal é uma etapa crucial para aumentar sua absorção oral, aumentando sua biodisponibilidade e, consequentemente, seus efeitos farmacológicos.

Diversas estratégias são utilizadas para aumentar a hidrossolubilidade e biodisponibilidade oral de fármacos pouco solúveis, como redução do tamanho das partículas para aumentar a área de superfície, utilização de pró-farmacos, utilização de sais e dispersões sólidas, as quais são consideradas umas das mais efetivas pelo aumento da molhabilidade e porosidade, diminuição do tamanho de partícula e/ou transformação para o estado amorfo do fármaco (LEUNER, CHRISTIAN e

DRESSMAN, JENNIFER, 2000; VO *et al.*, 2013). O princípio da técnica consiste basicamente em dispersar o fármaco hidrofóbico em um carreador hidrofílico, onde o carreador pode ser tanto cristalino quanto amorfo, e o fármaco pode encontrar-se molecularmente disperso como partículas amorfas ou cristalinas (MENG *et al.*, 2015).

O preparo de dispersões sólidas tem contribuído para gerar resultados promissores na dissolução e biodisponibilidade de flavonoides (KANAZE *et al.*, 2006; KAKRAN *et al.*, 2011; KHAN *et al.*, 2015). Mesmo sendo evidente a necessidade de melhorar a biodisponibilidade oral do kaempferol, pouco se tem investigado no que se refere ao desenvolvimento de formulações orais contendo kaempferol, e, até o momento, dispersões sólidas contendo kaempferol não foram exploradas. Assim, o desenvolvimento de dispersões sólidas contendo KPF é uma promissora e inédita estratégia com o objetivo de melhorar sua solubilidade aquosa e biodisponibilidade oral.

Portanto, o presente trabalho tem como objetivo desenvolver diferentes estratégicas farmacotécnicas, nanoemulsões e dispersões sólidas, a fim de melhorar as características biofarmacêuticas do kaempferol.

OBJETIVOS

Objetivo Geral

Desenvolver e caracterizar sistemas de liberação contendo kaempferol para administração intranasal e oral visando à melhoria de suas características biofarmacêuticas.

Objetivos específicos

Capítulo I:

− Desenvolver e validar métodos analítico e bioanalítico para a quantificação do KPF em nanoemulsões, em amostras de permeação/retenção através mucosa nasal e em cérebros de ratos;

− Desenvolver nanoemulsões contendo KPF e caracterizá-las quanto às propriedades físicas, químicas e físico-químicas;

− Estimar a distribuição cerebral do KPF após administração intranasal das nanoemulsões em ratos Wistar;

− Avaliar a atividade citotóxica do KPF incorporado nas nanoemulsões desenvolvidas em linhagem celular de glioblastoma multifome (C6);

Capítulo II:

− Realizar uma revisão com análise descritiva e quantitativa da literatura existente que utilizou a abordagem de dispersões sólidas para a melhoria da dissolução e biodisponibilidade oral de flavonoides.

− Selecionar o melhor carreador e desenvolver dispersões sólidas para administração oral contendo KPF;

− Caracterizar as dispersões sólidas através de Calorimetria Exploratória Diferencial (DSC), Espectroscopia de Infravermelho com Transformada de Fourier (FTIR), difração de raios X (DRX) e microscopia eletrônica de varredura (MEV);

− Avaliar o perfil de dissolução das dispersões desenvolvidas;

− Realizar estudo de farmacocinética da formulação otimizada em comparação ao KPF.

KAEMPFEROL

Flavonoides são metabólitos secundários caracterizados pela estrutura difenilpropano, consistindo em dois anéis benzeno unidos por uma cadeia linear de três carbonos (C6-C3-C6). Na maioria dos casos, os três carbonos formam um anel pirano fechado, formando assim uma estrutura de 15 átomos de carbono, compondo três anéis, denominados A, B e C, representado na Figura 1. As classes de flavonóides diferem no grau de oxidação e no padrão de substituição do anel C, enquanto que os compostos dentro de uma classe diferem no padrão de substituição dos anéis A e B. Dependendo das variações no anel heterocíclico C, os flavonóides podem ser divididos em subclasses: flavonas (apigenina, luteolina), flavonóis (quercetina, kaempferol, miricetina), flavanonas (naringenina, hesperitina), flavanonóis (taxifolin), flavanóis ou catequinas (catequina, epicatequina, epigalocatequina), isoflavonas (genisteína, daidzeína, glicetina), antocianinas e antocianidinas (cianidina, pelargonidina, petunidina) (YAO *et al.*, 2004; KUMAR e PANDEY, 2013).

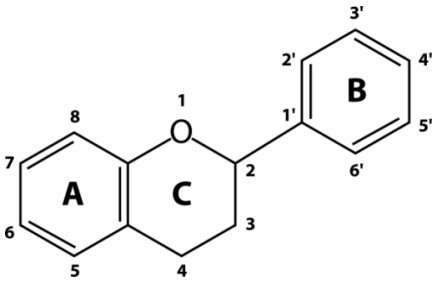

Figura 1. Estrutura básica dos flavonoides (KUMAR e PANDEY, 2013).

Estes compostos polifenólicos são amplamente encontrados em plantas e constituem grande parte da dieta humana, como frutas e vegetais (AHERNE e O'BRIEN, 2002; ROSS e KASUM, 2002). Além de suas funções fisiológicas nas plantas, os flavonoides apresentam diversas atividades terapêuticas, como forte atividade antioxidante, anti-inflamatória, antiproliferativa, hepatoprotetora, antibacteriana, dentre outras (YAO *et al.*, 2004; KUMAR e PANDEY, 2013).

O flavonoide Kaempferol (KPF, *3,5,7-trihydroxy-2-(4-hydroxyphenyl)-4H-1-benzopyran-4-one*), Figura 2, é um composto de coloração amarela com baixo peso

molecular (PM 286,2 g/mol), encontrado em diversas espécies de plantas, abundantemente encontrado na dieta humana (brócolis, maçã, morango, feijão, uva, etc) e em plantas medicinais (por exemplo, *Aloe vera, Ginkgo biloba, Rosmarinus officinalis, Crocus sativus* L., *Hypericum perforatum L., Equisetum spp,*) (MIEAN e MOHAMED, 2001; SULTANA e ANWAR, 2008; YANG *et al.*, 2008; CALDERON-MONTANO *et al.*, 2011). Em plantas, açúcares, tais como rutinose, ramnose, glicose e galactose podem estar ligados ao kaempferol para produzir a forma glicosídica do kaempferol, como por exemplo, astragalina (kaempferol-3-O-glucoside), onde somente uma enzima é necessária ao final de sua biossíntese (flavonol 3-O-glucosyltransferase), sendo esta enzima amplamente encontrada no reino vegetal (CALDERON-MONTANO *et al.*, 2011).

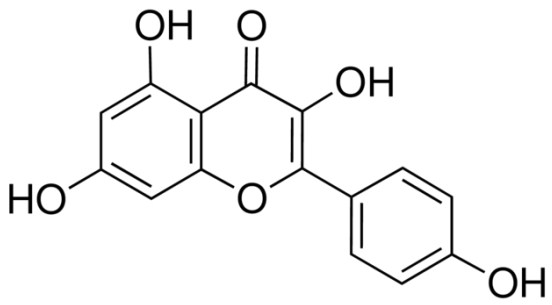

Figura 2. Estrutura química do kaempferol (CHEN e CHEN, 2013).

Após a administração oral de 100 e 250 mg/kg de KPF em ratos, o t_{max} foi observado entre 1 e 1,5 horas seguido por um declínio constante até 6h. Observou-se baixa a moderada absorção, com baixa biodisponibilidade relativa (~2%) e extenso metabolismo de primeira passagem (BARVE *et al.*, 2009). Kaempferol é comumente metabolizado em formas metil, sulfato ou glicuronídeo (BARVE *et al.*, 2009; CHEN *et al.*, 2010). Em um estudo onde avaliaram a permeabilidade intestinal de flavonoides em modelo de células Caco-2, verificou-se que KPF possui boa permeabilidade intestinal e que a taxa de transporte é controlada por gradiente de concentração (YANG *et al.*, 2014).

Amidon et al. classificou insumos farmacêuticos ativos (APIs, do inglês, *active pharmaceutical ingredient*) em 4 grupos com base em sua solubilidade e permeabilidade, conhecido como Sistema de Classificação Biofarmacêutica (BCS, do inglês, *Biopharmaceutics Classification System*), sendo uma ferramenta útil para a tomada de decisão no desenvolvimento de formulações do ponto de vista biofarmacêutico (AMIDON *et al.*, 1995). Este flavonoide é classificado como categoria II no Sistema de Classificação Biofarmacêutica, uma vez que possui baixa solubilidade e alta permeabilidade, tendo a biodisponibilidade oral limitada pela etapa de dissolução (AMIDON *et al.*, 1995; TIAN *et al.*, 2009; MERCADER-ROS *et al.*, 2010; XIE *et al.*, 2014). O log P (coeficiente de partição entre a solubilidade em octanol e água) do KPF foi calculado em aproximadamente 3,11 (ROTHWELL *et al.*, 2005).

Mesmo sendo evidente a necessidade de melhorar a biodisponibilidade oral do kaempferol, pouco se tem investigado no que se refere ao desenvolvimento de formulações orais contendo kaempferol. Na maioria dos estudos, foram desenvolvidas formulações sólidas contendo extratos vegetais, os quais apresentavam kaempferol em suas composições, como *Ginkgo biloba* (CHEN *et al.,* 2010; WANG *et al.,* 2015), persimmon leaf (LI *et al.*, 2011), e *Hippophae rhamnoides* L. (ZHAO *et al.*, 2013; DUAN *et al.*, 2016). Tzeng et al. (TZENG *et al.*, 2011), com o desenvolvimento de nanopartículas, verificou aumento da dissolução e melhora na atividade antioxidante quando comparado ao kaempferol livre. Zhang et al. (ZHANG, K. *et al.,* 2015) e Telang et al. (TELANGE *et al.,* 2016) realizaram a complexação do kaempferol com fosfolipídios e ambos demonstraram aumento na solubilidade, dissolução e biodisponibilidade oral em ratos.

Dados epidemiológicos sugerem que o alto consumo de alimentos contendo KPF pode reduzir o risco de desenvolvimento de doenças cardiovasculares e diversos tipo de câncer, como câncer de pulmão, pâncreas e ovário (LIN *et al.*, 2007; NOTHLINGS *et al.*, 2007; CUI *et al.*, 2008; GATES *et al.*, 2009). Entretanto, o número relativamente baixo de estudos e a presença de outros compostos potencialmente bioativos presentes nos alimentos faz com que esses dados sejam insuficientes para se ter uma conclusão sobre a relação do consumo e efeito protetor do

KPF. Diversos estudos experimentais, no entanto, mostram que KPF possui amplas atividades biológicas, envolvendo tanto a prevenção quanto o tratamento dessas e outras doenças (CALDERON-MONTANO *et al.*, 2011; RAJENDRAN *et al.*, 2014).

Embora diversos estudos *in vitro* e pré-clínicos tenham sido realizados com o KPF, até o presente momento, não foram encontrados ensaios clínicos (fases I, II, III e IV) com o KPF livre. Ensaios clínicos foram desenvolvidos com plantas ou extratos vegetais que continham KPF ou seus glicosídeos em suas composições (VAN DONGEN *et al.*, 2000; HAUNS *et al.*, 2001; PICON *et al.*, 2010; ATTIA *et al.*, 2012; BARTON *et al.*, 2013; SALES *et al.*, 2014).

Tanto na sua forma aglicona quanto na de seus glicosídeos, o KPF apresenta atividade antioxidante não somente *in vitro*, mas também *in vivo*. Diversos mecanismos para sua ação antioxidante foram relatados, podendo reagir com H_2O_2, HOCl, superóxido e óxido nítrico, prevenir peroxidação lipídica, inibir enzimas como xantina oxidase e aumentar a expressão ou atividade de enzimas antioxidantes como superóxido dismutase, catalase e heme oxigenase-1 (CALDERON-MONTANO *et al.*, 2011; RAJENDRAN *et al.*, 2014; DEVI *et al.*, 2015).

Diversos mecanismos explicam o efeito anti-inflamatório do KPF, como a inibição de TNF-α e IL-1β e expressão de IL-8. Além disso, KPF é potente inibidor das enzimas COX-1 e COX2 (LEE e KIM, 2010; LEE *et al.*, 2010; DEVI *et al.*, 2015).

O KPF induz morte celular em diferentes tecidos neoplásicos (pulmão, mama, cólon, próstata, fígado, pâncreas, pele, esôfago, cérebro e ovário) principalmente por apoptose, e os mecanismos envolvidos neste processo estão sendo elucidados (CALDERON-MONTANO *et al.*, 2011). KPF também possui ação antimetastática em linhagens de câncer de mama e é capaz de interromper a progressão do ciclo celular em células de câncer de colo (CHO e PARK, 2013; LEE *et al.*, 2014; LI *et al.*, 2015). Outro mecanismo que pode explicar sua ação antineoplásica é pela produção de espécies reativas de oxigênio (ROS) (BARVE *et al.*, 2009; CALDERON-MONTANO *et al.*, 2011).

Em gliomas, além de inibir a invasividade e migração das células, o KPF induz apoptose celular através da geração de ROS, (SHARMA *et al.*, 2007) sensibiliza células ao TRAIL (*tumor necrosis factor–related apoptosis inducing ligand*)

(SIEGELIN *et al.*, 2008), dentre outras vias (JEONG *et al.*, 2009; NAKATSUMA *et al.*, 2010; SEIBERT *et al.*, 2011).

Kaempferol é capaz de sensibilizar células cancerígenas aos efeitos citotóxicos de fármacos como doxorrubicina (SHARMA *et al.*, 2007), cisplatina (LUO *et al.*, 2010), 5-fluorouracil (ZHANG *et al.*, 2008), citarabina (NADOVA *et al.*, 2007), mitoxantrona e o metabolito ativo do irinotecano (SN-38) (IMAI *et al.*, 2004), podendo ter aplicações clínicas como adjuvante terapêutico no tratamento de neoplasias. Além disso, KPF causa menos efeitos adversos em comparação aos fármacos antineoplásicos disponíveis (CHEN e CHEN, 2013).

Este flavonoide também é capaz inibir a enzima CYP3A4 do citocromo p-450 e de inibir o efluxo de fármacos pela glicoproteína P (gp-P) (PATEL *et al.*, 2004). Estudos avaliaram a prévia administração de KPF a administração dos antineoplásicos tamoxifeno e etoposídeo e verificaram um aumento da biodisponibilidade destes, comprovando a inibição da gp-P e CYP3A4 pelo KPF (PIAO *et al.*, 2008; LI *et al.*, 2009).

Ao atingir a circulação sistêmica, os compostos que atuam como moduladores da função cerebral precisam atravessar a barreira hematoencefálica (BHE) para atingir o SNC (ALAM *et al.*, 2010). No entanto, a distribuição sistêmica e a penetração cerebral de flavonoides e seus metabólitos ainda não são bem compreendidas. Apenas um número limitado de estudos sobre a permeabilidade intestinal e cerebral do KPF foram publicados. Barrington et al. (2009) mostraram que, nas células Caco-2, o KPF sofre extenso metabolismo de fase 2, formando conjugados de sulfato e glicuronídeo, e que apenas uma pequena fração de KPF não conjugada penetra nas monocamadas de células Caco-2 (BARRINGTON *et al.*, 2009). Rangel-Ordóñez et al., (2010) relataram a distribuição cerebral em ratos após a administração oral de extrato de *Ginkgo biloba*, demonstrando que o KPF é capaz de atravessar a BHE (RANGEL-ORDONEZ et al., 2010). Recentemente, Yang et al. (2014) e Moradi-Afrapoli et al (2016) relataram a permeação do KPF em modelo de BHE e em células Caco-2 (YANG *et al.*, 2014; MORADI-AFRAPOLI *et al.*, 2016). Contudo, pouco se sabe sobre os perfis farmacocinéticos do KPF no cérebro, o que é provavelmente devido à baixa

quantidade cerebral acumulada de KPF, tendo em vista o efeito protetor da BHE, que limita a entrada de KPF no tecido cerebral (ZHANG, Q. *et al.*, 2015).

Portanto, é de suma importância a elaboração de estratégias para aumentar a biodisponibilidade oral, bem como facilitar a entrada do KPF ao SNC.

VIA NASAL

Tradicionalmente, os produtos nasais comercializados são para o tratamento local de doenças das vias respiratórias, como infecções, congestão e alergias na cavidade nasal. Entretanto, nas últimas décadas, um grande interesse nessa via de administração surgiu devido à possibilidade de veiculação de fármacos com problemas de aplicação pelas vias usuais (oral, tópica ou parenteral), e ao potencial desta via para o transporte de fármacos da cavidade nasal diretamente ao SNC, contornando a BHE. Isto é especialmente de interesse, não só para tratamento de doenças crônicas neurodegenerativas do SNC, tais como doença de Parkinson e doença de Alzheimer, câncer, psicose, depressão, mas também para o tratamento mais rápido de enxaqueca e dores de cabeça (ROMEO *et al.*, 1998; ILLUM, 2012).

A cavidade nasal humana, representada na Figura 3, é dividida verticalmente, em quase toda a sua extensão, pelo septo nasal, sendo cada cavidade nasal dividida em três regiões: o vestíbulo nasal, a região respiratória e a região olfatória (ILLUM, 2000). O vestíbulo nasal corresponde à porção anterior e é constituída por uma área de 0,6 cm^2, epitélio escamoso e rico em pelos, com a finalidade de filtração do ar durante a inalação. A região respiratória é a maior área superficial com cerca de 130 cm^2, maior grau de vascularização e é a principal região responsável pela absorção sistêmica através da mucosa nasal. A região respiratória inclui três estruturas: o corneto superior, médio e inferior. Essas estruturas são revestidas com epitélio respiratório, composto por células colunares ciliadas e não ciliadas, células basais e células globulares, responsáveis pela produção de muco (células de globet). A mucosa respiratória também é rica em células dendríticas importantes para a resposta imune local. Por fim, a região olfatória, com uma área de aproximadamente 10 cm^2, localiza-se na porção superior medial, logo abaixo da placa cribriforme do osso etmóide que

separa as duas cavidades nasais do cérebro. A camada epitelial olfativa contém predominantemente três tipos de células: células neurais olfativas, células de sustentação e células basais. As células basais são as células progenitoras que também proporcionam suporte mecânico aderindo às outras células. As células neurais olfativas ou os axônios são desmielinizados e intercalam-se entre as células de suporte. Eles se originam no bulbo olfatório no SNC e terminam na superfície apical do epitélio olfatório. Abaixo das camadas epiteliais olfatórias, encontra-se a lâmina própria, que contém vasos sanguíneos, glândulas secretoras de muco (glândulas de Bowman) e um suprimento neuronal constituído por feixes de axônios olfativos, fibras nervosas autonômicas e o ramo maxilar do nervo trigêmeo. Estes nervos são responsáveis pelo transporte de fármacos da cavidade nasal para o SNC ao longo da via neural. A vascularização sanguínea é essencialmente arterial a partir das ramificações da carótida, evitando, assim, o metabolismo de primeira passagem (ROMEO *et al.*, 1998; ILLUM, 2000; VYAS *et al.*, 2005; MISRA e KHER, 2012). O "neuroepitelio" olfativo é a única parte do SNC que está em contato direto com o ambiente externo (PARDESHI e BELGAMWAR, 2013).

Tanto o epitélio olfatório quanto o respiratório na cavidade nasal são fortemente ligados por junções intercelulares que circundam as células epiteliais. O diâmetro das *tight junction*, das células epiteliais nasais possuem entre 3,9 e 8,4 Å e, mesmo com o uso de promotores de absorção, o diâmetro máximo alcançado quando aberto é de 15 nm (COSTANTINO *et al.*, 2007). Assim, obviamente, mesmo que uma *tight junction* esteja aberta, não será permitida a passagem paracelular de nanopartículas, geralmente utilizadas na administração nasal, com diâmetro entre 50 e 500 nm (CASETTARI e ILLUM, 2014).

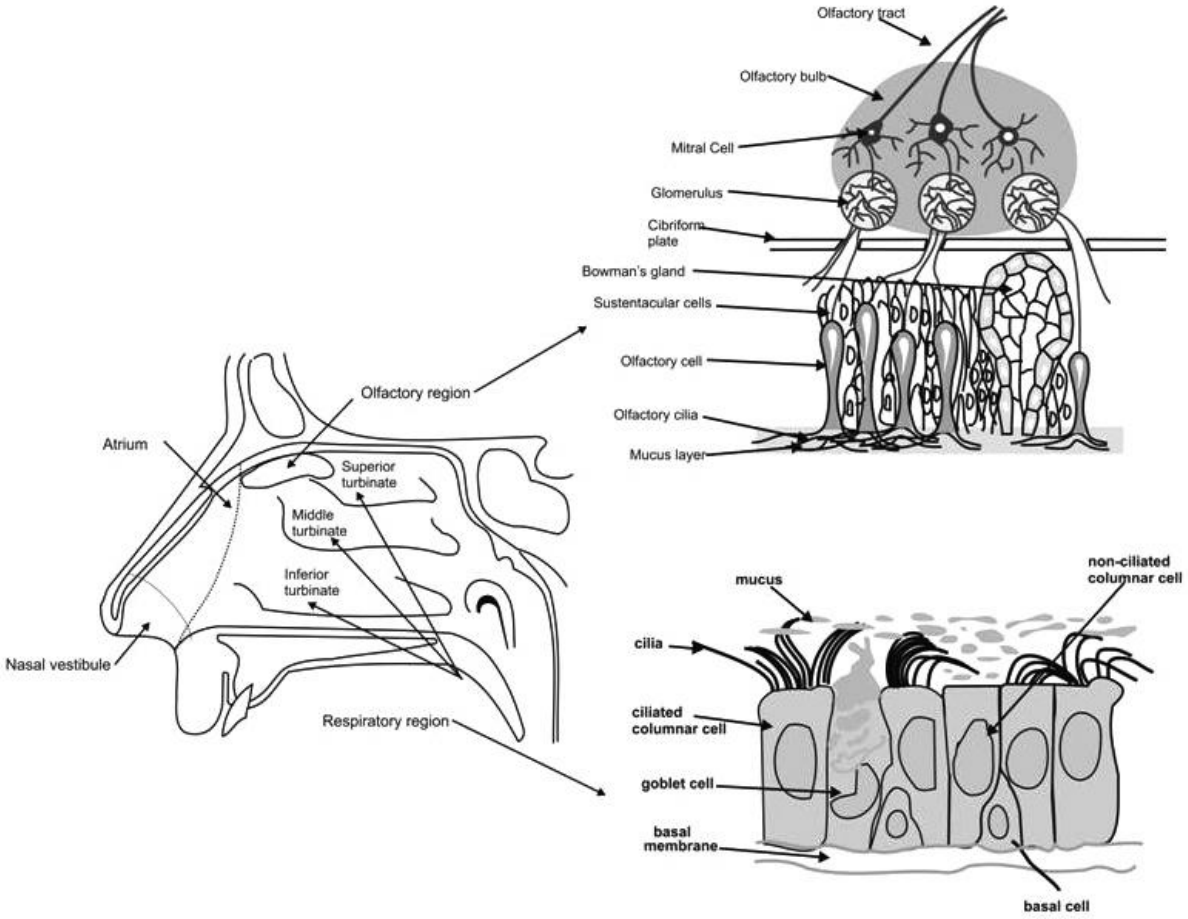

Figura 3. Anatomia da cavidade nasal (MISRA e KHER, 2012).

Assim, a via de administração nasal vem se mostrando uma importante alternativa às demais vias de administração por diversas razões: via não invasiva; entrega direta do fármaco ao cérebro de agentes terapêuticos com baixa ou nenhuma absorção cerebral após administração sistêmica, evitando a limitação imposta pela BHE; evita o metabolismo de primeira passagem, que poderia diminuir a porção de fármaco ativo; possibilidade da utilização de baixas doses com a diminuição dos possíveis efeitos adversos; possibilidade de autoadministração. O fármaco consegue alcançar o cérebro diretamente através da região olfatória e/ou ramificações do nervo trigêmeo, ou indiretamente, onde a porção de fármaco absorvido que atingir a circulação sistêmica pode alcançar a região cerebral se conseguir transpor à BHE (Figura 4) (ALAM *et al.*, 2010; KOZLOVSKAYA *et al.*, 2014; COMFORT *et al.*, 2015).

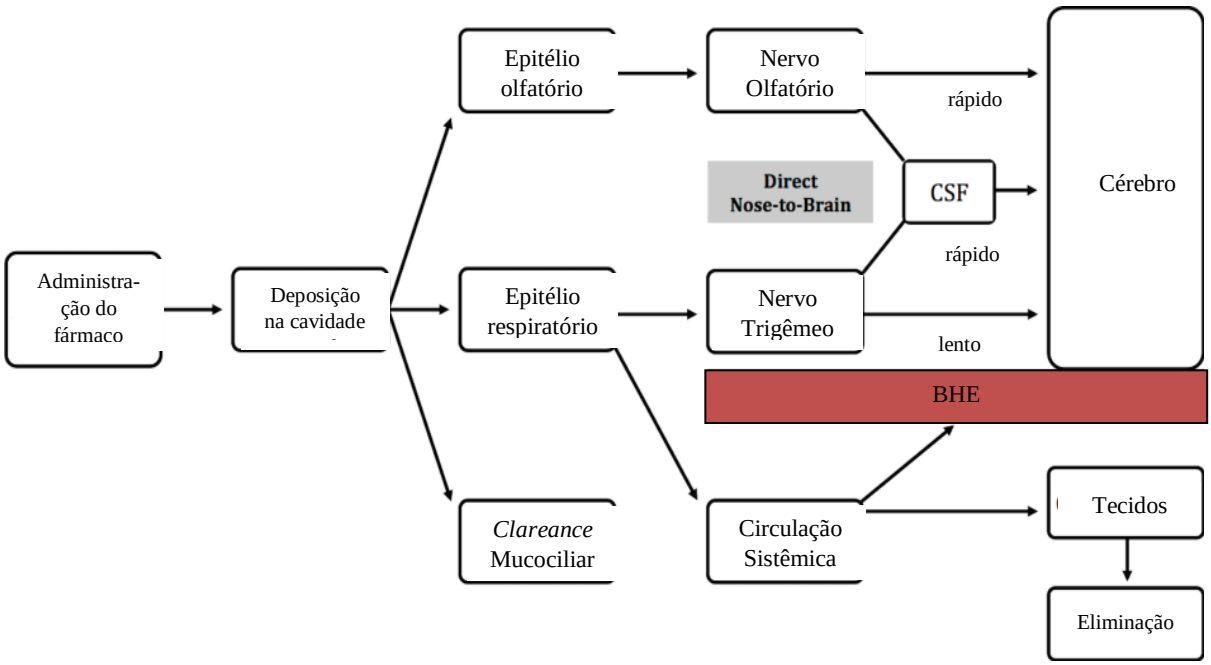

Figura 4. Vias de direcionamento cerebral após administração nasal. CSF: fuido cérebro espinhal. Adaptado de (COMFORT *et al.*, 2015).

Apesar das vantagens já apresentadas da via nasal, há algumas barreiras que limitam a absorção de fármacos, como o *clearance* mucociliar, que pode remover o ativo da cavidade nasal. O muco é uma secreção com papel de lubrificação e proteção, constituída por aproximadamente 95% de água, 2% de mucina, 1% de sais, 1% de outras proteínas, tais como albumina, imunoglobulinas, lisozimas e lactoferrina, e menos de 1% de lipídios. O pH das secreções mucosas varia de 5,5 a 6,5 em adultos e 5,0 e 6,7 em crianças. Em geral, a camada de muco da cavidade nasal é continuamente propelida com taxa de fluxo na faixa de 5 a 6 mm/min, sendo totalmente renovada a cada 15 – 20 min (ILLUM, 2003; MISRA e KHER, 2012; CASETTARI e ILLUM, 2014).

Também existe a possibilidade de degradação enzimática do fármaco pelas enzimas presentes na cavidade nasal, como isoformas da enzima citocromo P450 (CYP1A, CYP2A e CYP2E), carboxilesterases e glutationas S-transferases. Tal ocorrência é descrita como sendo um pseudo efeito de primeira passagem (MISRA e KHER, 2012).

Ainda, a transposição de dados experimentais de animais para seres humanos deve ser tratada com cautela, visto que há grandes diferenças anatômicas entre eles. Os roedores são respiradores nasais obrigatórios, enquanto os primatas são respiradores oronasais. A cavidade nasal em ratos é mais complexa do que em seres humanos e possui maior relação superfície-volume. Cavidades nasais em camundongos, ratos e humanos apresentam um volume de 0,032, 0,26 e 25 cm^3, respectivamente (VAN WOENSEL *et al.*, 2013). Kozlovskaya e colaboradores realizaram uma revisão com publicações entre 1970–2014, que abordavam o tema de liberação cerebral através da administração intranasal, e verificaram que a maioria dos estudos foram realizados em ratos (78,4%) ou camundongos (16,2%), seguido por coelhos (4,1%) e humanos (1,4%) (KOZLOVSKAYA *et al.*, 2014).

Pelas limitações apresentadas, para aumentar a eficácia e o potencial de transporte de fármacos aplicados na cavidade nasal ao cérebro, o desenvolvimento de formulações, como nanoemulsões, torna-se interessante, visto que elas podem aumentar a estabilidade do composto ativo frente à possível degradação e até mesmo oferecer maior especificidade ao tecido alvo.

ADMINISTRAÇÃO INTRANASAL DE NANOEMULSÕES

Diversas estratégias vêm sendo estudadas para reduzir as limitações impostas pela mucosa nasal e fundamentam-se em aumentar o tempo de permanência do fármaco na cavidade nasal, aumentar sua absorção ou modificar sua estrutura para produzir propriedades físico-químicas mais favoráveis para a absorção nasal. As principais técnicas incluem inibição enzimática nasal, utilização de promotores de permeação, utilização de pró-fármacos e sistemas de liberação, como micropartículas, nanopartículas e nanoemulsões (ALAGUSUNDARAM *et al.*, 2010).

Nas últimas décadas, a utilização de nanocarreadores oportunizou a incorporação de diversos agentes terapêuticos com limitações biofarmacêuticas, como baixa solubilidade ou alta degradabilidade, e também possibilitou a permeação através de barreiras biológicas, mostrando, assim, a potencialidade do emprego da

nanotecnologia para a liberação de fármacos ao cérebro (MODI *et al.*, 2010; KOZLOVSKAYA e STEPENSKY, 2013).

A absorção de fármacos pela mucosa nasal incorporados a nanossistemas pode ser decorrente da permeação do fármaco pela camada de células que compõem a cavidade nasal, bem como pela entrada das próprias nanopartículas. O tipo de revestimento da nanoestrutura também pode influenciar na absorção, o uso de quitosana, por exemplo, devido a sua capacidade de abrir as junções oclusivas, favorece a permeação dos ativos, bem como aumenta o tempo de permanência na cavidade nasal, devido às propriedades mucoadesivas (CASETTARI e ILLUM, 2014).

Nesse sentido, as nanoemulsões tem se destacado, pois tem o potencial de aumentar a absorção de fármacos, aumentar a estabilidade da formulação e o tempo de retenção na cavidade nasal (SOOD *et al.*, 2014).

Nanoemulsões são sistemas heterogêneos compostos por gotículas de óleo de tamanho submicrométrico dispersas em um meio aquoso estabilizadas por tensoativos (Figura 5). O diâmetro de gotícula geralmente encontra-se entre 50 e 500 nm. Substâncias de reduzida hidrossolubilidade encontram-se dissolvidas no interior do núcleo oleoso e/ou adsorvidas na interface óleo/água das nanoemulsões. Possuem maior capacidade de solubilização do que dispersões micelares simples e maior estabilidade cinética do que as emulsões grosseiras (COMFORT *et al.*, 2015; SINGH *et al.*, 2017).

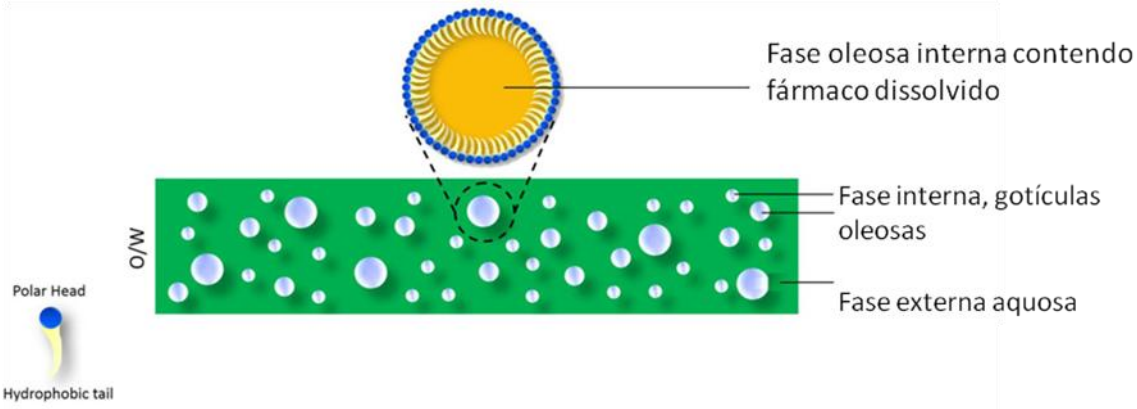

Figura 5. Estrutura de uma nanoemulsão. Adaptado de (SINGH *et al.*, 2017).

Alguns aspectos físico-químicos das nanoemulsões são essenciais para a sua estabilidade superior quando comparados com emulsões grosseiras. O tamanho das gotículas da fase dispersa permite que os movimentos brownianos e a taxa de difusão superem o efeito da força gravitacional que atua sobre o sistema, conduzindo a uma redução significativa de fenômenos tais como cremação, sedimentação e floculação durante o armazenamento. As propriedades do sistema também impedem a separação de fases por coalescência, uma vez que as gotículas não são facilmente deformáveis e a espessura significativa do tensoativo na superfície das gotas impede a instabilidade ou a ruptura do filme superficial que as separa. Embora as nanoemulsões tenham alta estabilidade, estão sujeitas a um aumento do tamanho das gotículas ao longo do tempo e, eventualmente, à sua ruptura, através do processo de maturação de Ostwald (TADROS *et al.*, 2004; SOLANS *et al.*, 2005; SINGH *et al.*, 2017).

Nanoemulsões são sistemas de "não-equilíbrio" e, portanto, não podem ser formadas espontaneamente. Dois métodos principais são descritos para sua produção: os métodos de baixa energia e os de alta energia. Métodos de baixa energia utilizam as propriedades físico-químicas intrínsecas aos componentes, como auto-emulsificação (emulsificação espontânea), inversão de fase e temperatura de inversão de fase. Já os métodos por alta energia requerem equipamentos específicos para gerar intensas forças desruptivas, capazes de dispersar a fase oleosa e formar gotículas de tamanho nanométrico, como ultrassons, microfluidizadores e homogeneizadores de alta pressão, que são industrialmente escalonáveis (TADROS *et al.*, 2004; SOLANS *et al.*, 2005; SINGH *et al.*, 2017).

Portanto, é importante otimizar as condições de emulsificação e homogeneização necessárias para a obtenção de nanoemulsões com estabilidade física. A seleção adequada dos componentes e do método de preparação é uma etapa crítica para o desenvolvimento de uma formulação estável e eficiente, devendo-se levar em consideração a via de utilização, solubilidade do fármaco, toxicidade e estabilidade.

Ainda, as nanoemulsões têm recebido crescente atenção para novas aplicações,como sistemas de administração para a liberação controlada de fármacos, administração dirigida de agentes antitumorais e vacinação através da mucosa (LOVELYN e ATTAMA, 2011). Elas podem ser utilizadas para administrar fármacos

hidrofílicos e lipofílicos, e são geralmente formulações não tóxicas e não irritantes. De fato, as nanoemulsões são geralmente fabricadas com baixas concentrações de tensoativos que são reconhecidos como seguro (*Generally Recognized As Safe*, GRAS) para consumo humano pelo FDA (*Food and Drug Administration*), tornando-os seguros para a administração enteral e através das mucosas (COMFORT *et al.*, 2015).

Além disso, as nanoemulsões apresentam grande área superficial e elevada energia livre, assegurando maior e mais rápida permeação de fármacos através das barreiras de absorção (epitélio intestinal, pele e superfícies mucosas). Consequentemente, há aumento da biodisponibilidade, não somente para fármacos pouco solúveis em água, mas também de peptídeos e proteínas. Outra vantagem das nanoemulsões é a proteção contra a hidrólise e a oxidação proporcionada pela encapsulação do fármaco nas gotículas dispersas (LU *et al.*, 2012; COMFORT *et al.*, 2015).

Diversos estudos descrevem a utilização de nanoemulsões para uso intranasal com objetivo de tratamento em desordens cerebrais, como nanoemulsões contendo risperidona, onde obteve-se um maior transporte e maior alcance do fármaco ao cérebro pela via de administração intranasal em ratos quando comparada a via intravenosa (KUMAR, MISRA, BABBAR, *et al.*, 2008). Resultados promissores também foram observados em estudos com tramadol (LALANI *et al.*, 2014), nitrendipino (JAIN e PATRAVALE, 2009), curcumina (SOOD *et al.*, 2014), sumatriptano (VYAS *et al.*, 2006), olanzapina (KUMAR, MISRA, MISHRA, *et al.*, 2008), saquinavir (MAHAJAN *et al.*, 2014), amilorida (JAIN *et al.*, 2011), tacrina (JOGANI *et al.*, 2008), zaleplon (HOSNY e BANJAR, 2013) e zidrasidona (BAHADUR e PATHAK, 2012). Notadamente, na maioria destes estudos, utilizou-se algum agente mucoadesivo, como a quitosana, e verificou-se que estes eram mais eficazes que as nanoemulsões simples para a liberação no SNC.

Apesar das vantagens da via nasal, há algumas barreiras que limitam a absorção de fármacos, como o mecanismo de depuração mucociliar que pode remover imediatamente a formulação da cavidade nasal, além da baixa permeabilidade do seu epitélio que dificulta a absorção de fármacos polares ou de alto peso molecular

(ILLUM, 2003; MAINARDES et al., 2006). Uma estratégia para vencer estas barreiras é o emprego de sistemas mucoadesivos.

Quitosana é um polissacarídeo derivado da desacetilação da quitina, originária em sua maioria de conchas de crustáceos. Compreende unidades ordenadas aleatoriamente de 2-acetamida-2-desoxi-p-D-glucopiranose (GlcNAc) e 2-amino-2-desoxi-p-D-glicopiranose (GlcN) (Figura 6) (CASETTARI e ILLUM, 2014).

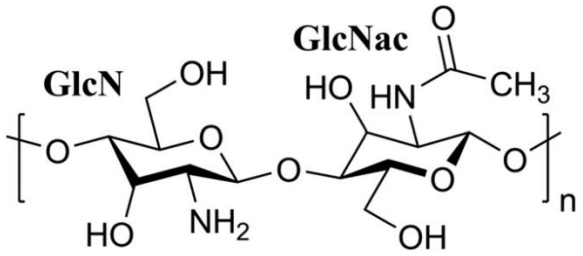

Figura 6. Estrutura química da quitosana (CASETTARI e ILLUM, 2014).

Esta substância contém aminas primárias, as quais se encontram positivamente carregadas na maioria dos fluidos fisiológico, sendo um dos polímeros mais estudados no campo da administração de fármaco através das mucosas (BERNKOP-SCHNURCH e DUNNHAUPT, 2012).

Quitosana é biocompatível, biodegradável (reconhecida como uma substância segura, GRAS) e apresenta propriedades mucoadesivas. Na administração intranasal, a utilização de quitosana na formulação aumenta o tempo de permanência na cavidade nasal. Além disso, tem a propriedade de abrir transientemente as *tight junctions* do epitélio, aumentando assim a permeabilidade de fármacos pela mucosa. (VAN WOENSEL *et al.*, 2013; CASETTARI e ILLUM, 2014). No pH fisiológico, a quitosana é capaz de interagir eletrostaticamente através dos seus grupos amino positivamente carregados, com ácido siálico e ésteres sulfatados, que apresentam carga negativa, presentes na camada de muco da mucosa nasal (KHUTORYANSKIY, 2011).

Sood e colaboradores (2014) relataram a utilização de quitosana em nanoemulsões contendo curcumina para administração intranasal. As formulações

desenvolvidas não apresentaram toxicidade e a adição de quitosana à nanoemulsão acarretou maior fluxo e permeação através da mucosa nasal (SOOD *et al.*, 2014).

Kumar e colabodores (2008) demonstraram que os níveis de risperidona no cérebro de ratos foram significativamente maiores em todos os tempos de análise após administração intranasal de nanoemulsão contendo quitosana, em comparação a nanoemulsão sem agente mucoadesivo (KUMAR, MISRA, BABBAR, *et al.*, 2008). Resultados similares também foram encontrados pelo mesmo grupo de pesquisa com nanoemulsões contendo olanzapina (KUMAR, MISRA, MISHRA, *et al.*, 2008).

GLIOMAS

Os gliomas são os tumores primários mais comuns e devastadores do sistema nervoso central (SNC) em adultos, correspondendo a cerca de 80% de todos os tumores desse sistema (SATHORNSUMETEE *et al.*, 2007). Gliomas foram descritos pela primeira vez por Virchou (1863-1865) como um enorme tumor cerebral, normalmente com lenta evolução clínica e sem limitação em relação ao tecido não tumoral (SCHERER, 1940). Sua incidência é maior em homens caucasianos com idade superior a 40 anos (PREUSSER *et al.*, 2006; OSTROM *et al.*, 2014). Em estudo analisado entre 2005 e 2009 nos Estados Unidos, os gliomas apresentaram incidência anual de 5,26 para cada 100.000 habitantes (DOLECEK *et al.*, 2012).

Historicamente, os gliomas foram classificados pela semelhança morfológica em relação às células gliais, sugerindo que astrocitomas, por exemplo, tenham se originado de astrócitos ou de precursores astrocíticos. Nesse sentido, a Organização Mundial da Saúde (OMS) classificou os gliomas em astrocitomas (grau I a IV), oligodendrogliomas (grau II e III), e oligoastrocitomas (grau II e III), sendo os gliomas de origem astrocítica classificados em quatro graus de malignidade (LOUIS *et al.*, 2007):

- Grau I: astrocitoma pilocítico, acometem principalmente crianças entre 5 e 15 anos, apresentam baixa capacidade invasiva e são facilmente removidos por ressecção cirúrgica;

- Grau II: astrocitoma de baixo grau, crescem de forma lenta, podendo ou não invadir o tecido cerebral normal adjacente;
- Grau III: astrocitoma anaplásico, são tumores recorrentes de neoplasias de baixo grau, apresentando uma taxa de crescimento maior e capacidade de invasão do tecido cerebral normal adjacente. Apresentam alta probabilidade de recorrência após o tratamento;
- Grau IV: glioblastoma multiforme (GBM), forma mais agressiva dos gliomas, alto grau de malignidade e alta capacidade de invasão.

O padrão atual de tratamento para pacientes com diagnóstico de GBM é tratamento com corticosteroides, ressecção cirúrgica seguida de radioterapia e quimioterapia com o agente alquilante temozolomida (Temodal®). O prognóstico é péssimo, pois mesmo com o tratamento preconizado, a sobrevida do paciente é de 14,6 meses desde o diagnóstico (ROBINS *et al.*, 2009; VAN WOENSEL *et al.*, 2013). Estas estatísticas fazem com que os gliomas estejam entre as formas mais mortais de câncer. A baixa sobrevida dos pacientes com esse tipo de tumor, altamente invasivo, está relacionada, principalmente a alta taxa de recorrência, ainda inevitável quando emprega-se terapias convencionais (LOUIS *et al.*, 2007). Apesar de pesquisa intensiva e uma variedade de quimioterapias, radioterapias e abordagens cirúrgicas, o prognóstico para os pacientes com estes tumores não mudou significativamente nas últimas décadas.

A falha na terapia quimioterápica se deve principalmente à natureza infiltrante, heterogeneidade celular e molecular, ausência de especificidade terapêutica de fármacos citotóxicos, quimiorresistência intrínseca e à barreira hematoencefálica (BHE), que limita a entrada dos quimioterápicos no SNC (VAN MEIR *et al.*, 2010; LIU *et al.*, 2014). A BHE é normalmente apenas permeável a moléculas lipofílicas, com um peso molecular (Mw) inferior a 600 Dalton (Da) e o LogP, estimado em 1,5-2,7 para um transporte eficiente sobre a BHE (ILLUM, 2000; PAJOUHESH e LENZ, 2005).

Além da limitação imposta pela BHE, mecanismos de resistência a multidrogas estão presentes como, por exemplo, a glicoproteína-P, que reduz a passagem de

fármacos pelas células endoteliais que compõem a BHE, diminuindo também o acúmulo de fármacos nas células tumorais pelo efluxo para o meio extracelular, limitando assim a eficácia terapêutica (SZAKACS *et al.*, 2006).

Tendo em vista o péssimo prognóstico para os pacientes com glioblastoma e os poucos avanços significativos da terapêutica nas últimas décadas, faz-se necessário o desenvolvimento de novas estratégias terapêuticas. A administração de fármacos ao SNC através da via intranasal proporciona uma alternativa promissora aos métodos tradicionais e invasivos, permitindo que os fármacos contornem a BHE, proporcionando uma distribuição direta e rápida ao cérebro e redução dos efeitos secundários sistêmicos (DHURIA *et al.*, 2010).

Considerando as vantagens da administração intranasal para a entrega de fármacos ao cérebro, diversos estudos foram feitos com vistas ao tratamento de glioblastoma, utilizando substâncias como metotrexato (SHINGAKI *et al.*, 2010), temozolamida (LI *et al.*, 2014), curcumina (SHINDE e DEVARAJAN, 2017), inibidor da telomerase GRN163 (HASHIZUME *et al.*, 2008), parvovírus H-1 (KIPRIANOVA *et al.*, 2011), células tronco neurais (REITZ *et al.*, 2012), álcool perílico (DA FONSECA *et al.*, 2011), dentre outros.

Nesse contexto, o desenvolvimento de uma nanoemulsão contendo quitosana para uso intranasal visando à liberação de fármacos no SNC torna-se interessante. A veiculação inédita de KPF nesse sistema mostra-se promissora para o avanço do estado da arte no que se refere ao tratamento de glioblastoma multiforme.

ADMINISTRAÇÃO ORAL DE DISPERSÕES SÓLIDAS

A administração de fármacos por via oral é a via mais utilizada devido à facilidade de administração e alta adesão ao tratamento pelo paciente. Devido à maior estabilidade, menor volume, dosagem precisa e fácil produção, as formas farmacêuticas orais sólidas apresentam muitas vantagens em relação a outros tipos de formas de dosagem oral (VASCONCELOS *et al.*, 2007). Quando uma fármaco é administrado por via oral, ele deve atravessar certos pontos de controle, o que varia de fármaco para fármaco, dentro do sistema biológico, incluindo dissolução em fluidos gastrointestinais, permeação através da membrana do intestino, metabolismo de

primeira passagem, para então finalmente chegar ao seu local de ação via circulação sistêmica (CHARMAN e CHARMAN, 2002).

A baixa taxa de dissolução e solubilidade aquosa de moléculas farmacologicamente ativas é um de desafios no desenvolvimento farmacêutico e está se tornando mais comum entre os novos candidatos a fármacos nas últimas décadas devido ao uso de ferramentas de triagem de alto rendimento e combinação durante a descoberta e fase de seleção (LIPINSKI, 2000; LIPINSKI *et al.*, 2001).

De acordo com o Sistema de Classificação Biofarmacêutica um composto é pouco solúvel se a dosagem mais alta não for solúvel em 250 mL de meio aquoso nas faixas de pH 1-7,5 a 37ºC (FDA, 2000). Estes compostos pertencem principalmente à Classe II, que são pouco solúveis e altamente permeáveis de acordo com o pH do fluido gastrointestinal, e tendem a apresentar absorção limitada pela dissolução (KAWABATA *et al.*, 2011). Apesar de sua alta permeabilidade, esses fármacos frequentemente apresentam baixa biodisponibilidade oral devido a sua lenta e limitada liberação no líquido gastrintestinal (VO *et al.*, 2013).

Neste contexto, várias abordagens (físicas, químicas e farmacotécnicas) para superar a baixa solubilidade aquosa de fármacos ou de candidatos a fármacos são empregadas (VASCONCELOS *et al.*, 2016). Abordagens químicas compreendem modificação molecular na estrutura do fármaco, como a inclusão de grupos polares ou ionizáveis, resultando na formação de um pró-fármaco e que podem apresentar diferente potência e perfil farmacocinético (VASCONCELOS *et al.*, 2007; SEO *et al.*, 2015). Outros exemplos incluem a formação de sais e co-cristais, mas sua aplicação é muito restrita. Os sais são viáveis apenas para ácidos fracos ou bases, e co-cristais geralmente não aumentam suficientemente a solubilidade do fármaco *in vivo* (SARKAR e ROHANI, 2015). O princípio básico por trás de todas as abordagens físicas é aumentar a área de superfície de contato através da redução do tamanho das partículas, resultando em cristais de tamanho micro ou nanométricos. A viabilidade desta abordagem nem sempre é adequada, uma vez que a redução tamanho do partícula acontece em torno de 2-5 µm, o que frequentemente não é o suficiente para melhorar consideravelmente a solubilidade da fármaco. Além disso, apresenta limitações técnicas quanto ao controle granulométrico (VASCONCELOS *et al.*, 2007;

GOUTHAMI *et al.*, 2015). Por fim, estratégias farmacotécnicas consistem na produção de sistemas líquidos ou sólidos baseados em veículos lipídicos, poliméricos e/ou tensoativos (VASCONCELOS *et al.*, 2016). Neste contexto, diversas formulações são empregadas, como complexação com ciclodextrinas, nanoemulsões, nanopartículas lipídicas e dispersões sólidas (DS). Dentre essas, DS são consideradas uma das estratégias mais bem sucedidas para melhorar o perfil de dissolução de moléculas pouco solúveis (VO *et al.*, 2013).

O conceito de "dispersões sólidas" foi proposto pela primeira vez por Sekiguchie Obi, onde foi observado que misturas eutéticas melhoraram a taxa de liberação de fármacos pouco solúveis em água (SEKIGUCHI *et al.*, 1964). Desde então, diferentes técnicas e carreadores vem sendo estudados. Convencionalmente, DS são definidas como "dispersão de um ou mais insumo farmacêutico ativo (API) dispersos em uma matriz inerte". O princípio desta técnica consiste em dispersar o API hidrofóbico em um carreador hidrofílico, resultando no aumento da molhabilidade, diminuição do tamanho de partícula e/ou geração de forma amorfa do API com alta solubilidade aquosa aparente. Carreadores usados em dispersões sólidas normalmente são farmacologicamente inertes e podem interagir com o API por ligações físicas fracas, como ligações de hidrogênio, forças de Van der Waals e interações eletrostáticas para formar um complexo mais solúvel e, portanto, melhorar a solubilidade aquosa e, desse modo, a dissolução e biodisponibilidade oral do API (MENG *et al.*, 2015).

Dispersões sólidas foram pela primeira vez classificadas por Chiou e Riegelman que classificaram-nas em seis grupos: misturas eutéticas simples, soluções sólidas, soluções vítreas, suspensões vítreas, precipitações amorfas em carreador cristalino, formação de complexa e combinações dos cinco tipos anteriores (CHIOU e RIEGELMAN, 1971). Vasconcelos et al. (2007) classificaram-nas em três gerações (VASCONCELOS *et al.*, 2007), e, posteriormente, Vo et al. (2013), acrescentaram a esta classificação, dispersões sólidas de liberação controlada, sendo a quarta geração (VO *et al.*, 2013). A figura 7 ilustra a classificação das dispersões sólidas nas quatro gerações.

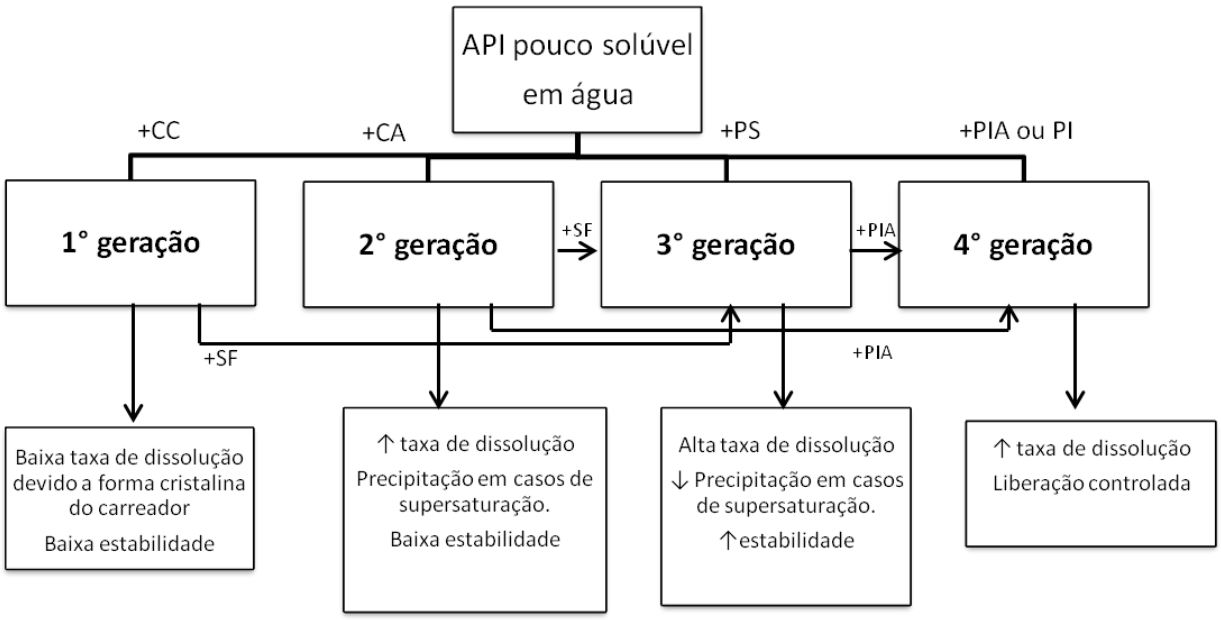

Figura 7. Composição e propriedades das quatro gerações de dispersões sólidas. CC: carreador cristalino; CA: carreador amorfo; PS: polímero surfactante; PIA: polímero insolúvel em água; PI: polímero intumescente; SF: surfactante. ↓: diminuição; ↑: aumento. Adaptado de VO *et al.* (2013).

A primeira geração é composta por dispersões sólidas cristalinas, onde o fármaco no estado cristalino é disperso em carreador também no estado cristalino, formando uma mistura eutética ou monotética. Em sistemas eutéticos, o fármaco e o carreador são completamente miscíveis no estado fundido e, após resfriamento, formam uma mistura com ponto de fusão inferior aquele do fármaco ou carreador. Já em sistemas monotéticos, o ponto de fusão do carreador e do fármaco são constantes (VO *et al.*, 2013). Os carreadores cristalinos incluem ureia e açúcares, como manitol, que foram os primeiros carreadores a serem empregados em dispersões sólidas. Eles têm a desvantagem de formar dispersões sólidas cristalinas, mais estáveis termodinamicamente, e assim, não liberaram o fármaco tão rapidamente quanto os carreadores amorfos (VASCONCELOS *et al.*, 2007; MISHRA *et al.*, 2015).

A segunda geração contem carreadores amorfos, geralmente polímeros, e formam dispersões sólidas amorfas. As dispersões sólidas amorfas podem ser classificadas em soluções sólidas amorfas (soluções vítreas) e suspensões sólidas amorfas de acordo com o estado físico do fármaco. Na solução sólida amorfa, o

fármaco e o carreador amorfo são completamente miscíveis para formar uma mistura molecularmente homogênea, enquanto que a suspensão sólida amorfa consiste em duas fases separadas. Suspensões sólidas amorfas são formadas quando o fármaco tem solubilidade limitada no carreador ou um ponto de fusão extremamente alto. Os principais polímeros utilizados nessa classe são polímeros totalmente sintéticos, como povidona (PVP), polietilenoglicóis (PEG) e polimetacrilatos; polímeros naturais como os derivados de celulose, como hidroxipropilmetilcelulose (HPMC) e hidroxipropilcelulose (HPC) (VO *et al.*, 2013; MISHRA *et al.*, 2015). Na DS de segunda geração, o fármaco está finamente disperso (a nível molecular, estado amorfo ou em pequenos cristais), e está no estado supersaturado devido à solubilização forçada no carreador, aumentando, assim, a molhabilidade e dispersibilidade do fármaco. Estas propriedades, juntamente com a taxa de dissolução rápida do carreador (baixa estabilidade termodinâmica), aumentam a solubilidade e a taxa de liberação do fármaco (VO *et al.*, 2013).

A dispersões sólidas de terceira geração são compostas por uma combinação de carreadores amorfos e, preferencialmente, por uma combinação de carreadores amorfos e tensoativos. A introdução de tensoativos ou emulsionantes em dispersões sólidas melhora não apenas o perfil de dissolução, mas também a estabilidade física e química do fármaco. Os tensoativos com estrutura anfifílica podem aumentar a miscibilidade dos fármacos e carreadores e, assim, reduzir a taxa de recristalização do fármaco. Além disso, são capazes de melhorar a molhabilidade dos fármacos e prevenir a precipitação do fármaco devido à supersaturação, absorvendo a camada externa das partículas do fármaco ou formando micelas para encapsular os fármacos. Os carreadores mais utilizados incluem poloxamer, gelucire 44/14, compritol 888 ATO e Soluplus®. Tensoativos, como o lauril sulfato de sódio (SLS), Tween 80 são utilizados como aditivos em dispersões sólidas (VO *et al.*, 2013; MISHRA *et al.*, 2015).

Por fim, a dispersão sólida de quarta geração é uma dispersão sólida de liberação controlada contendo fármacos pouco solúveis em água com uma meia-vida curta. Este tipo de dispersão possui dois alvos, aumento da solubilidade e liberação prolongada de maneira controlada, a qual é oferecida pelo emprego de polímeros

insolúveis ou que dissolvem lentamente em água ou polímeros intumecíveis, como Eudragit® (RS, RL), óxido de polietileno (PEO) e polímero carboxivinílico (Carbopol) (VO *et al.*, 2013).

As duas principais técnicas empregadas para preparar dispersões sólidas atualmente são os métodos de fusão e de evaporação do solvente. No método de fusão, o fármaco e o carreador são fundidos em um temperatura acima do ponto de fusão e, em seguida, resfriado. Um pré-requisito importante para este método é que o fármaco e o carreador devem ser miscíveis e termoestáveis (LEUNER, C. e DRESSMAN, J., 2000). Tachibana e Nakumura (1965) foram os primeiros a dissolver o fármaco e o carreador num solvente comum e depois evaporar o solvente para produzir uma dispersão sólida (TACHIBANA e NAKAMURA, 1965). O principal pré-requisito é que tanto o carreador quanto o fármaco devem ser solúveis no solvente empregado. Nesse método, a decomposição de fármacos termolábeis pode ser evitada, pois a evaporação do solvente orgânico ocorre em baixas temperaturas. Contudo, possui a desvantagem de empregar solventes orgânicos (VASCONCELOS *et al.*, 2016).

Apesar do alto interesse na pesquisa, o número de dispersões sólidas comercializadas ainda é baixo. Este baixo número deve-se principalmente ao escalonamento para escala industrial, problemas e instabilidade físico-química durante a produção e armazenamento, como separação de fases e recristalização (VO *et al.*, 2013). Na tabela 1 estão apresentados alguns exemplos de dispersões sólidas disponíveis no mercado atualmente.

Tabela 1. Exemplos de dispersões sólidas disponíveis comercialmente.

Nome	Fármaco	Carreador	Ano de aprovação
Cesamet®	Nabilone	PVP	1985 (FDA)
Sporanox®	Itraconazol	HPMC	1992 (FDA)
Prograf®	Tacrolimus	HPMC	1994 (FDA/MHRA)
Gris-PEG®	Griseofulvina	PEG	2000 (FDA)
Crestor®	Rosuvastatina	HPMC	2004 (EMA) 2002 (FDA)
Cymbalta®	Duloxetine	HPMCAS	2004 (EMA/FDA)
Kaletra®	Lopinavir/ Ritonavir	PVP-VA	2005 (FDA) 2001(EMA)
Fenoglide®	Fenofibrato	PEG/Polaxamer188	2010 (FDA)
Novir®	Ritonavir	PVP-VA	2010 (FDA) 2009 (EMA)
Zelboraf®	Vemurafenib	HPMCAS	2012 (EMA) 2011 (FDA)
Viekira® (EUA)/ Viekirax® (UE)	Ombitasvir/ Paritaprevir/ Ritonavir	PVP-VA/TPGS	2014 (EMA/FDA)
Orkambi®	Lumacaftor/Ivacaftor	HPMCAS/SLS	2015 (EMA/FDA)

HPMC: hidroxipropilmetilcelulose; HPMCAS: succinato do acetato de hidroxipropilmetilcelulose; PEG: polietilenoglicol; PVP: polivinilpirrolidona; PVP-VA: polivinilpirrolidona vinil acetato; SLS: Lauril sulfato de sódio; TPGS: succinato de d- alfa tocoferol polietilenoglicol 1000 EUA: Estados Unidos; UE: União Europeia; EMA: European Medicines Agency; FDA: Food and Drug Administration; MHRA: Medicines and Health Products Regulatory Agency.

Fonte: VASCONCELOS et al (2016).

A utilização de formulações a base de dispersões sólidas de flavonoides vem sendo empregada a fim de aumentar a solubilidade, dissolução e/ou biodisponibilidade

destas moléculas. Khan et. al (2015) desenvolveram dispersões sólidas contendo naringenina e Soluplus® e demonstraram aumento significativo da solubilidade do flavonoide, bem como melhora no perfil de dissolução e aumento significativo da ASC (área sob a curva) em estudos farmacocinéticos em comparação a naringenina livre (KHAN *et al.*, 2015). Kakran. e Sahoo (2011) realizaram a comparação de diferentes estratégias (complexação com ciclodextrinas, nanopartículas e dispersões sólidas) para melhorar a dissolução da quercetina e verificaram que na menor concentração de carreadores, as dispersões sólidas apresentaram melhor dissolução do que as demais estratégias, entretanto em maior concentração, não houve diferença significativa no perfil de dissolução das três formulações (KAKRAN *et al.*, 2011). Kanaze et al. (2006) desenvolveram dispersões sólidas de polivinilpirrolidona (PVP) e polietilenoglicol (PEG) com os glicosídeos naringina e hesperidina, e suas agliconas, naringenina e hesperetina, pelo método de evaporação por solvente e a dissolução destes atingiu 100% após 2 h usando PVP como carreador, enquanto no caso do PEG, o valor foi um pouco menor. Além disso, verificaram através de espectros de FTIR, presença de ligações de hidrogênio entre grupos carbonila do PVP com grupos hidroxila de ambas agliconas, as quais impedem a cristalização, já com o emprego do PEG, tanto glicosídeos quanto agliconas permaneceram principalmente na forma cristalina (KANAZE et al., 2006).

Uma revisão completa sobre a utilização de dispersões contendo flavonoides encontra-se no capítulo II, artigo I, da presente tese.

Uma vez que o preparo de dispersões sólidas tem contribuído para gerar resultados promissores na biodisponibilidade de muitos flavonoides, torna-se interessante o desenvolvimento de dispersões sólidas contendo kaempferol, tendo-se em vista sua baixa hidrossolubilidade e baixa biodisponibilidade oral.

CAPÍTULO I

Desenvolvimento de nanoemulsões contendo kaempferol para administração intranasal e avaliação da atividade citotóxica em glioma

INDRODUÇÃO

Visando ao tratamento de glioblastoma multiforme, no capítulo I da presente tese, nanoemulsões contendo kaempferol para administração intranasal foram desenvolvidas. Duas publicações são apresentadas.

A publicação I refere-se ao desenvolvimento e validação de uma metodologia analítica por cromatografia líquida de alta eficiência para a quantificação do kaempferol em diferentes matrizes (nanoemulsão, mucosa nasal suína e fluido receptor para experimentos de permeação/retenção, e cérebros de ratos para o estudo de biodistribuição cerebral).

Na publicação II, foram desenvolvidas duas nanoemulsões, uma sem agente mucoadesivo (KPF-NE) e outra contendo quitosana (KPF-MNE). As formulações foram caracterizadas quanto ao teor, tamanho de gotícula, potencial zeta, índice de polidispersão, pH, viscosidade, capacidade antioxidante, mucoadesividade, permeação através da mucosa nasal suína e quantificação do KPF em cérebros de ratos após a administração intranasal. Além disso, estudos de viabilidade celular após o tratamento com as nanoemulsões desenvolvidas em linhagem de GBM (células C6) também foram realizados.

CAPÍTULO I - Publicação I

Artigo publicado no periódico *Journal of Pharmaceutical and Biomedical Analysis*

Colombo, M., de Lima Melchiades, G., Figueiró, F., Battastini, A. M. O., Teixeira, H. F., & Koester, L. S. (2017). *Validation of an HPLC-UV method for analysis of Kaempferol-loaded nanoemulsion and its application to in vitro and in vivo tests. Journal of pharmaceutical and biomedical analysis, 145, 831-837.* http://dx.doi.org/10.1016/j.jpba.2017.07.046

VALIDATION OF AN HPLC-UV METHOD FOR ANALYSIS OF KAEMPFEROL-LOADED NANOEMULSION AND ITS APPLICATION TO *IN VITRO* AND *IN VIVO* TESTS

Mariana Colombo[a], Gabriela de Lima Melchiades[a], Fabrício Figueiró[b,c], Ana Maria Oliveira Battastini[b,c], Helder Ferreira Teixeira[a], Letícia Scherer Koester[a*]

[a]Programa de Pós-Graduação em Ciências Farmacêuticas, Faculdade de Farmácia, Universidade Federal do Rio Grande do Sul (UFRGS), Av. Ipiranga, 2752, 90610-000, Porto Alegre, RS, Brazil.

[b]Programa de Pós-Graduação em Ciências Biológicas: Bioquímica, Instituto de Ciências Básicas da Saúde, UFRGS, Av. Ramiro Barcelos, 2600, Anexo, 90035-003, Porto Alegre, RS, Brazil.

[c]Departamento de Bioquímica, Instituto de Ciências Básicas da Saúde, UFRGS, Av. Ramiro Barcelos, 2600, Anexo, 90035-003, Porto Alegre, RS, Brazil.

*Corresponding author: Dr. Letícia S. Koester, Faculdade de Farmácia/UFRGS, Av. Ipiranga, 2752/607, Porto Alegre-RS, 90.610-000, Brazil. E-mail:leticia.koester@ufrgs.br

ABSTRACT

A simple and reliable HPLC-UV method for Kaempferol (KPF) determination in a Kaempferol-loaded nanoemulsion (KPF-NE), samples from mucosa permeation/retention studies, and murine brain was developed and validated according to international guidelines. The analyses were performed on a reversed-phase C18 column at 35°C and under UV detection at 368 nm. The mobile phase was composed of methanol:formic acid 0.1% (75:25, v/v) and was eluted at an isocratic flow rate of 1.0 mL/min. The method was selective and sensitive for KPF analysis in matrix extracts, linear in the range of 0.25-7.5 µg/mL. The method was also considered precise, accurate, and robust. The recovery rates of KPF from the porcine nasal mucosa and murine brain were higher than 85%. Low matrix effect was observed to determine KPF, including biological matrices. The applicability of the method was

confirmed in all different approaches, i.e., quantification of KPF in nanoemulsion, *in vitro* permeation/retention of KPF across porcine nasal mucosa, and *in vivo* quantification of KPF in brain samples after nasal administration in rats. Thus, the method is effective and reliable to determine KPF in different real samples. The proposed method, therefore, provides a useful quantification approach to routine processes, to the development of drug delivery systems, and to KPF quantification in different biological matrices. Furthermore, the method is applicable in bioavailability studies and the developed formulation (KPF-NE) is suitable for preclinical trials in different brain disorders.

Keywords: Kaempferol, High-performance liquid chromatography, Validation, Nanoemulsion, Permeation/retention assays, Brain delivery

1. Introduction

Flavonoids are biologically active molecules commonly found in the plant kingdom and in ordinary human diets [1]. These phytochemicals have beneficial effects on the central nervous system (CNS), protecting neurons against stress-induced damage, suppressing mediators in neuroinflammation, and improving cognitive function [2]. Kaempferol (KPF, (*3,5,7-trihydroxy-2-(4hydroxyphenyl)-4H-1-benzopyran-4-one*) is a flavonol found mostly in onion, cabbage, carrot, and black tea [3]. KPF has a wide range of pharmacological properties, such as anti-inflammatory, antioxidative, antibacterial, antiviral, antifungal, and anti-tumoral activities [3-5], especially in CNS disorders [6, 7]. However, the therapeutic efficacy of KPF is limited by its poor water solubility, low bioavailability after oral administration, and rapid metabolism into the forms of methyl, sulfate or glucuronide [5, 8]. In this context, nanotechnology has emerged as a promising approach to improve tissue bioavailability of drugs. Moreover, alternative routes of administration as, for example, intranasal delivery of nanosized drug carriers, have also emerged as a strategy to deliver different drugs/carriers into the CNS [9, 10]. The intranasal route is a potential non-invasive pathway for drug delivery directly to the brain, bypassing the blood–brain barrier (BBB), avoiding gastrointestinal and hepatic first-pass metabolism, and promoting the

direct absorption into blood circulation. However, intranasal delivery has some limitations, such as rapid mucociliary clearance and low nasal permeability of drugs [9, 11]. Nanoemulsions (NE), which are composed of nanosized oil droplets dispersed in an aqueous phase stabilized by appropriate surfactants, are a potential alternative approach to overcome these problems, due to their stability, small droplet size, larger surface area, and optimal solubilization properties, increasing absorption and bioavailability of many drugs for nose-to-brain delivery like clonazepam, curcumin, olanzapine, risperidone, and saquinavir [12]. Thus, nanoemulsions may have a great potential in the nose-to-brain delivery of KPF.

Routine analysis of drugs in pharmaceutical dosage forms and biological samples have to be carefully evaluated to ensure the correct interpretation of data. Therefore, a reliable and fully validated analytical method to analyze trustworthy results has been prioritized. Although some techniques for the quantification of KPF in different matrices have been reported, none of them evaluated KPF selectivity in the presence of possible interferents from the porcine nasal mucosa, used as biological membrane in *ex-vivo* permeation/retention experiments, and from murine brain tissue. Therefore, the aim of the present work was to describe the development, validation, and application of a novel analytical and bioanalytical HPLC-UV method to determine KPF in complex matrices, like KPF-loaded nanoemulsion, receptor media, and biological membrane for *in vitro* permeation/retention experiments and murine brain delivery.

2. Experimental

2.1. Materials

The KPF (purity > 98.0%) was purchased from ShaanXi HuiKe Botanical (Xi'an, China). Egg-lecithin (Lipoid E-80s) and medium chain triglycerides (MCT) were purchased from Lipoid GmbH (Ludwigshafen, Germany). Polysorbate 80 was supplied from Sigma Aldrich (Steinheim, Germany). Methanol HPLC grade and formic acid 96% were obtained from Tedia (Rio de Janeiro, Brazil). Ultrapure water was obtained from a Milli-Q apparatus (Millipore, Billerica, USA). Porcine heads were purchased from Ouro do Sul Ltda (Harmonia, Brazil). All other used reagents were of analytical grade.

2.2. Chromatographic conditions

The HPLC apparatus consisted of a Shimadzu LC-10A system (Kyoto, Japan) equipped with a model LC-20AT pump, a SPD-20AV UV-VIS variable wavelength detector, a DGU-20A5 degasser, a CBM-20A system controller and SIL-20A injection valve with a 100-µL loop. KPF was analyzed using a XTerra® RP18 column (250 mm x 4.6 mm, 5-µm particle size). The mobile phase was a 75:25 (v/v) mixture of methanol and 0.1% formic acid in water. The injection volume was 20 µL and the HPLC system was operated at an isocratic flow of 1.0 mL/min, with detection at 368 nm and temperature of 35°C.

2.3. Sample preparation

2.3.1. Standard and matrices solutions

A stock solution of KPF (20 µg/mL) was prepared in methanol. The stock solution was then diluted with methanol to give a series of working standards solutions.

Blank nanoemulsions were prepared without KPF incorporation, according to section 2.5, and an adequate aliquot was diluted in methanol. For the *in vitro* permeation/retention experiments, Phosphate Buffered Saline (PBS) pH 6.4 containing 2% of polysorbate 80 was used as receptor media and porcine nasal mucosa was used as biological membrane. Porcine heads were obtained from a local slaughter house and an incision along the nasal septum was performed. They were maintained at 4°C during transport. Cartilages and adhered tissues were properly removed using a scalpel. The mucosal membrane was carefully removed from the nasal turbinates and washed as soon as shipped to the lab [13]. For the extraction procedure, the mucosa was cut into small pieces, placed in test tubes with methanol, and sonicated in an ultrasonic bath for 90 min. For the analysis of KPF content in murine brain samples, brain tissues from male Wistar rats (220-260 g) were removed and washed using PBS. Brain homogenates were obtained by homogenization of the brain tissue with methanol and sonicated in ultrasonic bath for 30 min. The samples were centrifuged (10^4 rpm for 15 min) and the supernatants were collected.

Animal experiments were conducted with prior approval from Ethical Committee of the Universidade Federal do Rio Grande do Sul (Protocol # 31216) and performed according to the guidelines given in “Principles of Laboratory Animal Care”, National Institutes of Health (NIH).

All matrices solutions were filtered through a 0.45-µm membrane before analysis.

2.4. Method validation

The quantification method was validated according to International Conference on Harmonization (ICH), European Medicine Agency (EMA), and US Food and Drug Administration (FDA) industry guidelines with respect to selectivity, linearity, limit of detection (LOD), limit of quantitation (LOQ), carry-over, precision, accuracy, robustness, and matrix effect for the matrices evaluated: nanoemulsion, receptor media, porcine nasal mucosa, and murine brain [14-16].

2.4.1. System Suitability

Before validation tests, system suitability parameters were measured and compared with specifications and recommended limits [17]. The evaluated parameters were theoretical plates, tailing factor, and retention time.

2.4.2. Selectivity and forced degradation study

A standard KPF solution (5.0 µg/mL, n = 3 in triplicate) was evaluated in the absence and in the presence of each matrix. A forced degraded assay was conducted to check the potential matrix interference peaks and degradation products. Data were analyzed considering both peak area and retention time. Data were expressed as mean ± S.D. and analyzed for statistical significance by the one-way analysis of variance (ANOVA) followed by Tukey’s test (GraphPad Software, San Diego, USA).

For stressing conditions, hydrochloric acid, sodium hydroxide, and hydrogen peroxide were added to the KPF stock solution. Acidic, alkaline, and oxidative conditions were 1.0 M for 24 h, 0.05 M for 5 min, and 3% for 24 h, respectively. The effect of heat was evaluated submitting the KPF standard solution (5.0 µg/mL) in a securely closed container and placing it in an oven at 60°C for 24 h. To evaluate the effect of light, the

KPF standard solution was stored in 1-cm covered quartz cell, which was exposed to mirror chambers equipped with UVA (352 nm) for 120 min.

Alternatively, after each endpoint analysis, solutions were properly neutralized and all samples were compared with a freshly prepared KPF solution (5.0 µg/mL), and peak purity analysis was performed by using a photodiode array detector.

2.4.3. Linearity, limits of detection (LOD) and limits of quantitation (LOQ)

Five different calibration curves, constructed on three consecutive days, were prepared by spiking each matrix with standard KPF solution to final concentrations of 0.25, 0.5, 1.0, 2.5, 5.0, and 7.5 µg/mL. Peak area for each solution against the corresponding concentration was measured, and linearity was evaluated by linear regression analysis, which was calculated by least squares regression analysis and the ANOVA test (α = 0.05).

The limits of detection and quantitation were determined by the standard deviation of the response and the slope, using the calibration curve data as follows: LOD = 3.3 SD/S; LOQ = 10 SD/S, where SD is the standard deviation of y-intercepts and S is the average slope obtained from the different calibration curves prepared for each matrix. LLOQ (lower limit of quantitation) was defined as the lowest concentration of KPF that could be quantitatively determined with accuracy and precision [15].

2.4.4. Carry-over

Carry-over was assessed by injecting blank samples immediately after both replicates of the upper limit of quantification (ULOQ = 7.5 µg/mL). Mean carry-over in the blank samples was then calculated [16].

2.4.5. Precision and accuracy

Repeatability (intra-day precision) was evaluated for three levels of KPF (0.5, 1.0, and 5.0 µg/mL) in the presence of different matrices by using five replicates of each concentration, on the same day. Intermediate precision (inter-day precision) was evaluated on three different days using the same KPF concentrations. The results were expressed as percentage of relative standard deviation (RSD).

To evaluate accuracy, a recovery experiment was performed. KPF concentrations of 0.5, 1.0, and 5.0 µg/mL were added to the previously extracted matrices solutions in five replicates and analyzed. Accuracy was evaluated as the difference between the measured value and the theoretical value.

2.4.6. Extraction recovery

The recovery method consisted of spiking porcine nasal mucosa and whole murine brain before the extraction procedure with known amounts of KPF solution, leading to a theoretical concentration of 0.25, 0.5, 2.5, and 5.0 µg/mL.

After solvent evaporation, mucosas were cut in small pieces and brain tissues were homogenized with IKA® Ultra-Turrax T8 mixer (IKA Works Inc., Wilmington, USA). Methanol was added, and the mixture was maintained in an ultrasound bath for 90 and 30 min, respectively. The samples were centrifuged (10^4 rpm for 15 min) and the supernatant was filtered through a 0.45-µm membrane and analyzed. KPF recovery was determined according the equation: RE(%) = (AM/A)*100, where: RE is extraction recovery, AM is the mean value of the peak area responses (obtained from biological matrix samples spiked with KPF before extraction), and A is the mean value of the peak area responses obtained from samples in the absence of the matrix.

2.4.7. Stock solution and processed sample stability

KPF stock solution was stored at 4°C for 120 days and then analyzed. Samples of KPF spiked matrices (5.0 µg/mL) were processed and stored in the HPLC vials at room temperature (25°C) for up to 48 h, intending to overestimated the time spent during routine analysis. The stability of these solutions was determined in comparison with freshly prepared solutions.

2.4.8. Robustness

Robustness in each matrix was assessed using a four-factor Plackett – Burman design with three centre points (in triplicate) in the Minitab 17 statistical software. The factors evaluated were: A, flow rate; B, column compartment temperature; C, detection wavelength; D, methanol content in the mobile phase (Table 1).

Table 1. Factors and their levels evaluated by four-factor Plackett–Burman robustness test.

Factor	Level		
	Low (-1)	Middle (0)	High (+1)
(A) Flow rate (mL/min)	0.97	1.00	1.03
(B) Column compartment temperature (°C)	34	35	36
(C) Detection wavelength (nm)	367	368	369
(D) Methanol content in the mobile phase (%)	74.7	75.0	75.3

The experimental errors were determined by seven dummy factors, and the experiments were carried out in randomized order to minimize the effects of uncontrolled factors that may introduce a bias into the response. A sample 5.0 µg/mL solution was used to measure the effect of factors, and the responses evaluated were the percentages of KPF in the obtained matrices in relation to the standard solution.

2.4.9. Evaluation of matrix effects

The matrix effect was determined based on the comparison of the slopes obtained in standard curves of KPF in methanol and in each matrix, as described in item 2.4.3 [18]. The equation used to calculate the matrix effect was ME% = 100 x [1-(Sm/Ss)], where Sm = slope of the calibration curves of KPF in methanol and Ss = slopes of the calibration curves of KPF in each matrix.

2.5. Nanoemulsion preparation and characterization

The Kaempferol-load nanoemulsion (KPF-NE) was prepared using the high-pressure homogenization technique. Oil and aqueous phases were separately prepared. The oil phase was prepared by dispersing KPF (0.1%, w/w) in 14.0 % (w/w) MCT and 5.0 % (w/w) egg-lecithin. The aqueous phase contained 1.0% (w/w) polysorbate 80 and

water. First, a coarse emulsion was prepared homogenizing both phases using an IKA® Ultra-Turrax T8 mixer (IKA Works Inc., Wilmington, USA) at 9500 rpm for 1 min. Second, the coarse emulsion was subjected to high-pressure homogenization (EmulsiFlex-C3, Avestin, Ottawa, Canada) at 750 bars to produce the final nanoemulsion. A blank nanoemulsion was prepared without KPF incorporation.

Mean particle size and size distribution (polydispersity index, PDI) were measured by photon correlation spectroscopy, and zeta potential was determined through electrophoretic mobility using a Malvern Zetasizer® Nano-ZS 90 at 25°C. To determine KPF content, an aliquot of KPF-NE was diluted in methanol to obtain a theoretical concentration of 5.0 µg/mL, then filtered and analyzed by HPLC as aforementioned. All analyses were carried out in triplicate.

2.6. Method applicability

The applicability of the method was assessed for the KPF quantitation in porcine nasal mucosa and receptor media after *in vitro* permeation/retention studies and murine brain after nasal administration in rats. An *ex-vivo* diffusion study of KPF-NE was conducted using freshly isolated pig nasal mucosa as previously described. A Franz diffusion cell was filled with of 12.0 mL of medium (PBS, pH 6.4, containing 2.0% Polysorbate 80) and stirred at 400 rpm at 34°C. A freshly excised porcine mucosa tissue (1.77 cm^2) was kept in PBS pH 6.4 for 15 min to equilibrate, and then fixed to the diffusion cell. The donor compartment was filled with 500 µL of a KPF-NE (1 mg/mL), maintaining the sink conditions for the assay. After 6 h, 1 mL of receptor media was withdrawn and filtered through a 0.45-µm membrane before analysis by HPLC. To analyze KPF retained on the porcine nasal mucosa, the tissue was cleaned using a cotton swab. Then, the tissue was cut into small pieces, placed in test tubes with methanol, and sonicated in an ultrasonic bath for 90 min. Receptor media and extractions were performed from each diffusion cell and the results are represent as mean ± SD.

For analysis of KPF content in brain, Wistar rats (weight: 300-400 g) were anesthetized with isoflurane before intranasal administration. Then, animals were placed in supine position and 100 µL of KPK-NE was given as three alternate

administrations into each nostril by nasal instillation using a micropipette (total of 100 µg of KPF/animal). After 1 h, the animals were decapitated, then the whole brain was removed and washed twice using normal saline to remove adhering tissue/fluid. Subsequently, brain tissues were homogenized with 3 mL of methanol per g of tissue using IKA® Ultra-Turrax T8 mixer (IKA Works Inc., Wilmington, USA) at 9500 rpm for 1 min, followed by centrifugation at 10^4 rpm at 4°C for 15 min. The supernatants were filtered and analyzed for drug content using the HPLC method described.

3. Results and discussion

3.1. Validation Tests

3.1.1. System suitability

Upon performing the system suitability tests, parameter values and their variability (RSD, %) for KPF were: 6.40 min (0.46) for migration time, 3869 (2.42) for theoretical plates, and 1.10 (0.79) for tailing factor. These parameters indicate that the system is suitable for the analysis according to official guidelines.

3.1.2. Selectivity and forced degradation study

The method was selective, since there were no interfering signals from all assessed matrices detected at 368 nm within the same retention time of KPF. The potentially interfering substances from the matrices eluted over the first 4 min of running, while KPF peak eluted after 6 min (Figure 1). Therefore, matrices interferents did not significantly change KPF retention time and peak area, demonstrating the selectivity of the method. High peak purity index for KPF (> 0.9999) was observed in all analyses.

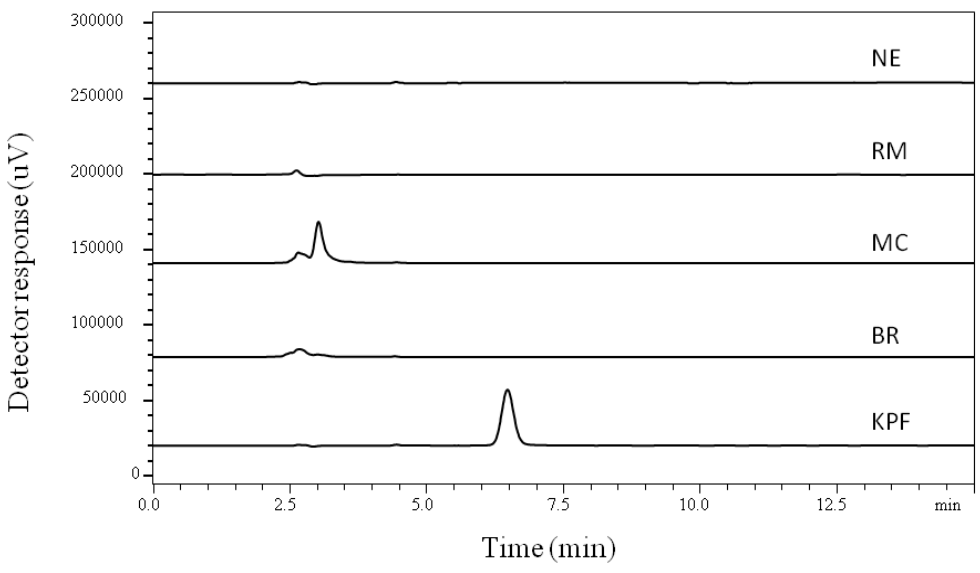

Figure 1. Representative HPLC chromatograms of KPF (kaempferol standard solution, 5.0 μg/mL), BR (murine brain), MC (porcine nasal mucosa), RM (receptor media), NE (blank nanoemulsion).

After, Kaempferol solutions were submitted to forced degradation using the following stress conditions: heat, UVA light, oxidative, and acid. There were no significant changes in KPF after these stress conditions (data not shown). Oppositely, when KPF was submitted to the alkaline condition for 5 min, a reduction in KPF peak area was observed (approximately 30%), without additional peaks. These experiments demonstrated proper stability under most of the stress conditions used, except under alkaline media, in agreement with previous reports [19-21]. The peak purity of KPF did not change due to exposure to any of the stress conditions used (> 0.9999).

3.1.3. Linearity, limits of detection (LOD) and limits of quantitation (LOQ)

The method presented linearity over the evaluated concentration range (0.25 - 7.5 μg/mL), since the determination coefficients (R^2) were always > 0.998, which complies with all regulatory requirements for this parameter. Moreover, the validity of the assay for all matrices was certified by ANOVA, which demonstrated linear regression with no deviation from linearity ($p < 0.05$). The equation, R^2, LOD, and LOQ are shown in Table 2. The low values of LOD and LOQ demonstrated the high sensitivity of the method. The LLOQ was 0.25 μg/mL, since the precision and accuracy at this concentration in all matrices were acceptable for bioanalytical parameters [15].

Table 2. Linearity evaluation and sensitivity data from KPF detected in different matrices.

Matrix	Equation	R^2	LOD (μg/mL)	LOQ (μg/mL)
Blank nanoemulsion	y = 76341x - 2557	0.999	0.03	0.10
Receptor media	y = 78801x - 3808	0.999	0.04	0.14
Porcine nasal mucosa	y = 75073x - 5712	0.998	0.07	0.21
Murine Brain	y = 77692x - 3041	0.999	0.04	0.13

R^2 = determination coefficient; LOD = limit of detection; LOQ = limit of quantitation;

3.1.4. Carry-over

Mean carry-over of KPF was less than 5.1% for all matrices, thus complying with the EMA recommendation, meaning that the carry-over effect was negligible [16]. Therefore, the carry-over effect did not affect the results of routine analysis.

3.1.5. Precision and accuracy

Repeatability, intermediate precision, and accuracy for the KPF spiked matrices are summarized in Table 3. All precision and accuracy parameters were in accordance with the acceptance criteria defined in international guidelines [14-16], indicating that the method has proper repeatability, low interday variability, and accuracy to determine KPF from different matrices.

Table 3. Results of precision and accuracy of KPF recovered from different matrices.

Matrix	Theoretical concentration (µg/mL)	Experimental concentration[a] (µg/mL)	Repeatability RSD[b] (%)	Intermediate precision RSD[b] (%)	Accuracy[a] (%)
Blank Nanoemulsion	0.25	0.26 ± 0.003	0.31	1.32	105.60 ± 1.39
	0.5	0.52 ± 0.009	0.88	1.70	104.37 ± 1.77
	1.0	1.02 ± 0.021	0.56	1.50	103.22 ± 2.16
	5.0	4.94 ± 0.032	0.27	0.64	99.58 ± 0.64
Receptor Media	0.25	0.28 ± 0.005	1.72	1.78	113.27 ± 2.01
	0.5	0.51 ± 0.004	0.52	0.81	103.82 ± 0.84
	1.0	1.03 ± 0.004	0.39	0.42	104.27 ± 0.43
	5.0	4.90 ± 0.023	0.32	0.46	98.75 ± 0.46
Mucosa	0.25	0.28 ± 0.004	1.37	0.62	112.52 ± 1.70
	0.5	0.53 ± 0.018	0.75	3.37	106.39 ± 3.59
	1.0	1.01 ± 0.016	0.45	1.63	101.90 ± 1.66
	5.0	4.93 ± 0.102	0.69	2.06	99.46 ± 2.05
Brain	0.25	0.28 ± 0.001	2.15	0.41	109.62 ± 2.59
	0.5	0.51 ± 0.006	0.39	1.17	104.83 ± 1.30
	1.0	1.01 ± 0.024	1.07	2.39	102.79 ± 1.46
	5.0	4.92 ± 0.030	1.18	0.61	99.55 ± 0.76

[a] Mean and standard deviation of samples. [b] RSD = relative standard deviation

3.1.6 Extraction Recovery

Table 4 shows the absolute extraction recoveries of KPF from mucosa and brain. The results are indicative of efficient quantitative extraction procedure and recovery, which is in agreement with the FDA recommendation for bioanalytical method validation [15]. Furthermore, RSD values were ≤ 5.78%, showing that the extraction procedure was precise. It is important to note that there was no sign of KPF degradation when the solution evaporated to dryness.

Table 4. Recovery of KPF added in biological matrices

Matrix	Amount added (µg/mL)	Recovery % (RSD)[a]
Mucosa	0.25	95.88 (2.97)
	0.5	88.94 (0.91)
	2.5	95.78 (1.58)
	5.0	92.22 (5.78)
Brain	0.25	89.45 (0.48)
	0.5	95.52 (3.58)
	2.5	93.21 (3.23)
	5.0	95.89 (1.55)

[a]n = 3; RSD = relative standard deviation

3.1.7. Stock solution and processed sample stability

Analysis showed that the percent recovery of KPF in the stock solution was 101.37%, indicating that the stock solution of KPF remained stable at least for 6 months at 4°C. At room temperature, no significant degradation of KPF was observed for 48 h, since the concentrations of KPF in blank nanoemulsion, receptor media, porcine nasal mucosa, and murine brain varied by no more than 1.41, 1.84, 1.64, and 0.29% relative to the freshly-made samples, respectively.

3.1.8. Robustness

To assess the method's robustness, the Plackett–Burman design was applied to evaluate the influence of the selected factors. The responses obtained for each matrix were processed to evaluate the significance of the effects, which were represented by a Pareto chart of the standardized effects. The chart includes a vertical line at the critical t-value for α of 0.01. As shown in Fig. 2, no significant factors were revealed for all analyses. The robustness of the developed method was demonstrated, since small changes introduced in the experimental conditions did not result in significant

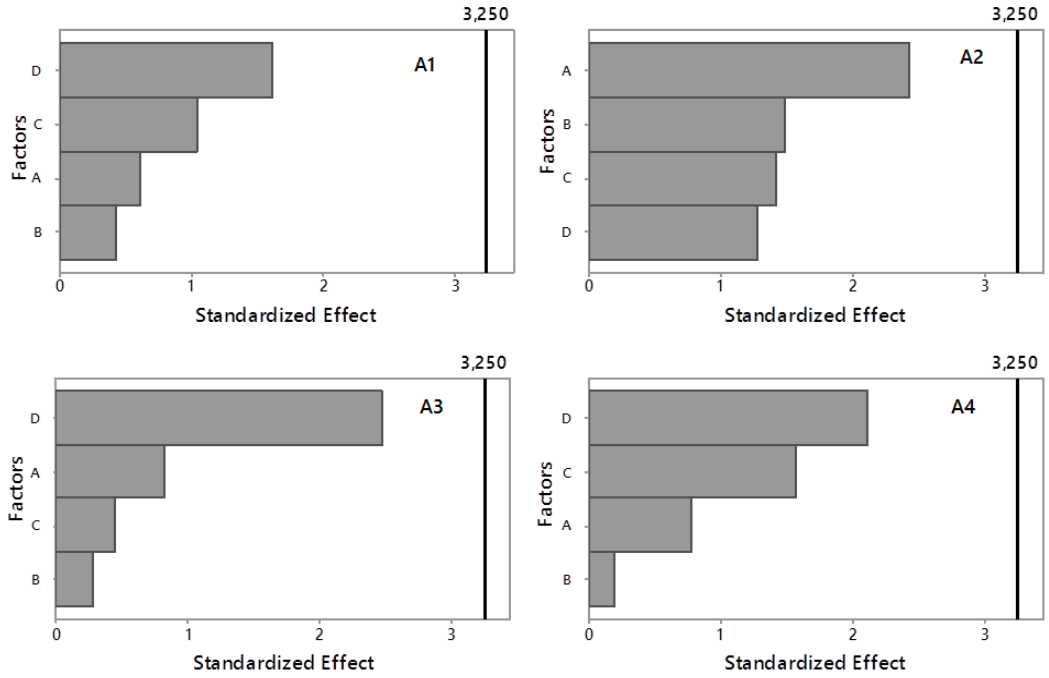

variations in the percent results of KPF contents.

Figure 2. Pareto charts obtained from the Plackett–Burman robustness test. A, flow rate (mL/min); B, temperature (°C); C, detection wavelength (nm); D, methanol content in the mobile phase (%); A_1: blank nanoemulsion; A_2: receptor media; A_3: porcine nasal mucosa; A_4: murine brain.

3.1.9. Evaluation of matrix effects

Endogenous components from biological samples can influence the response of the analyte of interest. These undesirable phenomena, called matrix effects, may result in

an inaccurate quantitation, becoming important issues in development and validation of quantification methods [22]. The matrix effects (ME%) for KPF were -1.67, 4.94, 0.02, and 3.47% in the presence of blank nanoemulsion, receptor media, porcine nasal mucosa, and murine brain, respectively. Therefore, the data show that the samples analyzed exhibited lower matrix effects when compared with the criteria reccomended by the European Medicine Agency [16].

3.2. Nanoemulsion preparations and characterization

The aforementioned nanoemulsion presented nanometric droplet size, low polydispersity index, and negative zeta potential. Droplet size was 139.6 ± 3.08 nm, zeta potential was -17.33 ± 0.06 mV, PDI was 0.20 ± 0.02, and KPF content was 93.6 ± 0.28% for an initial content of 1.0 mg/mL. In addition, physicochemical properties remained significantly unchanged 1 month into storage at 4^{o}C (data not shown).

3.3. Method applicability

The *in vitro* diffusion study was performed with the objective to assess drug release through a biological membrane simulating the actual *in vivo* barrier to drug absorption after intranasal administration. Porcine nasal mucosa was selected because the olfactory epithelium is large enough to afford to obtain workable mucosa pieces, besides the advantage that the morphology of epithelium and some aspects of mucus composition are similar for pigs and humans [23].

The amount of KPF permeated through the mucosa and assessed in the receptor compartment was 2.49 ± 0.36 μg/cm^2 for KPF-NE. KPF retention in the mucosa was 7.08 ± 0.58 μg/cm^2. The method allows determining KPF in porcine nasal mucosa and receptor media samples with adequate precision (RSD below 15% in all analysis), even considering the high variability of the Franz cell experiment [24]. To our best knowledge, no previous report a detailed study of KPF nasal permeation/retention and, although this methodology has been developed for the quantitation of KPF-NE, this HPLC method may be applied to other pharmaceutical forms containing KPF and its diffusion through the porcine nasal mucosa.

The method developed and validated also estimated KPF concentrations in rat brain tissue after intranasal administration of KPF-NE. The mean value of KPF concentration in murine brain was 0.205 ± 0.01 µg/mL. The assay was successfully employed in *in vivo* studies, with acceptable precision and sensitivity. This is the first study that quantified KPF in brains of rats after intranasal administration of a nanotechnological carrier.

The development and quality control of new products, including technology-based products, depends on reliable quantitative methods. Therefore, the development of a highly sensitive and fast analytical method with wide linear range for KPF quantitation in different complex matrices remains an important challenge. Unlike the analytical methods already reported for KPF quantification in biological samples, like rat plasma [8, 25], transport buffers [26], and pharmaceutical formulations [27-29], our method was shown to be simpler, since it uses isocratic reversed-phase liquid chromatography, which requires only binary solvent system containing acidified water and methanol [26-28]. Also, the method afforded shorter analysis time and high sensitivity [8, 25, 30]. To the best of our knowledge, this is the first report on the validation of a method for KPF quantification in complex samples such as porcine mucosa and murine brain.

4. Conclusion

The present study describes the first full validated method for determination of Kaempferol in nanotechnology-based products like nanoemulsion, receptor media for diffusion studies, porcine nasal mucosa as biological membrane, and murine brain, showing the versatility of the method. The method was selective, linear, sensitive, precise, accurate, robust, and had low matrix effect. Thus, it is suitable for routine assay, affording short analysis time. The successful application of this method to mucosa and receptor media samples from diffusion tests on Franz cells enabled the correct evaluation of permeation/retention of KPF. Furthermore, due to the increasing interest in intranasal administration of different drugs-loaded nanoparticles, the quantitation of KPF-NE through the nasal mucosa is interesting in the evaluation of this poorly soluble compound to the CNS. In addition, the method was successfully employed for *in vivo* quantification of KPF in rat brain. The aforementioned method

is applicable in bioavailability studies, and the formulation developed (KPF-NE) is suitable for preclinical trials in different brain disorders.

Acknowledgments

This work was financially supported by CNPq, CAPES/Brazil and FAPERGS. The authors would also like to thank these agencies for their research fellowships.

References

[1] S.A. Aherne, N.M. O'Brien, Dietary flavonols: chemistry, food content, and metabolism, Nutrition 18(1) (2002) 75-81.

[2] J.P. Spencer, Flavonoids: modulators of brain function?, Br J Nutr 99(1) (2008).

[3] J.M. Calderon-Montano, E. Burgos-Moron, C. Perez-Guerrero, M. Lopez-Lazaro, A review on the dietary flavonoid kaempferol, Mini-Reviews in Medicinal Chemistry 11(4) (2011) 298-344.

[4] K.P. Devi, D.S. Malar, S.F. Nabavi, A. Sureda, J. Xiao, S.M. Nabavi, M. Daglia, Kaempferol and inflammation: From chemistry to medicine, Pharmacological Research 99 (2015) 1-10.

[5] A.Y. Chen, Y.C. Chen, A review of the dietary flavonoid, kaempferol on human health and cancer chemoprevention, Food Chemistry 138(4) (2013) 2099-107.

[6] V. Sharma, C. Joseph, S. Ghosh, A. Agarwal, M.K. Mishra, E. Sen, Kaempferol induces apoptosis in glioblastoma cells through oxidative stress, Mol Cancer Ther 6(9) (2007) 2544-53.

[7] G. Filomeni, I. Graziani, D. De Zio, L. Dini, D. Centonze, G. Rotilio, M.R. Ciriolo, Neuroprotection of kaempferol by autophagy in models of rotenone-mediated acute toxicity: possible implications for Parkinson's disease, Neurobiol Aging 33(4) (2012) 767-85.

[8] A. Barve, C. Chen, V. Hebbar, J. Desiderio, C.L. Saw, A.N. Kong, Metabolism, oral bioavailability and pharmacokinetics of chemopreventive kaempferol in rats, Biopharmaceutics & Drug Disposition 30(7) (2009) 356-65.

[9] L. Kozlovskaya, M. Abou-Kaoud, D. Stepensky, Quantitative analysis of drug delivery to the brain via nasal route, J Control Release 189 (2014) 133-40.

[10] W.Y. Ong, S.M. Shalini, L. Costantino, Nose-to-brain drug delivery by nanoparticles in the treatment of neurological disorders, Curr Med Chem 21(37) (2014) 4247-56.

[11] L. Illum, Transport of drugs from the nasal cavity to the central nervous system, European Journal of Pharmaceutical Sciences 11(1) (2000) 1-18.

[12] C. Comfort, G. Garrastazu, M. Pozzoli, F. Sonvico, Opportunities and challenges for the nasal administration of nanoemulsions, Curr Top Med Chem 15(4) (2015) 356-68.

[13] F.C. Carvalho, M.L. Campos, R.G. Peccinini, M.P. Gremiao, Nasal administration of liquid crystal precursor mucoadhesive vehicle as an alternative antiretroviral therapy, European Journal of Pharmaceutics and Biopharmaceutics 84(1) (2013) 219-27.

[14] ICH, International Conference on Harmonization,Technical requirements for the registration of pharmaceutical for human use, Validation of Analytical Procedures: Text and Methodology Q2(R1), (2005) 1-13.

[15] FDA, Food and Drug Administration, Center for drug evaluation and research, Guidance for Industry: Bioanalytical Method Validation, (2013) 1-34.

[16] EMA, European Medicines Agency, EMEA/CHMP/EWP/192217/2009, Guideline on bioanalytical method validation, (2011) 1-22.

[17] FDA, Food and Drug Administration, Center for Drug Evaluation and Research, Reviewer Guidance: Validation of Chromatographic Methods, (1994) 1-30.

[18] M.C. Nemitz, F.K. Yatsu, J. Bidone, L.S. Koester, V.L. Bassani, C.V. Garcia, A.S. Mendez, G.L. von Poser, H.F. Teixeira, A versatile, stability-indicating and high-throughput ultra-fast liquid chromatography method for the determination of isoflavone aglycones in soybeans, topical formulations, and permeation assays, Talanta 134 (2015) 183-93.

[19] S.E. Bianchi, H.F. Teixeira, S. Kaiser, G.G. Ortega, P.H. Schneider, V.L. Bassani, A bioanalytical HPLC method for coumestrol quantification in skin permeation tests followed by UPLC-QTOF/HDMS stability-indicating method for identification of degradation products, J Chromatogr B Analyt Technol Biomed Life Sci 1 (2016) 43-52.

[20] J.P. Carini, S. Kaiser, G.G. Ortega, V.L. Bassani, Development, optimisation and validation of a stability-indicating HPLC method of achyrobichalcone quantification using experimental designs, Phytochem Anal 24(3) (2013) 193-200.
[21] A. Dube, K. Ng, J.A. Nicolazzo, I. Larson, Effective use of reducing agents and nanoparticle encapsulation in stabilizing catechins in alkaline solution, Food Chemistry 122(3) (2010) 662-667.
[22] M.L. Chiu, W. Lawi, S.T. Snyder, P.K. Wong, J.C. Liao, V. Gau, Matrix effects—a challenge toward automation of molecular analysis, Journal of the association for laboratory automation 15(3) (2010) 233-242.
[23] A. Mistry, S. Stolnik, L. Illum, Nose-to-Brain Delivery: Investigation of the Transport of Nanoparticles with Different Surface Characteristics and Sizes in Excised Porcine Olfactory Epithelium, Mol Pharm 12(8) (2015) 2755-66.
[24] S.F. Ng, J.J. Rouse, F.D. Sanderson, V. Meidan, G.M. Eccleston, Validation of a static Franz diffusion cell system for in vitro permeation studies, AAPS PharmSciTech 11(3) (2010) 1432-41.
[25] Q. Zhang, Y. Zhang, Z. Zhang, Z. Lu, Sensitive determination of kaempferol in rat plasma by high-performance liquid chromatography with chemiluminescence detection and application to a pharmacokinetic study, J Chromatogr B Analyt Technol Biomed Life Sci 877(29) (2009) 3595-600.
[26] F. Moradi-Afrapoli, M. Oufir, F.R. Walter, M.A. Deli, M. Smiesko, V. Zabela, V. Butterweck, M. Hamburger, Validation of UHPLC-MS/MS methods for the determination of kaempferol and its metabolite 4-hydroxyphenyl acetic acid, and application to in vitro blood-brain barrier and intestinal drug permeability studies, J Pharm Biomed Anal 128 (2016) 264-274.
[27] K. Zhang, L. Gu, J. Chen, Y. Zhang, Y. Jiang, L. Zhao, K. Bi, X. Chen, Preparation and evaluation of kaempferol-phospholipid complex for pharmacokinetics and bioavailability in SD rats, J Pharm Biomed Anal 114 (2015) 168-75.
[28] Y. Chao, C.T. Huang, L.T. Fu, Y.B. Huang, Y.H. Tsai, P.C. Wu, The effect of submicron emulsion systems on transdermal delivery of kaempferol, Chem Pharm Bull 60(9) (2012) 1171-5.

[29] S. Ilk, N. Saglam, M. Ozgen, Kaempferol loaded lecithin/chitosan nanoparticles: preparation, characterization, and their potential applications as a sustainable antifungal agent, Artif Cells Nanomed Biotechnol 45(5) (2017) 907-916.
[30] Y. Yang, L. Bai, X. Li, J. Xiong, P. Xu, C. Guo, M. Xue, Transport of active flavonoids, based on cytotoxicity and lipophilicity: an evaluation using the blood-brain barrier cell and Caco-2 cell models, Toxicol In Vitro 28(3) (2014) 388-96.

CAPÍTULO I - Publicação II

Artigo publicado no periódico *International Journal of Pharmaceutics*

Colombo, M., Figueiró, F., de Fraga Dias, A., Teixeira, H. F., Battastini, A. M. O., & Koester, L. S. (2018). *Kaempferol-loaded mucoadhesive nanoemulsion for intranasal administration reduces glioma growth in vitro. International journal of pharmaceutics, 543(1-2), 214-223*. https://doi.org/10.1016/j.ijpharm.2018.03.055

KAEMPFEROL-LOADED MUCOADHESIVE NANOEMULSION FOR INTRANASAL ADMINISTRATION REDUCES GLIOMA GROWTH *IN VITRO*

Mariana Colombo[a], Fabrício Figueiró[b,c], Amanda de Fraga Dias[c], Helder Ferreira Teixeira[a], Ana Maria Oliveira Battastini[b,c], Letícia Scherer Koester[a*]

[a]Programa de Pós-Graduação em Ciências Farmacêuticas, Faculdade de Farmácia, Universidade Federal do Rio Grande do Sul (UFRGS), Av. Ipiranga, 2752, 90610-000, Porto Alegre, RS, Brazil.

[b]Programa de Pós-Graduação em Ciências Biológicas: Bioquímica, Instituto de Ciências Básicas da Saúde, UFRGS, Av. Ramiro Barcelos, 2600, Anexo, 90035-003, Porto Alegre, RS, Brazil.

[c]Departamento de Bioquímica, Instituto de Ciências Básicas da Saúde, UFRGS, Av. Ramiro Barcelos, 2600, Anexo, 90035-003, Porto Alegre, RS, Brazil.

*Corresponding author: Dr. Letícia S. Koester, Faculdade de Farmácia/UFRGS, Av. Ipiranga, 2752/607, Porto Alegre-RS, 90.610-000, Brazil. E-mail:leticia.koester@ufrgs.br

Graphical Abstract:

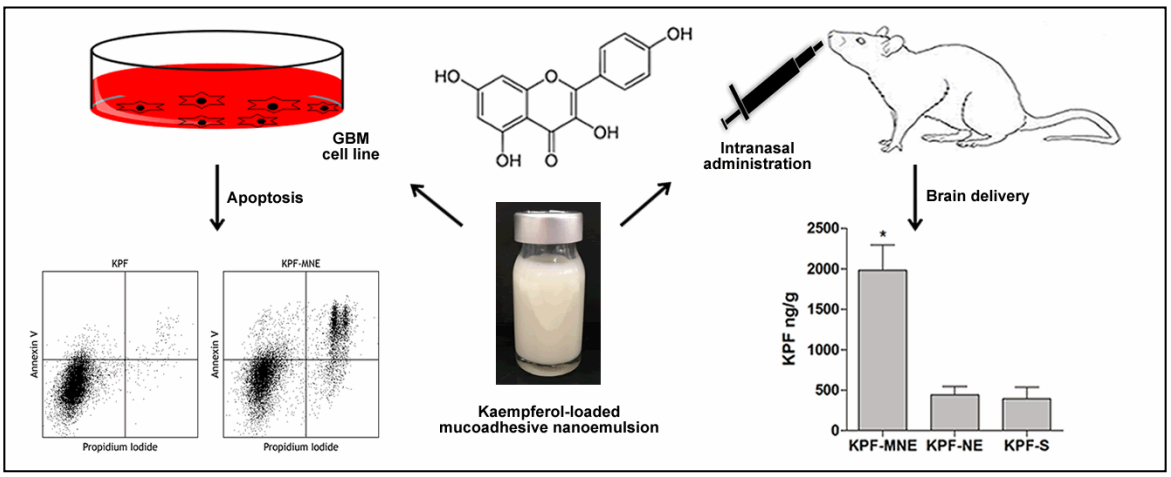

Abstract

In order to search for new approaches to treat glioma, intranasal administration has been proposed as an alternative route to deliver drugs into the brain. Among the drug alternatives, kaempferol (KPF) has been reported to induce glioma cell death. This study aimed to prepare nanoemulsions containing KPF with and without chitosan to investigate their potential for brain delivery following intranasal administration, and to evaluate their antitumor activity against glioma cells. KPF-loaded nanoemulsion (KPF-NE) and KPF-loaded mucoadhesive nanoemulsion (KPF-MNE) were prepared by high-pressure homogenization technique and were characterized for their globule size, zeta potential, drug content, pH, viscosity, mucoadhesive strength and morphology. KPF from KPF-MNE showed significantly higher permeation across the mucosa in *ex vivo* diffusion studies. Histopathological examination suggests both nanoemulsions to be safe for the nasal mucosa and able to preserve KPF antioxidant capability. KPF-MNE enhanced significantly the amount of drug into rat's brain following intranasal administration (5- and 4.5-fold higher than free drug and KPF-NE, respectively). In addition, KPF-MNE reduced C6 glioma cell viability through induction of apoptosis to a greater extent than either free KPF or KPF-NE. The mucoadhesive nanoemulsion developed for intranasal administration may be a promising system for delivery to the brain, and KPF-MNE is a candidate for further antiglioma trials.

Keywords: Kaempferol; mucoadhesive nanoemulsion; intranasal; brain delivery; glioma.

1. Introduction

Kaempferol (KPF; 3,4',5,7-tetrahydroxyflavone) is a natural flavonol present in different plant species, found abundantly in edible plants (broccoli, apples, strawberries and beans) and common medicinal plants (*Aloe vera, Ginkgo biloba, Rosmarinus officinalis*, *Crocus sativus* L., *Hypericum perforatum L., Equisetum spp*,) (Calderon-Montano et al., 2011; Sultana and Anwar, 2008).

KPF has been described to present anti-oxidant, anti-inflammatory, neuroprotective and anti-tumor activities (Chen and Chen, 2013; Devi et al., 2015; Lopez-Sanchez et

al., 2007). Recently, research studies have reported KPF presenting anti-cancer activity in various cancer cells, including glioma cells (Jeong et al., 2009; Nakatsuma et al., 2010; Seibert et al., 2011; Sharma et al., 2007; Siegelin et al., 2008). However, its low water solubility and bioavailability are not desired properties of a candidate drug, and limit its application in the clinical field (Barve et al., 2009; Chen et al., 2010; Luo et al., 2012). In this way, the identification of an appropriate formulation and route of administration is part of the accurate selection and optimization of a candidate drug.

Gliomas are the most common and deadly type of intrinsic brain tumor in adults, of which glioblastoma multiforme (GBM) represents the ultimate grade of malignancy. Despite multimodal therapy (neurosurgical resection, radiotherapy and chemotherapy), the median overall survival of patients with GBM does not exceed 15 months from diagnosis (Stupp et al., 2009). The dismal prognosis for GBM is due to its high capacity for proliferation and an infiltrative growth pattern, variability in the tumor histopathology and resistance to radiation- and chemotherapy (Van Meir et al., 2010). Moreover, another important factor that impairs the development of new therapeutic strategies for treating GBM is the presence of the blood–brain barrier (BBB), that hampers the drug penetration into the central nervous system (CNS), restricting the glioma therapy and inducing therapy failure (Behin et al., 2003; Van Meir et al., 2010).

Recognizing the need to improve patient survival, different drug delivery approaches have been studied, and the intranasal route of administration is a strategy that provides a noninvasive method to deliver therapeutic drugs into the brain (Alam et al., 2010). The intranasal route provides direct and rapid transport of drugs from the nasal cavity to the brain, involving three main pathways: olfactory nerve pathway, transport via the trigeminal nerves, and the systemic pathway (Illum, 2000; Pardeshi and Belgamwar, 2013). Furthermore, this strategy offers painless and efficient drug delivery by circumventing the BBB and avoiding hepatic first-pass metabolism by using the permeable nasal mucosa as a route to the brain (van Woensel et al., 2013).

Nanoemulsions hold great potential in nose-to-brain drug delivery, increasing the absorption and the bioavailability of many water-insoluble compounds by nasal administration. Because of their small diameter, nanoemulsions present large surface

area and high free energy, ensuring faster and higher drug permeation through biological membranes. Furthermore, these systems may offer protection from enzymatic and chemical degradation (Comfort et al., 2015; van Woensel et al., 2013).

To improve the nasal residence time of the formulation and to enhance permeation across the nasal membrane, chitosan has shown great potential, by decreasing mucociliary clearance due to its bioadhesive and permeation-enhancing properties (Casettari and Illum, 2014). Chitosan is one of the most studied polymers in the area of transmucosal drug delivery. This polycationic polymer is an *N*-deacetylated product of the polysaccharide chitin, and shows interesting properties, such as biocompatibility, biodegradability, and low local and systemic toxicity (Bernkop-Schnurch and Dunnhaupt, 2012).

Considering the advantages of nose-to-brain transport afforded by nanoemulsions, the main aims of the present study were to develop a kaempferol-loaded mucoadhesive nanoemulsion (KPF-MNE) and to evaluate both its potential as a delivery system to rat's brain following nasal administration, and its activity against a glioma cell line.

2. Materials and methods

2.1. Materials

KPF (purity > 98%) was purchased from ShaanXi HuiKe Botanical (Xi'an, China). Egg-lecithin (Lipoid E-80s) and medium-chain triglycerides (MCT) were purchased from Lipoid GmbH (Ludwigshafen, Germany). Polysorbate 80 was supplied from Sigma Aldrich (Steinheim, Germany). Chitosan (low molecular weight, degree of deacetylation 75–85%) was purchased from Sigma Aldrich (St Louis, USA). Methanol HPLC grade and Formic Acid 96% were obtained from Tedia (Rio de Janeiro, Brazil). Ultrapure water was obtained from a Milli-Q apparatus (Millipore, Billerica, USA). Porcine heads were purchased from Ouro do Sul Ltda (Harmonia, Brazil). Mucin from porcine stomach was from Sigma Aldrich (Sigma, St. Louis, USA). Dulbecco's modified Eagle's medium (DMEM), fetal bovine serum (FBS), penicillin/streptomycin, and 0.5% trypsin/EDTA solution were obtained from Gibco (Gibco BRL, Carlsbad, USA). Gentamicin was obtained from Schering do Brazil (Rio de Janeiro, Brazil). Propidium iodide (PI) and dimethyl sulfoxide (DMSO) were

obtained from Sigma (St. Louis, USA). Annexin V-FITC/PI was obtained from BD Biosciences (San Diego, USA). All other reagents used were of analytical grade.

2.2. High-performance liquid chromatography analysis

Quantification of KPF in formulations, nasal mucosa and brain was assessed by high-performance liquid chromatography (HPLC) using the chromatographic conditions previously validated by our research group (Colombo et al., 2017). In brief, HPLC apparatus consisted of a Shimadzu LC-10A system (Kyoto, Japan) equipped with a model LC-20AT pump, a SPD-20AV UV-vis variable wavelength detector, a DGU-20A5 degasser, a CBM-20A system controller, and an SIL-20A injection valve with a 100 μL loop. Kaempferol was analyzed using a XTerra® RP18 column (250 mm × 4.6 mm, 5 μm particle size). The mobile phase consisted of a 75:25 (v/v) mixture of methanol and 0.1% formic acid in water in isocratic flow at a flow rate of 1.0 mL/min, with detection at 368 nm and temperature of 35 °C.

2.3. Preparation of nanoemulsion and mucoadhesive nanoemulsion

The kaempferol-loaded nanoemulsion (KPF-NE) was prepared by a high-pressure homogenization technique (Colombo et al., 2017). The oil phase was prepared by dispersing KPF (0.1% w/w) in 16% (w/w) MCT and 5.0% (w/w) egg-lecithin. The aqueous phase contained 1.0% (w/w) polysorbate 80 and water. First, a coarse emulsion was prepared by the homogenization of both phases using an IKA® Ultra-Turrax T8 mixer (IKA® Works Inc., NC, USA) at 9500 rpm for 1 min. Afterwards, the coarse emulsion was subjected to high-pressure homogenization (EmulsiFlex-C3®, Avestin, Canada) for eight cycles at 750 bar to produce the final nanoemulsion.

The KPF-loaded mucoadhesive nanoemulsion was prepared after the KPF-NE. The nanoemulsion external phase was evaporated under reduced pressure to 75% of the initial volume and then adding the required volume of chitosan solution (1% w/v in 0.1% acetic acid) so the final concentration of polymer in the KPF-MNE was 0.25% (w/v). After addition of the chitosan solution, the KPF-MNE was allowed to homogenize for 10 min with continuous stirring on a magnetic stirrer. Blank

nanoemulsion (NE) and blank mucoadhesive nanoemulsion (MNE) were prepared without KPF incorporation.

2.4. Characterization of nanoemulsions

2.4.1. Globule size and zeta potential measurements

Globule size and polydispersity index (PDI) were evaluated by photon correlation spectroscopy. Each nanoemulsion was diluted in ultrapure water (1:1000) before measurement. The determination of the zeta potential was performed by eletrophoretic mobility, after dilution of the formulations in 1 mM NaCl (1:1000). All analyses were carried out in triplicate using a Malvern Nano-ZS90® (Malvern Instruments, England) at 25 °C.

2.4.2. Transmission electron microscopy (TEM)

Morphology and size of nanoemulsions were studied using transmission electron microscopy (TEM). Before analysis, samples were diluted with ultrapure water, placed on a carbon-coated copper grid (200 mesh) coated with Formvar/carbon, stained with 2.0% uranyl acetate aqueous solution, and examined using a JEM-1200 EXII instrument (JEOL, Tokyo, Japan).

2.4.3. Viscosity, pH and refractive index (RI)

Nanoemulsion viscosity and rheological behavior were determined in a rotational viscosimeter (Brookfield LVDVII+ Pro model, Middleboro, USA) equipped with a ULA spindle. For the determinations, samples (16 mL, n = 3) were conditioned in a Brookfield device coupled to a thermostated circulating water bath at 25 or 34 °C. The pH of formulations was measured at room temperature using a calibrated digital pH meter (Digimed, São Paulo, Brazil) by placing 10 ml of each formulation in a beaker. The refractive index (RI) of formulations was determined in triplicate using an Abbe-type refractometer in the presence of visible light at ambient temperature (USP, 2011).

2.4.4. KPF content and association efficiency (%AE)

KPF content in nanoemulsions was assayed by HPLC as previously described, after sample dilution in methanol to obtain a theoretical concentration of 5.0 µg/mL. To show the improvement in KPF solubility, saturation solubility in water was performed as follows: an excess amount of KPF was added to 2 mL of distilled water. The samples were sealed in triplicate and shaken for 48 h at 37 °C. The supernatant was filtered through a Millipore filter (pore size 0.45 µm), and assayed by HPLC. In order to determine the %AE, the free KPF content in the nanoemulsions was determined by measuring the nonincorporated KPF present in the aqueous phase using HPLC after ultrafiltration/centrifugation with Microcon® centrifugal filter devices (100,000 NMWL; Millipore, USA) for 15 min at 15,000 rpm. Values of %AE for each nanoemulsion, after triplicate measurements, were calculated using Eq. (1):

$$\%AE = (\text{total drug} - \text{free drug})/\text{total drug} \times 100 \quad \text{Eq. (1)}$$

2.5. *In vitro* DPPH assay for antioxidant activity

The antioxidant activity of the optimized formulations was compared with methanolic KPF solution using the DPPH assay method. The test was based on the free-radical scavenging activity of 2,2-diphenyl-1-picrylhydrazyl (DPPH), a stable nitrogen-centered free radical (Caddeo et al., 2013). A methanolic DPPH solution (0.004% w/v) was prepared, of which 3.9 mL were mixed with either 0.1 mL KPF nanoemulsions (KPF-NE or KPF-MNE) or 0.1 ml KPF solution (1 mg/mL in methanol) or blank nanoemulsions. Absorbance was measured after 60 min at 515 nm using methanol as blank (without the drug). The percentage inhibition was calculated using Eq. (2):

$$\text{DDPH inhibition } \% = [(A_0 - A_1)/A_0] \times 100 \quad \text{Eq. (2)}$$

where A_0 is the absorbance of the blank, and A_1 is the absorbance of the drug solution or nanoemulsion. All experiments were performed in triplicate.

2.6. *Ex vivo* diffusion study

An *ex vivo* diffusion study of formulations was determined using a Franz diffusion cell through a freshly isolated pig nasal mucosa obtained from a local slaughterhouse. Cartilages and adhered tissues were removed completely, and the mucosal membrane was washed with PBS, pH 6.4 (Carvalho et al., 2013). The receptor compartment was

filled with medium, volume 12.0 mL (PBS, pH 6.4, containing 2.0% Polysorbate 80), maintained at 34 °C by a circulating bath. A small magnetic bead was placed in the receptor compartment for stirring the medium at 400 rpm. Freshly excised porcine mucosa tissue (1.77 cm^2) was kept in PBS, pH 6.4, for 15 min to equilibrate, and then fixed to the diffusion cell. Receptor and donor compartments were tightly closed with a stainless steel clip. A comparative nasal diffusion study was performed by placing in the donor compartment 0.3 mL of KPF-NE, KPF-MNE or pure KPF suspension (1.0 mg/mL in water) maintaining the sink conditions for the assay (n = 4). After 6 h, 1 mL of receptor medium was withdrawn and filtered with a membrane filter of pore size 0.45 µm before analysis by HPLC. To analyze the KPF retained on the porcine nasal mucosa, the tissue was removed from the Franz cell and cleaned using a cotton swab. Then, the tissue was cut into small pieces, placed in test tubes with methanol and sonicated in an ultrasonic bath for 90 min. Samples were passed through a 0.45 µm membrane filter before analysis by HPLC.

2.7. Preliminary nasal toxicity studies

Nasal toxicity studies were carried out using freshly isolated porcine nasal mucosa collected from a local slaughterhouse (Carvalho et al., 2013). Each mucosa piece, of uniform thickness, was treated with KPF-NE, KPF-MNE, blank nanoemulsions, PBS pH 6.4 (as negative control), or isopropyl alcohol (as positive control). After treatment for 1 h, pieces of mucosa were washed with PBS and fixed in 10% v/v formalin solution overnight and embedded in paraffin. The sections (5 µm) were cut using a microtome, stained with hematoxylin–eosin and observed under the microscope (Nikon Eclipse TE 300) to evaluate any damage to the mucosa (Shah et al., 2016).

2.8. Measurement of *ex vivo* mucoadhesive strength

Mucoadhesive strength of formulations was evaluated by Texture analyzer (TA.XT.Plus, Stable Micro Systems, Surrey, UK) using freshly isolated porcine nasal mucosa (Shah et al., 2016). A cleaned piece of nasal mucosa was immersed in artificial nasal mucus (ANM) for 30 s prior to the test; excess ANM was removed with soft paper. ANM was prepared by dispersing 8% (w/v) of mucin type II from porcine

stomach in a solution of 7.45 mg/mL NaCl, 1.29 mg/mL KCl and 0.32 mg/mL $CaCl_2.2H_2O$ (Callens et al., 2003). Pieces of mucosa were attached both onto the base of the texture analyzer and onto the probe using two-sided adhesive tape. Each formulation (0.5 ml) was placed on the mucosa on the lower surface of the base. The mobile arm was lowered at a rate of 0.5 mm/s (pre-test speed) until contact with formulation was made. A contact force of 10 g was maintained for 150 s; subsequently, the probe was withdrawn from the membrane at a post-test speed of 0.1 mm/s. After an adhesive bond was formed, the strength (g) and the work of mucoadhesion (area under the force vs distance curve) (g.s) needed for detachment was registered. The acquired data was processed with Texture Exponent Lite software.

2.9. *In vivo* quantification of KPF in rat's brain

Animal experiments were conducted with prior approval from the Ethical Committee of the Universidade Federal do Rio Grande do Sul (Protocol # 31216) and performed according to the guidelines of "Principles of Laboratory Animal Care" from the National Institutes of Health (NIH).

Wistar rats (n = 4/group, weight: 300–400 g) were anesthetized with isoflurane before intranasal administration. Then, animals were placed in a supine position and treated with KPF-NE, KPF-MNE or KPF solution (KPF-S). KPF-S (KPF at 1.0 mg/mL) was prepared by solubilizing the drug in a mixture of 3% DMSO in PBS. Formulations were gently administered into each nostril (50 µl) with the help of a micropipette (equivalent to 100 µg of kaempferol per animal). After 1 h, the animals were decapitated and the whole brain was removed and washed twice using normal saline to remove adhering tissue/fluid. Subsequently, brain homogenates were obtained by homogenizing the tissues with 3 mL of methanol per g of tissue using IKA® Ultra-Turrax T8 mixer (IKA® Works Inc., NC, USA) at 9500 rpm for 1 min, and sonicated in an ultrasonic bath for 30 min. After centrifugation at 10000 rpm at 4 °C for 15 min, the supernatant was filtered at 0.45 µm and analyzed for drug content using HPLC.

2.10. Maintenance of cell lines

The C6 rat glioma cell line was obtained from American Type Culture Collection (ATCC) (Rockville, Maryland, USA). Cells at passage 5–30 were grown and maintained in 1% Dulbecco's modified Eagle's medium (DMEM) containing antibiotics (0.5 U/mL penicillin/streptomycin) and supplemented with 5% (v/v) fetal bovine serum (FBS). Cells were kept at 37 °C, a minimum relative humidity of 95%, and an atmosphere of 5% CO_2.

2.11. Assessment of glioma cell viability

The C6 glioma cells were seeded at 25×10^3 cells per well in DMEM 5% FBS in 24-well plates and allowed to grow until reaching semi-confluence. Glioma cells were treated with 1.0 µM of free KPF, KPF-NE or KPF-MNE for 72 h. Cells treated with 0.5% dimethyl sulfoxide (DMSO) or formulations without drugs were used as vehicle controls. After 72 h of treatment, the medium was removed. Cells were washed twice with 200 µL PBS, and 100 µL of 0.05% trypsin/EDTA solution was added to detach the cells, which were counted immediately in a hemocytometer by the Trypan blue dye exclusion test. Live cells that have intact membranes exclude the dye, whereas dead cells do not and are thus stained. In order to calculate IC50 values, treatment of C6 glioma cells with KPF, at concentrations of 0.25, 0.5, 0.75, and 1.0 µM for KPF-MNE, and 1.0, 5.0, 10.0 and 20.0 µM for free KPF for 72 h were performed.

2.12. Cellular uptake of kaempferol

For evaluation of KPF cellular uptake, cells were treated with KPF-MNE or free KPF at 5 µM. After 48 h of incubation, the medium was aspirated and the cells were washed twice with ice-cold PBS, and scraped. Protein concentration was determined using the BCA Protein Assay kit. KPF was extracted from the cells with 200 µL of methanol containing 1% acetic acid by sonication for 1 min. Samples were filtered at 0.45µm, and 20 µL was injected into the HPLC system for determining the concentrations of KPF (Bandaruk et al., 2014; Liu et al., 2006).

2.13. Cell-cycle analysis

Cells were plated in 6-well plates, and after reaching semi-confluence, and treated with 1.0 µM of free KPF or KPF-MNE for 72 h. Cells treated with 0.5% DMSO or MNE were used as vehicle controls. At the end of the treatment, the medium and the cells were harvested and centrifuged at 400×g for 6 min. Next, the supernatant was removed and the cells were washed twice with PBS (pH 7.4), centrifuged, and resuspended in 400 µL staining solution (3.5 mM trisodium citrate; 0.5 mM TRIS.HCl (pH 7.6); NP 40 0.1% (v/v); RNAse 100 µg/mL; PI 50 µg/mL) at a concentration of 10^6 cells/mL. After 15 min, the cells were analyzed using flow cytometry (FACS Calibur cytometry system, FACS Calibur, BD Bioscience, Mountain View, CA, USA). The data obtained were analyzed by FLOWJO® software.

2.14. Annexin V/PI assay

Apoptotic cells were quantified using an AnnexinV-FITC–propidium iodide (PI) double staining kit (BD Biosciences, San Diego, USA) according to the manufacturer's instructions. Cells were plated in 24-well plates and, after reaching semi-confluence, were treated with 1.0 µM of MNE-KPF or free KPF. Cells treated with 0.5% DMSO or MNE were used as vehicle controls. At the end of the treatment, the medium and the cells were harvested and centrifuged at 400×g for 6 min. Cells were washed twice in cold PBS (pH 7.4) and counted. Next, 10^5 cells were suspended in binding buffer containing FITC-conjugated AnnexinV and PI. The samples were mixed and incubated for 15 min at room temperature in the dark. Apoptotic and/or necrotic cells were quantified using a dual-color flow cytometry technique on a FACS Calibur cytometry system (FACS Calibur, BD Bioscience, Mountain View, CA, USA). The data obtained were analyzed by FLOWJO® software. Cells were classified as follows: live cells (Annexin−/PI−); early apoptotic (Annexin+/PI−); late apoptotic (Annexin+/PI+) and necrotic (Annexin−/PI+). A total apoptosis measurement was also performed (Annexin+/PI− plus Annexin+/PI+).

2.15. Statistical analysis

The experiments are expressed as mean ± standard deviation (SD). The significance of the differences was evaluated using one-way ANOVA followed by Tukey's test. The

statistical significance level was set at $p < 0.05$. All analyses were performed with GraphPad Prism 5 software (GraphPad Software, USA).

3. RESULTS AND DISCUSSION

3.1 Characterization of nanoemulsions

The developed KPF nanoemulsions presented an uniform milky yellowish aspect (data not shown). The physicochemical characteristics of formulations are shown in Table 1.

Table 1. Physicochemical properties of formulations [a].

Formulation	Globule size (nm)	PDI	ZP (mV)	Refractive Index
KPF-NE	145.07 ± 4.91	0.145 ± 0.015	-18.10 ± 2.55	1.354 ± 0.002
KPF-MNE	180.53 ± 4.90*	0.203 ± 0.022	+26.09 ± 2.67	1.359 ± 0.001
NE	137.07 ± 1.18	0.155 ± 0.015	-18.71 ± 1.72	1.350 ± 0.001
MNE	180.48 ± 8.37[#]	0.211 ± 0.023	+26.32 ± 2.26	1.350 ± 0.002

[a] Values for all characterization parameters are reported as mean ± SD (n = 3). *means statistical difference from the KPF-NE ($p < 0.05$). [#]means statistical difference from the NE ($p < 0.05$).

Formulations showed nanoscale droplets with low polydispersity index. Nanosized droplets present greater surface area and high free energy, assuring faster and greater drug permeation through absorption barriers such as mucosal surfaces (Comfort et al., 2015). The uniformity of droplet size in the nanoemulsions is indicated by the PDI value. The small PDI value found (less than 0.2) indicates a narrow size distribution. The significant increase ($p < 0.05$) in globule size upon inclusion of chitosan (KPF-MNE and MNE) is attributed to the chitosan coating on the nanoparticle surface and the previous evaporation step. After evaporating but before adding chitosan, the globule size was 170.4 ± 4.1 nm (n = 3). Furthermore, TEM of formulations confirmed their spherical shape and nanometric size (Figure 1). Also, the globule size observed by TEM is highly comparable to the average globule size measured by photon correlation spectroscopy. Formulations without coating presented a negative zeta

potential, due to phospholipids and free fatty acids from egg lecithin. The addition of chitosan conferred a positive zeta potential to the globules.

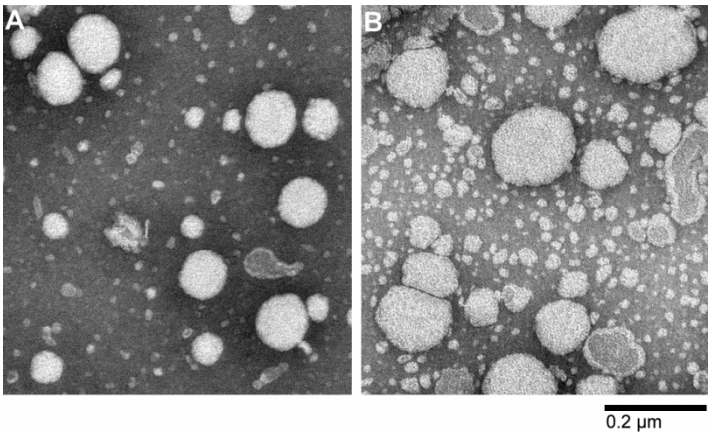

Figure 1. TEM analysis from developed formulations A) KPF-NE, B) KPF-MNE.

The refractive index was measured to evaluate the isotropic nature of the nanoemulsions, as the value of the refractive index is helpful to show the chemical interactions between the drug and excipients. No significant difference in the RI values was observed between the KPF-NE and blank NE, and between KPF-MNE and blank MNE, indicating that the nanoemulsion and mucoadhesive formulations were chemically stable and remained isotropic in nature.

KPF-NE and KPF-MNE showed pH values of 4.70 ± 0.02 and 5.56 ± 0.02, respectively, which is well tolerated within the limits of human nasal pH range (4.5–6.5) and therefore would not cause nasal irritation upon intranasal administration (Arora et al., 2002).

The viscosity of a formulation may affect absorption across the nasal mucosa, since it is related to the residence time in the nasal cavity. Formulations with higher viscosity tend to stay longer on the mucosa and increase the residence time in the nasal cavity; however, higher viscosity may also result in delay in release of the drug from the carrier to the mucosal surface (Furubayashi et al., 2007). KPF-NE showed viscosities of 2.23 ± 0.01 and 1.93 ± 0.02 cP at 25 and 34°C, respectively. KPF-MNE showed viscosities of 11.48 ± 0.13 and 8.98 ± 0.16 cP at 25 and 34°C, respectively. A Newtonian rheological behavior was demonstrated for the formulations, since they

exhibited constant viscosity; that is, the shear stress was directly proportional to the shear rate and viscosity was independent of shear rate (see Supplementary Data, Fig S1 and S2). As expected, the low viscosity of KPF-NE was very close to that of water, and the addition of chitosan increased considerably the viscosity of the system. The viscosity value of KPF-MNE may contribute to the high nasal absorption efficiency of KPF, according to the described relationship between formulation nasal absorption and viscosity, where moderate viscosity of the dosing formulation improved *in vivo* nasal absorption, while lower viscosity of the application decreased it, by mucociliary clearance (Furubayashi et al., 2007).

3.2. KPF content and association efficiency (%AE)

The amount of KPF present in the KPF-NE and KPF-MNE was found to be 97.52 ± 2.88% and 96.37 ± 2.67%, respectively, for an initial content of 1 mg/ml, indicating a good recovery of KPF in the developed nanoemulsions. The aqueous solubility of pure KPF in water was 0.33 ± 0.04 µg/mL. The incorporation into nanoemulsion showed significant improvement in KPF solubility. Moreover, the association efficiency was determined by measuring the unentrapped drug present in the supernatant, which was obtained after centrifugation of the formulations. The %AE values of KPF-NE and KPF-MNE were 99.38 ± 0.06% and 99.35 ± 0.10%, respectively. As expected, considering KPF lipophilicity, a higher amount of KPF was found in the inner phase of all prepared formulations.

3.3. *Ex vivo* permeation studies

Ex vivo permeation studies were carried out using porcine nasal mucosa as a diffusional barrier to evaluate the permeation from the pure drug KPF and the developed formulations. KPF is a lipophilic drug with log*P* value of 3.11, with limited solubility in aqueous phase (Rothwell et al., 2005). The solubility of a drug in the dissolution medium is essential to maintain sink condition. For this reason, KPF saturation solubility was determined in the receptor medium and was found to be 242.01 ± 7.49 µg/mL. As shown in Table 2, KPF-MNE exhibited higher permeation compared to free KPF and KPF-NE. The significant increase in the amount of KPF

that was able to reach the receptor fluid ($p < 0.0001$) may be attributed to the enhanced permeation activity of chitosan. This activity is due to the interaction of positively charged amino groups of chitosan with the anionic sites present in the mucous layers, mainly sialic acid, affecting the permeability of the epithelial membrane by the transient opening of the tight junctions in the epithelial cells of the mucosal barriers (Amidi et al., 2010; Vllasaliu et al., 2010). An advantage of using nanoparticle systems is that they provide a larger surface area for the interaction between the drug and the epithelial cells and, therefore, increasing the absorption through the nasal mucosa. Although the globule size is lower for KPF-NE, it has been observed that permeability is strongly related to the coating of the nanoparticle. Despite the addition of chitosan to the surface of the droplets increasing the mean diameter of KPF-MNE, KPF permeability was significantly higher in this system.

Another parameter analyzed in this study was the amount of KPF retained in the mucosa tissue after 6 h of experiment. The difference between the cumulative amount of retained KPF from KPF-NE and free-KPF was not statistically significant. On the other hand, there was a significant retention of KPF in the nasal mucosa when carried by mucoadhesive nanoemulsion, which could act as a deposit for its prolonged release ($p < 0.0001$). A justification for the lowest permeability of free KPF could be its hydrophobicity and incomplete solubilization in the solvent (Chao et al., 2012). The enhanced permeation due to the addition of chitosan to the formulation compared to the corresponding nanoemulsion without chitosan was also observed in other works (Kumar et al., 2009; Sood et al., 2014).

Table 2. *Ex vivo* KPF permeation from different formulations in porcine nasal mucosa.

Formulation	Nasal mucosa (μg/cm^2)	Receptor fluid (μg/cm^2)
Free-KPF	5.79 ± 1.15	0.43 ± 0.05
KPF-NE	5.72 ± 0.76	0.9 ± 0.04*
KPF-MNE	13.04 ± 1.97$^{\#}$	4.44 ± 0.36$^{\#}$

Data represent mean ± SD, n = 4, $^{\#}p < 0.001$, $*p < 0.05$ as compared to Free-KPF in each column.

3.4. *In vitro* DPPH assay for antioxidant activity

KPF is reported to be an excellent antioxidant compound, with a potential role in the prevention and treatment of oxidative stress (Calderon-Montano et al., 2011; Devi et al., 2015). The antioxidant capacity of KPF in the encapsulated form was assessed by the *in vitro* DPPH assay. The reduction capability of DPPH radicals was determined by the decrease in its absorbance at 515 nm, which is denoted by a purple color changing to yellow. As expected, a significant decrease in the concentration of the DPPH radical was observed due to the free-radical scavenging activity of KPF, even when incorporated into the nanoemulsion. As shown in Table 3, the average percentages of DPPH obtained in KPF solution, KPF-MNE and KPF-NE were not statistically different ($p < 0.05$). Thus, the nanoemulsion did not compromise the inherent antioxidant activity of KPF.

Table 3. Antioxidant activity of KPF solution, KPF nanoemulsions, and blank formulations, calculated as the inhibition percentage of DPPH radical.

Sample	DPPH inhibition % ± SD
NE	3.41 ± 0.74^{a}
MNE	4.07 ± 1.19^{a}
KPF-NE	93.85 ± 1.16^{b}
KPF-MNE	92.71 ± 0.24^{b}
KPF methanolic solution	92.44 ± 0.19^{b}

Values represent the mean ± standard deviations of 3 independent experiments. Different letters indicate significant statistical differences (ANOVA, Tukey test, $p < 0.05$).

3.5. Preliminary nasal toxicity studies

Nasal mucosa histopathology studies are useful to evaluate any potential toxic effects of a formulation on the integrity of the nasal mucosa. As shown in Figure 2, the mucosa treated with isopropyl alcohol (positive control) showed loss of epithelial cells, with internal tissue damage and shrinkage of the mucosal layer. The treatment with blank formulations, KPF-loaded formulations and PBS pH 6.4 (negative control)

caused no structural damage, and the epithelial layer was intact, indicating that the excipients used in the formulations are biocompatible and safe for nasal administration. Nanoemulsion safety for nasal administration has already been widely demonstrated through nasal toxicity tests (Bshara et al., 2014; Cho et al., 2012; Shah et al., 2015; Sood et al., 2014).

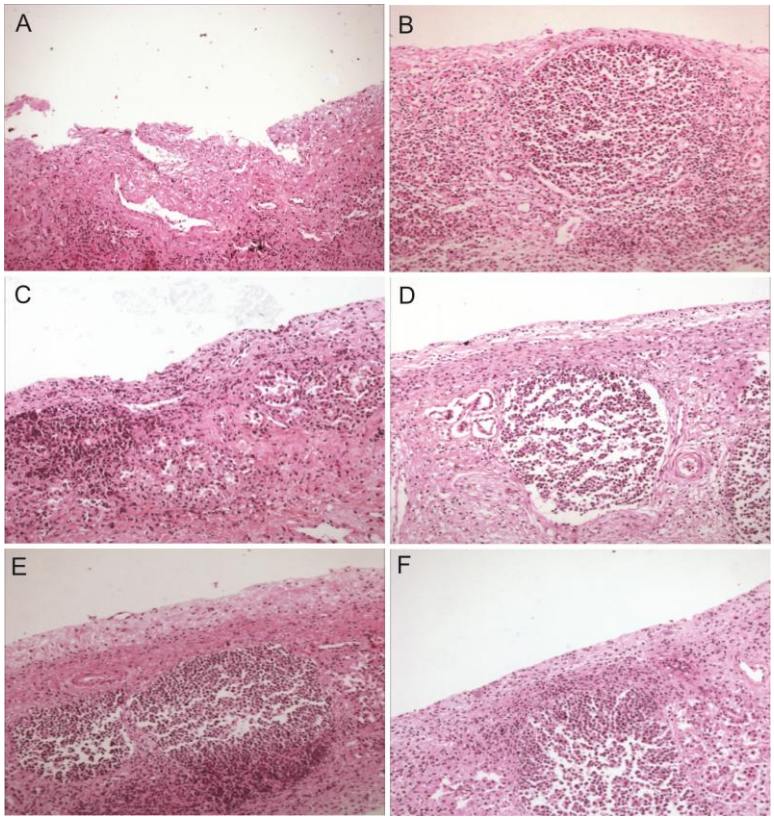

Figure 2. Histopathological sections of porcine nasal mucosa treated with A) IPA, B) PBS pH 6.4, C) NE, D) MNE, E) KPF-NE, F) KPF-MNE.

3.6. Measurement of *ex vivo* mucoadhesive strength

As a predictor of the mucoadhesiveness of the proposed formulations, the mucoadhesion peak and the mucoadhesion work of the nanoemulsions were measured, which are the maximum force required to detach the material under study from the mucosal surface, and the work (applied total force) required for this, respectively.

As shown in Figure 3, KPF-MNE presented significantly higher values of strength (g) and mucoadhesion work (g.s) when compared to KPF-NE ($p < 0.0001$), and both

formulations presented significant differences in comparison to the negative control (PBS) ($p < 0.001$).

The higher value of strength and mucoadhesion work for KPF-MNE compared to KPF-NE could be attributed to the presence of the mucoadhesion property of chitosan, indicating higher residence time at the site of absorption. The mucoadhesive property of the formulation depends on the presence of functional groups that allow mucoadhesion by interaction with mucin. For chitosan, a cationic polymer, the positive charge will allow binding and a strong electrostatic interaction with the negatively charged groups of sialic acid in the mucus present on the surface of the nasal mucosa, and hence the potential for a longer residence time (Bshara et al., 2014).

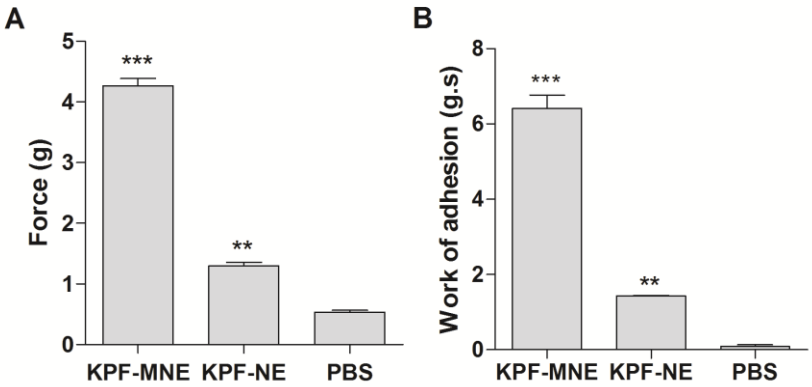

Figure 3. Force (A) and work of mucoadhesion (B) of samples measured by the mucoadhesive strength test. Data were analyzed with one-way ANOVA followed by Tukey's test. Significantly different from the control groups (**$p < 0.001$, ***$p < 0.0001$).

3.7. *In vivo* quantification of KPF in rat's brain

To evaluate the brain targeting after a single dose via intranasal administration, a preliminary brain distribution of KPF in rats was investigated. The drug concentration (ng/g of tissue) in brain tissue after 1 h of nasal administration is given in Figure 4. Extraction efficiency from brain homogenate was found to be greater than 89.45% when analyzed by HPLC, using our previously validated method (Colombo et al., 2017).

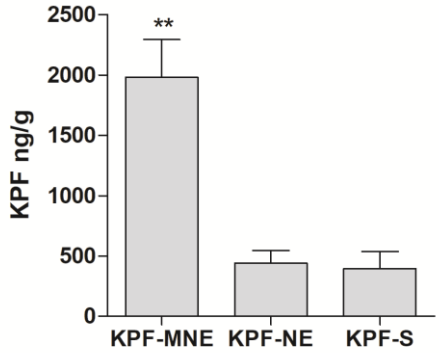

Figure 4. KPF concentration (ng/g of tissue) in rat's brain after 1 h of nasal administration of formulations. Data were analyzed with one-way ANOVA followed by Tukey's test. Significantly different from the control groups (**$p < 0.001$).

The concentration of KPF when loaded into KPF-MNE was found to be significantly higher compared to both KPF-S and KPF-NE (5- and 4.5-fold higher than KPF-S and KPF-NE, respectively). As is evident, the lower amount of KPF reaching the brain following intranasal administration of KPF-S and KPF-NE could be ascribed to rapid mucociliary clearance, as well as to nasal drainage. The use of nanoemulsions to improve nose-to-brain delivery of drugs is widely studied. The higher transport of a drug-loaded nanoemulsion from the nasal cavity to the brain is related to its small globule size, which allows the drug to be transported transcellulary through olfactory neurons to the brain via the various endocytic pathways of sustentacular or neuronal cells in the olfactory membrane (Comfort et al., 2015; Mistry et al., 2009). However, the formulation needs to contain an absorption enhancer and a mucobioadhesive agent for the maintenance of the drug at the site of absorption and to increase transport through the membrane. The addition of a mucoadhesive agent plays a key role in improving brain uptake as a result of the prolonged contact time of the applied formulation with the nasal mucosa (Comfort et al., 2015). Furthermore, chitosan was reported as an absorption enhancer by its ability to open tight junctions in the olfactory and respiratory epithelia (Casettari and Illum, 2014; Vllasaliu et al., 2010). Similar results were obtained by Kumar et al, (Kumar et al., 2008), who showed the superior performance of a mucoadhesive nanoemulsion containing risperidone in comparison to

the nanoemulsion without chitosan and to a simple risperidone solution, after intranasal administration.

To date, no study has been found that quantifies KPF in brain tissue after intranasal administration of KPF-loaded mucoadhesive nanosystems. The first study that proposed the intranasal administration of KPF was recently reported by our research group (Colombo et al., 2017). In our results, the nanoemulsion containing chitosan allowed a significantly better transport of KPF into the brain. This result is in agreement with the results obtained from viscosity, *ex-vivo* mucoadhesive strength and *ex vivo* permeation studies, wherein the formulation with suitable viscosity for nasal administration and the highest mucoadhesion exhibited higher permeation and higher uptake into the brain.

3.8. Assessment of glioma cell viability

In order to determine the antitumor activity of the formulations, rat glioma C6 cells were treated with free KPF, KPF-NE, KPF-MNE (all at 1.0 μM) and blank formulations. After 72 h of incubation, a Trypan blue dye exclusion test was used to evaluate cell viability. The percentage of cell viability was calculated in relation to untreated cells considered as 100% viable. As shown in Figure 5A, KPF-MNE caused a significant decrease in cell viability compared to all other treatment groups. The increased cytotoxic effect of KPF-MNE could be attributed to the better penetration of the drug into the glioma cells due to the positive charge of the carrier. Generally, positively charged nanoparticles exhibit better association with cells, as a result of attractive interactions with the negatively charged cell membrane, leading to a greater uptake rate, and, thus, greater cytotoxicity. Moreover, the small size of the nanoparticles facilitates their uptake by the cells (Hillaireau and Couvreur, 2009). Chitosan presents the ability to facilitate the active transport of nanoparticles via absorptive mediated transcytosis, and chitosan-coated nanoparticles have been extensively used as carriers for tumor targets (Anitha et al., 2012; Chuah et al., 2014; Liu et al., 2012; Yang et al., 2015; Zhu et al., 2009). Interestingly, for the cells treated with blank formulation and 1.0 μM KPF in solution, a significant decrease in cellular viability was not observed, evidencing the importance of the encapsulation of KPF in

the nanosystem. To a lower extent than KPF-MNE, the unloaded nanoformulations also decreased cell viability after 72 h of treatment in relation to untreated cells. This effect may be explained by the physical interaction between the formulation and the cells, allowing them to be detached from the plate. Cytotoxicity is often due to many factors, such as the size, shape, composition, surface charge, and surface hydrophobicity of the nanoparticles (Frohlich, 2012). In order better to understand the mechanisms underlying the anticancer effect, and based on its promising result, we selected KPF-MNE for further analysis of cell-cycle progression and apoptosis induction. As shown in Fig. 5B, the percentage viability of C6 cells decreased when treated with KPF at concentrations of 0.25 to 1.0 μM for KPF-MNE and 1 to 20 μM for free KPF. The IC50 for free KPF was 17.94 ± 5.41 μM, and for KPF-MNE it was 0.84 ± 0.15 μM.

Furthermore, time-dependent stability of KPF-MNE were demonstrated under cell culture conditions (see Suplementary Data, Fig. S3).

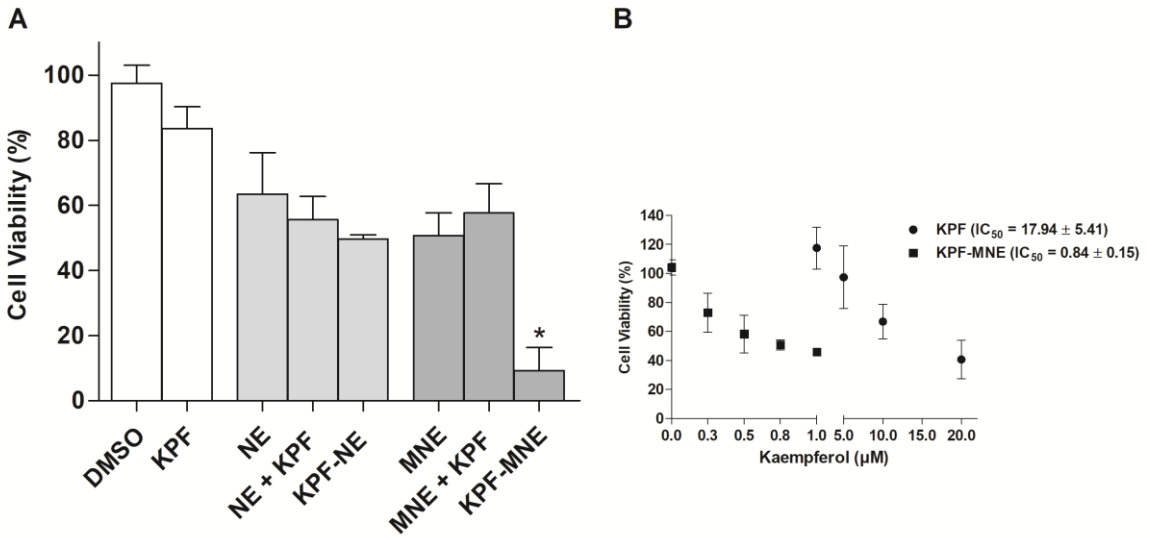

Figure 5. A) Antiproliferative effect of free KPF, KPF-NE and KPF-MNE at 1 μM by Trypan blue exclusion assays. B) Effect of kaempferol on C6 glioma cell line. Cell viability is presented in relation to control. Vehicle control (DMSO) did not interfere significantly with cell viability. The data represent the mean of three independent experiments performed in triplicate ± SD. Data were analyzed with one-way ANOVA followed by Tukey's test. Significantly different from the control groups (*$p < 0.05$).

3.9. Cellular uptake of kaempferol

For evaluation of cellular uptake, we tested different approaches with some limitations: After 24 h of treatment, KPF was detectable neither for KPF nor for KPF-MNE treatment. Treatment for 72 h resulted in significant death, and it was not possible to quantify the remaining cells. The treatment concentration of 5 µM was chosen since when it was treated at 1 µM, KPF was below the limit of quantification by HPLC. Thus, KPF and KPF-MNE were added at 5 µM for 48 h of treatment.

Results showed that cellular content of KPF carried by mucoadhesive nanoemulsion achieved 4.40 ± 1.5 nmol/mg protein. On the other hand, when cells were treated with free KPF, KPF was not detectable by HPLC analysis. No interfering peaks were observed within the time frame in which KPF is detected. Blank cell samples did not demonstrate any interference peaks. Therefore, considering the IC50 values, the cytotoxicity of KPF-MNE in GBM is about 20-fold greater than free KPF (Figure 5B) as result of higher cellular uptake when KPF is loaded into a mucoadhesive nanoemulsion.

3.10. Cell-cycle analysis

Considering that KPF-MNE inhibits cell growth in C6 cells, we decided to evaluate whether this inhibition effect could be due to an arrest of cell-cycle progression. Flow cytometry analysis showed that KPF-MNE did not alter the DNA content after treatment (Fig. 6), indicating that it did not affect the cell-cycle progression. Despite studies indicating that exposure to KPF resulted in cell-cycle arrest in different tumor cell lines (Cho and Park, 2013; Choi and Ahn, 2008; Dang et al., 2015; Song et al., 2014), there were no differences among free KPF, MNE, free KPF + MNE and KPF-MNE at 1µM after 72 h. It is a important finding, since cell-cycle arrest could be a reason for the failure of chemotherapy, where, after finishing the treatment, cancer cell may restore their proliferation capability (Silva et al., 2016).

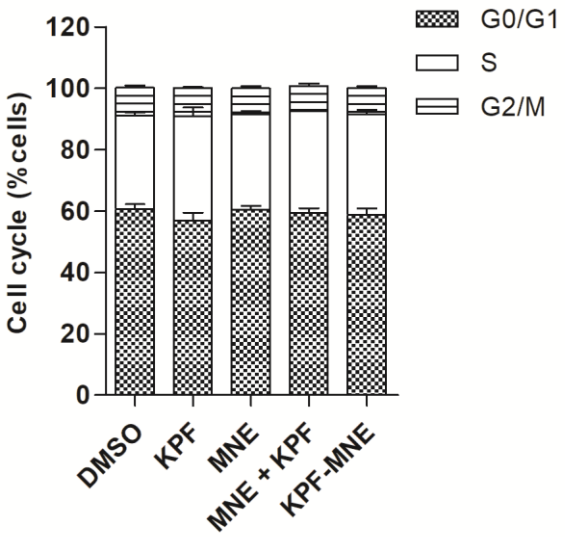

Figure 6. Representative histograms of the percentage of cells in the G1, S, G2/M and sub-G1 phase of the cell cycle after treatment with free KPF, MNE, MNE+ KPF and KPF-MNE at 1 μM for 72 h. Data were analyzed with one-way ANOVA followed by Tukey's test. Significantly different from the control groups (*$p < 0.05$).

3.11. Annexin V/PI assay

To verify whether KPF-MNE could induce apoptotic or necrotic cell death, glioma cells were treated with KPF 1.0 μM for 72 h and AnnexinV-PI assay was carried out by flow cytometry analysis. KPF-MNE did not increase PI incorporation in C6 cells, indicating the absence of necrotic cell death (data not shown). However, treatment of glioma cells with KPF-MNE promoted a significant increase in early apoptosis content (EA = 15.1 ± 4.2%) and late apoptosis (15.2 ± 6.2%) as shown in Figure 7E. Overall, KPF-MNE induced 30.4 ± 8.4% apoptosis after treatment (total apoptosis, Figure 7F). Free KPF (KPF) did not increase apoptosis at 1μM, confirming the higher cytotoxic potential of KPF-MNE. Treatments with MNE, MNE+KPF or DMSO did not show significant alterations in apoptotic cell death either (Figure 7A–D).

Kaempferol is known to induce apoptosis in numerous cancer cell lines (Chen and Chen, 2013). In vitro, KPF has been described to induce apoptosis in glioma cells by elevating intracellular oxidative stress by a decrease in the levels of redox active proteins SOD-1 and TRX-1, which are involved in maintaining cellular redox balance and through caspase-dependent mechanisms (Jeong et al., 2009; Sharma et al., 2007).

Seibert and collaborators (Seibert et al., 2011) have shown that cytotoxicity from KPF was not due to H_2O_2 generation in the culture medium. Importantly, concentrations of KPF protecting glioma cells under oxidative stress were identical to those causing cell damage under normal conditions (in the absence of oxidative stress) (Ruweler et al., 2008).

In addition to the antiproliferative effect, our results showed the ability of KPF-MNE to induce apoptosis in glioma cells at concentrations as low as 1.0 µM and to a greater extent than other studies that used free KPF (Jeong et al., 2009; Seibert et al., 2011; Sharma et al., 2007; Siegelin et al., 2008).

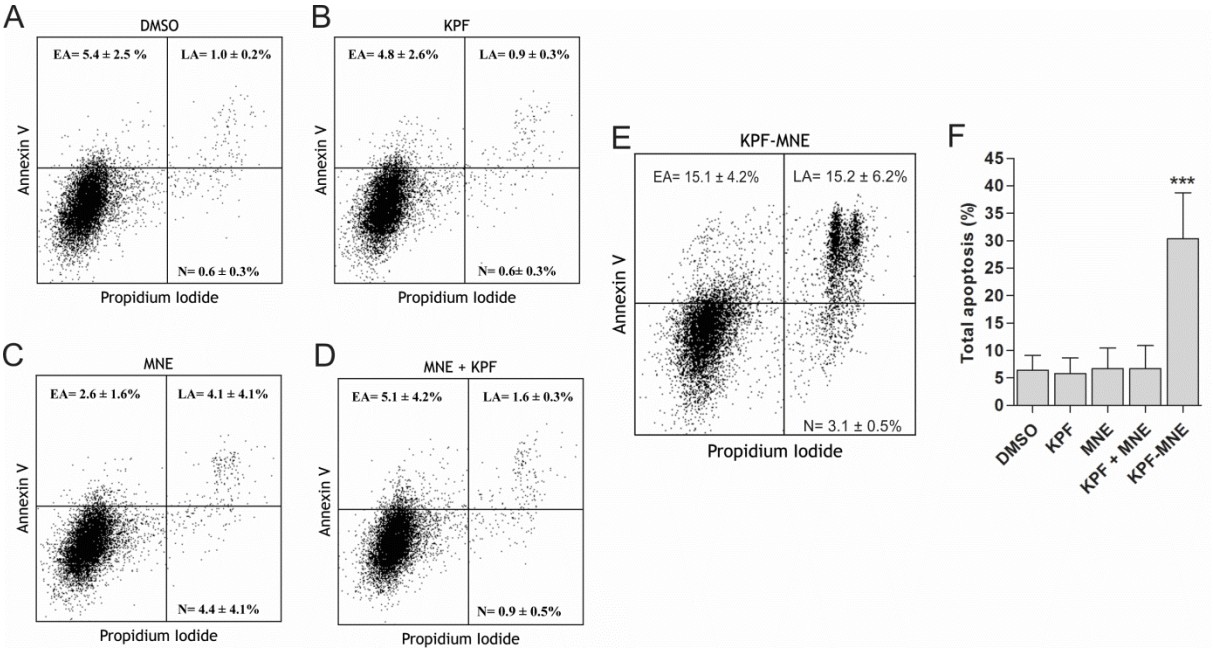

Figure 7. A–D) Representative images containing the average relative number of cells after treatment with DMSO, free KPF, MNE, MNE+ KPF and KPF-MNE at 1 µM for 72 h. E) Representative images containing the average relative number of cells after treatment with free KPF-MNE at 1 µM for 72 h. The gate settings distinguish between viable cells (bottom left), necrotic cells (top left), early apoptotic cells (bottom right) and late apoptotic cells (top right). F) Quantitative analysis of total apoptosis in cells treated with free KPF, KPF+MNE and KPF-MNE at 1 µM for 72 h. The values are presented as the means ± S.D. of three independent experiments. Data were analyzed with one-way ANOVA followed by Tukey's test. Significantly different from the control groups (*$p < 0.05$, ***$p < 0.0001$).

4. CONCLUSIONS

Kaempferol-loaded nanoemulsions and mucoadhesive nanoemulsions were successfully prepared via a high-pressure homogenization technique, and showed nanometric globule size, high loading capacity and entrapment efficiency, and were able to preserve their antioxidant potential. Furthermore, the developed nanoemulsions showed no toxicity towards nasal mucosa. *Ex vivo* permeation studies and *in vivo* biodistribution studies confirmed the superiority of the developed chitosan-coated nanoemulsion for brain targeting after intranasal administration compared to KPF-NE and free KPF. The mucoadhesive nanoemulsion decreased the viability of glioma cells by enhancing apoptosis, a goal for cancer treatment.

Taken together, KPF-MNE seems to be a promising approach for nose-to-brain delivery of KPF and hence provides an important therapeutic candidate for pre-clinical glioma treatment.

Acknowledgements

This work was financially supported by Coordenação de Aperfeiçoamento de Pessoal de Nível Superior/Ministério da Educação – CAPES/MEC, Brazil (Network Nanobiotec-grant 902/2009 and PROCAD-grant 552457/2011-6), Conselho Nacional de Desenvolvimento Científico e Tecnológico - CNPq (grants 453927/2014-9 and INCT 2014 - 465671/2014-4) and Fundação de Amparo à Pesquisa do Rio Grande do Sul – FAPERGS (Edital PqG 2017 – T.O. 17/2551-0001). The authors would also like to thank these agencies for their research fellowships.

REFERENCES

Alam, M.I., Beg, S., Samad, A., Baboota, S., Kohli, K., Ali, J., Ahuja, A., Akbar, M., 2010. Strategy for effective brain drug delivery. European Federation for Pharmaceutical Sciences 40, 385-403.

Amidi, M., Mastrobattista, E., Jiskoot, W., Hennink, W.E., 2010. Chitosan-based delivery systems for protein therapeutics and antigens. Advanced Drug Delivery Reviews 62, 59-82.

Anitha, A., Maya, S., Deepa, N., Chennazhi, K.P., Nair, S.V., Jayakumar, R., 2012. Curcumin-loaded N,O-carboxymethyl chitosan nanoparticles for cancer drug delivery. Journal of biomaterials science. Polymer edition. 23, 1381-1400.

Arora, P., Sharma, S., Garg, S., 2002. Permeability issues in nasal drug delivery. Drug Discovery Today 7, 967-975.

Bandaruk, Y., Mukai, R., Terao, J., 2014. Cellular uptake of quercetin and luteolin and their effects on monoamine oxidase-A in human neuroblastoma SH-SY5Y cells. Toxicology reports 1, 639-649.

Barve, A., Chen, C., Hebbar, V., Desiderio, J., Saw, C.L., Kong, A.N., 2009. Metabolism, oral bioavailability and pharmacokinetics of chemopreventive kaempferol in rats. Biopharmaceutics & Drug Disposition 30, 356-365.

Behin, A., Hoang-Xuan, K., Carpentier, A.F., Delattre, J.Y., 2003. Primary brain tumours in adults. Lancet 361, 323-331.

Bernkop-Schnurch, A., Dunnhaupt, S., 2012. Chitosan-based drug delivery systems. European Journal of Pharmaceutics and Biopharmaceutics 81, 463-469.

Bshara, H., Osman, R., Mansour, S., El-Shamy Ael, H., 2014. Chitosan and cyclodextrin in intranasal microemulsion for improved brain buspirone hydrochloride pharmacokinetics in rats. Carbohydr Polym 99, 297-305.

Caddeo, C., Manconi, M., Fadda, A.M., Lai, F., Lampis, S., Diez-Sales, O., Sinico, C., 2013. Nanocarriers for antioxidant resveratrol: formulation approach, vesicle self-assembly and stability evaluation. Colloids Surf B Biointerfaces 111, 327-332.

Calderon-Montano, J.M., Burgos-Moron, E., Perez-Guerrero, C., Lopez-Lazaro, M., 2011. A review on the dietary flavonoid kaempferol. Mini-Reviews in Medicinal Chemistry 11, 298-344.

Callens, C., Ceulemans, J., Ludwig, A., Foreman, P., Remon, J.P., 2003. Rheological study on mucoadhesivity of some nasal powder formulations. Eur J Pharm Biopharm 55, 323-328.

Carvalho, F.C., Campos, M.L., Peccinini, R.G., Gremiao, M.P., 2013. Nasal administration of liquid crystal precursor mucoadhesive vehicle as an alternative antiretroviral therapy. European Journal of Pharmaceutics and Biopharmaceutics 84, 219-227.

Casettari, L., Illum, L., 2014. Chitosan in nasal delivery systems for therapeutic drugs. Journal of Controlled Release 190, 189-200.

Chao, Y., Huang, C.T., Fu, L.T., Huang, Y.B., Tsai, Y.H., Wu, P.C., 2012. The effect of submicron emulsion systems on transdermal delivery of kaempferol. Chem Pharm Bull 60, 1171-1175.

Chen, A.Y., Chen, Y.C., 2013. A review of the dietary flavonoid, kaempferol on human health and cancer chemoprevention. Food Chemistry 138, 2099-2107.

Chen, Z.P., Sun, J., Chen, H.X., Xiao, Y.Y., Liu, D., Chen, J., Cai, H., Cai, B.C., 2010. Comparative pharmacokinetics and bioavailability studies of quercetin, kaempferol and isorhamnetin after oral administration of Ginkgo biloba extracts, Ginkgo biloba extract phospholipid complexes and Ginkgo biloba extract solid dispersions in rats. Fitoterapia 81, 1045-1052.

Cho, H.J., Ku, W.S., Termsarasab, U., Yoon, I., Chung, C.W., Moon, H.T., Kim, D.D., 2012. Development of udenafil-loaded microemulsions for intranasal delivery: in vitro and in vivo evaluations. Int J Pharm 423, 153-160.

Cho, H.J., Park, J.H., 2013. Kaempferol Induces Cell Cycle Arrest in HT-29 Human Colon Cancer Cells. J Cancer Prev 18, 257-263.

Choi, E.J., Ahn, W.S., 2008. Kaempferol induced the apoptosis via cell cycle arrest in human breast cancer MDA-MB-453 cells. Nutr Res Pract 2, 322-325.

Chuah, L.H., Roberts, C.J., Billa, N., Abdullah, S., Rosli, R., 2014. Cellular uptake and anticancer effects of mucoadhesive curcumin-containing chitosan nanoparticles. Colloids and Surfaces B: Biointerfaces 116, 228-236.

Colombo, M., Melchiades, G.d.L., Figueiró, F., Battastini, A.M.O., Teixeira, H.F., Koester, L.S., 2017. Validation of an HPLC-UV method for analysis of Kaempferol-loaded nanoemulsion and its application to in vitro and in vivo tests. Journal of pharmaceutical and biomedical analysis 145, 831-837.

Comfort, C., Garrastazu, G., Pozzoli, M., Sonvico, F., 2015. Opportunities and challenges for the nasal administration of nanoemulsions. Curr Top Med Chem 15, 356-368.

Dang, Q., Song, W., Xu, D., Ma, Y., Li, F., Zeng, J., Zhu, G., Wang, X., Chang, L.S., He, D., Li, L., 2015. Kaempferol suppresses bladder cancer tumor growth by inhibiting cell proliferation and inducing apoptosis. Mol Carcinog 54, 831-840.

Devi, K.P., Malar, D.S., Nabavi, S.F., Sureda, A., Xiao, J., Nabavi, S.M., Daglia, M., 2015. Kaempferol and inflammation: From chemistry to medicine. Pharmacol Res 99, 1-10.

Frohlich, E., 2012. The role of surface charge in cellular uptake and cytotoxicity of medical nanoparticles. International Journal of Nanomedicine 7, 5577-5591.

Furubayashi, T., Inoue, D., Kamaguchi, A., Higashi, Y., Sakane, T., 2007. Influence of formulation viscosity on drug absorption following nasal application in rats. Drug Metab Pharmacokinet 22, 206-211.

Hillaireau, H., Couvreur, P., 2009. Nanocarriers' entry into the cell: relevance to drug delivery. Cellular and Molecular Life Sciences 66, 2873-2896.

Illum, L., 2000. Transport of drugs from the nasal cavity to the central nervous system. European Journal of Pharmaceutical Sciences 11, 1-18.

Jeong, J.C., Kim, M.S., Kim, T.H., Kim, Y.K., 2009. Kaempferol induces cell death through ERK and Akt-dependent down-regulation of XIAP and survivin in human glioma cells. Neurochem Res 34, 991-1001.

Kumar, M., Misra, A., Babbar, A.K., Mishra, A.K., Mishra, P., Pathak, K., 2008. Intranasal nanoemulsion based brain targeting drug delivery system of risperidone. Int J Pharm 358, 285-291.

Kumar, M., Pathak, K., Misra, A., 2009. Formulation and characterization of nanoemulsion-based drug delivery system of risperidone. Drug Development and Industrial Pharmacy 35, 387-395.

Liu, J., Xu, L., Liu, C., Zhang, D., Wang, S., Deng, Z., Lou, W., Xu, H., Bai, Q., Ma, J., 2012. Preparation and characterization of cationic curcumin nanoparticles for improvement of cellular uptake. Carbohydrate Polymers 90, 16-22.

Liu, R., Wang, X., Zhao, Y., Wang, Z., Du, L., 2006. The uptake behaviors of kaempferol and quercetin through rat primary cultured cortical neurons. Biomedical Chromatography 20, 1178-1184.

Lopez-Sanchez, C., Martin-Romero, F.J., Sun, F., Luis, L., Samhan-Arias, A.K., Garcia-Martinez, V., Gutierrez-Merino, C., 2007. Blood micromolar concentrations of kaempferol afford protection against ischemia/reperfusion-induced damage in rat brain. Brain Res 28, 123-137.

Luo, H., Jiang, B., Li, B., Li, Z., Jiang, B.H., Chen, Y.C., 2012. Kaempferol nanoparticles achieve strong and selective inhibition of ovarian cancer cell viability. International Journal of Nanomedicine 7, 3951-3959.

Mistry, A., Stolnik, S., Illum, L., 2009. Nanoparticles for direct nose-to-brain delivery of drugs. Int J Pharm 379, 146-157.

Nakatsuma, A., Fukami, T., Suzuki, T., Furuishi, T., Tomono, K., Hidaka, S., 2010. Effects of kaempferol on the mechanisms of drug resistance in the human glioblastoma cell line T98G. Pharmazie 65, 379-383.

Pardeshi, C.V., Belgamwar, V.S., 2013. Direct nose to brain drug delivery via integrated nerve pathways bypassing the blood-brain barrier: an excellent platform for brain targeting. Expert Opin Drug Deliv 10, 957-972.

Rothwell, J.A., Day, A.J., Morgan, M.R., 2005. Experimental determination of octanol-water partition coefficients of quercetin and related flavonoids. J Agric Food Chem 53, 4355-4360.

Ruweler, M., Anker, A., Gulden, M., Maser, E., Seibert, H., 2008. Inhibition of peroxide-induced radical generation by plant polyphenols in C6 astroglioma cells. Toxicol In Vitro 22, 1377-1381.

Seibert, H., Maser, E., Schweda, K., Seibert, S., Gulden, M., 2011. Cytoprotective activity against peroxide-induced oxidative damage and cytotoxicity of flavonoids in C6 rat glioma cells. Food and Chemical Toxicology 49, 2398-2407.

Shah, B., Khunt, D., Misra, M., Padh, H., 2016. Non-invasive intranasal delivery of quetiapine fumarate loaded microemulsion for brain targeting: Formulation, physicochemical and pharmacokinetic consideration. European Journal of Pharmaceutical Sciences 91, 196-207.

Shah, B.M., Misra, M., Shishoo, C.J., Padh, H., 2015. Nose to brain microemulsion-based drug delivery system of rivastigmine: formulation and ex-vivo characterization. Drug Deliv 22, 918-930.

Sharma, V., Joseph, C., Ghosh, S., Agarwal, A., Mishra, M.K., Sen, E., 2007. Kaempferol induces apoptosis in glioblastoma cells through oxidative stress. Mol Cancer Ther 6, 2544-2553.

Siegelin, M.D., Reuss, D.E., Habel, A., Herold-Mende, C., von Deimling, A., 2008. The flavonoid kaempferol sensitizes human glioma cells to TRAIL-mediated apoptosis by proteasomal degradation of survivin. Mol Cancer Ther 7, 3566-3574.

Silva, A.O., Dalsin, E., Onzi, G.R., Filippi-Chiela, E.C., Lenz, G., 2016. The regrowth kinetic of the surviving population is independent of acute and chronic responses to temozolomide in glioblastoma cell lines. Exp Cell Res 348, 177-183.

Song, W., Dang, Q., Xu, D., Chen, Y., Zhu, G., Wu, K., Zeng, J., Long, Q., Wang, X., He, D., Li, L., 2014. Kaempferol induces cell cycle arrest and apoptosis in renal cell carcinoma through EGFR/p38 signaling. Oncol Rep 31, 1350-1356.

Sood, S., Jain, K., Gowthamarajan, K., 2014. Optimization of curcumin nanoemulsion for intranasal delivery using design of experiment and its toxicity assessment. Colloids and surfaces. B, Biointerfaces 113, 330-337.

Stupp, R., Hegi, M.E., Mason, W.P., van den Bent, M.J., Taphoorn, M.J., Janzer, R.C., Ludwin, S.K., Allgeier, A., Fisher, B., Belanger, K., Hau, P., Brandes, A.A., Gijtenbeek, J., Marosi, C., Vecht, C.J., Mokhtari, K., Wesseling, P., Villa, S., Eisenhauer, E., Gorlia, T., Weller, M., Lacombe, D., Cairncross, J.G., Mirimanoff, R.O., 2009. Effects of radiotherapy with concomitant and adjuvant temozolomide versus radiotherapy alone on survival in glioblastoma in a randomised phase III study: 5-year analysis of the EORTC-NCIC trial. Lancet Oncol 10, 459-466.

Sultana, B., Anwar, F., 2008. Flavonols (kaempeferol, quercetin, myricetin) contents of selected fruits, vegetables and medicinal plants. Food chemistry 108, 879-884.

USP, 2011. The United States Pharmacopeia. 33 ed. Rockville: United States Pharmacopeia Convetional.

Van Meir, E.G., Hadjipanayis, C.G., Norden, A.D., Shu, H.K., Wen, P.Y., Olson, J.J., 2010. Exciting new advances in neuro-oncology: the avenue to a cure for malignant glioma. CA Cancer J Clin 60, 166-193.

van Woensel, M., Wauthoz, N., Rosiere, R., Amighi, K., Mathieu, V., Lefranc, F., van Gool, S.W., de Vleeschouwer, S., 2013. Formulations for Intranasal Delivery of

Pharmacological Agents to Combat Brain Disease: A New Opportunity to Tackle GBM? Cancers 5, 1020-1048.

Vllasaliu, D., Exposito-Harris, R., Heras, A., Casettari, L., Garnett, M., Illum, L., Stolnik, S., 2010. Tight junction modulation by chitosan nanoparticles: comparison with chitosan solution. Int J Pharm 400, 183-193.

Yang, L., Gao, S., Asghar, S., Liu, G., Song, J., Wang, X., Ping, Q., Zhang, C., Xiao, Y., 2015. Hyaluronic acid/chitosan nanoparticles for delivery of curcuminoid and its in vitro evaluation in glioma cells. International Journal of Biological Macromolecules 72, 1391-1401.

Zhu, L., Ma, J., Jia, N., Zhao, Y., Shen, H., 2009. Chitosan-coated magnetic nanoparticles as carriers of 5-fluorouracil: preparation, characterization and cytotoxicity studies. Colloids and Surfaces B: Biointerfaces 68, 1-6.

Supplementary Material

KAEMPFEROL-LOADED MUCOADHESIVE NANOEMULSION FOR INTRANASAL ADMINISTRATION REDUCES GLIOMA GROWTH *IN VITRO*

Mariana Colombo, Fabrício Figueiró, Amanda de Fraga Dias, Helder Ferreira Teixeira, Ana Maria Oliveira Battastini, Letícia Scherer Koester

1) Viscosity and rheological behavior of formulations

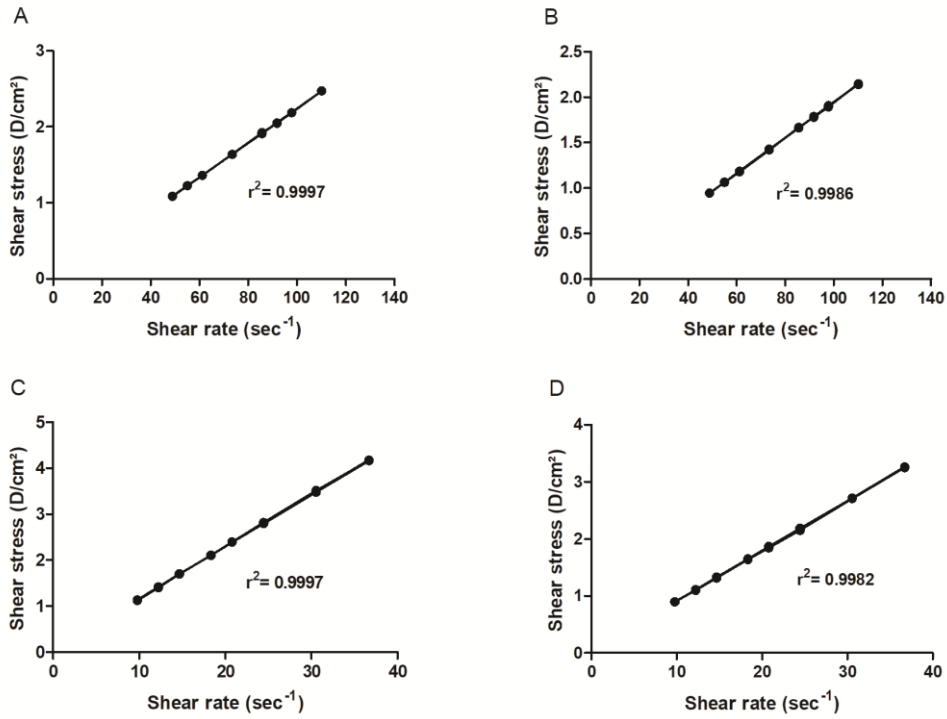

Fig. S1. Shear stress versus shear strain rate. A) KPF-NE (25 °C), B) KPF-NE (34 °C), C) KPF-MNE (25 °C), D) KPF-NE (34 °C).

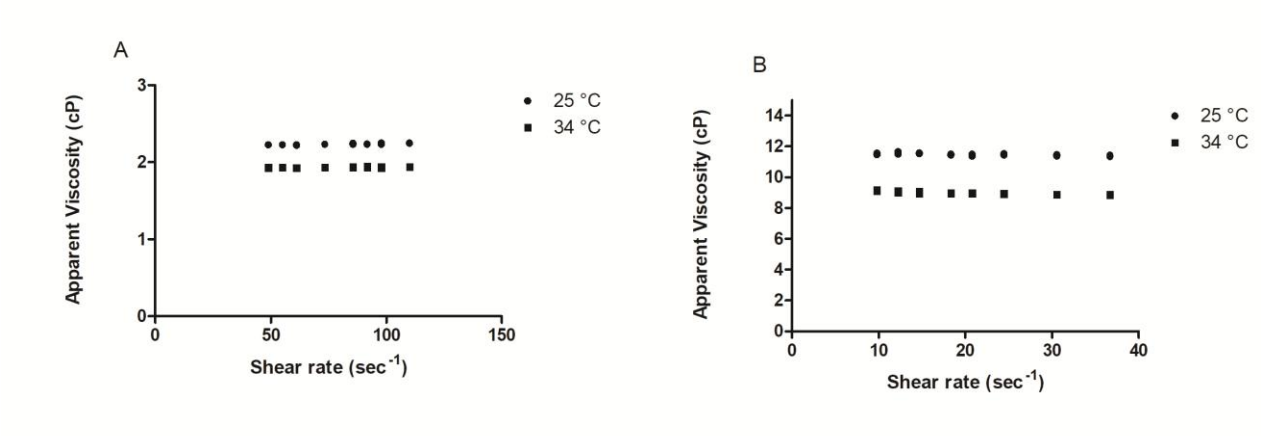

Fig. S2. Viscosity of formulations as function of shear rate. A) KPF-NE B) KPF-MNE.

2) Incubation time-dependent stability of KPF-MNE

KPF-MNE (at 1 μM) was dispersed in DMEM cell culture medium containing 5% FBS and maintained at 37 °C and 5% CO_2 up to 72 h. The measurements were conducted with the Zetasizer (ZS90, Malvern Instruments Ltd., UK). When nanoemulsion was added to the culture medium no change in the appearance of the medium was observed since a very low amount of nanoemulsion was added (0.029% v/v). Fig. S3 illustrates the time evolution of the particle size distribution curves during incubation. The inspection of the plots reveals similar Gaussian monomodal size distribution curves described the behavior of KPF-MNE up to 72 h of incubation, showing the stability of KPF-MNE during the *in intro* tests.

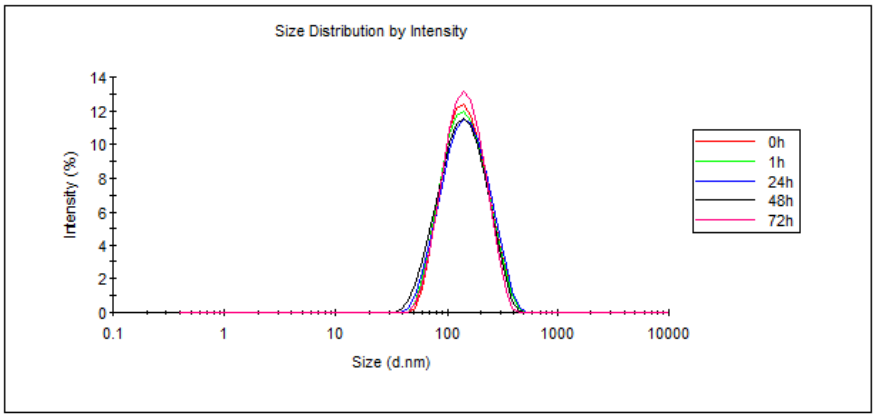

Fig. S3. Time evolution of the size distribution curves of KPF-MNE incubated (37 °C) in DMEM culture medium.

CAPÍTULO II

Desenvolvimento de dispersões sólidas contendo kaempferol para administração oral

INTRODUÇÃO

Uma vez que o KPF possui baixas hidrossolubilidade e biodisponibilidade oral, estratégias de formulação são necessárias para contornar tais características.

Seguindo no desenvolvimento de *drug delivery systems* de fácil administração e alta eficiência, como, por exemplo, desenvolvimento de nanoemulsões para uso intranasal (etapa já concluída no capítulo I da presente tese), o capítulo II apresenta o desenvolvimento e caracterização de dispersões sólidas para administração oral.

Primeiramente, verificou-se a ausência de estudos na literatura sobre dispersões sólidas contendo kaempferol. Assim, ampliou-se as ferramentas de busca e, na publicação I (artigo a ser submetido), foi realizada uma revisão sistemática sobre a utilização de dispersões sólidas como estratégia para melhorar o perfil de dissolução e biodisponibilidade de flavonoides.

Na publicação II, após a seleção do melhor carreador e proporção entre kaempferol e polímero, dois métodos de preparação foram utilizados, método por fusão e por evaporação do solvente. Ambas formulações foram caracterizadas por espectroscopia na região do infravermelho, difração de raios X, microscopia eletrônica de varredura, calorimetria exploratória diferencial, teor, solubilidade e dissolução em meio ácido. Além disso, após a administração oral a ratos, os perfis farmacocinéticos foram demonstrados.

CAPÍTULO II - Publicação I

Artigo a ser submetido

FLAVONOIDS DELIVERY BY SOLID DISPERSION: A SYSTEMATIC REVIEW

Mariana Colombo[a], Luana Roberta Michels[a], Helder Ferreira Teixeira[a], Letícia Scherer Koester[a*]

[a]Programa de Pós-Graduação em Ciências Farmacêuticas, Faculdade de Farmácia, Universidade Federal do Rio Grande do Sul (UFRGS), Av. Ipiranga, 2752, 90610-000, Porto Alegre, RS, Brazil.

*Corresponding author: Dr. Letícia S. Koester, Faculdade de Farmácia/UFRGS, Av. Ipiranga, 2752/607, Porto Alegre-RS, 90.610-000, Brazil. E-mail:leticia.koester@ufrgs.br

ABSTRACT

The poor water solubility of flavonoids composes the greatest challenge to increase the oral bioavailability of these compounds. Nevertheless, several potential positive effects of flavonoids are demonstrated by many studies and therefore much attention has been paid to the development of ways to improve their solubility, such as solid dispersions (SD). Therefore, the aim of this review is present a detailed analysis of the current literature which utilized SD approach to improve the solubility, dissolution, and oral bioavailability parameters of flavonoids to be useful in future researches. The results were presented evidencing the potential of the SD of flavonoids divided by their subclasses. In general, the studies concluded that SD developed by different methods using different carriers are an excellent alternative to improve solubility, dissolution and significantly increase the oral bioavailability of flavonoids.

Keywords: Solid dispersion, flavonoids, poor water solubility, dissolution, bioavailability.

1. Introduction

Polyphenols or phenolic compounds constitute one of the most numerous and widely distributed groups in the plant kingdom (Bravo, 1998). Polyphenols are secondary plant metabolites found in fruits, vegetables, spices, nuts, grains, tea, coffee or wine characterized by at least one aromatic ring with one or more hydroxyl groups (Kaur and Kaur, 2014). They differ in terms of number of aromatic rings and number and position of phenolic groups and are composed of more than 8,000 different compounds, among them over 4000 flavonoids have been identified (Bravo, 1998; Tsao, 2010). Polyphenols can be preliminarily classified in flavonoids (two aromatic rings connected by a three-carbon bridge) or non-flavonoids compounds (heterogeneous class of compounds) (Del Rio et al., 2013; Vittorio et al., 2017).

Flavonoids are characterized by a diphenylpropane structure, consisting of two benzene rings joined by a straight chain of three carbons (C6-C3-C6). In most cases, the three carbons form a closed pyran ring, thus forming a structure of 15 carbon atoms, comprising three rings, called A, B and C, shown in Figure 1. The classes of flavonoids differ in the degree of oxidation and in the C-ring substitution pattern, whereas compounds within a class differ in the substitution pattern of rings A and B. Depending on the variations in the heterocyclic ring C, flavonoids can be divided into subclasses: flavones (apigenin, luteolin), flavonols (quercetin, kaempferol, myricetin), flavanols or catechins (catechin, epicatechin, epigallocatechin), isoflavones (genistein, daidzein, glycetein, biochanin A, formononetin), flavanones (naringenin, hesperitin), flavanonols (taxifolin) and anthocyanidins (cyanidin, pelargonidine, petunidine). Chalcones, though lacking the heterocyclic ring C, are still categorized as members of the flavonoid family. The basic flavonoid structure is aglycone, however, in plants, most of flavonoids occur as glycosides (Del Rio et al., 2013; Kumar and Pandey, 2013; Tsao, 2010).

Extensive research in the past years shed light on various biological activities of these substances, including antioxidant, anti-inflammatory, and anticancer activities. Moreover, epidemiological studies have showed that periodic consumption of flavonoids is linked to a reduced risk of long-term diseases such as cancer and neurodegenerative diseases (Rodriguez-Mateos et al., 2014; Yao et al., 2004).

However, the efficacy of these compounds in *in vivo* is different from *in vitro* experiments. The effectives concentrations of flavonoids strongly depends of their metabolism and bioavailability (Hu et al., 2017b; Teng and Chen, 2018). They show a relatively low bioavailability due to intrinsic factors (chemical structure, molecular weight, and poor aqueous solubility), and extrinsic factors (instability in the gastrointestinal tract, extensive phase I and phase II metabolism, insufficient gastric residence time and rapid elimination) (Teng and Chen, 2018).

Drugs with dissolution-limited absorption often result in high intra-patient variability, which turns out difficult the therapeutic drug monitoring. The majority of flavonoids belong to class II (low solubility and high permeability) and class IV (low solubility and low permeability) BCS classes. Consequently, the clinical applications of these compounds are still limited (Kaur and Kaur, 2014; Leonarduzzi et al., 2010; Squillaro et al., 2018). To address this, several approaches can be successfully used to ameliorate the chemical stability, enhance the solubility and permeability rate of these compounds (Ciurana and Rodriguez, 2017; Hu et al., 2017a; Kaur and Kaur, 2014; Khushnud and Mousa, 2013; Squillaro et al., 2018). These techniques include micronization, formulation of inclusion complexes, solid lipid nanoparticles, polymeric nanoparticles, liposomes, self-emulsifying delivery system (SEDDS), and solid dispersion (SD) (Kaur and Kaur, 2014; Squillaro et al., 2018; Vittorio et al., 2017). From this varied list of approaches, SD is considered as one of the most successful strategies to overcome the low solubility and enhancing oral drug bioavailability of poorly water soluble drugs. Solid dispersions consists of a molecular or amorphous mixtures of poorly water soluble drugs in hydrophilic matrix at the solid state in which the polymer properties play an crucial role in the drug dissolution profile (Vo et al., 2013).

Numerous reviews have provided discussions of SD as an effective and versatile drug delivery system (Huang and Dai, 2014; Mishra et al., 2015; Vasconcelos et al., 2016; Vo et al., 2013). In the same way, there are many reviews focusing in flavonoids and their solubility and bioavailability issues (Kumar and Pandey, 2013; Leonarduzzi et al., 2010; Squillaro et al., 2018; Wang et al., 2013). Nevertheless, a review of the

studies that applied the principle of solid dispersions-based formulations for flavonoids is lacking.

The aim of this review is to provide a detailed analysis of the current literature which utilized solid dispersion approach to improve the solubility, dissolution, and oral bioavailability of flavonoids. Thus, this information could be useful and insightful for future research to facilitate the improvement of these flavonoid parameters in solid dispersion-based formulation.

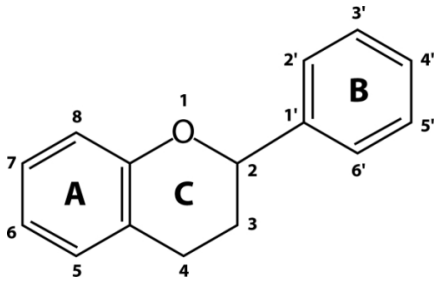

Figure 1. Basic flavonoid structure.

2. Methods

2.1 Search strategy

The internationally accepted Preferred Reporting Items for Systematic Reviews and Meta-Analyses (PRISMA) standard was used for this systematic review (Moher et al., 2009). A search of Medline and Embase databases was conducted for published studies. The keyword search terms were "solid dispersion" and the main classes of flavonoids. The date of the last search was December 12, 2018. The specific keywords that have been used in this search strategy are shown in Supplementary materials.

2.2. Study Selection and Evaluation

After removal of duplicates, the titles and/or abstracts of all articles resulting from the database searches were screened. A study was eligible for this review if it contained original data and a discussion on solid dispersion based formulation containing at least one flavonoid. Only English language papers were included.

Quantitative analyses were conducted to disclose the enhancement power of solid dispersion on drug oral bioavailability across different studies. Therefore, only studies that developed solid dispersion formulation for oral drug delivery, improving the

bioavailability of the flavonoid, have been used. From each eligible collected data, the bioavailability enhancement was calculated as fold-change compared to control group (pure drug), based on two major pharmacokinetic parameters: area under the plasma concentration time curve ($AUC_{0\rightarrow t}$) and maximum plasma concentration (Cmax).

3. Results and Discussion

3.1. General characteristics of literature search

The initial database search according to the applied strategy identified a total of 278 articles. After the review process by proofreading the relevant literatures, we included seven additional records obtained from references. Six studies were excluded because the full text was not found despite an extensive search. After removing duplicates and reviews, excluding some articles that did not discuss solid dispersion and polyphenols, 56 articles were included in this review (Figure 2). The studied flavonoid or herbal extract, solid carrier, preparation method, main analyzed parameters and bioavailability enhancement factor are described in Table 1 and Table 2.

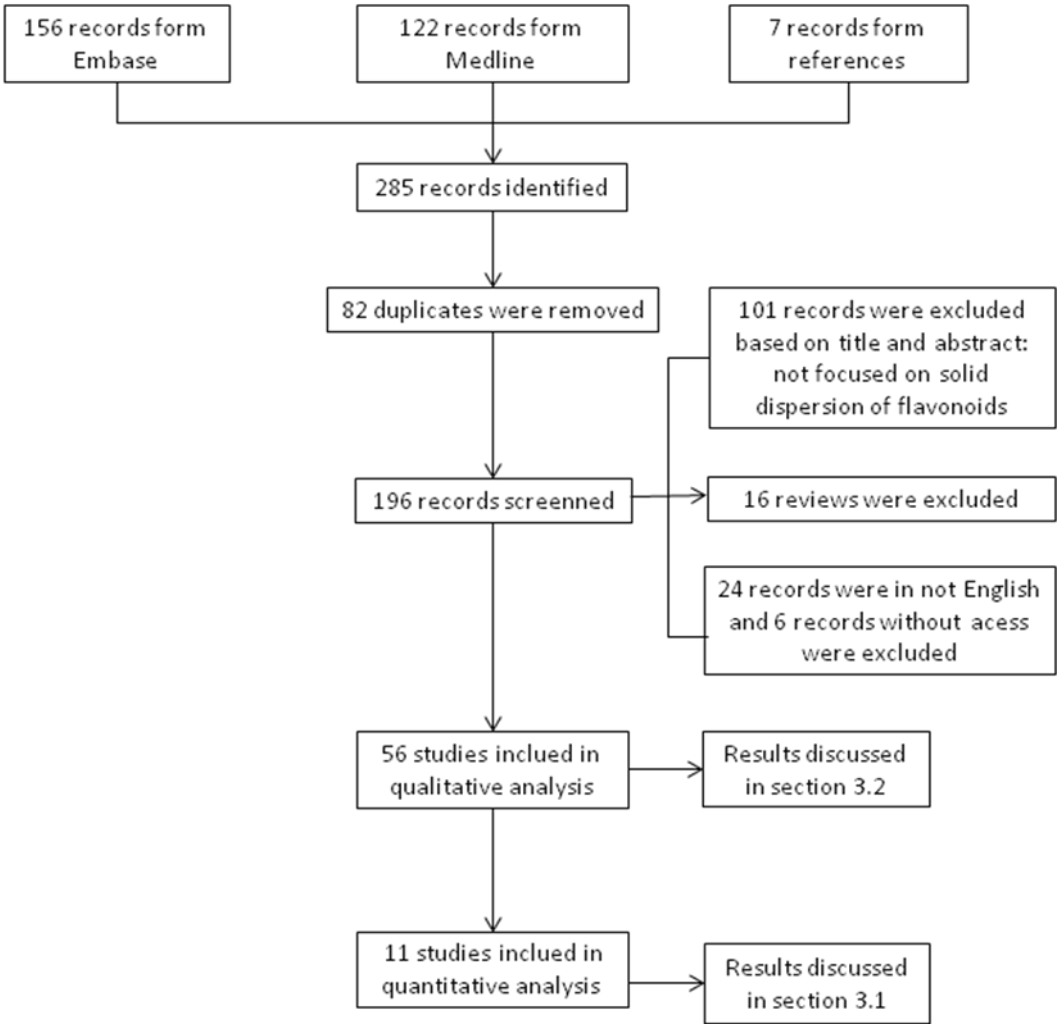

Figure 2. Flowchart of systematic literature search

Table 1. Summary of records that discussed solid dispersion formulations for the enhancement of the *in vitro* dissolution and/or oral bioavailability of flavonoids

Flavonoid	**Activity reported**	**Solid carrier**	**Method of process**	**Main parameters analyzed**	**Bioavailability parameter compared to pure drug**	**References**
Apigenin	Antiproliferative against pancreatic, colorectal, skin, neuroblastoma and breast cancer cell lines	Carbon nanopowders	Solvent method	Dissolution Bioavailability	↑ AUC (1.8-fold) ↑ Cmax (2.5-fold)	(Ding et al., 2014)
Apigenin	Anti-inflammatory, anti-cancer, antibiotic, antiviral, antidiabetic and anti-oxidant	Poloxamer-F-127	Melting, kneaded and microwave method	Dissolution Bioavailability	↑ AUC (3.1-fold) ↑ Cmax (2.8-fold)	(Alshehri et al., 2018)
Baicalein	Anti-inflammatory, antioxidative, anticancer, antiallergic and antiviral	Pluronic F68	Spray freeze drying Solvent method	Dissolution Bioavailability	↑ AUC (2.3-fold) ↑ Cmax (3.6-fold)	(He et al., 2011)
Baicalin	Anticancer Hepatoprotective	PVP	Solvent method	Dissolution Bioavailability	↑ AUC (3.2-fold) ↑ Cmax (4.6-fold)	(Li et al., 2013a; Li et al., 2011)

Biochanin A	Antioxidant, anti-inflammatory, antiviral, anti-carcinogenic and n inhibitor of P-glycoprotein	Solutol® HS15 and HPMC 2910	Solvent method	Dissolution Bioavailability	↑ AUC (3.1-fold) ↑ Cmax (2.8-fold)	(Han et al., 2011)
Catechin	Not reported	Eudragit1 S100 and PVAC	Melting method and hot-melt fluid bed coating method.	Dissolution *In vivo* release	Not studied	(Yang et al., 2004)
Chalcone Derivative, SU-740	Anti-ulcer	PEG 6000 and PVP K29-32	Melting or coprecipitação method	Dissolution	Not studied	(ITO et al., 1995)
Chrysosplenol C	Inhibitors of poliovirus and rhinovirus	PEG 6000, PVP K-25, SLS	Melting method	Dissolution	Not studied	(Ng et al., 2016)
Epigallocatechin gallate	Preventive agent against mammary cancer post-initiation, degenerative diseases, oxidative stress, cardiovascular and neurological disorders, and hepatotoxicity	(Hpmcas), (hpmcp), Soluplus®, cellulose acetate, or gelucire® 50/13	Lyophilization	Dissolution	Not studied	(Cao et al., 2017)
Genistein	Beneficial effects on cancer, cardiovascular diseases,	Pluronic F127	Solvent method and lyophilized followed	*In vitro* release Bioavailability	↑ AUC (3-fold) ↑ Cmax (4.7-	(Kwon et al., 2007)

	osteoporosis and postmenopausal symptoms		by a freeze Dry system		fold)	
Hesperetin	Antioxidant, antiaging, anti-inflammatory, blood lipid- and cholesterollowering, anticarcinogenic, and estrogenic activities.	Mannitol	Spray drying	*In vitro* release profile Caco-2 and mcf-7 cell uptake study *Ex vivo* intestinal uptake study Bioavailability	Not compared to pure drug	(Shete et al., 2015b)
Hesperetin	Potential antioxidant anti-inflammatory and anticancer agent	PVP, PEG, Pluronic F127 or Tween 80	Solvent method	Dissolution	Not studied	(Kakran et al., 2013)
Hesperetin and naringenin	Antioxidant, blood lipid-lowering, anti-inflammatory, anticarcinogenic and inhibit selected cytochrome P-450 enzymes	PVP, PEG and mannitol	Solvent method	Dissolution Bioavailability	Not compared to pure drug	(Kanaze et al., 2007; Kanaze et al., 2006a; Kanaze et al., 2006b)
Hesperetin or naringenin	Not reported	Mannitol	Spray drying	Crystallization kinetics	Not studied	(Shete et al., 2015a)

Ipriflavone	Reduce bone turnover rate mainly through an inibition of bolle resorption and in stimulating bone formation	PVP or PEG	Solvent method	Dissolution Bioavailability	Not compared to pure drug	(Li et al., 1999a; Li et al., 1999b)
Kaempferol	Antioxidant, anti-inflammatory, anticancer, cardioprotective, neuroprotective and antidiabetic activities	Polysaccharide arabinogalactan (AG) and disodium glycyrrhizinate (NA_2GA)	Mechanochemical technique	Dissolution Bioavailability	↑ AUC (4.6-6.1-fold) ↑ Cmax (5.7-7.2-fold)	(Xu et al., 2018)
Naringenin	Antioxidant, anti-inflammatory, anticancer, antifibrogenic and antiatherogenic	Soluplus®	Solvent and kneading Methods	Dissolution Bioavailability	↑ AUC (2.3-fold) ↑ Cmax (2.3-fold)	(Khan et al., 2015)
Naringenin	Antioxidant, anticancer, antiestrogenic, hepatoprotective, and protective effect against the lipid peroxidation	Mannitol	Solvent method With three drying methods (vacuum drying, microwave-vacuum drying, And spray drying)	Dissolution	Not studied	(Wang et al., 2011)
Naringenin	Anticancer, hepatoprotective,	PVP K-30	Solvent method	Dissolution	Not studied	(Zhong et

	antioxidant and antiestrogenic		with drying methods (vacuum drying, microwave-vacuum drying, and spray drying)			al., 2011)
Naringenin and quercetin	Antioxidant, antitumor and antibacterial agents	Pvp, eudragit e100, cmcab, Hpmc, hpmcasu or paa	Solvent method	Crystallization study	Not studied	(Wegiel et al., 2014)
Naringin	Antioxidant, anti-inflammatory, anti-apoptotic	PEG6000, F68 or PVP K30	Solvent melting method	Dissolution Bioavailability	↑ AUC (1.3-fold) ↑ Cmax (2-fold)	(Wang et al., 2018)
Nobiletin	Anti-dementia, anti-tumor, anti-apoptotic, anti-oxidative, anti-inflammatory and hepatoprotective	HPC-SSL	Wet-milling and subsequent freeze drying	Dissolution Bioavailability	↑ Cmax (4.1-fold)	(Onoue et al., 2013)
Nobiletin	Anti-inflammation, anticancer, and most notably ameliorative actions on memory impairment and β-amyloid pathology	HPC-SSL	Wet-milling technique followed by freeze drying	Dissolution Bioavailability	↑ Cmax (7-fold)	Onoue et al., 2011)
Quercetin	Strong inhibition of breast,	PVP and	Solvent method	Dissolution	Not studied	(Kakran et

	colon, lung, and ovarian cancer cell growth	pluronic F127				al., 2011)
Quercetin	Reduced risk of cardiovascular disease, cancer and diabetes and obesity	CCAB, HPMCCAS or CASub	Spray drying	Dissolution	Not studied	(Gilley et al., 2017)
Quercetin	Does not report	PVP, PEO-6000, and β-cyclodextrin	NA	Dissolution	Not studied	(Kovalevska et al., 2017)
Quercetin	Antioxidante, anti-inflammatory, antibacterial, antiviral, and muscle-relaxation	CMCAB, HPMCAS, CAAdP	Spray drying	Dissolution	Not studied	(Li et al., 2013b)
Quercetin	Anti-oxidant, anti-infammatory, and hepatoprotective	MPEG–PCL copolymer	Solvent method	Cellular uptake	Not studied for oral delivery	(Wu et al., 2013)
Quercetin	Reduce the arterial blood pressure	PVP	Solvent method	Pharmacokinetic study after i.v. injection	Not studied for oral delivery	(Porcu et al., 2018)
Quercetin	Antioxidante and chemopreventive	PEG-8000	Melting method	Dissolution	Not studied	(Dwi et al., 2018)
Quercetin	Antioxidants, anticancer and	HPMC	Solvent method	Dissolution	Not studied	(Setyawan et

	antivirus					al., 2017)
Quercetin	Anti-ulcer and gastroprotective effects	PVP K30	Solvent method	Biochemical studies	Not studied for oral delivery	(Abourehab et al., 2015)
Quercetin	Antiviral, antibacterial, anticancer and cardiovascular protective effects	PEG 8000 and PEG 400	Melting method	Dissolution	Not studied for oral delivery	(Otto et al., 2013)
Quercetin	Antioxidant and anticancer	Lecithin, cholesterol and PEG	Solvent method	*In vitro* Drug Release Assay	Not studied for oral delivery	(Long et al., 2013)
Quercetin	Antioxidant	PVP K30 and pluronic F 127	Spray drying	Dissolution	Not studied	(Ghanem et al., 2013)
Tectorigenin	Antidiabetic, antioxidant, preventing prostate cancer, estrogen-like effect, antiangiogenic and antitumor	PEG4000 and PVP	Solvent method	Dissolution Bioavailability	↑ AUC (4.8-fold) ↑ Cmax (13.1-fold)	(Shuai et al., 2016)

NA: not available; hydroxypropyl methylcellulose acetate succinate (HPMCAS); hydroxypropyl methylcellulose phthalate (HPMCP); polyvinylpyrrolidone (PVP), polyvinyl acetate (PVAc), polyethylene glycol (PEG); carboxymethylcellulose acetate butyrate (CMCAB), hydroxypropylmethylcellulose (HPMC), poly(acrylic acid) (PAA), hydroxypropyl cellulose SSL (HPC-SSL), 6-carboxycellulose acetate butyrate (CCAB), cellulose acetate suberate (CASub), polyethylene oxide (PEO), cellulose acetate adipate propionate (CAAdP); Sodium lauryl sulfate (SLS).

From the included literature, 71% investigated solid dispersion of an isolated flavonoid and 29% of articles accounted for herbal extracts that containing flavonoids (Fig. 3A). A total of 51 literatures reported applications of solid dispersion for improving the oral bioavailability of 17 different flavonoids and 7 herbal extracts containing flavonoids. Among all preparation methods, the majority of studies adopted the solvent evaporation method (Fig 3B). As shown in Fig. 3C, PVP was the most common carrier used for solid dispersion followed by PEG.

Ten *in vivo* studies were included in the calculation of the overall oral bioavailability, with respect to $AUC_{0\rightarrow t}$, of isolated flavonoids enhancement by SD. In general, SD could increase 3.39 ± 1.48-fold in the $AUC_{0\rightarrow t}$ of the studied formulation compared to the free flavonoid. The overall enhancement effect on C_{max} by solid dispersion is 5.59 ± 3.74-fold great than that free flavonoid in eleven analyzed studies. The most frequently employed animal model was male rats (11 out of 12), with 2 using Wistar rats and 7 using Sprague–Dawley rats (and 2 unspecified), followed by beagle dogs (1 out of 12).

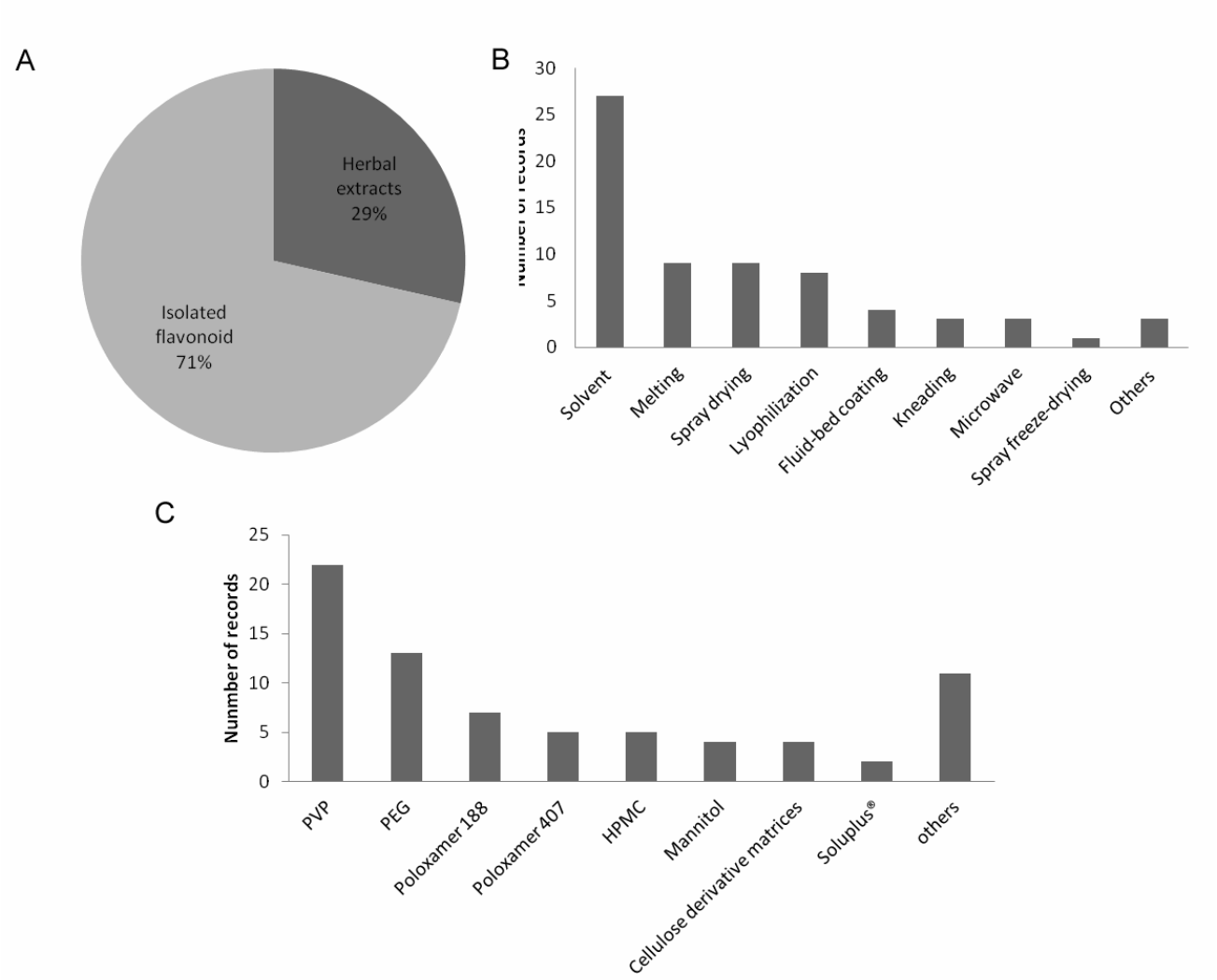

Figure 3. Summary of records employing solid dispersion of flavonoids in terms of (A) drugs being formulated; (B) the methods of preparation (C) the carriers employed.

3.2. Overview of literature on solid dispersion (SD)

Flavanols

Catechins (epicatechin (EC), epigallocatechin (EGC), epigallocatechin gallate (EGCG), and epicatechin gallate (ECG)) were formulated as SD chewing gum by hot-melt fluid bed coating method. The chewing gum prepared with Eudragit® S100 could sustain effective therapeutic concentrations of catechins over 30–40 min in human volunteers (Yang et al., 2004). Cao et al developed a epigallocatechin gallate (EGCG) solid dispersion with Soluplus® by lyophilization. EGCG-Soluplus® 50:50 (w/w) and showed a dissolution profile of only 50% EGCG being released for 20 min, with

sustained release for 24 h. This may also make it possible to increase the bioavailability of EGCG by extending its elimination time in plasma (Cao et al., 2017).

Flavanones

Several studies have developed SD with different flavanones to obtain an enhancement of their dissolutions. Kanaze et al. (Kanaze et al., 2006b) reported a SD systems with flavanone glycosides, naringin and hesperidin, and their aglycones, naringenin and hesperetin, prepared using solvent evaporation method. In order to select an appropriate carrier, they used polyvinylpyrrolidone (PVP) (PVP-K30), polyethylene glycol (PEG 4000) and mannitol. PVP carrier showed better solubilization feature than PEG and mannitol of the aglycones, due to the presence of the drug compounds in crystalline state in both matrices. PVP was an effective polymer matrix to form amorphous nano-dispersion systems with the flavanone aglycones, while did not form with their glycosides, indicating that bulky molecules are very difficult to form amorphous dispersions. Through FTIR (fourier-transform infrared spectroscopy) spectra, the same authors showed the presence of hydrogen bonds between PVP carbonyl groups and hydroxyl groups of both flavanone aglycones, which prevent the crystallization of naringenin and hesperetin aglycones in the PVP matrix (Kanaze et al., 2006a). One year later, Kanaze et al. (Kanaze et al., 2007) evaluated the pharmacokinetic parameters of hesperetin and naringenin in human plasma and urine, after their single oral administration in humans in the form of SD developed in their previous work. However, authors did not compared both with a control group, i.e. pure aglicones, only concluding that the absorption of both hesperetin and naringenin was rapid and much faster than previous studies after oral administration of their flavanone glycosides, either as pure compounds or in the form of citrus juices.

Formulating poorly water-soluble drugs as nanocrystals can increase the apparent solubility and dissolution rate, improving the oral bioavailability, and increasing adhesiveness to surfaces/cell membranes. The crystallization kinetics of amorphous hesperetin (HRN) and naringenin (NRN), alone and in presence of mannitol as crystallization-inducing excipient was studied. Mannitol accelerated crystallization of both flavonoids, however NRN exhibited great crystallization rate than HRN, in

presence of mannitol (Shete et al., 2015a). Nanocrystalline SD of HRN in crystalline mannitol was developed using a novel spray drying based process. The SD of HRN showed significantly enhanced oral bioavailability (2.25-fold) due to higher release rate, apparent solubility, and penetration into gastric mucosa and intestinal cells as compared to the control (physical mixture) (Shete et al., 2015b).

Another carrier to produce SD of naringenin was employed: Soluplus®. Two methods were tested, solvent evaporation and kneading methods, where the first one showed better drug release profile. The dissolution of naringenin up to 100±2.6% after 2 h was achieved by solvent method while in the case of kneading method the value was lower (53±3%). They attributed this difference due to the efficiency of technique to convert drug to amorphous form as well as produce a homogeneous dispersion. Possible hydrogen bonding between the hydroxyl groups, 4'-OH and 7-OH of drug and terminal OH groups in the Soluplus® enhance the miscibility between carrier and naringenin, preventing recrystalization and keeping them in molecular dispersion. Moreover, the SD revealed a significant increase in naringenin absorption compared to naringenin alone (Khan et al., 2015).

SD with different carriers (PEG6000, F68 and PVPK30) was developed to improve the dissolution rate and oral bioavailability of naringin. Despite PVPK30 showed more remarkable improvement on solubility than PEG6000, dispersion with PEG6000 showed more notable enhancement on the dissolution rate than PVPK30. Compared to control (suspension of naringin), SD had a significant higher AUC (Wang et al., 2018).

SD with quercetin and naringenin were developed with different polymers, as poly(vinylpyrrolidone) (PVP), Eudragit E100 (E100), carboxymethylcellulose acetate butyrate (CMCAB), hydroxypropylmethylcellulose (HPMC), HPMC acetate succinate (HPMCAS) and poly(acrylic acid) (PAA). The results of this study showed that E100 was the best polymer for formation of the amorphous SD as well as one of the best polymers for stability. It is suggested that this is due to the proposed ionic interaction in the flavonoid–E100 dispersions. On the other hand, PAA was the least effective polymer for inhibiting crystallization of the polyphenols during solvent evaporation, and high polymer concentrations being required. They concluded that less polymer was required to form an amorphous dispersion for polymers that developed stronger

hydrogen bonding interactions with the polyphenols, being more stable against crystallization when exposed to high relative humidity and high temperatures (Wegiel et al., 2014).

A better dissolution and possible intermolecular hydrogen bond between the drug and carriers was also demonstrated by developed naringenin SD with mannitol and polyvinyl pyrrolidone k-30 (PVP k-30), respectively. The dissolution rate of naringenin from SD with mannitol was significantly improved by SD compared to the pure drug and physical mixture (Wang et al., 2011). The SD with PVP-k30 has demonstrated also an improvement in the dissolution rate and a significantly extent of naringenin compared with the pure drug and physical mixtures (Zhong et al., 2011).

Ternary SD systems of hesperetin with the polymers PVP or PEG and a surfactant (Pluronic F127 or Tween 80®) prepared by solvent method possessed great solubility and dissolution rates compared to free drugs and also their binary dispersions (composed by drug and PVP or PEG). Drug dispersions in PVP showed superior dissolution as compared to those in PEG and the ternary dispersions with Tween 80® presented better dissolution than those with F127. Furthermore, the ternary systems were physically more stable than the binary dispersions in terms of crystalline nature of the drug (Kakran et al., 2013).

Flavones

Two studies developed SD of nobiletin (NOB), a polymethoxylated flavone. First, SD was prepared by wet-milling and subsequent freeze-drying technique. An improvement in the dissolution behavior compared with that of crystalline NOB was noticed. Increases of bioavailability and central nervous system (CNS) distribution by 13- and 7-fold, respectively, compared with those of crystalline NOB (Onoue et al., 2011). This research group utilized the same formulation of a previous study (Onoue et al., 2011) and showed enhanced hepatoprotective effects of SD compared with crystalline NOB in rats. They suggesting that higher dose of NOB might result in enhanced bioavailability (Onoue et al., 2013).

SD of apigenin (AP) with a novel carbon nanopowder (CNP) were prepared by solvent evaporation method. AP from SD after 1h of dissolution improved by 275% compared

with that of AP alone. After oral administration, the bioavailability was significantly improved with AP AUC value almost 2 times higher for the SD system than free AP and physical mixture. Moreover, no toxic effects were observed on rats mucosa after 2 weeks of treatment (Ding et al., 2014).

Microwave, melting and kneading methods were used to prepare solid dispersion of AP using pluronic-F127 as carrier. All technologies changed the crystalline nature of AP to amorphous form and significantly improved the release profile of AP. Pharmacokinetics studies in rats showed that microwave method increased maximum *in vivo* absorption compared to free AP, marketed capsule and SD prepared by melting and kneading technology (Alshehri et al., 2018).

SD of baicalin (BA) and its aglycone baicalein have been reported to improve its dissolution profile and oral bioavailability. Two methods, spray freeze drying and the solvent evaporation were used to prepared solid dispersions of baicalein with Pluronic F68. The spray freeze drying technology inhibited the majority of baicalein from recrystallizing, producing stable and amorphous solid dispersion at a 1:4 (drug/carrier) weight ratio, which could not be obtained by the solvent method. Moreover, the dissolution rate of SD prepared by spray freeze drying was significantly enhanced compared to the SD prepared by solvent evaporation. The relative bioavailability of the SD by comparing the $AUC_{0\text{-}12}$ was 233% higher than free baicalein, demonstrating the significantly improvement of oral bioavailability when baicalein prepared by spray freeze drying was delivered by solid dispersion (He et al., 2011). Baicalin-polyvinylpyrrolidone (PVP) coprecipitate was prepared by solvent method of solid dispersion technology using polyvinylpyrrolidone (PVP-K30) at a drug-to-polymer composition ratio of 1:3. This flavonoid was present in an amorphous or molecular state in the coprecipitate. The dissolution rate of BA from the developed formulation was 21.4-fold great than BA in 0.1 mol L^{-1} HCl. An intermolecular hydrogen bond was formed between the 4-OH of the glucuronide of baicalin and the O of the carbonyl group from PVP (Li et al., 2011). The same research group continued the studies and observed improvements in the dissolution of the baicalin–PVP in a 0.1 mol/l HCl solution, at pH 4.5 phosphate buffering solution (PBS), and in distilled water compared to free BA. However, the dissolution of BA from the formulation was

slightly lower than free BA at pH 6.8 PBS. After oral administration of SD in beagle dogs, a significant improvement in the absorption of baicalin with an increase of oral bioavailability by 2.4-fold compared to free BA (Li et al., 2013a).

SD of Chrysosplenol C (CR) was prepared by melting method. Binary systems consisting of CR and a single hydrophilic polymer (PVP or PEG 6000) and ternary systems composed by CR and two polymers (PVP and PEG 6000) in different combinations were prepared. Solubility in water of CR was significantly improved in the ternary SD binary systems. The formulation P3 composed by CRSP/PVP/PEG 6000 at a weight ratio of 2/1.8/0.2 was the formula that improved the solubility of the drug by 11.4-fold compared to the drug powder alone, and showed the highest dissolution rate. However, the dissolution rates were still low (<50%), the surfactants SLS were added to the formula. The new formulation, CRSP/PEG 6000/PVP/SLS at a weight ratio of 2/0.2/1.1/0.7, improved the total CR accumulative release by 2.1-fold versus the formulation P3 (Ng et al., 2016).

Flavonols

Quercetin (3,3',4',5,7-pentahydroxyflavone) is one of the most prominent flavonoid in dietary antioxidants. It is a potent chemopreventive and has demonstrated strong inhibition of breast, colon, lung, and ovarian cancer cell growth. To improve its use in pharmaceutical field, different strategies have been studied to enhance the dissolution rate of quercetin (QUE) and its poor bioavailability due to low solubility and fast metabolism. Nanoparticles as drug delivery system, using complexes with β-cyclodextrin and SD with PVP and pluronic F127 were developed by evaporative precipitation of nanosuspension method. SD of quercetin with PVP and F127 are better than nanoparticles and its complex with β-cyclodextrin as they show great dissolution even at lower concentrations of polymers. However, both carries show similar dissolution profile indicating that both are equally efficient to improve the dissolution rate of QUE (Kakran et al., 2011).

SD with different weight ratios of quercetin and PVP10 were obtained by using a co-solvent evaporation method. Drug/polymer weight ratio of 1:12 showed the maximal improvement of QUE water solubility (almost 20,000 fold). Although no differences

between freeze-drying and evaporation until dryness were observed, freeze-dried powders were chosen for *in vivo* studies because are more suitable for parenteral formulations. After iv administration, the arterial blood pressure was reduced in rats with rapid decrease of QUE plasma concentration. Metabolites, isorhamnetin and possibly quercetin-3-O-glucoronide, could contribute to the vasodilatory effect. An important finding in this study is the possibility of sterilization by autoclaving of the formulation dissolved in saline in terms of QUE content, viscosity and injectability, confirming the feasibility of the process on the reconstituted powder (Porcu et al., 2018).

Cellulose derivative matrices (carboxymethylcellulose acetate butyrate (CMCAB), hydroxypropylmethylcellulose acetate succinate (HPMCAS), and cellulose acetate adipate propionate (CAAdP)) were investigated to form spray-dried SD with QUE. However, even an hydrogen bonding between QUE and the matrix cellulose derivative matrices which may aid disruption of QUE crystalline structure, SD prepared with PVP (as control) showed faster release, more complete and prevented QUE chemical degradation (Li et al., 2013b). Blends of cellulose acetate suberate (CASub) and PVP, most significantly enhanced QUE solution concentration under intestinal pH conditions, increasing dissolution area under the concentration/time curve 18-fold compared to QUE alone (Gilley et al., 2017).

Hydroxypropyl methyl cellulose (HPMC), a cellulose derivative, was employed to produce QUE solid dispersion. Probably due to the formation of molecular dispersion or microstructural dispersion and the formation of micellar structure with the media, solubility and dissolution rate of QUE were significantly higher compared to the flavonoid alone and physical mixtures, especially in the ratio of 1:3 (Setyawan et al., 2017).

PVP was also employed to form SD with QUE, but in comparison with polyethylene oxide (PEO-600) and β-CD, PVP showed the lowest value of QUE dissolved, but still higher than QUE alone (Kovalevska et al., 2017). Combination of famotidine alginate beads plus QUE solid dispersion, formulated with PVP K30 by solvent evaporation technique, promisingly improved effectiveness in treatment of gastric ulcer in a rat model compared with the commercial famotidine tablets (Abourehab et al., 2015)

SD in PEG8000 increased the solubility and dissolution rate of QUE (Dwi et al., 2018), however in other study, dissolution profiles showed a decrease in dissolved flavonol concentration with time, suggesting phase separation between PEG and flavonol during release. An alternative for this phenomenon would be to administer the formulation at the site of absorption, as suppositories for rectal administration, to ensure absorption prior to phase separation (Otto et al., 2013).

Binary and ternary microstructured solid dispersions of QUE were formulated with different ratios of PVP K30 and pluronic F127 (PF 127) by spray drying, indicating possible amorphization of the drug and formation of narrow size distribution of microstructured particles. The highest improvement in dissolution rate was obtained from ternary systems composed QUE/PVP (1:1) with 5% of the total weight of PF 127 (Ghanem et al., 2013).

Other strategies for increasing solubility for intravenous administration of QUE can also be applied. Micelles and liposomes were formulated using solid dispersion method with Poly(ethylene glycol) monomethyl ether (Wu et al., 2013) or PEG4000 with lecithin and cholesterol (Long et al., 2013), respectively. After the co-evaporation process, the solid mass was dissolved in normal saline to self-assemble into QUE encapsulated micelles or liposomes. Using a dialysis method, both studies demonstrated a sustained release behavior when compared with QUE alone. QUE liposomes were an effective agent to inhibit tumor growth in both cisplatin-sensitive and cisplatin-resistant human ovarian cancers. QUE micelles improved cytotoxicity, apoptosis induction, antiangiogenesis, anti-metastasis, and cellular uptake *in vitro* compared to QUE alone.

Supramolecular complexes of kaempferol (KPF) with the natural polysaccharide arabinogalactan (AG) and disodium glycyrrhizinate (Na_2GA) were prepared by mechanochemical process using a ball mill. The reduction of particle sizes and partly amorphization of milled complexes revealed the formation of solid dispersion, which significantly improved the dissolution of KPF. The peak plasma concentrations of KPF-AG and KPF-Na2GA complex were significantly higher than free KPF (7.2 and 5.7 times, respectively) (Xu et al., 2018).

Isoflavones

Ipriflavone (7-isopropoxyisoflavone, IP) is a isoflavone derivative, currently used in several countries for prevention and treatment of postmenopausal osteoporosis. SD of Ipriflavone (IP) were prepared by solvent method with PVP or PEG as carrier and the results proved that PVP promote a better dissolution profile (Li et al., 1999a). After oral administration in rats, the relative bioavailability for IP solid dispersion was enhanced by 200% over the control (physical mixture of IP and PVP at the same proportion as the SD) (Li et al., 1999b).

In another study, PVP and PEG were employed to developed SD by solvent method with the isoflavone tectorigenin (TG) at weight ratio of 7:54:9. The i*n vitro* release was 4.35-fold higher than free drug after 150 min. The oral bioavailability in rats of the SD was also enhanced, with AUC and C_{max} of SD 4.8- and 13.1-fold higher than TG alone, respectively (Shuai et al., 2016).

Genistein-loaded polymeric micelles using Pluronic F127 was prepared by a SD method. The release rate of genistein from micelles at both tested pH (1.2 and 6.8) was faster than genistein alone. In the same way, the oral bioavailability in rats of genistein-loaded micelles was higher than suspension of genistein, with AUC approximately 3-fold greater (Kwon et al., 2007).

A biochanin A solid dispersion using Solutol® HS15 and HPMC 2910 increased the solubility and provided a rapid and complete dissolution (approximately 100% within 1 h) of biochanin A. After oral administration of SD, Cmax and AUC of biochanin A were increased by approximately 13 and 5-folds, respectively (Han et al., 2011).

Chalcones

ITO et al. compared three techniques (size reduction, solid dispersion and inclusion complexation with ciclodextrins) for improvement of the dissolution rate of 4-tert-butyl-2'-carboxymethoxy-4'-(3-methyl-2-butenyloxy) chalcone (SU-740). The solid dispersions of SU-740 were prepared with polyethyleneglycol 6000 (PEG) or polyvinylpyrrolidone K29/32 (PVP). The dissolution rates of SU-740 from the PVP and the β-CyD complex were similar and much larger than size-reduced form and PEG SD. However, after accelerated storage (40°C and 75% relative humidity) for one

month, inclusion complex was better than SD containing less PVP (1:5, drug:PVP), since it showed a decrease in the dissolution rate. On the other hand, the dissolution rate of SD containing higher proportion of PVP (1:10, drug:PVP), showed no change in the dissolution profile (ITO et al., 1995). Besides that, the appearance of SD changed during the storage, whereas inclusion complex showed no change. The authors concluded that inclusion complex with β-CyD was the better alternative for the formulation design of the drug. (ITO et al., 1995).

Herbal extracts

Seven different herbal extracts containing flavonoids showed significant enhancement in the solubility, *in vitro* dissolution and/or bioavailability after being formulated as solid dispersion (Table 2).

Table 2. Solid dispersion formulations of flavonoids from herbal extracts

Herbal Extract	**Activity reported**	**Markers**	**Solid Carrier**	**Method of process**	**Parameters analyzed**	**Reference**
Erigeron breviscapinus	Treatment of cardiovascular disorders	Scutellarin	PVP K30, microcrystalline cellulose and crospovidone	Solvent method	Dissolution, Bioavailability	(Cong et al., 2014)
Ginkgo biloba	Treatment and prevention of cardiovascular and cerebrovascular diseases	Total flavone glycosides	PEG 6000.	Melting method	Solubility Dissolution	(Ge, 2010)
Ginkgo biloba	Treatments of peripheral vascular disease, Alzheimer's, dementia of elderly people, tinnitus, inhibitation of platelet aggregation, antioxidant, protection of central nervous system	Quercetin, kaempferol and isorhamnetin	Poloxamer 188	Solvent method	Dissolution Bioavailability	(Chen et al., 2010)
Ginkgo biloba	Cardiovascular and neurodegenerative diseases	Quercetin , kaempferol and isorhamnetin	Kollidon® VA64/Kolliphor® RH40 (85:15)	Hot-melt Extrusion	Dissolution Bioavailability	(Wang et al., 2015)

Glycine max (L.) Merr.	Protect against hormone-dependent cancers, increase bone density, decrease the risk of heart diseases, prevent breast and prostate cancers, and decrease thrombogenicity and low-density lipoprotein (LDL) levels	Daidzein and genistein	Gelatin	Spray drying	Dissolution	(Panizzon et al., 2014)
Hippophae rhamnoides L.	Antioxidant, antibacterial, anti-atherogenic, radioprotective, cardioprotective and hepatoprotective	Isorhamnetin, quercetin, and Kaempferol	Poloxamer 188	Solvent method	Bioavailability	(Duan et al., 2016)
Hippophae rhamnoides L.	Antioxidant, antiulcerogenic, cardioprotective and hepatoprotective	Total flavones	Poloxamer 188	Solvent method	Dissolution	(Xie et al., 2009)
Hippophae rhamnoides L.	Antioxidant, antiulcerogenic, hypoglycemic, cardioprotective and hepatoprotective	Isorhamnetin, quercetin and kaempferol	Poloxamer 188	Solvent method	Solubility, intestinal permeation, dissolution, Bioavailability	(Zhao et al., 2013)
Kaempferia	Prevention of myocardial	5,7,4′-	HPMC and	Solvent	Dissolution	*(Weerapol*

parviflora	ischemic reperfusion, decreasing vascular responsiveness to phenylephrine and decreasing fasting serum glucose and triglyceride levels	trimethoxyflavone	PVA-co-PEG	method	Stability	*et al., 2017)*
Radix scutellariae	Anti-inflammatory, anti-allergic and anti-oxidant	Baicalein, wogonin, and oroxylin A.	PVP K-30	Solvent method	Dissolution Solubility Bioavailability	(Yu et al., 2017)
Silybum marianum L. Gaertn	Antihepatotoxic	Flavonolignan silibinin	PVP	One-step fluid-bed coating	Dissolution Bioavailability	(Sun et al., 2008a; Sun et al., 2008b)
Silybum marianum L. Gaertn	Hepatoprotectant	Taxifolin, silychristin, silydianin, isosilybin and silybin	PVP	Fluid-bed coating Technique	*In vitro* release	(Xie et al., 2013)
Silybum marianum L. Gaertn	Hepatoprotectant	Silymarin (qualtification by UV spectrometry	PEG 6000	Fusion method	Dissolution	(Qiu et al., 2005)
Silybum	Hepatoprotectant	Taxifolin,	PEG 6000 or	Melting	Dissolution	(Lu et al.,

marianum L. Gaertn		silychristin, silydianin, isosilybin and silybin	Poloxamer 188	method		2007)
Silybum marianum L. Gaertn	Antihepatotoxic	Silymarin (qualtification by UV spectrometry	HPMC E 15LV	Kkneading, spray drying and co-precipitation methods	Dissolution	(Sonali et al., 2010)

Erigeron breviscapinus (Vant.) Hand-Mazz

Scutellarin is the major compound of breviscapine, a crude extract of several flavonoids extracted from a Chinese herb *Erigeron breviscapinus (Vant.) Hand-Mazz*. However, its clinical application is severely restrict due to poor water solubility and low bioavailability *in vivo*. To overcome these problems, a breviscapine SD tablets with PVP K30, microcrystalline cellulose and crospovidone was prepared using a modified solvent evaporation method. The dissolution profile of scutellarin in the SD was improved compared to the commercial product. Furthermore, after oral administration in beagle dogs, bioavailability of scutellarin was 3.45-fold higher compared to commercial tablets, suggesting that SD tablets are a great solution to improve the bioavailability and the dissolution rate of breviscapine (Cong et al., 2014).

Silybum marianum Gaertn

Silymarin, a mixture of flavonolignans (natural products, composed of a flavonoid moiety and a lignan part), is isolated from the milk thistle plant *Silybum marianum* Gaertn. SD of silymarin in the form of "dripping pills" prepared at a 1:4 ratio by fusion method with polyethylene glycol 6000 (PEG 6000) showed an improvement in the solubility and higher dissolution rate compared to commercial products (Qiu et al., 2005). SD of silymarin with PVP were prepared by one-step solvent method in a fluid-bed coater. At lower PVP/ silymarin ratios, SD showed slower dissolution rate than silymarin powder. However, when PVP/silymarin ratios increased to 4/1, 5/1 and 6/1, a great dissolution rate was observed (about 10-fold higher) compared to silymarin powders. Interestingly, when the SD was at the ratio (PVP/silymarin) of 6/1, the dissolution rate decreased slightly, compared to SD at the ratio 4/1 and 5/1, which means PVP/ silymarin ratio can neither be too high nor too low (Sun et al., 2008a). Further study was performed and the relative oral bioavailability of SD (4/1) pellets in beagle dogs based on quantification of silibinin, the major active component, was about 5-fold than silymarin suspension (Sun et al., 2008b). Lu et al provided a synchronized release of the active components of silymarin by SD prepared by fusion method with glyceryl monostearatem and polyethylene glycol 6000 (PEG 6000) or poloxamer 188 (Lu et al., 2007). However, these systems suffer from limited total

release when the content of the lipid increased to achieve higher synchronicity. From the formulation developed by Sun el al. (Sun et al., 2008a), silymarin osmotic tablets were prepared and controlled release of the multiple components of silymarin was achvied in a solubilized state through the release orifices (Xie et al., 2013). Different methods of preparation of silymarin SD were studied using HPMC E15LV. All preparation (kneading, spray drying and co-precipitation) methods enhanced silymarin dissolution from SD. However, the co-precipitation method provided a stable amorphous SD with 2.5 more dissolution rate than free drug (Sonali et al., 2010).

Ginkgo biloba

Ginkgo biloba is a traditional Chinese medicinal plant which is used to treat various diseases, especially to treat and prevent cardiovascular and neurodegenerative diseases. Standardized leaf extracts from *Ginkgo biloba* is mainly composed for flavones (quercetin, kaempferol and isorhamnetin) and triterpene lactones (Wang et al., 2015). Some researchers have been reported advantages in formulate SD with extract of *Ginkgo biloba*, aiming the improvement in the dissolution and oral bioavailability of the major components. An example is a study comparison between SD of *Ginkgo biloba* (GBS), *G. biloba* phospholipid complex (GBP) and *Ginkgo biloba* extract (GBE). The results of dissolution of total flavones from GBP and GBS increased about 2-fold and 9-fold compared to the GBE, respectively. They also showed that GBP and GBS highly increased the bioavailabilities of quercetin, kaempferol and isorhamnetin in rats via oral route compared with GBE. However, the bioavailability of quercetin, kaempferol and isorhamnetin from SD was lower than phospholipid formulation (Chen et al., 2010). An improved dissolution rate and oral bioavailability of total flavonoids (quercetin, kaempferol, and isorhamnetin) from *Ginkgo biloba* extract was found through the preparation of SD via hot-melt extrusion with Kollidon® VA64/Kolliphor® RH40 (85:15) (Wang et al., 2015). Based on these studies, it has been demonstrated that each flavonoid showed different increased degrees of bioavailability, probably due the difference chemical structure among them. It has been shown that PEG 6000 is also suitable for the development of SD with *Ginkgo biloba* extract by melting method. The SD at high drug loading (30-50%)

present a total flavones-controlled dissolution, but at low drug loading (10-20%), the formulation present a carrier-controlled dissolution (Ge, 2010).

Hippophae rhamnoides L.

The major constituents of *Hippophae rhamnoides* L. (TFH, sea buckthorn) include quercetin, isorhamnetin and kaempferol. SD using poloxamer 188 as carrier, for example, prepared by solvent evaporation method, promoted a dissolution enhancement of TFH. For optimization of the formulation a 32 full-factorial design approach was used. Amount of solvent and the drug-to-polymer ratio were used as independent variables and the percentage of TFH dissolved in 10 min was selected as the dependent variable. The 1:4 ratio was selected for the subsequent studies and showed enhancement of TFH dissolution probably due to the conversion of TFH into a less crystalline and/or an amorphous form (Xie et al., 2009).

Solubility, dissolution, permeability and pharmacokinetics on rats of isorhamnetin, quercetin and kaempferol in different TFH formulations have been investigated comparing two types of formulation: SD composed by Poloxamer 188 and self-emulsifying (SE) composed by medium chain triglycerides, Cremophor EL and 1,2-propanediol. For each flavonoid, SD showed higher dissolution rate than self-emulsifying system. However, both formulations could not significantly increase the intestinal permeability of flavonoids of TFH. On the other hand, oral bioavailability of isorhamnetin, quercetin and kaempferol in rats increased remarkably after oral administration of TFH SD formulations compared to free TFH, but for the SE formulations there was no significant difference on the pharmacokinetic parameters of these flavonoids between TFH SE and TFH alone (Zhao et al., 2013). The same research group has studied the pharmacokinetic parameters of isorhamnetin, quercetin, and kaempferol in TFH SD or SE formulations in another animal species, beagle dogs. Some pharmacokinetic differences in flavonoids in TFH between rats and beagle dogs were observed. The AUC of isorhamnetin and quercetin in TFH-SD were 5.9- and 3.1-fold higher than TFH alone, respectively, while the AUCs of isorhamnetin and quercetin in TFH-SE were 3.4- and 2.4-fold higher than TFH alone. Kaempferol was not detectable in plasma in beagle plasma samples (Duan et al., 2016).

Radix scutellariae

Radix scutellariae is an important herb in traditional Chinese medicine prepared from the roots of *Scutellaria baicalensis* Georgi. SD of the *Radix scutellariae* extract has been prepared by solvent method to enhance the solubility and dissolution rate of three major hydrophobic components, the flavones baicalein, wogonin and oroxylin A. After screening with various polymers (PEG 3400, PEG 8000, PVP K-30, poloxamer 188 and poloxamer 407), PVP K-30 showed the highest solubility rate. All three components showed 100% release in pH 6.8 medium within 6 h from SD with Vitamin C, an anti-oxidant to prevent degradation of these flavonoids. Moreover, after oral administration on SD in rats, the plasma concentrations of baicalein were significantly higher than free baicalein (40.3% increase of AUC) (Yu et al., 2017).

Kaempferia parviflora

Kaempferia parviflora, member of the family Zingiberaceae, is found in the northern part of Thailand. SD formulations of *Kaempferia parviflora* extract (KPD) can be developed using HPMC and PVA-co-PEG polymers (ratio of KPD to polymer of 1:2 and 1:1, for KPD/HPMC and KPD/PVA-co-PEG SD, respectively) by solvent method, using the methoxyflavone 5,7,4′-trimethoxyflovone (TMF) as marker. This formulation significantly improves the dissolution rate of TMF comparing with free KPD with both polymers. The stability of SD was also good after 6-month storage in both longterm and accelerated conditions and to improve the aqueous solubility of TMF for at least 5 times, compared to the KPD alone. However, studies observed that the excess of polymer at a ratio of 1:4 (KPD:polymer) decreased the dissolution of KPS (Weerapol et al., 2017).

Glycine max (L.) Merr.

The soy isoflavones, daidzein (DAI) and genistein (GEN) had its dissolution drastically increased when formulated as a SD using a gelatin matrix to microencapsulate DAI and GEN from soy extract (SE) by spray drying (Panizzon et al., 2014).

Limitations and Future Perspectives

In the current review, we have evaluated classical groups of flavonoids formulated as solid dispersions: flavones, flavonols, flavanols, isoflavones, flavanones, and chalcones. Up to now, based on our search equation, no flavanonols and anthocyanidins were attempted to improve their solubility and oral bioavailability by SD strategy. Even though the two databases utilized in our search (Medline and Embase) are recommended for systematic searches for medical studies (Lunny et al., 2018), amount of records might be underreported due to limitations including the possibility of other types of publication, regarding reports, commentaries, patents, clinical trials, and conferences. Moreover, language restriction limits our research. Regardless of these limitations, to our knowledge, this review is the first to provide a summary in a systematic and quantitative evaluation of studies applying the solid dispersion technology for improvement of oral bioavailability of flavonoids.

It is known that researchers tend to select "publishable" results for publication, resulting in publication bias. From all 56 articles evaluated, only one study showed that solid dispersion present inferior oral bioavailability compared to the phospholipid formulation, but still higher than free quercetin, kaempferol and isorhamnetin (Chen et al., 2010).

Great heterogeneity among different studies was founded regarding the method of preparation, kind of polymers and the rate of drug/carrier.

Up to 2015, there were 23 solid dispersion commercially available products and none of them include a flavonoid or herbal extract (Zhang et al., 2018). Future studies regarding solid dispersion, including preclinical and clinical, needs to be carried out for improving the bioavailability of flavonoids.

Conclusion

This review attempt to provide an insight view on the development of solid dispersion of flavonoids for improving their dissolution-limited absorption. Also, we encourage the application of this formulation technology in the pharmaceutical development of flavonoids products to explore their pharmacological properties. Solid dispersion could enhance the solubility, dissolution and in general triplicate the oral bioavailability of

flavonoids. Thus, solid dispersion is a feasible and successful approach for overcoming the low solubility and low bioavailability of flavonoids.

Acknowledgements

This study was financially supported by Coordenação de Aperfeiçoamento de Pessoal de Nível Superior/Ministério da Educação−CAPES/MEC and FAPERGS (Edital PqG 2017-T.O. 17/2551-0001043-4). M.C. would like to thank CAPES-MEC for her research fellowship.

References

Abourehab, M.A., Khaled, K.A., Sarhan, H.A., Ahmed, O.A., 2015. Evaluation of combined famotidine with quercetin for the treatment of peptic ulcer: in vivo animal study. Drug design, development and therapy 9, 2159.

Alshehri, S.M., Shakeel, F., Ibrahim, M.A., Elzayat, E.M., Altamimi, M., Mohsin, K., Almeanazel, O.T., Alkholief, M., Alshetaili, A., Alsulays, B., 2018. Dissolution and bioavailability improvement of bioactive apigenin using solid dispersions prepared by different techniques. Saudi Pharmaceutical Journal.

Bravo, L., 1998. Polyphenols: chemistry, dietary sources, metabolism, and nutritional significance. Nutr Rev 56, 317-333.

Cao, Y., Teng, J., Selbo, J., 2017. Amorphous solid dispersion of epigallocatechin gallate for enhanced physical stability and controlled release. Pharmaceuticals 10, 88.

Chen, Z.-p., Sun, J., Chen, H.-x., Xiao, Y.-y., Liu, D., Chen, J., Cai, H., Cai, B.-c., 2010. Comparative pharmacokinetics and bioavailability studies of quercetin, kaempferol and isorhamnetin after oral administration of Ginkgo biloba extracts, Ginkgo biloba extract phospholipid complexes and Ginkgo biloba extract solid dispersions in rats. Fitoterapia 81, 1045-1052.

Ciurana, J., Rodriguez, C.A., 2017. Trends in Nanomaterials and Processing for Drug Delivery of Polyphenols in the Treatment of Cancer and Other Therapies. Curr Drug Targets 18, 135-146.

Cong, W., Shen, L., Xu, D., Zhao, L., Ruan, K., Feng, Y., 2014. Solid dispersion tablets of breviscapine with polyvinylpyrrolidone K30 for improved dissolution and bioavailability to commercial breviscapine tablets in beagle dogs. European journal of drug metabolism and pharmacokinetics 39, 203-210.

Del Rio, D., Rodriguez-Mateos, A., Spencer, J.P.E., Tognolini, M., Borges, G., Crozier, A., 2013. Dietary (Poly)phenolics in Human Health: Structures, Bioavailability, and Evidence of Protective Effects Against Chronic Diseases. Antioxidants & Redox Signaling 18, 1818-1892.

Ding, S.-m., Zhang, Z.-h., Song, J., Cheng, X.-d., Jiang, J., Jia, X.-b., 2014. Enhanced bioavailability of apigenin via preparation of a carbon nanopowder solid dispersion. International journal of nanomedicine 9, 2327.

Duan, J., Dang, Y., Meng, H., Wang, H., Ma, P., Li, G., Wu, T., Xie, Y., 2016. A comparison of the pharmacokinetics of three different preparations of total flavones of Hippophae rhamnoides in beagle dogs after oral administration. European journal of drug metabolism and pharmacokinetics 41, 239-249.

Dwi, S., Febrianti, S., Zainul, A., Retno, S., 2018. PEG 8000 increases solubility and dissolution rate of quercetin in solid dispersion system. Marmara Pharmaceutical Journal 22.

Ge, Y., 2010. An investigation into the mechanisms of rapid release of standard extract from Ginkgo biloba leaf in polyethylene glycol 6000 solid dispersions. Yakugaku Zasshi 130, 425-430.

Ghanem, A.S.M., Ali, H.S.M., El-Shanawany, S.M., Ibrahim, E.-S.A., 2013. Solubility and dissolution enhancement of quercetin via preparation of spray dried microstructured solid dispersions. Thai Journal of Pharmaceutical Sciences 37.

Gilley, A.D., Arca, H.C., Nichols, B.L., Mosquera-Giraldo, L.I., Taylor, L.S., Edgar, K.J., Neilson, A.P., 2017. Novel cellulose-based amorphous solid dispersions enhance quercetin solution concentrations in vitro. Carbohydrate polymers 157, 86-93.

Han, H.-K., Lee, B.-J., Lee, H.-K., 2011. Enhanced dissolution and bioavailability of biochanin A via the preparation of solid dispersion: in vitro and in vivo evaluation. International journal of pharmaceutics 415, 89-94.

He, X., Pei, L., Tong, H.H., Zheng, Y., 2011. Comparison of spray freeze drying and the solvent evaporation method for preparing solid dispersions of baicalein with Pluronic F68 to improve dissolution and oral bioavailability. AAPS PharmSciTech 12, 104-113.

Hu, B., Liu, X., Zhang, C., Zeng, X., 2017a. Food macromolecule based nanodelivery systems for enhancing the bioavailability of polyphenols. Journal of food and drug analysis 25, 3-15.

Hu, M., Wu, B., Liu, Z., 2017b. Bioavailability of Polyphenols and Flavonoids in the Era of Precision Medicine. Molecular Pharmaceutics 14, 2861-2863.

Huang, Y., Dai, W.G., 2014. Fundamental aspects of solid dispersion technology for poorly soluble drugs. Acta Pharm Sin B 4, 18-25.

ITO, S., DEMACHI, M., TORIUMI, Y., ADACHI, T., ITAI, S., HIRAYAMA, F., UEKAMA, K., 1995. Improvement of dissolution characteristics of a new chalcone derivative, SU-740: Comparison between size reduction, solid dispersion and inclusion complexation. Chemical and pharmaceutical bulletin 43, 2221-2225.

Kakran, M., Sahoo, N., Li, L., 2011. Dissolution enhancement of quercetin through nanofabrication, complexation, and solid dispersion. Colloids and Surfaces B: Biointerfaces 88, 121-130.

Kakran, M., Sahoo, N.G., Tan, Y.W., Li, L., 2013. Ternary dispersions to enhance solubility of poorly water soluble antioxidants. Colloids and Surfaces A: Physicochemical and Engineering Aspects 433, 111-121.

Kanaze, F., Bounartzi, M., Georgarakis, M., Niopas, I., 2007. Pharmacokinetics of the citrus flavanone aglycones hesperetin and naringenin after single oral administration in human subjects. European journal of clinical nutrition 61, 472.

Kanaze, F., Kokkalou, E., Niopas, I., Georgarakis, M., Stergiou, A., Bikiaris, D., 2006a. Dissolution enhancement of flavonoids by solid dispersion in PVP and PEG matrixes: A comparative study. Journal of applied polymer science 102, 460-471.

Kanaze, F., Kokkalou, E., Niopas, I., Georgarakis, M., Stergiou, A., Bikiaris, D., 2006b. Thermal analysis study of flavonoid solid dispersions having enhanced solubility. Journal of thermal analysis and calorimetry 83, 283-290.

Kaur, H., Kaur, G., 2014. A Critical Appraisal of Solubility Enhancement Techniques of Polyphenols. Journal of Pharmaceutics 2014, 14.

Khan, A.W., Kotta, S., Ansari, S.H., Sharma, R.K., Ali, J., 2015. Enhanced dissolution and bioavailability of grapefruit flavonoid Naringenin by solid dispersion utilizing fourth generation carrier. Drug Development and Industrial Pharmacy 41, 772-779.

Khushnud, T., Mousa, S.A., 2013. Potential role of naturally derived polyphenols and their nanotechnology delivery in cancer. Mol Biotechnol 55, 78-86.

Kovalevska, I., Ruban, E., Kutsenko, S., Kutova, O., Kovalenko, S.M., 2017. Study of physical and chemical properties of solid dispersions of quercetin.

Kumar, S., Pandey, A.K., 2013. Chemistry and biological activities of flavonoids: an overview. The Scientific World Journal 2013.

Kwon, S.H., Kim, S.Y., Ha, K.W., Kang, M.J., Huh, J.S., Kim, Y.M., Park, Y.M., Kang, K.H., Lee, S., Chang, J.Y., 2007. Pharmaceutical evaluation of genistein-loaded pluronic micelles for oral delivery. Archives of pharmacal research 30, 1138-1143.

Leonarduzzi, G., Testa, G., Sottero, B., Gamba, P., Poli, G., 2010. Design and development of nanovehicle-based delivery systems for preventive or therapeutic supplementation with flavonoids. Curr Med Chem 17, 74-95.

Li, B., He, M., Li, W., Luo, Z., Guo, Y., Li, Y., Zang, C., Wang, B., Li, F., Li, S., 2013a. Dissolution and pharmacokinetics of baicalin–polyvinylpyrrolidone coprecipitate. Journal of Pharmacy and Pharmacology 65, 1670-1678.

Li, B., Konecke, S., Harich, K., Wegiel, L., Taylor, L.S., Edgar, K.J., 2013b. Solid dispersion of quercetin in cellulose derivative matrices influences both solubility and stability. Carbohydrate polymers 92, 2033-2040.

Li, B., Wen, M., Li, W., He, M., Yang, X., Li, S., 2011. Preparation and characterization of baicalin-poly -vinylpyrrolidone coprecipitate. International Journal of Pharmaceutics 408, 91-96.

Li, Y.-P., Zhang, X.-Y., Zhou, J.-J., Pei, Y.-Y., 1999a. Preparation and dissolution property of ipriflavone solid dispersion. Zhongguo yao li xue bao= Acta pharmacologica Sinica 20, 957-960.

Li, Y.-P., Zhou, J.-J., Zhang, X.-Y., Pei, Y.-Y., 1999b. Pharmacokinetics of intragastric ipriflavone solid dispersion in rats. Zhongguo yao li xue bao= Acta pharmacologica Sinica 20, 1035-1038.

Long, Q., Xie, Y., Huang, Y., Wu, Q., Zhang, H., Xiong, S., Liu, Y., Chen, L., Wei, Y., Zhao, X., 2013. Induction of apoptosis and inhibition of angiogenesis by PEGylated liposomal quercetin in both cisplatin-sensitive and cisplatin-resistant ovarian cancers. Journal of biomedical nanotechnology 9, 965-975.

Lu, C., Lu, Y., Chen, J., Zhang, W., Wu, W., 2007. Synchronized and sustained release of multiple components in silymarin from erodible glyceryl monostearate matrix system. European Journal of Pharmaceutics and Biopharmaceutics 66, 210-219.

Lunny, C.A., Salzwedel, D.M., Liu, T., Ramasubbu, C., Gerrish, S., Puil, L., Mintzes, B., Wright, J.M., 2018. Protocol for the validation of four search strategies for retrieval of Clinical Practice Guidelines in MEDLINE, Embase and PubMed. PeerJ Preprints 6, e27149v27141.

Mishra, D.K., Dhote, V., Bhargava, A., Jain, D.K., Mishra, P.K., 2015. Amorphous solid dispersion technique for improved drug delivery: basics to clinical applications. Drug Deliv Transl Res 5, 552-565.

Moher, D., Liberati, A., Tetzlaff, J., Altman, D.G., 2009. Preferred reporting items for systematic reviews and meta-analyses: the PRISMA statement. PLoS Med 6, 21.

Ng, C.L., Lee, S.E., Lee, J.K., Kim, T.H., Jang, W.S., Choi, J.S., Kim, Y.H., Kim, J.K., Park, J.S., 2016. Solubilization and formulation of chrysosplenol C in solid dispersion with hydrophilic carriers. Int J Pharm 512, 314-321.

Onoue, S., Nakamura, T., Uchida, A., Ogawa, K., Yuminoki, K., Hashimoto, N., Hiza, A., Tsukaguchi, Y., Asakawa, T., Kan, T., 2013. Physicochemical and biopharmaceutical characterization of amorphous solid dispersion of nobiletin, a citrus polymethoxylated flavone, with improved hepatoprotective effects. European journal of pharmaceutical sciences 49, 453-460.

Onoue, S., Uchida, A., Takahashi, H., Seto, Y., Kawabata, Y., Ogawa, K., Yuminoki, K., Hashimoto, N., Yamada, S., 2011. Development of high-energy amorphous solid dispersion of nanosized nobiletin, a citrus polymethoxylated flavone, with improved oral bioavailability. Journal of pharmaceutical sciences 100, 3793-3801.

Otto, D.P., Otto, A., de Villiers, M.M., 2013. Experimental and mesoscale computational dynamics studies of the relationship between solubility and release of quercetin from PEG solid dispersions. International journal of pharmaceutics 456, 282-292.

Panizzon, G.P., Bueno, F.G., Ueda-Nakamura, T., Nakamura, C.V., Dias Filho, B.P., 2014. Preparation of spray-dried soy isoflavone-loaded gelatin microspheres for enhancement of dissolution: formulation, characterization and in vitro evaluation. Pharmaceutics 6, 599-615.

Porcu, E.P., Cossu, M., Rassu, G., Giunchedi, P., Cerri, G., Pourová, J., Najmanová, I., Migkos, T., Pilařová, V., Nováková, L., 2018. Aqueous injection of quercetin: An approach for confirmation of its direct in vivo cardiovascular effects. International journal of pharmaceutics 541, 224-233.

Qiu, M.-f., Jia, W., Li, S.-s., Xu, Z.-h., Sun, X., Wang, X.-r., Zhang, Y.-y., Xie, G.-x., 2005. A new silymarin preparation based on solid dispersion technique. Advances in therapy 22, 595-600.

Rodriguez-Mateos, A., Vauzour, D., Krueger, C.G., Shanmuganayagam, D., Reed, J., Calani, L., Mena, P., Del Rio, D., Crozier, A., 2014. Bioavailability, bioactivity and impact on health of dietary flavonoids and related compounds: an update. Arch Toxicol 88, 1803-1853.

Setyawan, D., Fadhil, A.A., Juwita, D., Yusuf, H., Sari, R., 2017. Enhancement of solubility and dissolution rate of quercetin with solid dispersion system formation using hydroxypropyl methyl cellulose matrix. Thai Journal of Pharmaceutical Sciences 41.

Shete, G., Modi, S.R., Bansal, A.K., 2015a. Effect of mannitol on nucleation and crystal growth of amorphous flavonoids: implications on the formation of nanocrystalline solid dispersion. Journal of pharmaceutical sciences 104, 3789-3797.

Shete, G., Pawar, Y.B., Thanki, K., Jain, S., Bansal, A.K., 2015b. Oral bioavailability and pharmacodynamic activity of hesperetin nanocrystals generated using a novel bottom-up technology. Molecular pharmaceutics 12, 1158-1170.

Shuai, S., Yue, S., Huang, Q., Wang, W., Yang, J., Lan, K., Ye, L., 2016. Preparation, characterization and in vitro/vivo evaluation of tectorigenin solid dispersion with

improved dissolution and bioavailability. European journal of drug metabolism and pharmacokinetics 41, 413-422.

Sonali, D., Tejal, S., Vaishali, T., Tejal, G., 2010. Silymarin-solid dispersions: characterization and influence of preparation methods on dissolution. Acta Pharmaceutica 60, 427-443.

Squillaro, T., Cimini, A., Peluso, G., Giordano, A., Melone, M.A.B., 2018. Nano-delivery systems for encapsulation of dietary polyphenols: An experimental approach for neurodegenerative diseases and brain tumors. Biochem Pharmacol 154, 303-317.

Sun, N., Wei, X., Wu, B., Chen, J., Lu, Y., Wu, W., 2008a. Enhanced dissolution of silymarin/polyvinylpyrrolidone solid dispersion pellets prepared by a one-step fluid-bed coating technique. Powder Technology 182, 72-80.

Sun, N., Zhang, X., Lu, Y., Wu, W., 2008b. In vitro evaluation and pharmacokinetics in dogs of solid dispersion pellets containing Silybum marianum extract prepared by fluid-bed coating. Planta medica 74, 126-132.

Teng, H., Chen, L., 2018. Polyphenols and Bioavailability: an update. Crit Rev Food Sci Nutr 6, 1437023.

Tsao, R., 2010. Chemistry and biochemistry of dietary polyphenols. Nutrients 2, 1231-1246.

Vasconcelos, T., Marques, S., das Neves, J., Sarmento, B., 2016. Amorphous solid dispersions: Rational selection of a manufacturing process. Advanced drug delivery reviews 100, 85-101.

Vittorio, O., Curcio, M., Cojoc, M., Goya, G.F., Hampel, S., Iemma, F., Dubrovska, A., Cirillo, G., 2017. Polyphenols delivery by polymeric materials: challenges in cancer treatment. Drug Deliv 24, 162-180.

Vo, C.L., Park, C., Lee, B.J., 2013. Current trends and future perspectives of solid dispersions containing poorly water-soluble drugs. Eur J Pharm Biopharm 85, 799-813.

Wang, G.F., Dai, C.L., Liao, Z.G., Zhao, G.W., Liang, X.L., Yang, M., Zhong, S.J., Zhang, N., 2011. Characterization, physical stability, and dissolution behavior of naringenin/mannitol solid dispersions prepared by solvent evaporation method with three drying methods, Advanced Materials Research. Trans Tech Publ, 2264-2272.

Wang, J., Ye, X., Lin, S., Liu, H., Qiang, Y., Chen, H., Jiang, Z., Zhang, K., Duan, X., Xu, Y., 2018. Preparation, characterization and in vitro and in vivo evaluation of a solid dispersion of Naringin. Drug development and industrial pharmacy 44, 1725-1732.

Wang, S., Zhang, J., Chen, M., Wang, Y., 2013. Delivering flavonoids into solid tumors using nanotechnologies. Expert Opin Drug Deliv 10, 1411-1428.

Wang, W., Kang, Q., Liu, N., Zhang, Q., Zhang, Y., Li, H., Zhao, B., Chen, Y., Lan, Y., Ma, Q., 2015. Enhanced dissolution rate and oral bioavailability of Ginkgo biloba extract by preparing solid dispersion via hot-melt extrusion. Fitoterapia 102, 189-197.

Weerapol, Y., Tubtimsri, S., Jansakul, C., Sriamornsak, P., 2017. Improved dissolution of Kaempferia parviflora extract for oral administration by preparing solid dispersion via solvent evaporation. asian journal of pharmaceutical sciences 12, 124-133.

Wegiel, L.A., Mauer, L.J., Edgar, K.J., Taylor, L.S., 2014. Mid-infrared spectroscopy as a polymer selection tool for formulating amorphous solid dispersions. Journal of Pharmacy and Pharmacology 66, 244-255.

Wu, Q., Deng, S., Li, L., Sun, L., Yang, X., Liu, X., Liu, L., Qian, Z., Wei, Y., Gong, C., 2013. Biodegradable polymeric micelle-encapsulated quercetin suppresses tumor growth and metastasis in both transgenic zebrafish and mouse models. Nanoscale 5, 12480-12493.

Xie, Y., Li, G., Yuan, X., Cai, Z., Rong, R., 2009. Preparation and in vitro evaluation of solid dispersions of total flavones of Hippophae rhamnoides L. Aaps Pharmscitech 10, 631-640.

Xie, Y., Lu, Y., Qi, J., Li, X., Zhang, X., Han, J., Jin, S., Yuan, H., Wu, W., 2013. Synchronized and controlled release of multiple components in silymarin achieved by the osmotic release strategy. International journal of pharmaceutics 441, 111-120.

Xu, W., Wen, M., Yu, J., Zhang, Q., Polyakov, N.E., Dushkin, A.V., Su, W., 2018. Mechanochemical preparation of kaempferol intermolecular complexes for enhancing the solubility and bioavailability. Drug development and industrial pharmacy 44, 1924-1932.

Yang, X., Wang, G., Zhang, X., 2004. Release kinetics of catechins from chewing gum. Journal of pharmaceutical sciences 93, 293-299.

Yao, L.H., Jiang, Y.M., Shi, J., Tomas-Barberan, F.A., Datta, N., Singanusong, R., Chen, S.S., 2004. Flavonoids in food and their health benefits. Plant Foods Hum Nutr 59, 113-122.

Yu, H., Chang, J.-S., Kim, S.Y., Kim, Y.G., Choi, H.-K., 2017. Enhancement of solubility and dissolution rate of baicalein, wogonin and oroxylin A extracted from Radix scutellariae. International journal of pharmaceutics 528, 602-610.

Zhang, J., Han, R., Chen, W., Zhang, W., Li, Y., Ji, Y., Chen, L., Pan, H., Yang, X., Pan, W., Ouyang, D., 2018. Analysis of the Literature and Patents on Solid Dispersions from 1980 to 2015. Molecules (Basel, Switzerland) 23, 1697.

Zhao, G., Duan, J., Xie, Y., Lin, G., Luo, H., Li, G., Yuan, X., 2013. Effects of solid dispersion and self-emulsifying formulations on the solubility, dissolution, permeability and pharmacokinetics of isorhamnetin, quercetin and kaempferol in total flavones of Hippophae rhamnoides L. Drug development and industrial pharmacy 39, 1037-1045.

Zhong, S.J., Wang, G.F., Dai, C.L., Liao, Z.G., Zhang, N., Wang, C.L., Han, X.Z., 2011. Preparation, Characterization and Evaluation In Vitro of Naringenin-PVP K-30 Solid Dispersions, Advanced Materials Research. Trans Tech Publ, 2422-2428.

Supplementary Material

FLAVONOIDS DELIVERY BY SOLID DISPERSION: A SYSTEMATIC REVIEW

Mariana Colombo, Luana R. Michels, Helder F. Teixeira, Letícia S. Koester

The specific keywords that have been used in this search strategy: (solid dispersion) AND (plant OR extract OR herbal OR polyphenol OR flavonoid OR isoflav OR chalcon OR neoflavonoid OR dihydrochalcon OR dihydroflavonol OR flavone OR flavonol OR flavanone OR flavanonol OR dihydroflavonol OR flavanol OR quercetin OR kaempferol OR myricetin OR isorhamnetin OR daidzein OR genistein OR formononetin OR glycitein OR biochanin OR dalbergin OR phloretin OR xanthohumol OR apigenin OR luteolin OR taxifolin OR naringenin OR hesperetin OR tangeretin OR nobiletin OR proanthocyanidin OR flavan-3-ols OR catechin OR epicatechin OR gallocatechin OR anthocyanidin OR procyanidin OR theaflavin OR cyanidin OR delphinidin OR pelargonidin OR malvidin OR peonidin OR petunidin)

CAPÍTULO II- Publicação II

Artigo publicado no periódico *AAPS PharmSciTech*

Colombo, M., de Lima Melchiades, G., Michels, L.R. Figueiró, F., Bassani, V.L., Teixeira, H. F., & Koester, L. S. (2017). *Solid Dispersion of Kaempferol: Formulation Development, Characterization, and Oral Bioavailability Assessment.* AAPS PharmSciTech (2019) 20: 106. https://doi.org/10.1208/s12249-019-1318-y

SOLID DISPERSION OF KAEMPFEROL: FORMULATION DEVELOPMENT, CHARACTERIZATION AND ORAL BIOAVAILABILITY ASSESSMENT

Mariana Colombo[a], Gabriela de Lima Melchiades[a], Luana Roberta Michels[a], Fabrício Figueiró[b,c], Valquiria Linck Bassania, Helder Ferreira Teixeira[a], Letícia Scherer Koester[a]*

[a]Laboratório de Desenvolvimento Galênico, Programa de Pós-Graduação em Ciências Farmacêuticas, Faculdade de Farmácia, Universidade Federal do Rio Grande do Sul, Avenida Ipiranga, 2752, Porto Alegre, RS, Brazil.

[b]Programa de Pós-Graduação em Ciências Biológicas: Bioquímica, Instituto de Ciências Básicas da Saúde, Universidade Federal do Rio Grande do Sul, Avenida Ramiro Barcelos, 2600-anexo, 90035-003, Porto Alegre, RS, Brazil.

[c]Departamento de Bioquímica, Instituto de Ciências Básicas da Saúde, Universidade Federal do Rio Grande do Sul, Avenida Ramiro Barcelos, 2600, Anexo, 90035-003, Porto Alegre, RS, Brazil.

*Corresponding author at: Dr. Letícia S. Koester, Faculdade de Farmácia, Universidade Federal do Rio Grande do Sul, Avenida Ipiranga, 2752-607, Porto Alegre-RS, Brazil. Email: leticia.koester@ufrgs.br

ABSTRACT

Kaempferol (KPF), an important flavonoid, has been reported to exert antioxidant, anti-inflammatory, and anticancer activity. However, this compound has low water solubility and hence poor oral bioavailability. This work aims to prepare a solid dispersion (SD) of KPF using Poloxamer 407 in order to improve the water solubility, dissolution rate, and pharmacokinetic properties KPF. After optimization, SD were prepared at a 1:5 weight ratio of KPF:carrier using solvent method (SD_{SM}) and melting method (SD_{MM}). Formulations were characterized by Fourier transform infrared spectroscopy (FTIR), X-ray diffractometry (XRD) analysis, differential scanning calorimetry (DSC), and scanning electron microscopy (SEM). The solubility in water of carried-KPF was about 4,000-fold greater than that of free KPF. Compared to free KPF or the physical mixture, solid dispersions significantly increased the extent of drug release (approximately 100% within 120 min) and the dissolution rate. Furthermore, after oral administration of SD_{MM} in rats, the area under the curve (AUC) and the peak plasma concentration (Cmax) of KPF from SD_{MM} were two-fold greater than those of free KPF ($p<0.05$). In conclusion, SD with Poloxamer 407 is a feasible pharmacotechnical strategy to ameliorate the dissolution and bioavailability of KPF.

Keywords: Kaempferol, Poloxamer 407, solid dispersion, dissolution, bioavailability

Introduction

Kaempferol (KPF) is a flavonoid compound present in various edible plants (grapes, red fruits, onions, and citrus fruits) and it has been also found in various medicinal plants, such as *Ginkgo biloba, Tilia spp, Hypericum perforatum L.,* and *Hippophae rhamnoides* (1, 2). KPF has been reported with potential antioxidant and free radical scavenging, anti-inflammatory, and anticancer properties (1). However, these activities may not be relevant to clinical applications whether this compound does not reach the therapeutic targets at the required concentrations. Kaempferol is poorly absorbed, and present poor oral bioavailability (1-4). KPF is a Biopharmaceutical Classification Scheme class (BCS) II drug having sparingly solubility in water, with considerably high permeability (5). When absorbed, KPF is frequently metabolized into sulfate, methyl, or glucuronide forms (2, 5). Therefore, enhancing the solubility of KPF in the gastrointestinal system is crucial to increasing absorption and, consequently, improving the clinical response.

Multiple approaches have been applied in order to increase the druggability of new candidates such as particle size reduction, salt formation, prodrug formation, complexation with cyclodextrin, nanoemulsions, and solid dispersion (SD); the latter is a common pharmaceutical method and considered one of the most effective approaches to enhance the solubility and dissolution profile of poorly water-soluble drugs (6-8). The basis of the SD method is to disperse the drug in a hydrophilic matrix. Using this technique, wettability and porosity are increased, particles present a reduced particle size, and amorphous forms with high apparent aqueous solubility are generated (9). Drugs in this system are dispersed in separate molecules, in crystalline particles or amorphous form. The carrier is used in the crystalline or amorphous state (6). Different techniques are used for SD preparation, but the solvent method (SM) and melting method (MM) are the major conventional techniques. Regarding MM, the matrix is melted and the drug is added, and then the liquid mixture returns to a solid state by cooling or solidification of the sample. For SM, a volatile solvent is used to dissolve the polymer and the drug. To obtain a uniform diffusion of the drug in the matrix, the mixture is stirred and the solvent is evaporated (10).

The solubility of drugs in different carriers prepared by the SD technique can affect the physicochemical properties of the drug, as well as the dissolution profile and oral bioavailability of the drug (11). Hence, proper selection of the carrier and method of preparation are crucial in the development of SD. Some studies have explored the design of oral formulations containing KPF. Most of them developed solid formulations from vegetal extracts containing KPF, such as *Ginkgo biloba* extract (12, 13), persimmon leaf extract (14), and *Hippophae rhamnoides* L. (15, 16). Tzeng and colleagues (17) demonstrated enhanced dissolution and antioxidant activity of KPF-loaded nanoparticles than pure KPF dissolved in water by applying a nanoparticle engineering process. In addition, Kummar and colleagues (18) developed a layer by layer polyelectrolyte nano-matrix on a KPF-loaded $CaCO_3$ template. This formulation significantly increased bioavailability compared to unloaded KPF in rats. Zhang and colleagues (19) and Telang and colleagues (20) performed phospholipid complexation with KPF and both demonstrated enhanced solubility, dissolution rate, and bioavailability of KPF after oral administration in rats. To date, solid dispersion has never been studied as a system containing pure KPF.

In this work, solid dispersion systems of KPF were prepared by MM and SM using a hydrophilic carrier, i.e. Poloxamer 407, after proper selection and characterized by Fourier transform infrared spectroscopy (FTIR), differential scanning calorimetry (DSC), X-ray diffractometry (XRD), and scanning electron microscopy (SEM). Moreover, the solubility and dissolution profile were investigated to assess the benefits of this approach. Finally, the pharmacokinetics were assessed to investigate the performance of KPF-solid dispersion systems *in vivo*.

Material and methods

Materials

KPF (>98.0%) was obtained from Shaanxi Huike Botanical Development (Xi'an, China). Ultra-pure water was acquired from Milli-Q apparatus (Billerica, USA). Poloxamer 407 was kindly donated from BASF (São Paulo, Brazil). Polysorbate 80 was purchased from Sigma-Aldrich (St Louis, USA). Formic acid 96% and methanol

(HPLC grade) were purchased from Tedia (Rio de Janeiro, Brazil). All other materials and solvents were of analytical grade.

High performance liquid chromatography analysis (HPLC)

In vitro *samples*

Kaempferol content in the *in vitro* samples was assessed by HPLC by a previously validated method (21). The column used was XTerra®RP18 (250 mm x 4.6 mm, 5 µm). The mobile phase was composed of a mixture of methanol and 0.1% formic acid in water (75:25, v/v) pumped at 1.0 mL/min. The wavelength was adjusted to 368 nm, and the injection volume was 20.0 µL.

Plasma samples

The kaempferol content in plasma samples was obtained by an HPLC assay as described in the section on *In vitro samples* with slight modifications, employing an HPLC Shimadzu Proeminence (Tokyo, Japan). The flow rate, column, and mobile phase were the same as for the in vitro samples. The injection volume was 40.0 µL. Three calibration curves, constructed on three consecutive days, were prepared by spiking the plasma matrix with standard KPF solution to final concentrations of 0.025, 0.0375, 0.05, 0.1, 0.25, 0.5, 0.75, and 1.0 µg/mL. Each concentration level was analyzed in three replicates. The precision and accuracy of the method were assessed in plasma by performing replicates at four levels (0.025, 0.0375, 0.05, and 0.5 µg/mL), by using 3 replicates of each concentration on 3 consecutive days. The recovery of KPF from plasma was determined at 3 concentrations (30, 100 and 500 ng/mL) in triplicate by analyzing the peak area from plasma samples containing KPF before extraction with the peak area from samples without the plasma matrix. The matrix effect was determined based on the comparison of the slopes obtained in standard curves of KPF in methanol and in plasma matrix (22).

Phase-solubility studies

To determine the best choice of carrier for solid dispersion manufacturing, the aqueous solubility KPF was examined in aqueous solutions of different excipients (Gelucire

44/14, Poloxamer 188, Poloxamer 407, and Soluplus). Solubility studies were conducted using the method reported by Higuchi and Connors (23). An excess quantity of KPF was added to the carrier water solutions at concentrations of 0-10% w/v. The vials were closed and shaken for 48 h in a water bath at 37 ± 0.5 °C. Then, the samples were centrifuged at 10,000 rpm for 20 min. Samples were filtered through a 0.45 μm membrane filter and diluted with methanol to measured by HPLC (21).
The apparent stability constant (Ks) was determined by Eq. 1.

$$Ks=\frac{\text{Slope}}{\text{intercept}}/(1-\text{Slope}) \qquad \text{(Eq. 1)}$$

The values of Gibbs free energy of transfer ($\Delta G°_{tr}$) of KPF were computed using Eq. 2,

$$\Delta G°_{tr}= - 2.303\ RT \log S_0/Ss \qquad \text{(Eq. 2)}$$

where S_0 and Ss are the molar solubility of KPF in aqueous solutions of each carrier to that in pure water, respectively. T is absolute temperature and R (8.31 J $K^{-1}mol^{-1}$) is the general gas constant.

Preparation of solid dispersions (SD)

SDs were prepared by SM and aqueous solubility was determined at various weight ratios of KPF:Poloxamer 407 (1:1, 1:2, 1:3, 1:4, 1:5) for the optimization of the polymer ratio. KPF and the carrier were accurately weighed and dissolved in acetone with continuous stirring for 10 min at ambient temperature. The solvent was removed by a rotary evaporator (Heidolph, Germany). The mass was dried for 48 h in a desiccator, removing traces of the solvent. After optimization, SD_{MM} were prepared at a 1:5 weight ratio of KPF and polymer by MM. KPF was added to the molten carrier, and the blend was warmed at 10°C above the melting point of the polymer with continuous stirring for 10 min. After cooling to ambient temperature, solidified samples were milled to obtain powders. The physical mixture (PM) were prepared by

gently mixing the carrier with KPF for 10 min with a pestle in a glass mortar. Subsequently, the obtained dry powders were passed through sieve #60 (250 μm). All samples were kept in a desiccator.

Saturation solubility studies

The saturation solubility was evaluated individually by adding an excess amount of KPF (20 mg/mL), PM, SD_{MM}, and SD_{SM} in 2.0 mL of distilled water. The flasks were shaken in a water bath at 37 ± 0.5°C for 48 h. Then, the samples were centrifuged for 20 min at 10,000 rpm. Supernatants were filtered through a 0.45 μm membrane filter, appropriately diluted with methanol, and evaluated by HPLC (21).

Solid state characterization

Fourier transform infrared spectroscopy (FTIR)

The FTIR analysis of KPF, carrier, PM, and SD were conducted on a Nicolet iS10 FTIR Spectrometer (Madison, WI, USA). Pellets were prepared from mixtures of the sample and KBr. The spectra were recorded at a resolution of 4 cm^{-1} over a frequency range of 4,000-400 cm^{-1}.

Differential scanning calorimetry (DSC)

DSC measurements of KPF, carrier, PM, and SD were performed on a DSC-60 Shimadzu (Tokyo, Japan) instrument. Samples were placed in aluminum pans and heated from 30°C to 350°C at a rate of 10°C/min with a dynamic nitrogen atmosphere at a flow rate of 100 mL/min. The instrument was calibrated with zinc and indium patterns.

X-ray diffractometry (XRD)

X-ray diffractometry measurements of KPF, carrier, PM, and SD were investigated on a diffractometer Siemens D500 (Berlin, Germany). Measurements were performed using Cu Kα radiation (γ = 1.5406 A), tube current 20 mA, 40 kV voltage, and angular speed 1° (2θ) per minute.

Scanning electron microscopy (SEM)

Morphological characteristics of KPF, carrier, PM, and SD were obtained on a scanning electron microscope Jeol LV-6610 (Tokyo, Japan) at a voltage of 15 kV. Samples were fixed with double-sided tape over aluminum stubs and covered with a gentle layer of gold.

Dissolution studies

Dissolution experiments were carried out in triplicate using the USP II dissolution test apparatus (Nova Ética, Brazil) under predetermined sink conditions. A sample amount equivalent to 25 mg KPF (pure drug, PM, and SD) was filled in an hard gelatin capsule and added to 900 mL of dissolution medium (0.1 N HCl containing 1% w/v Polysorbate 80) at 37°C ± 0.2°C) and shaked at 75 rpm. Each capsule was trapped in a metal sinker in order to avoid floating. At predetermined sampling intervals over 180 min, 1 mL of samples were withdrawn, filtered through a 0.45 μm membrane filter and assayed by HPLC (21). The volume withdrawn was replaced by fresh medium after each sampling. Dissolution efficiency (DE) was computed from the area under the dissolution curve at time and represented as percentage of the rectangle area corresponding to 100% of dissolution (24). The dissolution profiles of SD were examined by difference factor (f_1) and similarity factor (f_2) (25).

Pharmacokinetics in rats

The oral bioavailability of free KPF and SD_{MM} were assessed in male albino Wistar rats (300 ± 20 g). Before the beginning of the assay, animals were deprived of food 12 h, with free access to water. Then, the rats were separated into two groups of four animals per group and administered via oral gavage with the following samples: free KPF, suspended in carboxymethyl-cellulose sodium solution (0.5%) at a dose of 100 mg/kg and SD, suspended in water at a dose of 100 mg/kg. Blood samples (250 μL) were obtained from the tail vein into a heparinized tube at 0.25, 0.5, 1.0, 2.0, 4.0, 6.0, 12.0, and 24 h post-treatment. The plasma fraction were prepared by centrifuging at 10,000 rpm for 10 min, and were preserved at −20°C until analysis. To 100 μL aliquots of plasma, 300 μL of cooled methanol containing 0.1% formic acid was

added. The samples were vortexed for 1 min and centrifuged at 10,000 rpm for 5 min. Next, samples were injected directly into the HPLC.

Animal experiments were approved by Ethical Committee of the Universidade Federal do Rio Grande do Sul (Protocol #31216) and conducted in accordance with "Principles of Laboratory Animal Care", National Institutes of Health (NIH).

Pharmacokinetic analysis

Pharmacokinetic parameters were quantified using PK Solver (version 2.0) (26). The maximum plasma concentration (Cmax) and the time to reach Cmax (Tmax) were determined. The area under the plasma concentration time curve (AUC) were computed by the linear trapezoidal method.

Statistical analysis

All data are expressed as mean ± S.D. (standard deviation). The significant differences were determined statistically using one-way ANOVA followed by Tukey's test or t-test at the 0.05 level of significance using GraphPad Prism 5 software (GraphPad Software, USA).

Results and discussion

Phase-solubility studies

Since various carriers may be utilized in SD preparation and their selection impacts in the solubility of the poorly soluble drugs, the solubility of KPF was determined with different carrier options. The phase-solubility diagrams were arranged using the concentration of each carrier in water versus the concentration of KPF. The solubility of pure KPF in water and with carriers (0 to 10%) is shown in Figure 1. The enhance in KPF solubility with the increasing concentration of each carrier indicates the solvent properties of all tested carriers for KPF. The solubility parameters are presented in Table 1. The KPF solubility in water was 0.36 ± 0.01 µg/mL. Figure 1 shows the phase solubility diagrams for all carriers evaluated.

The values of Ks depend on slope values. The higher the value of the slope, the greater the solubilization capacity of the carrier. Poloxamer 407 showed the highest slope value, suggesting the best capacity to solubilize KPF. The r^2 values obtained for Poloxamer 407 and Gelucire 44/14 were higher than 0.99, demonstrating a positive impact of these excipients on KPF hydrosolubility, giving AL-type solubility diagrams. The ΔG_{tr} ° values give an indication if the reaction condition is unfavorable or favorable for the drug solubilization in each carrier solution. All ΔG_{tr} ° values were negative, indicating a favorable interaction and spontaneous KPF solubilization. The ΔG_{tr} ° values were more negative for Poloxamer 407 than the other tested carries, indicating better solubilization of KPF in the presence of this carrier. In the last years, Poloxamer 407 has been used as a relevant carrier in solid dispersion systems (27-31). Poloxamer 407 is a non-ionic polyoxyethylene-polyoxypropylene copolymer. Above the critical micelle concentration, Poloxamer 407 self-assembles into micelles. The hydrophobic core (propylene oxide) of the micelles can incorporate lipophilic drugs, resulting in improved KPF solubility (32). In addition, the high hydrophilicity and surfactant properties of Poloxamer 407 enhanced the wettability of KPF by decreasing the interfacial tension between KPF and water (33). Based on the solubility studies, Poloxamer 407 was selected for further investigations.

Table 1. Phase solubility of kaempferol (µg/mL) at various concentrations of carriers (n=3).

	Gelucire 44/14		Poloxamer 188		Poloxamer 407		Soluplus	
Conc. of carrier (%w/v)	Conc. of KPF (µg/mL)	ΔG_{tr} ° (kJ/mol)	Conc. of KPF (µg/mL)	ΔG_{tr} ° (kJ/mol)	Conc. of KPF (µg/mL)	ΔG_{tr} ° (kJ/mol)	Conc. of KPF (µg/mL)	ΔG_{tr} ° (kJ/mol)
0	0.36 ± 0.01	-	0.36 ± 0.01	-	0.36 ± 0.01	-	0.36 ± 0.0	-
1	20.04 ± 2.18	-10.36± 0.29	6.71 ± 0.85	-7.54 ± 0.33	110.16 ± 6.14	-14.76 ± 0.15	121.82 ± 1.29	-15.03 ± 0.03
2.5	74.57 ± 4.59	-13.76 ± 0.16	24.88 ± 2.92	-10.92 ± 0.31	316.27 ± 29.40	-17.48 ± 0.25	300.14 ± 19.27	-17.35 ± 0.17
5	175.82 ± 18.51	-15.96 ± 0.27	58.77 ± 0.55	-13.15 ± 0.02	816.39 ± 26.13	-19.75± 0.32	583.26 ± 59.10	-19.23 ± 0.35
10	418.7 ± 47.54	-18.20 ± 0.30	69.18 ± 1.63	-13.16 ± 0.71	1670.16 ± 90.53	-21,68 ± 0,19	944.71 ± 17.08	-20.31 ± 0.05
r^2	0.9913		0.8862		0.9965		0.9845	
Slope	42.66 ± 2.31		7.258 ± 1.50		170.9 ± 5.89		94.35 ± 6.83	
Ks	89.17		8.85		583.52		215.03	

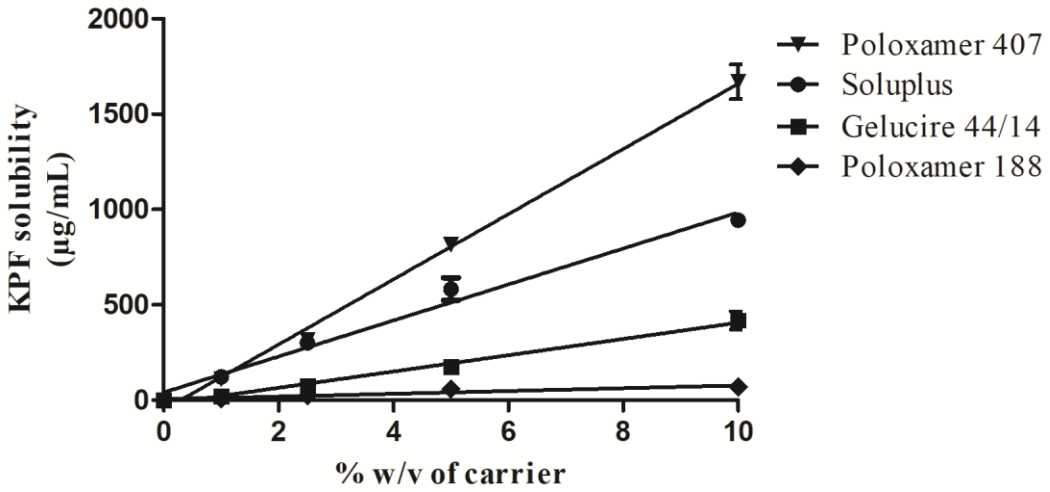

Figure 1. Diagram of phase solubility for KPF in the presence of various carriers in distilled water (mean ± S.D.; n = 3).

***Preparation* of solid dispersions (SD)**

SD were prepared in drug/Poloxamer 407 ratios (1:1, 1:2, 1:3, 1:4, and 1:5) by SM. The effect of the amount of carrier on the KPF solubility is shown in Figure 2. The increase in the solubility was linear as the proportion of the polymer increased up to a weight ratio of 1:5 ($p < 0.0001$) compared to other tested proportions. At 1:5, the solubility increased by about 4,000-fold compared to free KPF.

The choice of the SD method suitable for formulation development should be economical, environmentally friendly, and prevent drug degradation. The solvent technique is commonly used to prepare SD on a small scale (9), but MM is suitable for industrial production due its simplicity and affordability. Additionally, MM requires no organic solvent. The solid dispersion prepared by MM and SM at the 1:5 drug/polymer ratio increased the aqueous solubility of KPF to 1428.66 ± 52.27 µg/ml and 1414.51 ± 41.16 µg/ml, respectively. Both methods, i.e. MM and SM, were found to be efficient to produce SD with a KPF uniform distribution (RSD < 2.59%) and a KPF content of 107.48 ± 2.79% and 105.84 ± 1.22%, respectively.

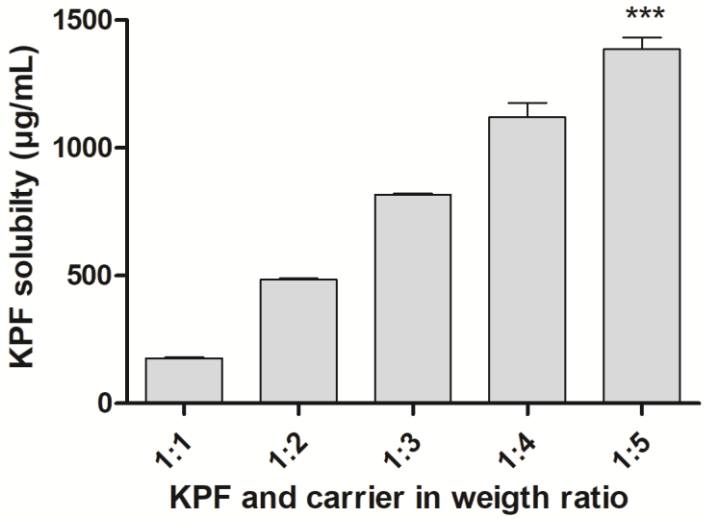

Figure 2. Solubility of KPF from solid dispersions composed of Poloxamer 407 at various drug: carrier weight ratio prepared by solvent method (mean ± S.D.; n = 3). ***$p < 0.0001$, compared to the other groups.

Fourier transform infrared spectroscopy (FTIR)

The FTIR spectra of KPF, carrier, solid dispersions, and the physical mixture are illustrated in Figure 3. The KPF spectrum (Figure 3A) exhibited characteristic peaks, i.e. hydroxyl (OH) stretching at 3324 cm^{-1}, C=O stretching at 1657 cm^{-1}, and benzene ring vibrations close to 1512 cm^{-1}. In the Poloxamer 407 spectrum (Figure 3B), the characteristic peaks at 1344 cm^{-1}, 2887 cm^{-1} and 1110 cm^{-1} were observed to stretching vibrations of the in-plane O-H bending, C-H aliphatic stretching, and C-O stretching, respectively. Figure 3D and 3E show the spectra of the SDs and physical mixture (Figure 3C) are very similar to the overlap of spectra of the single components, while the intensities were attenuated, probably due to the lower proportion of KPF. However, the absorption peak of OH of the KPF was shifted, which could indicate the existence of intermolecular interactions (hydrogen bonding) between KPF and the carrier, which may disrupt the crystalline structure of KPF (19, 34, 35). Since Poloxamer 407 molecule presents two terminal OH groups, KPF molecules may create hydrogen bonds with the polymer (36, 37). The lack of any additional peaks in the spectra of SD suggests the absence of chemical interactions.

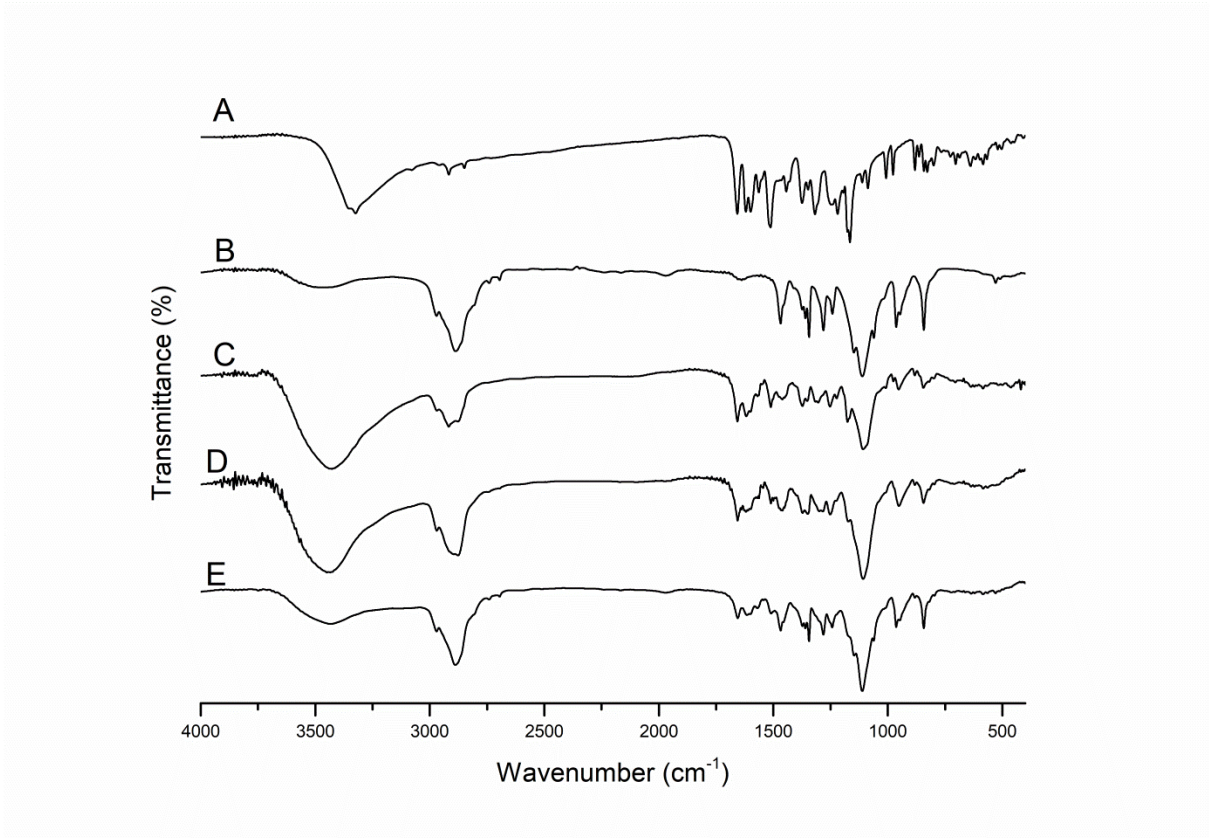

Figure 3. Fourier transform infrared spectroscopy spectra of KPF (A), Poloxamer 407 (B), physical mixture (C), SDMM (D), and SDSM (E).

Differential scanning calorimetry (DSC)

Figure 4 illustrates the DSC thermograms of KPF, Poloxamer 407, physical mixture and SDs. The thermogram of KPF (Figure 4A) shows at 287°C a sharp endothermic peak, indicating its crystalline nature and its melting point (17). The thermogram of Poloxamer 407 (Figure 4B) showed an endothermic peak relative to its melting point (49°C). Poloxamer was stable up to 160°C, after that the baseline was raised, indicating decomposition (38). In Figure 3C, thermogram of the physical mixture was very similar to thermograms of SD, and the melting point of KPF was not detectable. Moreover, the decomposition of poloxamer was not more detectable. In the thermograms of SD (Figure 3D and 3E), the melting endotherms of the polymer were almost unchanged, while the melting peak of KPF disappeared. This could be due the solubilization of KPF in the molten carrier or due to a lack of equipment sensitivity, since the lower proportion of KPF, as also observed in the thermogram of the physical mixture.

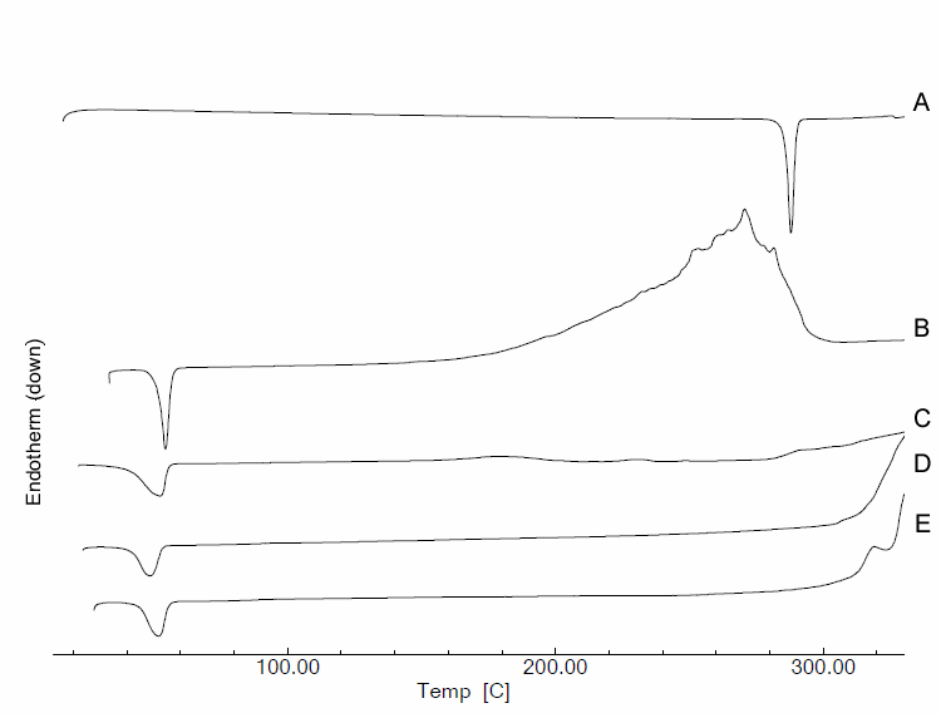

Figure 4. Differential scanning calorimetry thermograms of KPF (A), Poloxamer 407 (B), physical mixture (C), SDMM (D), and SDSM (E).

X-Ray diffraction (XRD)

The XRD patterns of KPF, Poloxamer 407, physical mixture and SDs are illustrated in Figure 5. The diffraction spectra of KPF (Figure 5A) showed intensive diffraction peaks, with the most prominent being 17.4°, 21.6°, 22.3°, and 25.7°, suggesting that KPF was present as a crystalline material. Poloxamer 407 (Figure 5B) had an XRD pattern with two prominent diffraction peaks at 19.1° and 23.2°, suggesting the presence of crystalline domains within the amorphous carrier (36). The diffraction spectra of the physical mixture (Figure 5C) and SD (Figure 5D and 5E) showed peaks at 19.1° and 23.2°, assigned to the carrier, which underwent no alteration in its crystalline nature. The principal peaks of KPF and Poloxamer 407 were showed in the physical mixture (Figure 5C) and SD (Figure 5D and 5E), although with lower intensity, which might be due to the lower proportion of KPF (1:5). However, compared to the physical mixture, some characteristic peaks of KPF disappeared in the solid dispersions, i.e. 17.4°, 18.1°, 21.6° and 22.3° indicating some proportion of drug in the amorphous form. This indicates that some of the drug crystallinity was reduced by Poloxamer 407 in the SD, after the melting/solidification and solubilization/evaporation processes.

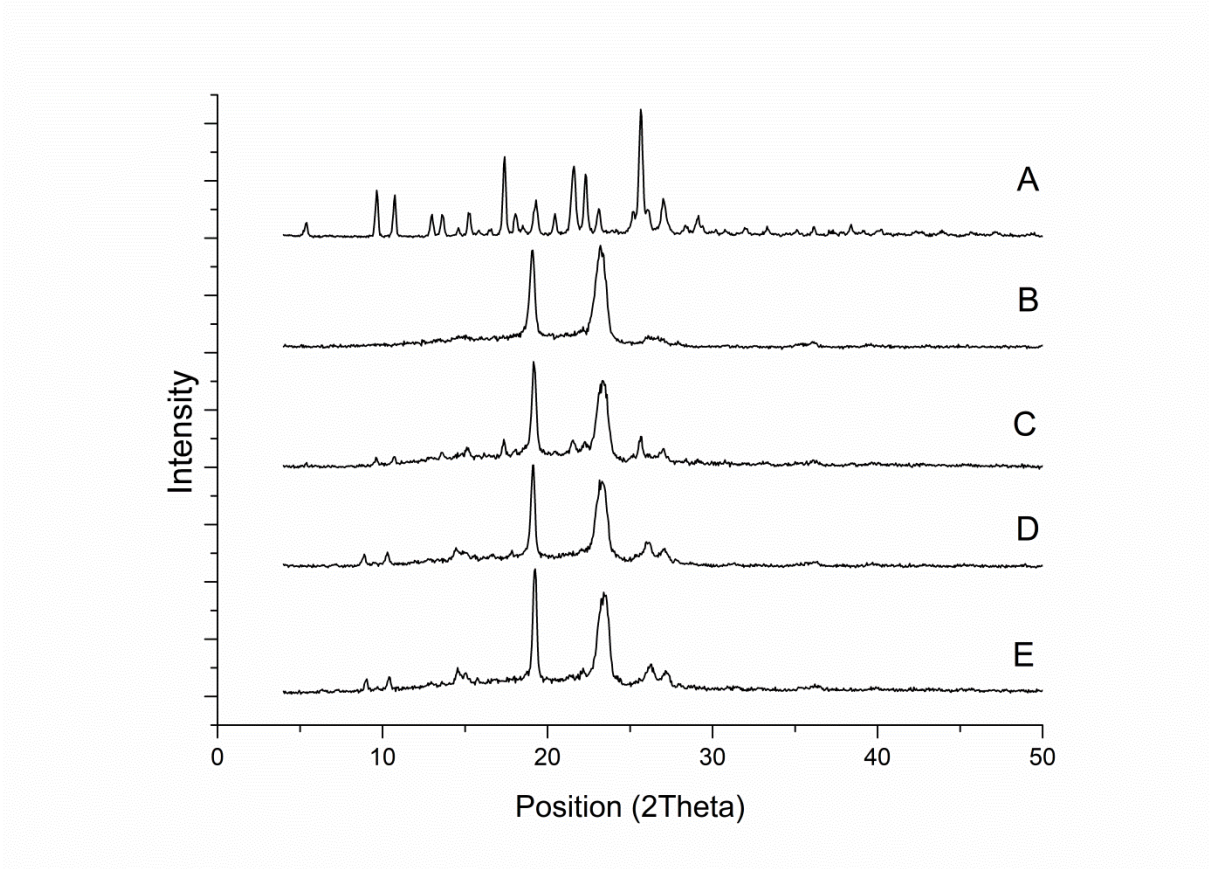

Figure 5. X-ray diffraction patterns of KPF (A), Poloxamer 407 (B), physical mixture (C), SDMM (D), and SDSM (E).

Scanning electron microscopy (SEM)

Images of KPF, Poloxamer 407, physical mixture and the two types of SD are shown in Figure 6. The KPF appeared to be irregular crystalline solids in size and shape (Figure 6A). Poloxamer 407 was presented as spherical smooth-surfaced particles (Figure 6B). The physical mixture showed (Figure 6C) KPF crystals adhered to the surface of Poloxamer 407 and some of the drug was dispersed in the carrier matrix during the physical mixture preparation. The SD systems prepared by MM (Figure 6D) and SM (Figure 6E) showed a similar wrinkled and irregular surface and the absence of visible KPF crystals, demonstrating the presence of dissolved KPF in the polymeric carrier or partial conversion into an amorphous form. The characteristic surface of Poloxamer 407 and KPF were changed during the process of solubilization or

evaporation and melting or solidification, suggesting the successful formation of solid dispersions by solvent and melting method. Furthermore, the irregular surface increased the surface area, responsible for the enhancement of solubility. It was not possible to distinguish any differences between the SD prepared by MM or SM.

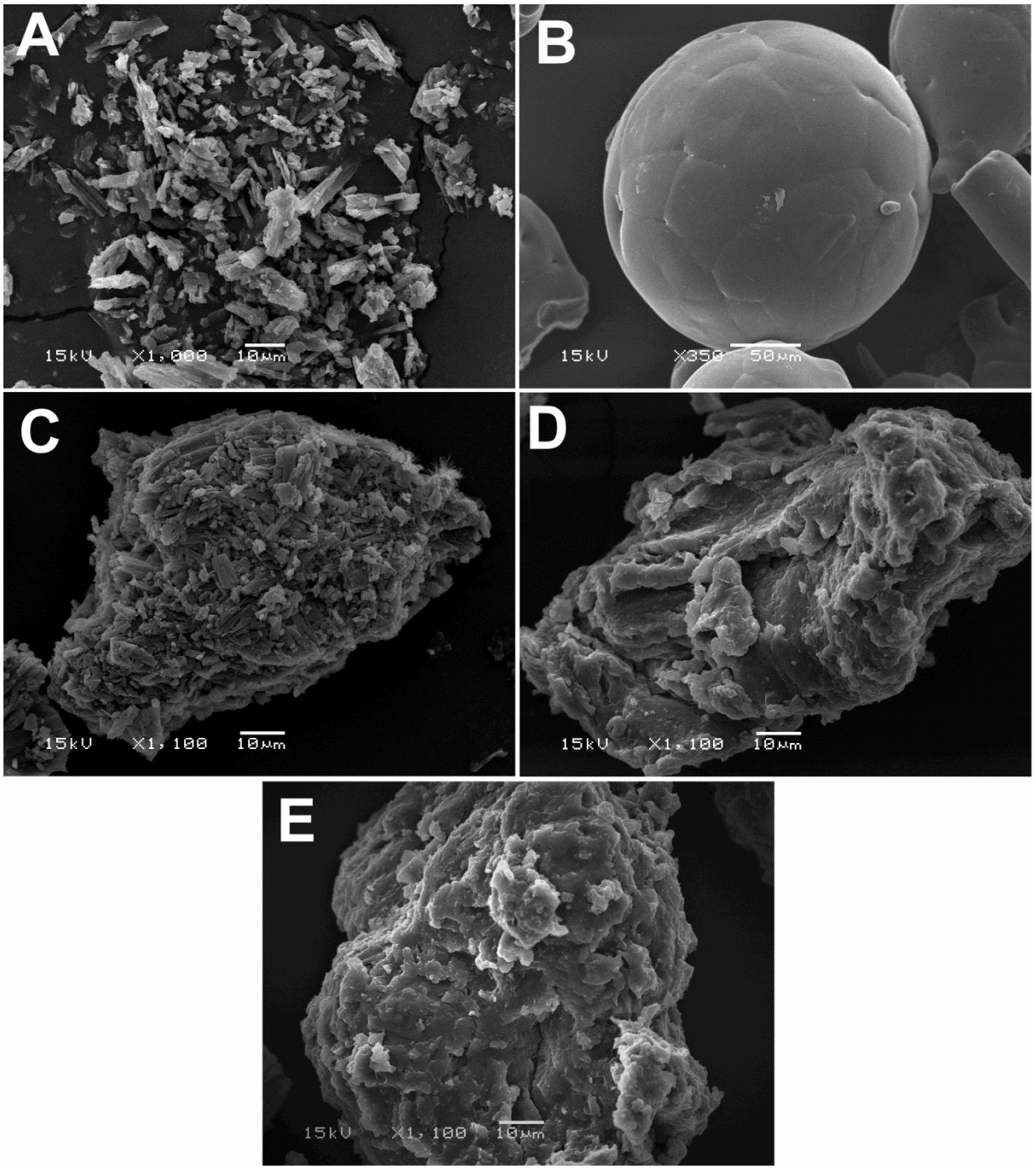

Figure 6. Scanning electron microscopic images of KPF (A), Poloxamer 407 (B), physical mixture (C), SDMM (D), and SDSM (E).

Dissolution studies

Before conducting the dissolution studies, KPF solubility in dissolution media (0.1 N HCl containing 1% w/v Polysorbate 80) was determined to ensure that the experiment was conducted under sink conditions (volume of medium at least 3-fold greater than that required to create a saturated solution of the drug). In the dissolution medium, KPF solubility corresponded to 92.40 ± 3.19 µg/mL. The dissolution profile of the formulations is illustrated in Figure 7. The pure drug displayed poor and incomplete dissolution (62.45% ± 9.32) after 180 min of dissolution. This poor dissolution is mainly attributed to its low solubility in water in addition to its poor wetting property. Such a limited dissolution rate frequently results in poor oral bioavailability, as compounds with water solubility lower than 100 µg/mL commonly show dissolution-limited absorption (39). However, the dissolution rate of KPF from the SD was significantly greater than pure KPF. Complete drug release (~100% within 120 min) was observed in the SD of Poloxamer 407 prepared by SM and MM, whereas PM showed incomplete drug release. SM and MM showed significantly higher dissolution efficiency (74.76 ± 1.34% and 73.32 ± 2.71%, respectively) compared to PM and pure KPF (57.12 ± 0.45% and 22.45 ± 2.37%, respectively; $p < 0.0001$).

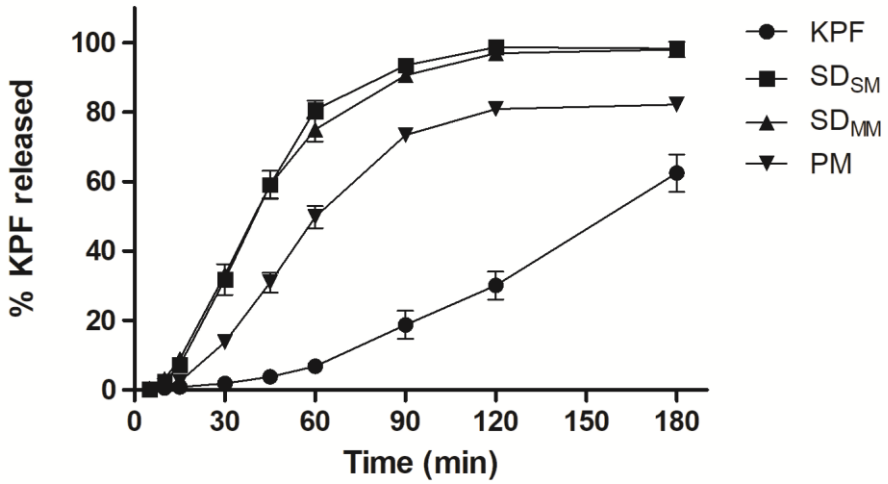

Figure 7. Dissolution profiles from different preparations of kaempferol (mean ± S.D.; n = 3).

The dissolution profiles were compared for similarity by the difference factor (f_1) and the similarity factor (f_2) tests. The f_1 is a measurement of the relative error between two curves, while the f_2 is a measure of the resemblance in the percent of dissolution between two curves. Profiles are treated as "similar" when f_1 is close to 0 and f_2 is close to 100. Current FDA guidelines (40-42) suggest that two profiles can be considered similar if f_1 is less than 15 (0-15) and f_2 is higher than 50 (50-100), which is equivalent to a mean difference of 10% at all sampling time points. The f_1 and f_2 values between SD prepared by SM and MM profiles were 4.62 and 79.6, respectively. This means that the dissolution behavior of SM and MM were similar. It is known that fast solvent removal in SD prepared by SM may leave channels in the SD structure, which increases the surface specific area, the porosity, and the dissolution rate of drugs (6). However, no difference was detect in water solubility and the dissolution profile between SD prepared by MM or SM. Eloy et al. also showed no difference in terms of ursolic acid dissolution between these two methods in SD prepared with Poloxamer 407 (27). Conversely, the comparison between the pure KPF, PM, and SD (SM and MM) dissolution profiles cannot be considered equivalent to each other (data not shown).

The enhanced dissolution rate obtained from the SD was not purely due to increased wetting of KPF in the presence of the Poloxamer 407 once the physical mixture showed a poor improvement in KPF dissolution compared to both SD. Therefore, the loss of KPF crystallinity in SD indicated by X-ray analyses and possible hydrogen bonding between the hydroxyl groups of KPF and carrier by FTIR, resulted in an improved drug dissolution profile.

Pharmacokinetic studies

The calibration curve of KPF was linear from 10 to 1000 ng/ml with $r^2 = 0.9978$. The precision values (repeatability and intermediate precision) were all < 10%. The accuracy was between 99.43 and 112.78%. The recovery of KPF from plasma samples was from 96.35 to 101.54%, meeting the requirements of quantitative analysis. The matrix effect for KPF was -4.06%, indicating low matrix effect.

Based on the results of solid characterization and dissolution tests, SD prepared by MM was chosen for an *in vivo* study of bioavailability. Figure 8 shows the mean plasma concentration-time profile of pure KPF and SD_{MM} in rats. The pharmacokinetic parameters were also determined and are summarized in Table 2. SD_{MM} displayed a primary peak at 1 h followed by a secondary peak at 6 h. Double peaks may be caused by enterohepatic circulation (43). DuPont et al. (2004), Zhang et al. (2009), and Zhang et al. (2010) reported two plasma peak in the concentration time curve, suggesting a potential enterohepatic recirculation of kaempferol after oral administration (44-46). However, this hypothesis needs a more detailed investigation.

While the Tmax of SD was not significantly different from pure KPF, the Cmax of SD was significantly higher (approximately 2.2-fold). The AUC value of KPF was 1.85 greater than that of pure KPF, indicating that SD may improve the oral bioavailability of KPF in rats. These findings indicate improved KPF oral bioavailability after the administration of SD-loaded KPF in rats, which may be attributed to the effective solubilization of KPF from SD. Through different formulation strategies, Kummar et al. (18), based on layer-by-layer nano-matrix, and Zhang et al. (19), based on phospholipid complex, also have shown improvement in oral bioavailability of KPF.

Table 2. Pharmacokinetic parameters of KPF and SDMM after oral administration to rats at 100 mg/Kg (n=4; mean ± S.D.)

Parameter	KPF	SD
Cmax (ng/mL)	117.08 ± 35.13	257.86± 51.63**
Tmax (h)	1.94 ± 2.73	2.50 ± 2.65
AUC 0-t (ng*h/mL)	1042.67 ± 429.72	1932.99 ± 486.89*

C_{max}: peak concentration; T_{max}: time to reach peak concentration; AUC: area under the plasma concentration-time curve; * $p < 0.05$ compared to pure KPF. ** $p < 0.01$ compared to pure KPF.

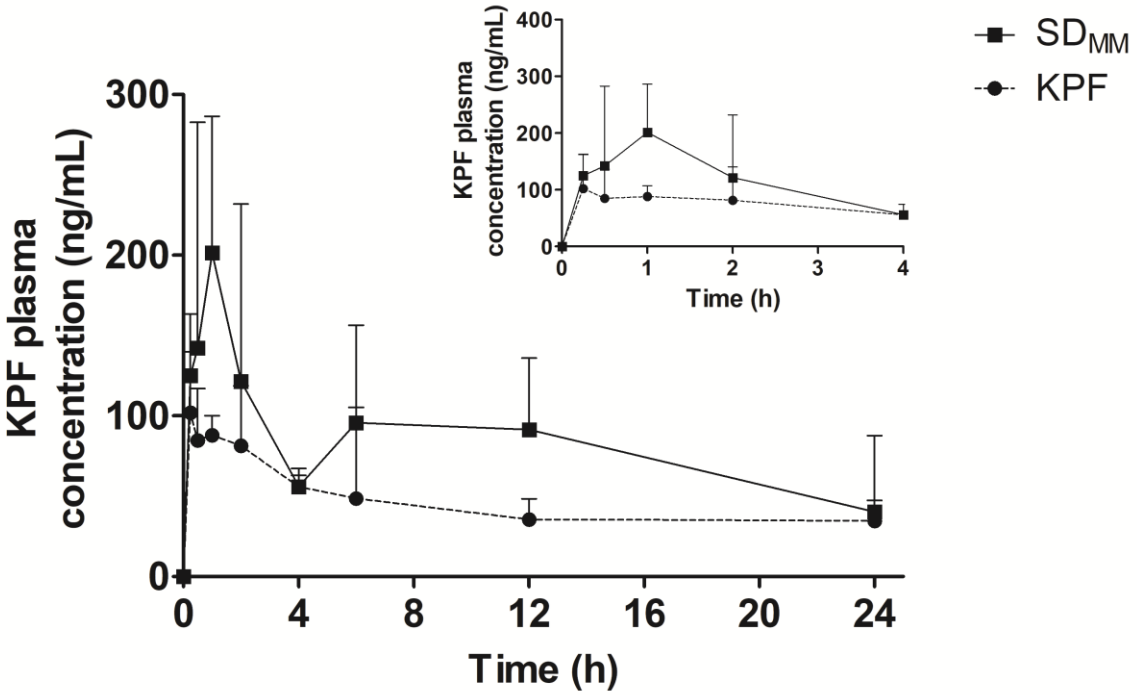

Figure 8. KPF plasma concentration upon oral administration in rats (100 mg/kg) of pure KPF and SDMM (KPF: Poloxamer 407, 1:5) (mean ± S.D., n= 4).

Conclusion

Solid dispersions with Poloxamer 407 appeared to be effective at ameliorating the solubility and dissolution of KPF. The lack of chemical interactions between KPF and the carrier, a reduction in the crystallinity of KPF, and the partial transformation of KPF into an amorphous form in SD formulations were demonstrated. Improved solubility and dissolution were observed with the SD compared to pure KPF. Furthermore, pharmacokinetic studies indicated that SD is an appropriate technology to improve the druggability of KPF, improving oral bioavailability in rats. These results could be an indication that SD_{MM} is an adequate strategy for the development of pharmaceutical formulations carrying KPF.

Acknowledgements

This study was financially supported by CAPES-MEC, Brazil (Network Nanobiotec-grant #902/2009 and PROCAD-grant 552457/2011-6), CNPq (grant #453927/2014-9)

and FAPERGS (Edital PqG 2017-T.O. 17/2551-0001043-4 and 17/2551-0000 970-3). M.C. thanks CAPES for her scholarship.

References

1. Calderon-Montano JM, Burgos-Moron E, Perez-Guerrero C, Lopez-Lazaro M. A review on the dietary flavonoid kaempferol. Mini-Reviews in Medicinal Chemistry. 2011;11:298-344. doi: BSP/MRMC/ Epub/196 [pii].

2. Devi KP, Malar DS, Nabavi SF, Sureda A, Xiao J, Nabavi SM, et al. Kaempferol and inflammation: From chemistry to medicine. Pharmacol Res. 2015;99:1-10.

3. Chen AY, Chen YC. A review of the dietary flavonoid, kaempferol on human health and cancer chemoprevention. Food Chemistry. 2013;138:2099-107. doi: 10.1016/j.foodchem.2012.11.139
S0308-8146(12)01917-6 [pii].

4. Rothwell JA, Day AJ, Morgan MR. Experimental determination of octanol-water partition coefficients of quercetin and related flavonoids. J Agric Food Chem. 2005;53:4355-60.

5. Xie Y, Luo H, Duan J, Hong C, Ma P, Li G, et al. Phytic acid enhances the oral absorption of isorhamnetin, quercetin, and kaempferol in total flavones of Hippophae rhamnoides L. Fitoterapia. 2014;93:216-25. doi: 10.1016/j.fitote.2014.01.013
S0367-326X(14)00019-7 [pii].

6. Vo CL, Park C, Lee BJ. Current trends and future perspectives of solid dispersions containing poorly water-soluble drugs. Eur J Pharm Biopharm. 2013;85:799-813.

7. Chiou WL, Riegelman S. Pharmaceutical applications of solid dispersion systems. J Pharm Sci. 1971;60:1281-302.

8. Leuner C, Dressman J. Improving drug solubility for oral delivery using solid dispersions. European Journal of Pharmaceutics and Biopharmaceutics. 2000;50:47-60. doi: https://doi.org/10.1016/S0939-6411(00)00076-X.

9. Meng F, Gala U, Chauhan H. Classification of solid dispersions: correlation to (i) stability and solubility (ii) preparation and characterization techniques. Drug Dev Ind Pharm. 2015;41:1401-15.
10. Vasconcelos T, Marques S, das Neves J, Sarmento B. Amorphous solid dispersions: Rational selection of a manufacturing process. Advanced drug delivery reviews. 2016;100:85-101. doi: https://doi.org/10.1016/j.addr.2016.01.012.
11. Mustapha O, Kim KS, Shafique S, Kim DS, Jin SG, Seo YG, et al. Comparison of three different types of cilostazol-loaded solid dispersion: Physicochemical characterization and pharmacokinetics in rats. Colloids Surf B Biointerfaces. 2017;154:89-95.
12. Chen ZP, Sun J, Chen HX, Xiao YY, Liu D, Chen J, et al. Comparative pharmacokinetics and bioavailability studies of quercetin, kaempferol and isorhamnetin after oral administration of Ginkgo biloba extracts, Ginkgo biloba extract phospholipid complexes and Ginkgo biloba extract solid dispersions in rats. Fitoterapia. 2010;81:1045-52.
13. Wang W, Kang Q, Liu N, Zhang Q, Zhang Y, Li H, et al. Enhanced dissolution rate and oral bioavailability of Ginkgo biloba extract by preparing solid dispersion via hot-melt extrusion. Fitoterapia. 2015;102:189-97.
14. Li W, Yi S, Wang Z, Chen S, Xin S, Xie J, et al. Self-nanoemulsifying drug delivery system of persimmon leaf extract: Optimization and bioavailability studies. International Journal of Pharmaceutics. 2011;420:161-71. doi: 10.1016/j.ijpharm.2011.08.024
S0378-5173(11)00786-1 [pii].
15. Zhao G, Duan J, Xie Y, Lin G, Luo H, Li G, et al. Effects of solid dispersion and self-emulsifying formulations on the solubility, dissolution, permeability and pharmacokinetics of isorhamnetin, quercetin and kaempferol in total flavones of Hippophae rhamnoides L. Drug Development and Industrial Pharmacy. 2013;39:1037-45. doi: 10.3109/03639045.2012.699066.
16. Duan J, Dang Y, Meng H, Wang H, Ma P, Li G, et al. A comparison of the pharmacokinetics of three different preparations of total flavones of Hippophae

rhamnoides in beagle dogs after oral administration. Eur J Drug Metab Pharmacokinet. 2016;41:239-49.

17. Tzeng CW, Yen FL, Wu TH, Ko HH, Lee CW, Tzeng WS, et al. Enhancement of dissolution and antioxidant activity of kaempferol using a nanoparticle engineering process. J Agric Food Chem. 2011;59:5073-80.

18. Kumar A, Gupta GK, Khedgikar V, Gautam J, Kushwaha P, Changkija B, et al. In vivo efficacy studies of layer-by-layer nano-matrix bearing kaempferol for the conditions of osteoporosis: a study in ovariectomized rat model. Eur J Pharm Biopharm. 2012;82:508-17.

19. Zhang K, Gu L, Chen J, Zhang Y, Jiang Y, Zhao L, et al. Preparation and evaluation of kaempferol-phospholipid complex for pharmacokinetics and bioavailability in SD rats. J Pharm Biomed Anal. 2015;114:168-75.

20. Telange D, Patil A, Pethe A, Tatode A, Sridhar A, Dave V. Kaempferol-Phospholipid Complex: Formulation, and Evaluation of Improved Solubility, In Vivo Bioavailability, and Antioxidant Potential of Kaempferol2016.

21. Colombo M, Melchiades GdL, Figueiró F, Battastini AMO, Teixeira HF, Koester LS. Validation of an HPLC-UV method for analysis of Kaempferol-loaded nanoemulsion and its application to in vitro and in vivo tests. Journal of pharmaceutical and biomedical analysis. 2017;145:831-7. doi: http://dx.doi.org/10.1016/j.jpba.2017.07.046.

22. Nemitz MC, Yatsu FK, Bidone J, Koester LS, Bassani VL, Garcia CV, et al. A versatile, stability-indicating and high-throughput ultra-fast liquid chromatography method for the determination of isoflavone aglycones in soybeans, topical formulations, and permeation assays. Talanta. 2015;134:183-93.

23. Higuchi T, Connors KA. Phase solubility techniques. Adv Anal Chem Instrum. 1965:117–212.

24. Khan KA. The concept of dissolution efficiency. J Pharm Pharmacol. 1975;27:48-9.

25. Moore JW, Flanner HH. Mathematical comparison of dissolution profiles. Pharm Technol. 1996;20:64-74.

26. Zhang Y, Huo M, Zhou J, Xie S. PKSolver: An add-in program for pharmacokinetic and pharmacodynamic data analysis in Microsoft Excel. Comput Methods Programs Biomed. 2010;99:306-14.

27. Eloy JO, Marchetti JM. Solid dispersions containing ursolic acid in Poloxamer 407 and PEG 6000: A comparative study of fusion and solvent methods. Powder Technology. 2014;253:98-106. doi: https://doi.org/10.1016/j.powtec.2013.11.017.

28. Simonazzi A, Davies C, Cid AG, Gonzo E, Parada L, Bermudez JM. Preparation and Characterization of Poloxamer 407 Solid Dispersions as an Alternative Strategy to Improve Benznidazole Bioperformance. J Pharm Sci. 2018;107:2829-36.

29. Dugar RP, Gajera BY, Dave RH. Fusion Method for Solubility and Dissolution Rate Enhancement of Ibuprofen Using Block Copolymer Poloxamer 407. AAPS PharmSciTech. 2016;17:1428-40. doi: 10.1208/s12249-016-0482-6.

30. Chaudhari SP, Dugar RP. Application of surfactants in solid dispersion technology for improving solubility of poorly water soluble drugs. Journal of Drug Delivery Science and Technology. 2017;41:68-77. doi: https://doi.org/10.1016/j.jddst.2017.06.010.

31. Tambe A, Pandita N. Enhanced solubility and drug release profile of boswellic acid using a poloxamer-based solid dispersion technique. Journal of Drug Delivery Science and Technology. 2018;44:172-80. doi: https://doi.org/10.1016/j.jddst.2017.11.025.

32. Dumortier G, Grossiord JL, Agnely F, Chaumeil JC. A review of poloxamer 407 pharmaceutical and pharmacological characteristics. Pharm Res. 2006;23:2709-28.

33. Rowe RC, Sheskey PJ, Owen SC. Handbook of pharmaceutical excipients: Pharmaceutical press London; 2006.

34. Li B, Konecke S, Harich K, Wegiel L, Taylor LS, Edgar KJ. Solid dispersion of quercetin in cellulose derivative matrices influences both solubility and stability. Carbohydr Polym. 2013;92:2033-40.

35. Mehanna MM, Motawaa AM, Samaha MW. In sight into tadalafil - block copolymer binary solid dispersion: Mechanistic investigation of dissolution enhancement. Int J Pharm. 2010;402:78-88.
36. Ali W, Williams AC, Rawlinson CF. Stochiometrically governed molecular interactions in drug: poloxamer solid dispersions. Int J Pharm. 2010;391:162-8.
37. Khan AW, Kotta S, Ansari SH, Sharma RK, Ali J. Enhanced dissolution and bioavailability of grapefruit flavonoid Naringenin by solid dispersion utilizing fourth generation carrier. Drug Dev Ind Pharm. 2015;41:772-9.
38. Cavallari C, Gonzalez-Rodriguez M, Tarterini F, Fini A. Image analysis of lutrol/gelucire/olanzapine microspheres prepared by ultrasound-assisted spray congealing. European Journal of Pharmaceutics and Biopharmaceutics. 2014;88:909-18. doi: https://doi.org/10.1016/j.ejpb.2014.08.014.
39. Kawabata Y, Wada K, Nakatani M, Yamada S, Onoue S. Formulation design for poorly water-soluble drugs based on biopharmaceutics classification system: Basic approaches and practical applications. International Journal of Pharmaceutics. 2011;420:1-10. doi: https://doi.org/10.1016/j.ijpharm.2011.08.032.
40. FDA. Guidance for Industry: Dissolution Testing of Immediate Release Solid Oral Dosage Forms. Rockville, MD1997.
41. FDA. Guidance for Industry: SUPAC-MR: Modified Release Solid Oral Dosage Forms Scale-Up and Postapproval Changes: Chemistry, Manufacturing, and Controls; In Vitro Dissolution Testing and In Vivo Bioequivalence Documentation. Rockville, MD1997.
42. FDA. Guidance for Industry: Waiver of In Vivo Bioavailability and Bioequivalence Studies for Immediate-Release Solid Oral Dosage Forms Based on a Biopharmaceutics Classification System. Rockville, MD2000.
43. Xing J, Chen X, Zhong D. Absorption and enterohepatic circulation of baicalin in rats. Life Sci. 2005;78:140-6.
44. DuPont MS, Day AJ, Bennett RN, Mellon FA, Kroon PA. Absorption of kaempferol from endive, a source of kaempferol-3-glucuronide, in humans. Eur J Clin Nutr. 2004;58:947-54.

45. Zhang WD, Wang XJ, Zhou SY, Gu Y, Wang R, Zhang TL, et al. Determination of free and glucuronidated kaempferol in rat plasma by LC-MS/MS: application to pharmacokinetic study. J Chromatogr B Analyt Technol Biomed Life Sci. 2010;878:2137-40.

46. Zhang Q, Zhang Y, Zhang Z, Lu Z. Sensitive determination of kaempferol in rat plasma by high-performance liquid chromatography with chemiluminescence detection and application to a pharmacokinetic study. Journal of Chromatography B. 2009;877:3595-600. doi: https://doi.org/10.1016/j.jchromb.2009.08.046.

DISCUSSÃO GERAL

A baixa expectativa de vida dos pacientes diagnosticados com GBM está diretamente relacionada à falha da quimioterapia convencional (ALIFIERIS e TRAFALIS, 2015). A baixa resposta a terapia se deve principalmente à natureza infiltrante, ausência de especificidade terapêutica e a presença da BHE, que limita a entrada dos quimioterápicos no SNC (VAN MEIR *et al.*, 2010; LIU *et al.*, 2014). Ainda, existem mecanismos de resistência a multidrogas como, por exemplo, a ação da glicoproteína-P que reduz a passagem de fármacos pelas células endoteliais que compõe a BHE e também diminui o acúmulo de fármacos dentro das células tumorais pelo efluxo para o meio extracelular, com consequente diminuição da eficácia terapêutica (SZAKACS *et al.*, 2006).

Neste contexto, buscam-se estratégias capazes de aumentar a biodisponibilidade dos quimioterápicos no SNC, onde se destaca a via de administração intranasal, bem como a utilização sistemas nanoestruturados de liberação de fármacos.

O capítulo I da presente tese teve como premissa o fato de o KPF ter atividade contra linhagens celulares de glioma já descrita na literatura (SHARMA *et al.*, 2007; JEONG *et al.*, 2009; NAKATSUMA *et al.*, 2010; SEIBERT *et al.*, 2011). Entretanto, as baixas hidrossolubilidade e biodisponibilidade do KPF limitam sua utilização terapêutica (BARVE *et al.*, 2009). O desenvolvimento de formas farmacêuticas para melhorar tais características torna-se fundamental para que este flavonoide possa ser um candidato quimioterápico para o tratamento de glioblastoma. Assim, buscou-se investigar o efeito de sua veiculação em nanoemulsões, já que sistemas nanoestruturados estão atraindo cada vez mais atenção para tratamento de neoplasias, bem como sua administração intranasal.

Os métodos analíticos, empregados para a determinação quantitativa de fármacos em amostras biológicas e em formas farmacêuticas, podem influenciar a avaliação e interpretação dos resultados do desenvolvimento e controle de qualidade da forma farmacêutica, bem como dos dados farmacocinéticos. Portanto, é essencial empregar métodos analíticos validados, seguindo os guias de validação internacionais, para a obtenção de resultados confiáveis (FDA, 1994; ICH, 2005; EMA, 2011; FDA, 2013).

Neste contexto, o primeiro passo para a elaboração dessa tese foi a validação da metodologia analítica e bioanalítica. No capítulo I, artigo I, desenvolveu-se um método de cromatografia líquida de alta eficiência, que requer apenas um sistema de solvente binário, contendo água acidificada e metanol, além de fornecer um rápido tempo de análise. Inicialmente, realizou-se a validação analítica em cada tipo de amostra onde o KPF seria quantificado, ou seja, nanoemulsão, mucosa nasal suína e fluido receptor nos experimentos de permeação/retenção, e cérebros de ratos para o estudo preliminar de biodistribuição cerebral. Como pode ser observado nos cromatogramas da Figura 1 (Capítulo I, artigo I), os componentes das matrizes não afetaram a quantificação do KPF. Além disso, o método demonstrou ser linear, preciso, exato e robusto, obteve-se baixos limites de quantificação (0,1 a 0,2 µg/mL), demonstrando a sensibilidade do método. Por fim, verificou-se a aplicabilidade do método nos experimentos de permeação/retenção bem como de quantificação do KPF em cérebros de ratos após administração intranasal. Assim, garante-se que o método cumpriu todos os requisitos de validação analítica e bioanalítica do guias internacionais já citados e se mostrou adequado para a consecução para os estudos subsequentes.

O interesse da veiculação de polifenóis em nanopartículas para a liberação cerebral após administração intranasal é recente e crescente, como em estudos com rutina (AHMAD *et al.*, 2016), quercetina (AHMAD *et al.*, 2017), curcumina (WANG *et al.*, 2012; SOOD *et al.*, 2014; SHINDE e DEVARAJAN, 2017), resveratrol (PANGENI *et al.*, 2014), associação de curcumina e resveratrol (NASR, 2016), própolis (RASSU *et al.*, 2015) e ácido rosmarínico (BHATT *et al.*, 2015). Entretanto, até o início do desenvolvimento da presente tese, não haviam sido descritos na literatura estudos que avaliassem a liberação de KPF pela via intranasal, seja livre ou veiculado em um nanocarreador.

Em sequência, foram desenvolvidas duas nanoemulsões, uma sem agente mucoadesivo (KPF-NE) e outra contendo quitosana (KPF-MNE). Para a escolha da composição da nanoemulsão de partida, um planejamento Box-Behnken com três fatores e três níveis foi realizado através do Software Minitab® 16. As variáveis de entrada (independentes) foram: concentração de lecitina de ovo (2, 3,5 e 5%), triglicerídeos de cadeia média (8, 14 e 20%) e polissorbato 80 (1, 2 e 3%) (Tabela 1

em Anexo). As variáveis de resposta analisadas (dependentes) foram tamanho de gotícula, índice de polidispersão, potencial zeta e teor de KPF. Na totalidade, quinze formulações foram desenvolvidas e analisadas (Tabela 2 em Anexo). Por meio da otimização da formulação dada pelo software, a composição final da formulação foi 5% de lecitina de ovo, 14,88% de triglicerídeos de cadeia média e 1% de polissorbato 80 (Figura 1 em Anexo). Entretanto, optou-se por não adicionar essa etapa de otimização do trabalho ao artigo II do Capítulo I, pois ao realizarmos a análise estatística dos resultados, somente a variável polissorbato 80 em relação ao índice de polidispersão foi significativa (Figura 1 em Anexo). A partir disso, conclui-se que dentre as variações que testamos, todas levaram ao mesmo resultado estatisticamente. Após a escolha da composição da nanoemulsão, realizou-se a adição da quitosana e assim obteve-se a nanoemulsão mucoadesiva (KPF-MNE).

Devido às características versáteis, como biocompatibilidade, biodegradabilidade, propriedades bioadesivas e aumento da permeabilidade da membrana celular tanto *in vitro* e *in vivo*, a quitosana é um polímero mucoadesivo amplamente utilizado em formulações intranasais (CASETTARI e ILLUM, 2014).

Ambas as formulações apresentaram tamanho de gotícula nanométrico e população monodispersa. Como esperado, a adição de quitosana a NE, possibilitou reverter o potencial zeta, tornando-o positivo (+26,09 ± 2,67), bem como foi observado um aumento do diâmetro de gotícula em cerca de 35 nm, podendo-se inferir que houve adsorção da quitosana a superfície da gotícula (Capítulo I, artigo II, Tabela 1). Além disso, ambas as formulações preservaram o potencial antioxidante quando comparado ao KPF em solução.

Os demais resultados de caracterização mostraram a superioridade da formulação mucoadesiva com vistas à administração intranasal. Nos estudos de permeação/retenção, observou-se maior permeação e retenção do KPF ($p < 0,0001$) na mucosa quando veiculado a MNE em comparação ao KPF livre ou veiculado a NE (Tabela 2, Capítulo I, artigo II). Esse aumento de KPF permeado foi de aproximadamente 5 e 10 vezes em relação a KPF-NE e KPF livre, respectivamente. Já para o KPF retido na mucosa, o aumento de KPF quando veiculado por MNE foi de aproximadamente 2 vezes tanto para NE quanto para KPF livre, podendo, portanto,

exercer função de reservatório. O aumento da permeação devido à adição de quitosana na formulação também foi obervado em outros trabalhos ao comparar com a nanoemulsão correspondente sem adição de quitosana (KUMAR *et al.*, 2009; SOOD *et al.*, 2014).

Quitosana já é sabidamente conhecida por ser promotora de permeação e de mucoadesão (CASETTARI e ILLUM, 2014). Entretanto, em experimentos de células do tipo Franz, fica evidente somente a promoção de permeação. Neste aparato, a questão da mucoadesão torna-se irrelevante, uma vez que as formulações ficam em contato com a mucosa durante todo experimento ou até toda formulação passar ao compartimento receptor e/ou ficar retida na própria mucosa, sem a ação do *clereance* mucociliar.

Como parâmetro preditor da mucoadesividade do nanocarreador proposto, foram determinados a força e o trabalho de mucoadesão, ou seja, a força máxima requerida para separar a formulação da superfície da mucosa e o trabalho (força total aplicada) necessário, respectivamente (CARVALHO *et al.*, 2010). Ao se observar a Figura 3 (Capítulo I, artigo II), nota-se que a presença de quitosana na nanoemulsão aumentou significativamente ($p<0,0001$) o comportamento mucoadesivo, ou seja, maior força e maior trabalho de mucoadesão em comparação a KPF-NE e ao controle negativo PBS. A quitosana exibe fortes propriedades mucoadesivas devido à formação de ligações de hidrogênio entre suas cargas positivas dos grupos amino e cargas carregadas negativamente de resíduos de ácido siálico da mucina. Assim, com uma maior força mucoadesiva, infere-se que a KPF-MNE ficaria mais tempo na cavidade nasal, resistindo mais ao *clereance* mucociliar, sendo, portanto, o KPF mais absorvido pelo epitélio nasal. Resultados similares foram observados em outros trabalhos que também utilizaram esta técnica (CARVALHO *et al.*, 2013; BARBI MDA *et al.*, 2015; SHAH *et al.*, 2016).

No estudo preliminar de distribuição cerebral, após administração intranasal de KPF-MNE, observou-se um aumento significativo ($p<0,001$) do teor de KPF quantificado nos cérebros dos animais em comparação ao KPF livre e a KPF-NE, com um incremento de aproximadamente 5 vezes em relação a ambos. Este resultado

corrobora com os demais resultados obtidos de viscosidade, resistência mucoadesiva e de permeação/retenção, em que a formulação com viscosidade adequada à administração nasal, maior força mucoadesiva, apresentou maior permeação e maior liberação do KPF ao cérebro.

No capítulo I, artigo II, também foi demonstrado que o KPF carreado pela nanoemulsão mucoadesiva (KPF-MNE) diminuiu significativamente ($p<0,0001$) a viabilidade das células de GBM *in vitro* na concentração de 1µM após 72h de tratamento, quando comparadas ao grupo veículo (MNE) e KPF em solução (Figura 5A, Capítulo I, artigo II). Nessa mesma figura, nota-se que KPF-MNE diminuiu significativamente ($p<0.0001$) a viabilidade celular em relação a KPF-NE. Esse resultado pode ser explicado pelo fato de que nanopartículas positivamente carregadas exibem melhor associação com as membranas celulares, levando assim a maior internalização e, consequentemente, maior efeito citotóxico (HILLAIREAU e COUVREUR, 2009; FROHLICH, 2012). Nanopartículas contendo quitosana têm sido amplamente estudas para o tratamento de neoplasias (TAHARA *et al.*, 2008; ZHU *et al.*, 2009; ANITHA *et al.*, 2012; LIU *et al.*, 2012; CHUAH *et al.*, 2014; YANG *et al.*, 2015).

A maior atividade nos experimentos *in vitro* pode ser explicada pela maior captação do KPF veiculado na nanoemulsão mucoadesiva em comparação ao KPF livre e também ao rápido metabolismo das células cancerígenas, que aumentam a eficiência da captação (BHATTACHARJEE *et al.*, 2010). Além disso, uma vez internalizadas, uma única nanopartícula pode carrear várias moléculas de KPF, aumentando a concentração intracelular efetiva.

Resultados similares, da diferença da toxicidade entre KPF livre e KPF carreado, já haviam sido demonstrados com nanopartículas poliméricas constituídas por poli(óxido de etileno)-poli(óxido de propileno)-poli(óxido de etileno) ou poli(ácido lático-co-ácido glicólico) (PLGA) em células de câncer de ovário após 24h de tratamento a 10 e 25µM, justificando o aprofundamento de estudos com essa molécula em nanossistemas (LUO *et al.*, 2012).

Ainda a partir da Figura 5A (Capítulo I, artigo II), verificou-se que o tratamento com as formulações brancas (NE e MNE) também levou a uma importante redução na

viabilidade celular, 63,49 ± 12,74% e 50,70 ± 6,99%, respectivamente. Sabe-se que os principais fatores de influência para a citotoxicidade são a composição, tamanho, forma, carga superficial e hidrofobicidade superficial das nanopartículas (FROHLICH, 2012). Embora não seja significativa a diferença de citotoxicidade entre elas, é visível a maior citotoxicidade da formulação positiva em relação a negativa. Essa observação pode ser devido às cargas positivas disponíveis, que podem interagir diretamente com as membranas celulares carregadas negativamente e causar possíveis danos celulares (ROMØREN *et al.*, 2004; FROHLICH, 2012). Além das características das nanopartículas, como tamanho, forma e revestimento, poderem alterar a absorção celular, Cho e colaboradores (2011) mostraram a importância do efeito de sedimentação em experimentos *in vitro*. Após a adição das nanopartículas ao meio de cultura, elas podem agregar e alterar suas características físicas. Além disso, nanopartículas grandes e pesadas podem sedimentar rapidamente, fazendo com que a dose de nanopartículas na superfície da célula possa variar (CHO *et al.*, 2011). Essa questão foi inclusive um dos pontos questionados por um dos revisores desse artigo. Seguindo sua sugestão, incubou-se KPF-MNE no meio de cultura (sem células) e avaliou-se durante todo período de tratamento (Figura S3, material suplementar do artigo II, Capítulo I). As gotículas permaneceram estáveis em relação ao tamanho de gotícula durante a incubação (72h).

Importante salientar que só foi observada diferença na viabilidade celular entre os grupos testados após 72h de tratamento. Esse achado reforça a necessidade de tempo de incubação para a internalização e atividade citotóxica do KPF-MNE.

Interessantemente, quando ao mesmo poço de tratamento foi adicionado formulação branca MNE e KPF em solução a 1µM, não foi obervado o mesmo comportamento quando comparado a KPF carreado pela nanoemulsão, evidenciando a importância da veiculação do KPF para a interação com a célula e liberação do composto citotóxico.

Aliado ao fato da necessidade da veiculação do KPF para atividade, observou-se que o tratamento por 72h com KPF-MNE levou à morte celular apoptótica ao contrário do KPF em solução, que não causou o mesmo efeito (Figura 7, Capítulo I, artigo II). Os resultados encontrados corroboram com os dados da literatura que

mostram apoptose em células de glioma após tratamento com KPF em solução, porém com concentração 50 vezes maior (50 µM) à concentração veiculada por MNE (1µM) (SHARMA *et al.*, 2007; SIEGELIN *et al.*, 2008; JEONG *et al.*, 2009). Ainda, após o tratamento com KPF-MNE e KPF livre por 48h, só foi possível realizar a quantificação do KPF internalizado pelas células quando tratadas com KPF-MNE (4.40 ± 1.5 nmol/mg proteína). O KPF internalizado pela célula após o tratamento com KPF livre foi abaixo do limite de quantificação por HPLC.

Mesmo com diminuição da viabilidade das células tratadas com MNE sem KPF (50,70 ± 6,99%), não foi constatada morte por apoptose, necrose ou parada no ciclo celular, ou seja, o mecanismo pelo qual as células morreram é outro. Experimentalmente, foi observado que as células tratadas com ambas nanoemulsões (MNE e NE) com ou sem KPF, soltavam-se da placa, provavelmente por perda da adesão celular. Em nossos experimentos preliminares, verificou-se que, quando menores volumes de formulação eram adicionados ao poço, menor variação na viabilidade celular era observado, ou seja, a perda de adesão celular pode estar relacionada ao número de partículas em contato com as células (dados não mostrados).

A adesão celular é a capacidade de uma célula aderir uma a outra célula ou a uma matriz extracelular e está envolvida na regulação da diferenciação celular, ciclo celular, migração e sobrevivência celular (KHALILI e AHMAD, 2015). O desprendimento das células ou a perda de ancoragem nas células adesivas é um marcador comum de morte celular, que pode ser monitorado como um sinal de citotoxicidade (YANG *et al.*, 2017). O desprendimento de células da matriz extracelular induz a uma variedade de fenótipos de morte celular: anoikis, entosis, autofagia e transdiferenciação escamosa (ISHIKAWA *et al.*, 2015). A análise por citometria de fluxo demonstrou que KPF-MNE não alterou a progressão do ciclo celular, bem como para os demais tratamentos (Figura 6).

Srinivas Raghavan e colaboradores (2015) desenvolveram nanopartículas de ouro contendo KPF e verificaram que, após o tratamento com 14,5 µg / mL por 24 e 48h, houve redução na viabilidade de células de câncer de mama de 50,6 ± 2,4 e 37,1 ± 5,8 %, respectivamente. Já a viabilidade das células quando tratadas com KPF livre (7,2 µg/mL) foi maior de 80%. Os autores verificaram indução de apoptose (16,9 ±

1,2% no tratamento com 2,4 µg/mL após 24h, bem como inibição da angiogênese com 7,2 µg/mL (SRINIVAS RAGHAVAN *et al.*, 2015). Em nossos resultados, com concentração cerca de 8 vezes inferior, já foi verificada indução a apoptose, embora com tempo de tratamento superior (72h).

O conjunto dos resultados obtidos indica que a nanoemulsão mucoadesiva desenvolvida (KPF-MNE) é um eficiente sistema de liberação do KPF ao sistema nervoso central, além de diminuir a viabilidade das células de GBM. Além disso, o primeiro e o segundo artigo deste capítulo foram os primeiros trabalhos que verificaram a liberação de KPF pela via intranasal, livre ou veiculado em um nanocarreador.

O capítulo II da presente tese apresenta uma revisão sistemática sobre a utilização de dispersões sólidas (DS) como estratégia para melhorar a dissolução e biodisponibilidade oral de flavonoides, bem como o desenvolvimento e caracterização de DS contendo KPF.

Com o intuito de melhorar a dissolução e biodisponibilidade oral do KPF, pensou-se em utilizar DS para veicular este flavonoide, visto o sucesso dessa estratégia para diversos fármacos pouco solúveis. Entretanto, ao realizarmos uma profunda busca na literatura para nos situarmos no contexto atual deste tema, nada foi encontrado sobre a utilização de DS contendo KPF. Assim, surgiu a ideia de realizar uma revisão sistemática, ampliando para a classe flavonoides, já que também não havia nenhum trabalho que abordasse esta temática.

O sucesso das dispersões sólidas em aumentar a dissolução e biodisponibilidade oral de flavonoides foi amplamente discutida no artigo I do Capítulo II. Neste trabalho, verificou-se que o método mais utilizado para a preparação de DS contendo flavonoides é a técnica de evaporação do solvente e o polímero mais empregado como carreador foi o PVP. Aproximadamente 70% dos trabalhos utilizaram o flavonoide livre, enquanto cerca de 30% investigaram extratos vegetais contendo flavonoides. Importante ressaltar que não foi possível estabelecer se determinado polímero, proporção ou método de preparação são as melhores opções para a classe de flavonoides. A literatura ainda está carente de trabalhos no tema para que se possa

chegar a tais conclusões. Verificou-se que todos os trabalhos encontraram resultados promissores, onde observaram um aumento na solubilidade em água, melhor perfil de dissolução e aumento da biodisponibilidade oral em relação ao flavonoide livre. Dos 56 trabalhos analisados, somente um deles demonstrou que a DS desenvolvida apresentou biodisponibilidade oral inferior a outra formulação, neste caso fosfolipídica, mas ainda assim, a DS apresentou ASC superior aos flavonoides livres (CHEN *et al.*, 2010).

Concomitantemente a realização da revisão sistemática, realizou-se o desenvolvimento de DS contendo KPF, gerando a publicação II do Capítulo II.

Com o objetivo de selecionar o carreador mais adequado para o preparo de dispersões sólidas contendo KPF, foram inicialmente realizados testes de solubilidade com os principais carreadores utilizados: Gelucire 44/14, Poloxamer 188, Poloxamer 407 e Soluplus®. Verificou-se que o Poloxamer 407 foi o carreador que mais aumentou a solubilidade do KPF em água. Por esse motivo, este foi o polímero escolhido para o desenvolvimento das dispersões. Poloxâmeros (comumente conhecidos por seus nomes comerciais Pluronic® ou Lutrol®) são copolímeros tribloco não-iônicos de polioxietileno-polioxipropileno-polioxietileno que apresentam propriedades tensoativas (ALI *et al.*, 2010).

Após esta triagem inicial para a seleção do carreador, foram desenvolvidas dispersões em diferentes proporções KPF:polímero (1:1, 1:2, 1:3, 1:4, 1:5, 1:7 e 1:9) pelo método de evaporação do solvente. Quanto maior a proporção de poloxamer, maior foi a solubilidade do KPF em água. Entretanto, o tamanho da forma farmacêutica final também tem papel importante na escolha da melhor proporção, descartando-se, assim, as proporções 1:7 e 1:9. Diferentemente da abordagem convencional utilizada no processo de desenvolvimento farmacotécnico, onde a dissolução é realizada posteriormente a caracterização físico-química, decidiu-se realizar um ensaio preliminar de dissolução. Verificou-se que a proporção 1:5 apresentou melhor perfil de dissolução em meio ácido em comparação as demais proporções (dados não apresentados) e foi a escolhida para a continuidade dos estudos.

Dois principais métodos são usados para produzir dispersões sólidas: evaporação do solvente e fusão. Ambos são úteis nas escalas laboratorial e industrial

(VASCONCELOS *et al.*, 2016). A escolha do método de preparo das dispersões da primeira etapa presente capítulo foi o método de evaporação do solvente, umas vez que DS preparadas pelo método de evaporação do solvente podem apresentar estrutura porosa com alguns canais na estrutura sólida, aumentando assim a porosidade, a área de superfície e, assim, a taxa de dissolução do fármaco (VO *et al.*, 2013).

Nas etapas seguintes deste estudo, ao compararmos com a dispersão sólida (1:5, KPF:poloxamer, p:p) preparada pelo método de fusão, esperávamos um comportamento superior das dispersões preparadas pelo método de evaporação do solvente pelo motivo apresentado acima. Entretanto, ambos os métodos apresentaram comportamento muito semelhante em relação a solubilidade, perfil de dissolução, bem como na caracterização por difração de raio X, FTIR, DSC e MEV. Como o método por fusão apresenta reduzido custo de produção, simplicidade operacional e não emprega solventes orgânicos, esse foi o método escolhido para os estudos de farmacocinética.

Através da análise de FTIR, foi observado uma possível interação por ligações de hidrogênio entre o KPF e o poloxamer, visto que o flavonoide apresenta quatro OH e o carreador duas OH para tal interação. Resultado semelhante também foi encontrado por Khan e colaboradores, onde eles sugerem ligações de hidrogênio entre as hidroxilas do flavonoide naringenina e do carreador, onde também observaram alteração na banda característica de hidroxila (KHAN *et al.*, 2015). Através das análises de difração de raio X, foi verificada uma diminuição da cristalinidade do KPF nas dispersões, visto que somente alguns picos característicos do KPF não foram observados. Já através das análises de DSC, as dispersões apresentaram o mesmo perfil que a mistura física, onde não foi observado o pico relativo ao ponto de fusão do KPF. Essa observação pode ser devido a solubilização do KPF no polímero fundido ou pela baixa proporção de KPF na mistura física e dispersões, fato também observado por Eloy e Marchetti (ELOY e MARCHETTI, 2014). Nas análises por MEV também não foi obervada nenhuma diferença visual entre as dispersões. Ambas dispersões apresentaram uma superfície rugosa e irregular e a ausência de cristais de KPF visíveis, indicando que a KPF está dissolvido no transportador polimérico ou que

ocorreu conversão parcial em uma forma amorfa. Por outro lado, as imagens da mistura física mostraram cristais de KPF sob a massa de poloxamer.

Nos ensaios de dissolução, ambos os métodos de preparação testados, método de fusão e de evaporação do solvente, levaram ao mesmo perfil de dissolução das dispersões, comprovadas pelo valor de *f1* e *f2* das curvas. Já a dissolução do KPF a partir da mistura física não se mostrou tão eficiente quanto a partir das dispersões, evidenciando a necessidade da dispersão sólida como estratégia farmacotécnica para melhorar a dissolução do KPF. Após a administração da dispersão sólida (100 mg/kg de KPF) em ratos, o C_{max} foi significativamente maior (2,2 vezes, $p < 0,05$) e o valor de ASC_{0-24h} de KPF foi 1,85 maior que o KPF livre, indicando que a dispersão sólida melhorou significativamente a exposição do KPF.

Importante ressaltar que o aumento observado, tanto nos valores de $ASC_{0\rightarrow t}$ quanto de C_{max}, para a dispersão sólida desenvolvida (aproximadamente 2 vezes para ambos parâmetros) estão compreendidos dentro da faixa de valores encontrados na revisão sistemática realizada (Artigo I, Capítulo II). Nestes trabalhos, em geral, as dispersões sólidas aumentaram em média 3,39 ± 1,48 vezes a $AUC_{0\rightarrow t}$ em relação ao flavonoide livre. Já para o C_{max} este aumento foi em média foi de 5,59 ± 3,74.

Mesmo com um grande aumento na solubilidade em água a partir da DS (aproximadamente de 4 mil vezes) e melhora significativa no perfil de dissolução, ambos em relação ao KPF livre, o aumento na ASC não foi tão grande quanto o esperado. Conclui-se que, por mais que o KPF seja classificado como classe II no Sistema de Classificação Biofarmacêutica (XIE *et al.*, 2014), a extensão de absorção dele depende de fatores que não foram avaliados em nosso estudo, como metabolização, permeabilidade e mecanismos de absorção e efluxo (BARVE *et al.*, 2009). Barve e colaboradores demonstraram que o KPF apresenta baixa a moderada absorção, com biodisponibilidade oral de aproximadamente 2%. Os autores atribuem esse baixo valor em parte ao extenso metabolismo de primeira passagem pela fase I (metabolismo oxidativo) e fase II (glicuronidação no intestino e fígado) (BARVE *et al.*, 2009).

Conforme dito anteriormente, ao realizarmos o planejamento e desenvolvimento da revisão (artigo I, Capítulo II) nenhum trabalho na literatura foi

encontrado no que tange a dispersões sólidas contendo KPF isolado, ou seja, sem o KPF estar em um extrato vegetal. Entretanto, em setembro de 2018, Xu e colaboradores desenvolveram complexos intermoleculares com o polissacarídeo arabinogalactano (AG) e glicirrizinato dissódico (Na_2GA) pela técnica "mecanoquímica" de moinhos de bolas. Os autores não atribuem o nome de "dispersão sólida" a formulação, embora afirmem que a redução do tamanho das partículas e a destruição das formas cristalinas revelaram a formação de uma dispersão sólida (XU *et al.*, 2018). Portanto, de forma inédita, pode-se considerar que, nesta tese, foram desenvolvidas dispersões sólidas contendo KPF por métodos consolidados com resultados promissores.

CONCLUSÕES

Por meio do trabalho realizado pode-se concluir que:

- O método desenvolvido e validado por cromatografia líquida de alta eficiência para quantificação de kaempferol em nanoemulsões, mucosa nasal suína, fluido receptor e cérebro de rato apresentou-se específico, linear, preciso, exato, sensível e robusto;

- O método por homogeneização a alta pressão mostrou-se adequado para a obtenção de nanoemulsões contendo KPF com elevado teor e taxa de associação, preservando sua atividade antioxidante;

- Foram obtidas nanoemulsões monodispersas contendo KPF com reduzido tamanho de gotícula e elevado potencial zeta;

- A adição de quitosana a nanoemulsão KPF-NE para a obtenção da nanoemulsão mucoadesiva KPM-MNE aumentou a força mucoadesiva bem como promoveu maior permeação e retenção do KPF na mucosa nasal suína no estudo de permeação *ex vivo*;

- A administração intranasal da nanoemulsão KPF-MNE aumentou o teor de KPF no cérebro de ratos quando comparado a KPF livre e a nanoemulsão sem agente mucoadesivo;

- O tratamento com KPF+MNE resultou em atividade citotóxica inferior quando comparada a KPF-MNE, demonstrando a importância da internalização do KPF no nanossistema;

- KPF-MNE aumentou a resposta contra glioma *in vitro* por apoptose em comparação a KPF-NE e ao composto livre, sugerindo um aumento da biodisponibilidade intracelular;

- Através da revisão sistemática, verificou-se grande interesse e sucesso na utilização de dispersões sólidas como estratégia para melhorar a dissolução e biodisponibilidade oral de flavonoides;

- A dispersão sólida SD_{MM} contendo KPF com o carreador Poloxamer 407 mostrou-se uma adequada estratégia farmacotécnica para a promoção da solubilidade, dissolução e biodisponibilidade oral do KPF;

- Observou-se perda da cristalinidade do KPF nas dispersões sólidas (SDMM e SDSM) indicada por análises de raios X e possível ligação de hidrogênio entre os grupos hidroxila do KPF e Poloxamer por FTIR.

REFERÊNCIAS

AHERNE, S. A.; O'BRIEN, N. M. Dietary flavonols: chemistry, food content, and metabolism. **Nutrition,** v. 18, n. 1, p. 75-81, Jan 2002.

AHMAD, N.; AHMAD, R.; NAQVI, A. A.; ALAM, M. A.; ASHAFAQ, M.; ABDUR RUB, R.; AHMAD, F. J. Intranasal delivery of quercetin-loaded mucoadhesive nanoemulsion for treatment of cerebral ischaemia. **Artificial Cells, Nanomedicine, and Biotechnology,** v. 12, p. 1-13, 2017.

AHMAD, N.; AHMAD, R.; NAQVI, A. A.; ALAM, M. A.; ASHAFAQ, M.; SAMIM, M.; IQBAL, Z.; AHMAD, F. J. Rutin-encapsulated chitosan nanoparticles targeted to the brain in the treatment of Cerebral Ischemia. **International Journal of Biological Macromolecules,** v. 91, p. 640-55, 2016.

ALAGUSUNDARAM, M.; CHENGAIAH, B.; GNANAPRAKASH, K.; RAMKANTH, S.; CHETTY, C. M.; DHACHINAMOORTHI, D. Nasal drug delivery system-an overview. **International Journal of Research in Pharmaceutical Sciences,** v. 1, n. 4, p. 454-465, 2010.

ALAM, M. I.; BEG, S.; SAMAD, A.; BABOOTA, S.; KOHLI, K.; ALI, J.; AHUJA, A.; AKBAR, M. Strategy for effective brain drug delivery. **European Federation for Pharmaceutical Sciences,** v. 40, n. 5, p. 385-403, Aug 11 2010.

ALI, W.; WILLIAMS, A. C.; RAWLINSON, C. F. Stochiometrically governed molecular interactions in drug: poloxamer solid dispersions. **Int J Pharm,** v. 391, n. 1-2, p. 162-8, 2010.

ALIFIERIS, C.; TRAFALIS, D. T. Glioblastoma multiforme: Pathogenesis and treatment. **Pharmacology & Therapeutics,** v. 152, p. 63-82, 2015.

AMIDON, G. L.; LENNERNAS, H.; SHAH, V. P.; CRISON, J. R. A theoretical basis for a biopharmaceutic drug classification: the correlation of in vitro drug product dissolution and in vivo bioavailability. **Pharmaceutical Research,** v. 12, n. 3, p. 413-20, Mar 1995.

ANITHA, A.; MAYA, S.; DEEPA, N.; CHENNAZHI, K. P.; NAIR, S. V.; JAYAKUMAR, R. Curcumin-loaded N,O-carboxymethyl chitosan nanoparticles for cancer drug delivery. **Journal of biomaterials science. Polymer edition.,** v. 23, n. 11, p. 1381-400, 2012.

ATTIA, A.; RAPP, S. R.; CASE, L. D.; D'AGOSTINO, R.; LESSER, G.; NAUGHTON, M.; MCMULLEN, K.; ROSDHAL, R.; SHAW, E. G. Phase II study of Ginkgo biloba in irradiated brain tumor patients: effect on cognitive function, quality of life, and mood. **Journal of Neuro-Oncology,** v. 109, n. 2, p. 357-63, 2012.

BAHADUR, S.; PATHAK, K. Buffered nanoemulsion for nose to brain delivery of ziprasidone hydrochloride: preformulation and pharmacodynamic evaluation. **Current Drug Delivery,** v. 9, n. 6, p. 596-607, 2012.

BARBI MDA, S.; CARVALHO, F. C.; KIILL, C. P.; BARUD HDA, S.; SANTAGNELI, S. H.; RIBEIRO, S. J.; GREMIAO, M. P. Preparation and Characterization of Chitosan Nanoparticles for Zidovudine Nasal Delivery. **Journal of Nanoscience and Nanotechnology,** v. 15, n. 1, p. 865-74, 2015.

BARRINGTON, R.; WILLIAMSON, G.; BENNETT, R. N.; DAVIS, B. D.; BRODBELT, J. S.; KROON, P. A. Absorption, Conjugation and Efflux of the Flavonoids, Kaempferol and Galangin, Using the Intestinal CACO-2/TC7 Cell Model. **Journal of Functional Foods,** v. 1, n. 1, p. 74-87, 2009.

BARTON, D. L.; BURGER, K.; NOVOTNY, P. J.; FITCH, T. R.; KOHLI, S.; SOORI, G.; WILWERDING, M. B.; SLOAN, J. A.; KOTTSCHADE, L. A.; ROWLAND, K. M., JR.; DAKHIL, S. R.; NIKCEVICH, D. A.; LOPRINZI, C. L. The use of Ginkgo biloba for the prevention of chemotherapy-related cognitive dysfunction in women receiving adjuvant treatment for breast cancer, N00C9. **Support Care Cancer,** v. 21, n. 4, p. 1185-92, 2013.

BARVE, A.; CHEN, C.; HEBBAR, V.; DESIDERIO, J.; SAW, C. L.; KONG, A. N. Metabolism, oral bioavailability and pharmacokinetics of chemopreventive kaempferol in rats. **Biopharmaceutics & Drug Disposition,** v. 30, n. 7, p. 356-65, Oct 2009.

BERNKOP-SCHNURCH, A.; DUNNHAUPT, S. Chitosan-based drug delivery systems. **European Journal of Pharmaceutics and Biopharmaceutics,** v. 81, n. 3, p. 463-9, 2012.

BHATT, R.; SINGH, D.; PRAKASH, A.; MISHRA, N. Development, characterization and nasal delivery of rosmarinic acid-loaded solid lipid nanoparticles for the effective management of Huntington's disease. **Drug delivery,** v. 22, n. 7, p. 931-9, 2015.

BHATTACHARJEE, H.; BALABATHULA, P.; WOOD, G. C. Targeted nanoparticulate drug-delivery systems for treatment of solid tumors: a review. **Therapeutic Delivery,** v. 1, n. 5, p. 713-34, 2010.

CALDERON-MONTANO, J. M.; BURGOS-MORON, E.; PEREZ-GUERRERO, C.; LOPEZ-LAZARO, M. A review on the dietary flavonoid kaempferol. **Mini-Reviews in Medicinal Chemistry,** v. 11, n. 4, p. 298-344, Apr 2011.

CARVALHO, F. C.; BRUSCHI, M. L.; EVANGELISTA, R. C.; GREMIÃO, M. P. D. Mucoadhesive drug delivery systems. **Brazilian Journal of Pharmaceutical Sciences,** v. 46, n. 1, p. 1-17, 2010.

CARVALHO, F. C.; CAMPOS, M. L.; PECCININI, R. G.; GREMIAO, M. P. Nasal administration of liquid crystal precursor mucoadhesive vehicle as an alternative antiretroviral therapy. **European Journal of Pharmaceutics and Biopharmaceutics,** v. 84, n. 1, p. 219-27, 2013.

CASETTARI, L.; ILLUM, L. Chitosan in nasal delivery systems for therapeutic drugs. **Journal of Controlled Release,** v. 190, p. 189-200, 2014.

CHARMAN, W. N.; CHARMAN, S. A. Oral Modified-Release Delivery Systems. In: (Ed.). **Modified-release drug delivery technology**: CRC Press, 2002. p.25-34.

CHEN, A. Y.; CHEN, Y. C. A review of the dietary flavonoid, kaempferol on human health and cancer chemoprevention. **Food chemistry,** v. 138, n. 4, p. 2099-107, Jun 15 2013.

CHEN, Z. P.; SUN, J.; CHEN, H. X.; XIAO, Y. Y.; LIU, D.; CHEN, J.; CAI, H.; CAI, B. C. Comparative pharmacokinetics and bioavailability studies of quercetin, kaempferol and isorhamnetin after oral administration of Ginkgo biloba extracts, Ginkgo biloba extract phospholipid complexes and Ginkgo biloba extract solid dispersions in rats. **Fitoterapia,** v. 81, n. 8, p. 1045-52, 2010.

CHIOU, W. L.; RIEGELMAN, S. Pharmaceutical applications of solid dispersion systems. **Journal of Pharmaceutical Sciences,** v. 60, n. 9, p. 1281-1302, 1971.

CHO, E. C.; ZHANG, Q.; XIA, Y. The effect of sedimentation and diffusion on cellular uptake of gold nanoparticles. **Nature Nanotechnology,** v. 6, n. 6, p. 385-391, 2011.

CHO, H. J.; PARK, J. H. Kaempferol Induces Cell Cycle Arrest in HT-29 Human Colon Cancer Cells. **Journal of Cancer Prevention,** v. 18, n. 3, p. 257-63, Sep 2013.

CHUAH, L. H.; ROBERTS, C. J.; BILLA, N.; ABDULLAH, S.; ROSLI, R. Cellular uptake and anticancer effects of mucoadhesive curcumin-containing chitosan nanoparticles. **Colloids and Surfaces B: Biointerfaces,** v. 116, p. 228-36, 2014.

COMFORT, C.; GARRASTAZU, G.; POZZOLI, M.; SONVICO, F. Opportunities and challenges for the nasal administration of nanoemulsions. **Current Topics in Medicinal Chemistry,** v. 15, n. 4, p. 356-68, 2015.

COSTANTINO, H. R.; ILLUM, L.; BRANDT, G.; JOHNSON, P. H.; QUAY, S. C. Intranasal delivery: physicochemical and therapeutic aspects. **International Journal of Pharmaceutics,** v. 337, n. 1-2, p. 1-24, 2007.

CUI, Y.; MORGENSTERN, H.; GREENLAND, S.; TASHKIN, D. P.; MAO, J. T.; CAI, L.; COZEN, W.; MACK, T. M.; LU, Q. Y.; ZHANG, Z. F. Dietary flavonoid

intake and lung cancer--a population-based case-control study. **Cancer,** v. 112, n. 10, p. 2241-8, 2008.

DA FONSECA, C. O.; SIMAO, M.; LINS, I. R.; CAETANO, R. O.; FUTURO, D.; QUIRICO-SANTOS, T. Efficacy of monoterpene perillyl alcohol upon survival rate of patients with recurrent glioblastoma. **Journal of Cancer Research and Clinical Oncology,** v. 137, n. 2, p. 287-93, 2011.

DEVI, K. P.; MALAR, D. S.; NABAVI, S. F.; SUREDA, A.; XIAO, J.; NABAVI, S. M.; DAGLIA, M. Kaempferol and inflammation: From chemistry to medicine. **Pharmacological Research,** v. 99, p. 1-10, 2015.

DHURIA, S. V.; HANSON, L. R.; FREY, W. H., 2ND. Intranasal delivery to the central nervous system: mechanisms and experimental considerations. **Journal of Pharmaceutical Sciences,** v. 99, n. 4, p. 1654-73, 2010.

DOLECEK, T. A.; PROPP, J. M.; STROUP, N. E.; KRUCHKO, C. CBTRUS statistical report: primary brain and central nervous system tumors diagnosed in the United States in 2005-2009. **Neuro Oncol,** v. 14 Suppl 5, p. v1-49, Nov 2012.

DUAN, J.; DANG, Y.; MENG, H.; WANG, H.; MA, P.; LI, G.; WU, T.; XIE, Y. A comparison of the pharmacokinetics of three different preparations of total flavones of Hippophae rhamnoides in beagle dogs after oral administration. **Eur J Drug Metab Pharmacokinet,** v. 41, n. 3, p. 239-49, 2016.

ELOY, J. O.; MARCHETTI, J. M. Solid dispersions containing ursolic acid in Poloxamer 407 and PEG 6000: A comparative study of fusion and solvent methods. **Powder Technology,** v. 253, p. 98-106, 2014/02/01/ 2014.

EMA. European Medicines Agency, EMEA/CHMP/EWP/192217/2009, Guideline on bioanalytical method validation. p. 1-22, 2011.

FDA. Food and Drug Administration, Center for Drug Evaluation and Research, Reviewer Guidance: Validation of Chromatographic Methods. p. 1-30, 1994.

FDA. **Guidance for Industry Waiver of In Vivo Bioavailability and Bioequivalence Studies for Immediate-Release Solid Oral Dosage Forms Based on a Biopharmaceutics Classification System (CDER, FDA)**. 2000.

FDA. Food and Drug Administration, Center for drug evaluation and research, Guidance for Industry: Bioanalytical Method Validation. p. 1-34, 2013.

FROHLICH, E. The role of surface charge in cellular uptake and cytotoxicity of medical nanoparticles. **International Journal of Nanomedicine,** v. 7, p. 5577-91, 2012.

GATES, M. A.; VITONIS, A. F.; TWOROGER, S. S.; ROSNER, B.; TITUS-ERNSTOFF, L.; HANKINSON, S. E.; CRAMER, D. W. Flavonoid intake and ovarian cancer risk in a population-based case-control study. **International Journal of Cancer,** v. 124, n. 8, p. 1918-25, 2009.

GOUTHAMI, K. S.; KUMAR, D.; THIPPARABOINA, R.; CHAVAN, R. B.; SHASTRI, N. R. Can crystal engineering be as beneficial as micronisation and overcome its pitfalls?: A case study with cilostazol. **International Journal of Pharmaceutics,** v. 491, n. 1-2, p. 26-34, 2015.

HASHIZUME, R.; OZAWA, T.; GRYAZNOV, S. M.; BOLLEN, A. W.; LAMBORN, K. R.; FREY, W. H., 2ND; DEEN, D. F. New therapeutic approach for brain tumors: Intranasal delivery of telomerase inhibitor GRN163. **Neuro-Oncology,** v. 10, n. 2, p. 112-20, 2008.

HAUNS, B.; HARING, B.; KOHLER, S.; MROSS, K.; UNGER, C. Phase II study of combined 5-fluorouracil/ Ginkgo biloba extract (GBE 761 ONC) therapy in 5-fluorouracil pretreated patients with advanced colorectal cancer. **Phytotherapy Research,** v. 15, n. 1, p. 34-8, 2001.

HILLAIREAU, H.; COUVREUR, P. Nanocarriers' entry into the cell: relevance to drug delivery. **Cellular and Molecular Life Sciences,** v. 66, n. 17, p. 2873-96, 2009.

HOSNY, K. M.; BANJAR, Z. M. The formulation of a nasal nanoemulsion zaleplon in situ gel for the treatment of insomnia. **Expert Opinion Drug Delivery,** v. 10, n. 8, p. 1033-41, 2013.

ICH. International Conference on Harmonization,Technical requirements for the registration of pharmaceutical for human use, Validation of Analytical Procedures: Text and Methodology Q2(R1). p. 1-13, 2005.

ILLUM, L. Transport of drugs from the nasal cavity to the central nervous system. **European Journal of Pharmaceutical Sciences,** v. 11, n. 1, p. 1-18, 2000.

ILLUM, L. Nasal drug delivery--possibilities, problems and solutions. **Journal of Controlled Release,** v. 87, n. 1-3, p. 187-98, 2003.

ILLUM, L. Nasal drug delivery - recent developments and future prospects. **Journal of Controlled Release,** v. 161, n. 2, p. 254-63, 2012.

IMAI, Y.; TSUKAHARA, S.; ASADA, S.; SUGIMOTO, Y. Phytoestrogens/flavonoids reverse breast cancer resistance protein/ABCG2-mediated multidrug resistance. **Cancer Research,** v. 64, n. 12, p. 4346-52, 2004.

ISHIKAWA, F.; USHIDA, K.; MORI, K.; SHIBANUMA, M. Loss of anchorage primarily induces non-apoptotic cell death in a human mammary epithelial cell line

under atypical focal adhesion kinase signaling. **Cell Death & Disease,** v. 6, p. e1619, 2015.

JAIN, N.; AKHTER, S.; JAIN, G. K.; KHAN, Z. I.; KHAR, R. K.; AHMAD, F. J. Antiepileptic intranasal Amiloride loaded mucoadhesive nanoemulsion: development and safety assessment. **Journal of Biomedical Nanotechnology,** v. 7, n. 1, p. 142-3, 2011.

JAIN, R.; PATRAVALE, V. B. Development and evaluation of nitrendipine nanoemulsion for intranasal delivery. **Journal of Biomedical Nanotechnology,** v. 5, n. 1, p. 62-8, 2009.

JEONG, J. C.; KIM, M. S.; KIM, T. H.; KIM, Y. K. Kaempferol induces cell death through ERK and Akt-dependent down-regulation of XIAP and survivin in human glioma cells. **Neurochemical Research,** v. 34, n. 5, p. 991-1001, May 2009.

JOGANI, V. V.; SHAH, P. J.; MISHRA, P.; MISHRA, A. K.; MISRA, A. R. Intranasal mucoadhesive microemulsion of tacrine to improve brain targeting. **Alzheimer Disease and Associated Disorders,** v. 22, n. 2, p. 116-24, Apr-Jun 2008.

KAKRAN, M.; SAHOO, N.; LI, L. Dissolution enhancement of quercetin through nanofabrication, complexation, and solid dispersion. **Colloids and Surfaces B: Biointerfaces,** v. 88, n. 1, p. 121-130, 2011.

KANAZE, F.; KOKKALOU, E.; NIOPAS, I.; GEORGARAKIS, M.; STERGIOU, A.; BIKIARIS, D. Dissolution enhancement of flavonoids by solid dispersion in PVP and PEG matrixes: A comparative study. **Journal of applied polymer science,** v. 102, n. 1, p. 460-471, 2006.

KAWABATA, Y.; WADA, K.; NAKATANI, M.; YAMADA, S.; ONOUE, S. Formulation design for poorly water-soluble drugs based on biopharmaceutics classification system: Basic approaches and practical applications. **International Journal of Pharmaceutics,** v. 420, n. 1, p. 1-10, 2011/11/25/ 2011.

KHALILI, A. A.; AHMAD, M. R. A review of cell adhesion studies for biomedical and biological applications. **International journal of molecular sciences,** v. 16, n. 8, p. 18149-18184, 2015.

KHAN, A. W.; KOTTA, S.; ANSARI, S. H.; SHARMA, R. K.; ALI, J. Enhanced dissolution and bioavailability of grapefruit flavonoid Naringenin by solid dispersion utilizing fourth generation carrier. **Drug Development and Industrial Pharmacy,** v. 41, n. 5, p. 772-779, 2015.

KHUTORYANSKIY, V. V. Advances in mucoadhesion and mucoadhesive polymers. **Macromolecular Bioscience,** v. 11, n. 6, p. 748-64, 2011.

KIPRIANOVA, I.; THOMAS, N.; AYACHE, A.; FISCHER, M.; LEUCHS, B.; KLEIN, M.; ROMMELAERE, J.; SCHLEHOFER, J. R. Regression of glioma in rat models by intranasal application of parvovirus h-1. **Clinical Cancer Research,** v. 17, n. 16, p. 5333-42, 2011.

KOZLOVSKAYA, L.; ABOU-KAOUD, M.; STEPENSKY, D. Quantitative analysis of drug delivery to the brain via nasal route. **Journal of Controlled Release,** v. 189, p. 133-40, Sep 10 2014.

KOZLOVSKAYA, L.; STEPENSKY, D. Quantitative analysis of the brain-targeted delivery of drugs and model compounds using nano-delivery systems. **Journal of Controlled Release,** v. 171, n. 1, p. 17-23, 2013.

KUMAR, M.; MISRA, A.; BABBAR, A. K.; MISHRA, A. K.; MISHRA, P.; PATHAK, K. Intranasal nanoemulsion based brain targeting drug delivery system of risperidone. **International Journal of Pharmaceutics,** v. 358, n. 1-2, p. 285-91, Jun 24 2008.

KUMAR, M.; MISRA, A.; MISHRA, A. K.; MISHRA, P.; PATHAK, K. Mucoadhesive nanoemulsion-based intranasal drug delivery system of olanzapine for brain targeting. **Journal of Drug Targeting,** v. 16, n. 10, p. 806-14, Dec 2008.

KUMAR, M.; PATHAK, K.; MISRA, A. Formulation and characterization of nanoemulsion-based drug delivery system of risperidone. **Drug Development and Industrial Pharmacy,** v. 35, n. 4, p. 387-95, 2009.

KUMAR, S.; PANDEY, A. K. Chemistry and biological activities of flavonoids: an overview. **The Scientific World Journal,** v. 29, n. 162750, 2013.

LALANI, J.; BARADIA, D.; LALANI, R.; MISRA, A. Brain targeted intranasal delivery of tramadol: comparative study of microemulsion and nanoemulsion. **Pharmaceutical Development and Technology**, p. 1-10, Sep 17 2014.

LEE, H. S.; CHO, H. J.; KWON, G. T.; PARK, J. H. Kaempferol Downregulates Insulin-like Growth Factor-I Receptor and ErbB3 Signaling in HT-29 Human Colon Cancer Cells. **Journal of Cancer Prevention,** v. 19, n. 3, p. 161-9, Sep 2014.

LEE, J. H.; KIM, G. H. Evaluation of antioxidant and inhibitory activities for different subclasses flavonoids on enzymes for rheumatoid arthritis. **Journal of Food Science,** v. 75, n. 7, p. 1750-3841, 2010.

LEE, K. M.; LEE, K. W.; JUNG, S. K.; LEE, E. J.; HEO, Y. S.; BODE, A. M.; LUBET, R. A.; LEE, H. J.; DONG, Z. Kaempferol inhibits UVB-induced COX-2 expression by suppressing Src kinase activity. **Biochemical Pharmacology,** v. 80, n. 12, p. 2042-9, 2010.

LEUNER, C.; DRESSMAN, J. Improving drug solubility for oral delivery using solid dispersions. **Eur J Pharm Biopharm,** v. 50, n. 1, p. 47-60, 2000.

LEUNER, C.; DRESSMAN, J. Improving drug solubility for oral delivery using solid dispersions. **European Journal of Pharmaceutics and Biopharmaceutics,** v. 50, n. 1, p. 47-60, 2000/07/03/ 2000.

LI, C.; LI, X.; CHOI, J. S. Enhanced bioavailability of etoposide after oral or intravenous administration of etoposide with kaempferol in rats. **Archives of Pharmacal Research,** v. 32, n. 1, p. 133-8, Jan 2009.

LI, C.; ZHAO, Y.; YANG, D.; YU, Y.; GUO, H.; ZHAO, Z.; ZHANG, B.; YIN, X. Inhibitory effects of kaempferol on the invasion of human breast carcinoma cells by downregulating the expression and activity of matrix metalloproteinase-9. **Biochemistry and Cell Biology,** v. 93, n. 1, p. 16-27, Feb 2015.

LI, W.; YI, S.; WANG, Z.; CHEN, S.; XIN, S.; XIE, J.; ZHAO, C. Self-nanoemulsifying drug delivery system of persimmon leaf extract: Optimization and bioavailability studies. **International Journal of Pharmaceutics,** v. 420, n. 1, p. 161-71, Nov 25 2011.

LI, Y.; GAO, Y.; LIU, G.; ZHOU, X.; WANG, Y.; MA, L. [Intranasal administration of temozolomide for brain-targeting delivery: therapeutic effect on glioma in rats]. **Journal of Southern Medical University,** v. 34, n. 5, p. 631-5, 2014.

LIN, J.; REXRODE, K. M.; HU, F.; ALBERT, C. M.; CHAE, C. U.; RIMM, E. B.; STAMPFER, M. J.; MANSON, J. E. Dietary intakes of flavonols and flavones and coronary heart disease in US women. **American Journal of Epidemiology,** v. 165, n. 11, p. 1305-13, 2007.

LIPINSKI, C. A. Drug-like properties and the causes of poor solubility and poor permeability. **Journal of pharmacological and toxicological methods,** v. 44, n. 1, p. 235-249, 2000.

LIPINSKI, C. A.; LOMBARDO, F.; DOMINY, B. W.; FEENEY, P. J. Experimental and computational approaches to estimate solubility and permeability in drug discovery and development settings. **Adv Drug Deliv Rev,** v. 46, n. 1-3, p. 3-26, 2001.

LIU, J.; XU, L.; LIU, C.; ZHANG, D.; WANG, S.; DENG, Z.; LOU, W.; XU, H.; BAI, Q.; MA, J. Preparation and characterization of cationic curcumin nanoparticles for improvement of cellular uptake. **Carbohydrate Polymers,** v. 90, n. 1, p. 16-22, 2012.

LIU, L.; ZHANG, X.; LOU, Y.; RAO, Y. Cerebral microdialysis in glioma studies, from theory to application. **Journal of pharmaceutical and biomedical analysis,** v. 96, p. 77-89, Aug 5 2014.

LOUIS, D. N.; OHGAKI, H.; WIESTLER, O. D.; CAVENEE, W. K.; BURGER, P. C.; JOUVET, A.; SCHEITHAUER, B. W.; KLEIHUES, P. The 2007 WHO classification of tumours of the central nervous system. **Acta neuropathologica,** v. 114, n. 2, p. 97-109, 2007.

LOVELYN, C.; ATTAMA, A. A. Current state of nanoemulsions in drug delivery. **Journal of Biomaterials and Nanobiotechnology,** v. 2, n. 05, p. 626, 2011.

LU, Y.; QI, J.; WU, W. Absorption, disposition and pharmacokinetics of nanoemulsions. **Current Drug Metabolism,** v. 13, n. 4, p. 396-417, 2012.

LUO, H.; DADDYSMAN, M. K.; RANKIN, G. O.; JIANG, B. H.; CHEN, Y. C. Kaempferol enhances cisplatin's effect on ovarian cancer cells through promoting apoptosis caused by down regulation of cMyc. **Cancer Cell International,** v. 10, n. 16, p. 1475-2867, 2010.

LUO, H.; JIANG, B.; LI, B.; LI, Z.; JIANG, B. H.; CHEN, Y. C. Kaempferol nanoparticles achieve strong and selective inhibition of ovarian cancer cell viability. **International Journal of Nanomedicine,** v. 7, p. 3951-9, 2012.

MAHAJAN, H. S.; MAHAJAN, M. S.; NERKAR, P. P.; AGRAWAL, A. Nanoemulsion-based intranasal drug delivery system of saquinavir mesylate for brain targeting. **Drug delivery,** v. 21, n. 2, p. 148-54, 2014.

MENG, F.; GALA, U.; CHAUHAN, H. Classification of solid dispersions: correlation to (i) stability and solubility (ii) preparation and characterization techniques. **Drug Dev Ind Pharm,** v. 41, n. 9, p. 1401-15, 2015.

MERCADER-ROS, M. T.; LUCAS-ABELLAN, C.; GABALDON, J. A.; FORTEA, M. I.; MARTINEZ-CACHA, A.; NUNEZ-DELICADO, E. Kaempferol complexation in cyclodextrins at basic pH. **Journal of agricultural and food chemistry,** v. 58, n. 8, p. 4675-80, Apr 28 2010.

MIEAN, K. H.; MOHAMED, S. Flavonoid (myricetin, quercetin, kaempferol, luteolin, and apigenin) content of edible tropical plants. **Journal of agricultural and food chemistry,** v. 49, n. 6, p. 3106-12, 2001.

MISHRA, D. K.; DHOTE, V.; BHARGAVA, A.; JAIN, D. K.; MISHRA, P. K. Amorphous solid dispersion technique for improved drug delivery: basics to clinical applications. **Drug delivery and translational research,** v. 5, n. 6, p. 552-565, 2015.

MISRA, A.; KHER, G. Drug delivery systems from nose to brain. **Current Pharmaceutical Biotechnology,** v. 13, n. 12, p. 2355-79, 2012.

MODI, G.; PILLAY, V.; CHOONARA, Y. E. Advances in the treatment of neurodegenerative disorders employing nanotechnology. **Annals of the New York Academy of Sciences**, 2010.

MORADI-AFRAPOLI, F.; OUFIR, M.; WALTER, F. R.; DELI, M. A.; SMIESKO, M.; ZABELA, V.; BUTTERWECK, V.; HAMBURGER, M. Validation of UHPLC-MS/MS methods for the determination of kaempferol and its metabolite 4-hydroxyphenyl acetic acid, and application to in vitro blood-brain barrier and intestinal drug permeability studies. **Journal of pharmaceutical and biomedical analysis,** v. 128, p. 264-274, 2016.

NADOVA, S.; MIADOKOVA, E.; CIPAK, L. Flavonoids potentiate the efficacy of cytarabine through modulation of drug-induced apoptosis. **Neoplasma,** v. 54, n. 3, p. 202-6, 2007.

NAKATSUMA, A.; FUKAMI, T.; SUZUKI, T.; FURUISHI, T.; TOMONO, K.; HIDAKA, S. Effects of kaempferol on the mechanisms of drug resistance in the human glioblastoma cell line T98G. **Pharmazie,** v. 65, n. 5, p. 379-83, 2010.

NASR, M. Development of an optimized hyaluronic acid-based lipidic nanoemulsion co-encapsulating two polyphenols for nose to brain delivery. **Drug delivery,** v. 23, n. 4, p. 1444-52, 2016.

NOTHLINGS, U.; MURPHY, S. P.; WILKENS, L. R.; HENDERSON, B. E.; KOLONEL, L. N. Flavonols and pancreatic cancer risk: the multiethnic cohort study. **American Journal of Epidemiology,** v. 166, n. 8, p. 924-31, 2007.

OSTROM, Q. T.; BAUCHET, L.; DAVIS, F. G.; DELTOUR, I.; FISHER, J. L.; LANGER, C. E.; PEKMEZCI, M.; SCHWARTZBAUM, J. A.; TURNER, M. C.; WALSH, K. M.; WRENSCH, M. R.; BARNHOLTZ-SLOAN, J. S. The epidemiology of glioma in adults: a "state of the science" review. **Neuro-Oncology,** v. 16, n. 7, p. 896-913, 2014.

PAJOUHESH, H.; LENZ, G. R. Medicinal chemical properties of successful central nervous system drugs. **NeuroRx : the journal of the American Society for Experimental NeuroTherapeutics.,** v. 2, n. 4, p. 541-53, 2005.

PANGENI, R.; SHARMA, S.; MUSTAFA, G.; ALI, J.; BABOOTA, S. Vitamin E loaded resveratrol nanoemulsion for brain targeting for the treatment of Parkinson's disease by reducing oxidative stress. **Nanotechnology,** v. 25, n. 48, p. 0957-4484, 2014.

PARDESHI, C. V.; BELGAMWAR, V. S. Direct nose to brain drug delivery via integrated nerve pathways bypassing the blood-brain barrier: an excellent platform for brain targeting. **Expert Opinion on Drug Delivery,** v. 10, n. 7, p. 957-72, 2013.

PATEL, J.; BUDDHA, B.; DEY, S.; PAL, D.; MITRA, A. K. In vitro interaction of the HIV protease inhibitor ritonavir with herbal constituents: changes in P-gp and CYP3A4 activity. **American Journal of Therapeutics,** v. 11, n. 4, p. 262-77, Jul-Aug 2004.

PIAO, Y.; SHIN, S. C.; CHOI, J. S. Effects of oral kaempferol on the pharmacokinetics of tamoxifen and one of its metabolites, 4-hydroxytamoxifen, after oral administration of tamoxifen to rats. **Biopharmaceutics & Drug Disposition,** v. 29, n. 4, p. 245-9, May 2008.

PICON, P. D.; PICON, R. V.; COSTA, A. F.; SANDER, G. B.; AMARAL, K. M.; ABOY, A. L.; HENRIQUES, A. T. Randomized clinical trial of a phytotherapic compound containing Pimpinella anisum, Foeniculum vulgare, Sambucus nigra, and Cassia augustifolia for chronic constipation. **BMC Complement Altern Med,** v. 10, n. 17, p. 1472-6882, 2010.

PREUSSER, M.; HABERLER, C.; HAINFELLNER, J. A. Malignant glioma: neuropathology and neurobiology. **Wiener medizinische Wochenschrift.,** v. 156, n. 11-12, p. 332-7, 2006.

RAJENDRAN, P.; RENGARAJAN, T.; NANDAKUMAR, N.; PALANISWAMI, R.; NISHIGAKI, Y.; NISHIGAKI, I. Kaempferol, a potential cytostatic and cure for inflammatory disorders. **European Journal of Medicinal Chemistry,** v. 86, p. 103-12, 2014.

RANGEL-ORDONEZ, L.; NOLDNER, M.; SCHUBERT-ZSILAVECZ, M.; WURGLICS, M. Plasma levels and distribution of flavonoids in rat brain after single and repeated doses of standardized Ginkgo biloba extract EGb 761(R). **Planta Med,** v. 76, n. 15, p. 1683-90, 2010.

RASSU, G.; COSSU, M.; LANGASCO, R.; CARTA, A.; CAVALLI, R.; GIUNCHEDI, P.; GAVINI, E. Propolis as lipid bioactive nano-carrier for topical nasal drug delivery. **Colloids and Surfaces B: Biointerfaces,** v. 136, p. 908-17, 2015.

REITZ, M.; DEMESTRE, M.; SEDLACIK, J.; MEISSNER, H.; FIEHLER, J.; KIM, S. U.; WESTPHAL, M.; SCHMIDT, N. O. Intranasal delivery of neural stem/progenitor cells: a noninvasive passage to target intracerebral glioma. **Stem cells translational medicine,** v. 1, n. 12, p. 866-73, 2012.

ROBINS, H. I.; LASSMAN, A. B.; KHUNTIA, D. Therapeutic advances in malignant glioma: current status and future prospects. **Neuroimaging clinics of North America,** v. 19, n. 4, p. 647-56, Nov 2009.

ROMEO, V. D.; DEMEIRELES, J.; SILENO, A. P.; PIMPLASKAR, H. K.; BEHL, C. R. Effects of physicochemical properties and other factors on systemic nasal drug delivery. **Advanced drug delivery reviews,** v. 29, n. 1-2, p. 89-116, 1998.

ROMØREN, K.; THU, B. J.; BOLS, N. C.; EVENSEN, Ø. Transfection efficiency and cytotoxicity of cationic liposomes in salmonid cell lines of hepatocyte and macrophage origin. **Biochimica et Biophysica Acta (BBA) - Biomembranes,** v. 1663, n. 1–2, p. 127-134, 2004.

ROSS, J. A.; KASUM, C. M. Dietary flavonoids: bioavailability, metabolic effects, and safety. **Annual review of nutrition,** v. 22, p. 19-34, 2002.

ROTHWELL, J. A.; DAY, A. J.; MORGAN, M. R. Experimental determination of octanol-water partition coefficients of quercetin and related flavonoids. **J Agric Food Chem,** v. 53, n. 11, p. 4355-60, 2005.

SALES, D. S.; CARMONA, F.; DE AZEVEDO, B. C.; TALEB-CONTINI, S. H.; BARTOLOMEU, A. C.; HONORATO, F. B.; MARTINEZ, E. Z.; PEREIRA, A. M. Eugenia punicifolia (Kunth) DC. as an adjuvant treatment for type-2 diabetes mellitus: a non-controlled, pilot study. **Phytother Res,** v. 28, n. 12, p. 1816-21, 2014.

SARKAR, A.; ROHANI, S. Molecular salts and co-crystals of mirtazapine with promising physicochemical properties. **Journal of pharmaceutical and biomedical analysis,** v. 110, p. 93-99, 2015.

SATHORNSUMETEE, S.; REARDON, D. A.; DESJARDINS, A.; QUINN, J. A.; VREDENBURGH, J. J.; RICH, J. N. Molecularly targeted therapy for malignant glioma. **Cancer,** v. 110, n. 1, p. 13-24, Jul 1 2007.

SCHERER, H. J. A Critical Review: The Pathology of Cerebral Gliomas. **Journal of neurology and psychiatry,** v. 3, n. 2, p. 147-77, 1940.

SEIBERT, H.; MASER, E.; SCHWEDA, K.; SEIBERT, S.; GULDEN, M. Cytoprotective activity against peroxide-induced oxidative damage and cytotoxicity of flavonoids in C6 rat glioma cells. **Food and Chemical Toxicology,** v. 49, n. 9, p. 2398-407, 2011.

SEKIGUCHI, K.; OBI, N.; UEDA, Y. Studies on Absorption of Eutectic Mixture. II. Absorption of fused Conglomerates of Chloramphenicol and Urea in Rabbits. **Chemical and Pharmaceutical Bulletin,** v. 12, n. 2, p. 134-144, 1964.

SEO, J. H.; PARK, J. B.; CHOI, W.-K.; PARK, S.; SUNG, Y. J.; OH, E.; BAE, S. K. Improved oral absorption of cilostazol via sulfonate salt formation with mesylate and besylate. **Drug design, development and therapy,** v. 9, p. 3961, 2015.

SHAH, B.; KHUNT, D.; MISRA, M.; PADH, H. Non-invasive intranasal delivery of quetiapine fumarate loaded microemulsion for brain targeting: Formulation, physicochemical and pharmacokinetic consideration. **European Journal of Pharmaceutical Sciences,** v. 91, p. 196-207, 2016.

SHARMA, V.; JOSEPH, C.; GHOSH, S.; AGARWAL, A.; MISHRA, M. K.; SEN, E. Kaempferol induces apoptosis in glioblastoma cells through oxidative stress. **Molecular Cancer Therapeutics,** v. 6, n. 9, p. 2544-53, Sep 2007.

SHINDE, R. L.; DEVARAJAN, P. V. Docosahexaenoic acid-mediated, targeted and sustained brain delivery of curcumin microemulsion. **Drug delivery,** v. 24, n. 1, p. 152-161, 2017.

SHINGAKI, T.; INOUE, D.; FURUBAYASHI, T.; SAKANE, T.; KATSUMI, H.; YAMAMOTO, A.; YAMASHITA, S. Transnasal delivery of methotrexate to brain tumors in rats: a new strategy for brain tumor chemotherapy. **Molecular pharmaceutics,** v. 7, n. 5, p. 1561-8, 2010.

SIEGELIN, M. D.; REUSS, D. E.; HABEL, A.; HEROLD-MENDE, C.; VON DEIMLING, A. The flavonoid kaempferol sensitizes human glioma cells to TRAIL-mediated apoptosis by proteasomal degradation of survivin. **Molecular Cancer Therapeutics,** v. 7, n. 11, p. 3566-74, 2008.

SINGH, Y.; MEHER, J. G.; RAVAL, K.; KHAN, F. A.; CHAURASIA, M.; JAIN, N. K.; CHOURASIA, M. K. Nanoemulsion: Concepts, development and applications in drug delivery. **Journal of Controlled Release,** v. 252, p. 28-49, 2017.

SOLANS, C.; IZQUIERDO, P.; NOLLA, J.; AZEMAR, N.; GARCIA-CELMA, M. J. Nano-emulsions. **Current Opinion in Colloid & Interface Science,** v. 10, n. 3–4, p. 102-110, 2005.

SOOD, S.; JAIN, K.; GOWTHAMARAJAN, K. Optimization of curcumin nanoemulsion for intranasal delivery using design of experiment and its toxicity assessment. **Colloids and surfaces. B, Biointerfaces,** v. 113, p. 330-7, Jan 1 2014.

SRINIVAS RAGHAVAN, B.; KONDATH, S.; ANANTANARAYANAN, R.; RAJARAM, R. Kaempferol mediated synthesis of gold nanoparticles and their cytotoxic effects on MCF-7 cancer cell line. **Process Biochemistry,** v. 50, n. 11, p. 1966-1976, 2015/11/01/ 2015.

SULTANA, B.; ANWAR, F. Flavonols (kaempeferol, quercetin, myricetin) contents of selected fruits, vegetables and medicinal plants. **Food chemistry,** v. 108, n. 3, p. 879-84, 2008.

SZAKACS, G.; PATERSON, J. K.; LUDWIG, J. A.; BOOTH-GENTHE, C.; GOTTESMAN, M. M. Targeting multidrug resistance in cancer. **Nature reviews. Drug discovery,** v. 5, n. 3, p. 219-34, 2006.

TACHIBANA, T.; NAKAMURA, A. A methode for preparing an aqueous colloidal dispersion of organic materials by using water-soluble polymers: Dispersion ofB-carotene by polyvinylpyrrolidone. **Kolloid-Zeitschrift und Zeitschrift für Polymere,** v. 203, n. 2, p. 130-133, 1965/06/01 1965.

TADROS, T.; IZQUIERDO, P.; ESQUENA, J.; SOLANS, C. Formation and stability of nano-emulsions. **Advances in Colloid and Interface Science,** v. 109, p. 303-18, 2004.

TAHARA, K.; SAKAI, T.; YAMAMOTO, H.; TAKEUCHI, H.; KAWASHIMA, Y. Establishing chitosan coated PLGA nanosphere platform loaded with wide variety of nucleic acid by complexation with cationic compound for gene delivery. **International Journal of Pharmaceutics,** v. 354, n. 1-2, p. 210-6, 2008.

TELANGE, D.; PATIL, A.; PETHE, A.; TATODE, A.; SRIDHAR, A.; DAVE, V. **Kaempferol-Phospholipid Complex: Formulation, and Evaluation of Improved Solubility, In Vivo Bioavailability, and Antioxidant Potential of Kaempferol**. 2016. 89

TIAN, X. J.; YANG, X. W.; YANG, X.; WANG, K. Studies of intestinal permeability of 36 flavonoids using Caco-2 cell monolayer model. **International Journal of Pharmaceutics,** v. 367, n. 1-2, p. 58-64, Feb 9 2009.

TZENG, C. W.; YEN, F. L.; WU, T. H.; KO, H. H.; LEE, C. W.; TZENG, W. S.; LIN, C. C. Enhancement of dissolution and antioxidant activity of kaempferol using a nanoparticle engineering process. **J Agric Food Chem,** v. 59, n. 9, p. 5073-80, 2011.

VAN DONGEN, M. C.; VAN ROSSUM, E.; KESSELS, A. G.; SIELHORST, H. J.; KNIPSCHILD, P. G. The efficacy of ginkgo for elderly people with dementia and age-associated memory impairment: new results of a randomized clinical trial. **Journal of the American Geriatrics Society,** v. 48, n. 10, p. 1183-94, 2000.

VAN MEIR, E. G.; HADJIPANAYIS, C. G.; NORDEN, A. D.; SHU, H. K.; WEN, P. Y.; OLSON, J. J. Exciting new advances in neuro-oncology: the avenue to a cure for malignant glioma. **CA: a cancer journal for clinicians,** v. 60, n. 3, p. 166-93, May-Jun 2010.

VAN WOENSEL, M.; WAUTHOZ, N.; ROSIERE, R.; AMIGHI, K.; MATHIEU, V.; LEFRANC, F.; VAN GOOL, S. W.; DE VLEESCHOUWER, S. Formulations for Intranasal Delivery of Pharmacological Agents to Combat Brain Disease: A New Opportunity to Tackle GBM? **Cancers,** v. 5, n. 3, p. 1020-48, 2013.

VASCONCELOS, T.; MARQUES, S.; DAS NEVES, J.; SARMENTO, B. Amorphous solid dispersions: Rational selection of a manufacturing process. **Advanced drug delivery reviews,** v. 100, p. 85-101, 2016/05/01/ 2016.

VASCONCELOS, T.; SARMENTO, B.; COSTA, P. Solid dispersions as strategy to improve oral bioavailability of poor water soluble drugs. **Drug Discovery Today,** v. 12, n. 23-24, p. 1068-1075, 2007.

VINOGRADOV, S. V.; BRONICH, T. K.; KABANOV, A. V. Nanosized cationic hydrogels for drug delivery: preparation, properties and interactions with cells. **Advanced drug delivery reviews,** v. 54, n. 1, p. 135-47, 2002.

VO, C. L.; PARK, C.; LEE, B. J. Current trends and future perspectives of solid dispersions containing poorly water-soluble drugs. **Eur J Pharm Biopharm,** v. 85, n. 3 Pt B, p. 799-813, 2013.

VYAS, T. K.; BABBAR, A. K.; SHARMA, R. K.; SINGH, S.; MISRA, A. Preliminary brain-targeting studies on intranasal mucoadhesive microemulsions of sumatriptan. **AAPS PharmSciTech,** v. 7, n. 1, 2006.

VYAS, T. K.; SHAHIWALA, A.; MARATHE, S.; MISRA, A. Intranasal drug delivery for brain targeting. **Current Drug Delivery,** v. 2, n. 2, p. 165-75, 2005.

WANG, S.; CHEN, P.; ZHANG, L.; YANG, C.; ZHAI, G. Formulation and evaluation of microemulsion-based in situ ion-sensitive gelling systems for intranasal administration of curcumin. **Journal of Drug Targeting,** v. 20, n. 10, p. 831-40, 2012.

WANG, W.; KANG, Q.; LIU, N.; ZHANG, Q.; ZHANG, Y.; LI, H.; ZHAO, B.; CHEN, Y.; LAN, Y.; MA, Q.; WU, Q. Enhanced dissolution rate and oral bioavailability of Ginkgo biloba extract by preparing solid dispersion via hot-melt extrusion. **Fitoterapia,** v. 102, p. 189-97, 2015.

XIE, Y.; LUO, H.; DUAN, J.; HONG, C.; MA, P.; LI, G.; ZHANG, T.; WU, T.; JI, G. Phytic acid enhances the oral absorption of isorhamnetin, quercetin, and kaempferol in total flavones of Hippophae rhamnoides L. **Fitoterapia,** v. 93, p. 216-25, Mar 2014.

XU, W.; WEN, M.; YU, J.; ZHANG, Q.; POLYAKOV, N. E.; DUSHKIN, A. V.; SU, W. Mechanochemical preparation of kaempferol intermolecular complexes for enhancing the solubility and bioavailability. **Drug development and industrial pharmacy,** v. 44, n. 12, p. 1924-1932, 2018.

YANG, F.; RIEDEL, R.; DEL PINO, P.; PELAZ, B.; SAID, A. H.; SOLIMAN, M.; PINNAPIREDDY, S. R.; FELIU, N.; PARAK, W. J.; BAKOWSKY, U.; HAMPP, N. Real-time, label-free monitoring of cell viability based on cell adhesion measurements

with an atomic force microscope. **Journal of Nanobiotechnology,** v. 15, n. 1, p. 017-0256, 2017.

YANG, L.; GAO, S.; ASGHAR, S.; LIU, G.; SONG, J.; WANG, X.; PING, Q.; ZHANG, C.; XIAO, Y. Hyaluronic acid/chitosan nanoparticles for delivery of curcuminoid and its in vitro evaluation in glioma cells. **International Journal of Biological Macromolecules,** v. 72, p. 1391-401, 2015.

YANG, R. Y.; LIN, S.; KUO, G. Content and distribution of flavonoids among 91 edible plant species. **Asia Pacific journal of clinical nutrition,** v. 1, p. 275-9, 2008.

YANG, Y.; BAI, L.; LI, X.; XIONG, J.; XU, P.; GUO, C.; XUE, M. Transport of active flavonoids, based on cytotoxicity and lipophilicity: an evaluation using the blood-brain barrier cell and Caco-2 cell models. **Toxicology in Vitro,** v. 28, n. 3, p. 388-96, Apr 2014.

YAO, L. H.; JIANG, Y. M.; SHI, J.; TOMAS-BARBERAN, F. A.; DATTA, N.; SINGANUSONG, R.; CHEN, S. S. Flavonoids in food and their health benefits. **Plant foods for human nutrition,** v. 59, n. 3, p. 113-22, 2004.

ZHANG, K.; GU, L.; CHEN, J.; ZHANG, Y.; JIANG, Y.; ZHAO, L.; BI, K.; CHEN, X. Preparation and evaluation of kaempferol-phospholipid complex for pharmacokinetics and bioavailability in SD rats. **J Pharm Biomed Anal,** v. 114, p. 168-75, 2015.

ZHANG, Q.; WU, D.; WU, J.; OU, Y.; MU, C.; HAN, B. Improved blood-brain barrier distribution: effect of borneol on the brain pharmacokinetics of kaempferol in rats by in vivo microdialysis sampling. **Journal of Ethnopharmacology,** v. 162, p. 270-7, 2015.

ZHANG, Y.; CHEN, A. Y.; LI, M.; CHEN, C.; YAO, Q. Ginkgo biloba extract kaempferol inhibits cell proliferation and induces apoptosis in pancreatic cancer cells. **Journal of Surgical Research,** v. 148, n. 1, p. 17-23, 2008.

ZHAO, G.; DUAN, J.; XIE, Y.; LIN, G.; LUO, H.; LI, G.; YUAN, X. Effects of solid dispersion and self-emulsifying formulations on the solubility, dissolution, permeability and pharmacokinetics of isorhamnetin, quercetin and kaempferol in total flavones of Hippophae rhamnoides L. **Drug Development and Industrial Pharmacy,** v. 39, n. 7, p. 1037-45, Jul 2013.

ZHU, L.; MA, J.; JIA, N.; ZHAO, Y.; SHEN, H. Chitosan-coated magnetic nanoparticles as carriers of 5-fluorouracil: preparation, characterization and cytotoxicity studies. **Colloids and Surfaces B: Biointerfaces,** v. 68, n. 1, p. 1-6, 2009.

ANEXOS

Tabela 1. Variáveis no planejamento experimental Box-Behnken.

Fator	Baixo (-)	Alto(+)	Ponto Central
Triglicerídeos de cadeia média (%)	8	20	14
Lecitina de ovo (%)	1	5	3,5
Polissorbato 80 (%)	1	3	2

Tabela 2. Respostas obtidas através do planejamento experimental Box-Behnken.

TCM (%)	Lecitina (%)	Polisorbato 80 (%)	Content (%)	Size (nm)	PDI	Potencial Zeta (mV)
20	5	2	88,36	131,23	0,19	-15,57
14	2	1	88,15	145,20	0,18	-10,60
8	5	2	94,91	123,53	0,36	-10,83
8	2	2	89,56	131,53	0,39	-11,37
20	3,5	3	93,76	141,93	0,29	-11,97
14	5	3	86,32	128,80	0,34	-11,27
14	3,5	2	91,79	138,33	0,31	-15,93
20	3,5	1	83,65	155,27	0,11	-9,99
14	2	3	88,57	118,13	0,35	-17,47
20	2	2	89,77	132,70	0,19	-15,87
14	5	1	88,08	126,70	0,19	-10,73
14	3,5	2	87,66	116,83	0,28	-8,12
8	3,5	1	85,51	123,00	0,35	-11,77
14	3,5	2	85,52	148,70	0,24	-11,33
8	3,5	3	85,22	190,90	0,42	-34,00

Figura 1. Resultados da análise estatística obtidos através do Software Minitab ®16.

Regressão de Superfície de Resposta: Size (nm) versus TCM (%); Lecitin (%); Polisorbate 80

Análise de Variância

Fonte	GL	SQ (Aj.)	QM (Aj.)	Valor F	Valor-P
Modelo	9	3462,62	384,74	1,37	0,380
Linear	3	154,60	51,53	0,18	0,903
TCM (%)	1	7,67	7,67	0,03	0,875
Lecitin (%)	1	37,41	37,41	0,13	0,730
Polisorbate 80 (%)	1	109,52	109,52	0,39	0,559
Quadrado	3	1434,96	478,32	1,71	0,280
TCM (%)*TCM (%)	1	305,57	305,57	1,09	0,344
Lecitin (%)*Lecitin (%)	1	720,54	720,54	2,57	0,170
Polisorbate 80 (%)*Polisorbate 80 (%)	1	302,78	302,78	1,08	0,346
Interação com 2 Fatores	3	1873,06	624,35	2,23	0,203
TCM (%)*Lecitin (%)	1	10,67	10,67	0,04	0,853
TCM (%)*Polisorbate 80 (%)	1	1649,71	1649,71	5,89	0,060 ←
Lecitin (%)*Polisorbate 80 (%)	1	212,67	212,67	0,76	0,424
Erro	5	1401,13	280,23		
Falta de ajuste	3	872,73	290,91	1,10	0,508
Erro puro	2	528,40	264,20	*	*
Total	14	4863,76			

Sumário do Modelo

S	R2	R2(aj)	R2(pred)
16,7400	71,19%	19,34%	0,00%

Regressão de Superfície de Resposta: PDI versus TCM (%); Lecitin (%); Polisorbate 80 (%)

Análise de Variância

Fonte	GL	SQ (Aj.)	QM (Aj.)	Valor F	Valor-P
Modelo	9	0,112951	0,012550	19,06	0,002
Linear	3	0,107952	0,035984	54,64	0,000 ←
TCM (%)	1	0,068204	0,068204	103,56	0,000 ←
Lecitin (%)	1	0,000080	0,000080	0,12	0,741
Polisorbate 80 (%)	1	0,039668	0,039668	60,23	0,001
Quadrado	3	0,001486	0,000495	0,75	0,567
TCM (%)*TCM (%)	1	0,000909	0,000909	1,38	0,293
Lecitin (%)*Lecitin (%)	1	0,000458	0,000458	0,70	0,442
Polisorbate 80 (%)*Polisorbate 80 (%)	1	0,000006	0,000006	0,01	0,926
Interação com 2 Fatores	3	0,003514	0,001171	1,78	0,267
TCM (%)*Lecitin (%)	1	0,000361	0,000361	0,55	0,492
TCM (%)*Polisorbate 80 (%)	1	0,003099	0,003099	4,71	0,082
Lecitin (%)*Polisorbate 80 (%)	1	0,000054	0,000054	0,08	0,787
Erro	5	0,003293	0,000659		
Falta de ajuste	3	0,000976	0,000325	0,28	0,839
Erro puro	2	0,002317	0,001158	*	*
Total	14	0,116244			

Sumário do Modelo

S	R2	R2(aj)	R2(pred)
0,0256624	97,17%	92,07%	82,08%

Regressão de Superfície de Resposta: Content (%) versus TCM (%); Lecitin (%); Polisorbate

Análise de Variância

Fonte	GL	SQ (Aj.)	QM (Aj.)	Valor F	Valor-P
Modelo	9	78,219	8,6910	0,70	0,697
Linear	3	9,332	3,1108	0,25	0,858
TCM (%)	1	0,015	0,0150	0,00	0,974
Lecitin (%)	1	0,326	0,3255	0,03	0,878
Polisorbate 80 (%)	1	8,992	8,9919	0,73	0,433
Quadrado	3	29,194	9,7312	0,79	0,551
TCM (%)*TCM (%)	1	2,314	2,3140	0,19	0,684
Lecitin (%)*Lecitin (%)	1	8,708	8,7082	0,70	0,440
Polisorbate 80 (%)*Polisorbate 80 (%)	1	15,941	15,9412	1,29	0,308
Interação com 2 Fatores	3	39,693	13,2309	1,07	0,441
TCM (%)*Lecitin (%)	1	11,429	11,4289	0,92	0,381
TCM (%)*Polisorbate 80 (%)	1	27,071	27,0714	2,18	0,199
Lecitin (%)*Polisorbate 80 (%)	1	1,192	1,1924	0,10	0,769
Erro	5	61,951	12,3902		
Falta de ajuste	3	41,670	13,8899	1,37	0,448
Erro puro	2	20,281	10,1406	*	*
Total	14	140,170			

Sumário do Modelo

S	R2	R2(aj)	R2(pred)
3,51997	55,80%	0,00%	0,00%

Otimização da Resposta: PDI; Size (nm)

Parâmetros

Resposta	Meta	Inferior	Alvo	Superior	Peso	Importância
PDI	Mínimo		0,109	0,417	1	1
Size (nm)	Mínimo		116,833	190,900	1	1

Solução

Solução	TCM (%)	Lecitin (%)	Polisorbate 80 (%)	PDI Ajuste	Size (nm) Ajuste	Desirability Composta
1	15,8788	5	1	0,161302	124,010	0,866442

Predição de Múltiplas Respostas

Variável	Configurações
TCM (%)	15,8788
Lecitin (%)	5
Polisorbate 80 (%)	1

Resposta	Ajuste	EP do Ajustado	IC de 95%	IP de 95%
PDI	0,1613	0,0228	(0,1027; 0,2199)	(0,0731; 0,2495)
Size (nm)	124,0	14,9	(85,8; 162,2)	(66,4; 181,6)

Gráficos de Contorno de PDI

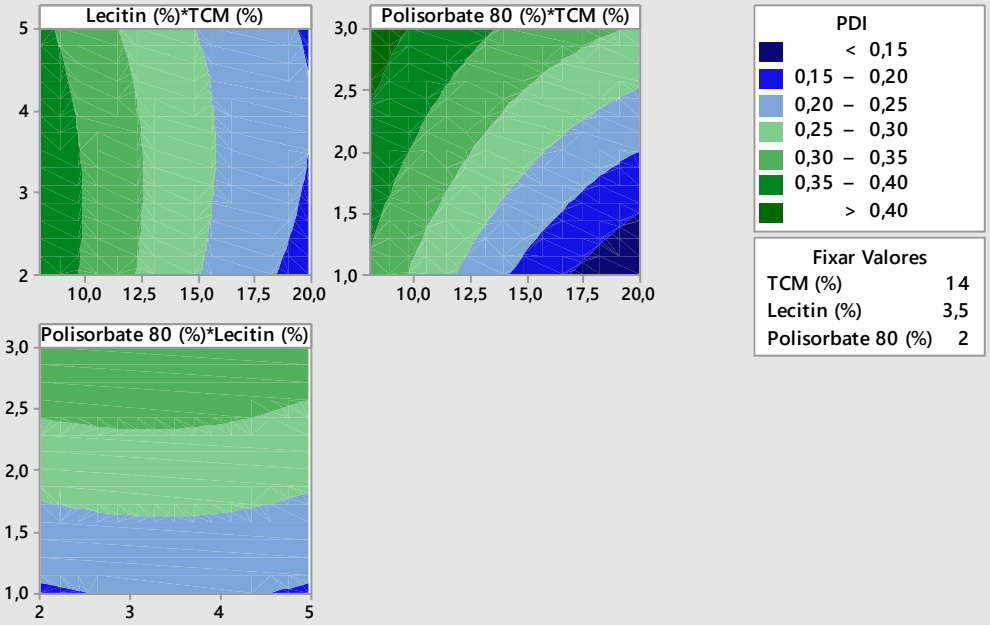

Gráficos de Contorno de Size (nm)

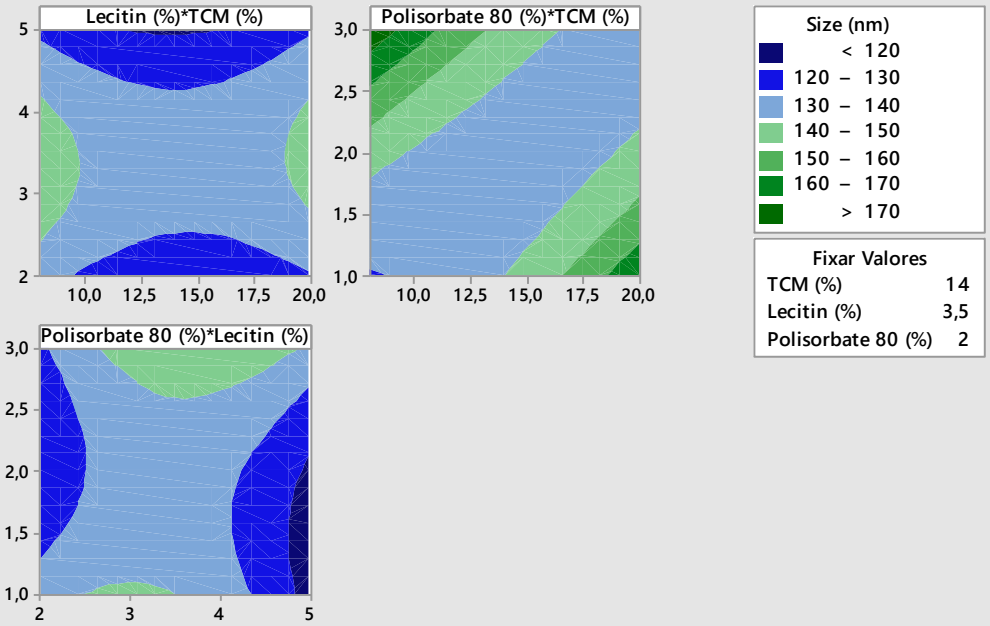

U F R G S
UNIVERSIDADE FEDERAL DO RIO GRANDE DO SUL

PRÓ-REITORIA DE PESQUISA

Comissão De Ética No Uso De Animais

CEUA UFRGS

CARTA DE APROVAÇÃO

Comissão De Ética No Uso De Animais analisou o projeto:

Número: 31216

Título: DESENVOLVIMENTO E CARACTERIZAÇÃO DE NANOEMULSÕES CONTENDO KAEMPFEROL E AVALIAÇÃO DA ATIVIDADE ANTINEOPLÁSICA

Vigência: 28/04/2016 à 31/12/2018

Pesquisadores:

Equipe UFRGS:

ANA MARIA OLIVEIRA BATTASTINI - coordenador desde 28/04/2016
LETICIA SCHERER KOESTER - coordenador desde 28/04/2016
MARIANA COLOMBO - Aluno de Doutorado desde 28/04/2016

Comissão De Ética No Uso De Animais aprovou o mesmo , em reunião realizada em 29/08/2016 - SALA 330 DO ANEXO I DO PRÉDIO DA REITORIA - CAMPUS CENTRO - UFRGS- AV. PAULO DA GAMA,110 BAIRRO FARROUPILHA, em seus aspectos éticos e metodológicos, para a utilização de 101 ratos Wistar machos, de 8 a 9 semanas, pesando entre 220 e 300 gramas, provenientes do Biotério do Departamento de Bioquímica da UFRGS; de acordo com os preceitos das Diretrizes e Normas Nacionais e Internacionais, especialmente a Lei 11.794 de 08 de novembro de 2008, o Decreto 6899 de 15 de julho de 2009, e as normas editadas pelo Conselho Nacional de Controle da Experimentação Animal (CONCEA), que disciplinam a produção, manutenção e/ou utilização de animais do filo Chordata, subfilo Vertebrata (exceto o homem) em atividade de ensino ou pesquisa.

Porto Alegre, Sexta-Feira, 9 de Setembro de 2016

MARCELO MELLER ALIEVI
Coordenador da comissão de ética

1